Comptes Rendus
de l'Académie des sciences

1778-7025 (electronic)

Géoscience
Sciences de la Planète

Volume 354, Special Issue S3, 2022

Special issue / *Numéro thématique*

Integrated stratigraphy of the Jurassic and the Cretaceous: a tribute to Jacques Rey / *Stratigraphie intégrée du Jurassique et du Crétacé : un hommage à Jacques Rey*

Guest editors / *Rédacteurs en chef invités*

Carine Lézin, Thomas Saucède

Académie des sciences — Paris

INSTITUT DE FRANCE
Académie des sciences

CENTRE MERSENNE

Comptes Rendus

Géoscience

Objective of the journal

Comptes Rendus Géoscience is an internationally peer-reviewed electronic journal covering the full range of earth sciences and sustainable development. It publishes original research articles, review articles, historical perspectives, pedagogical texts, and conference proceedings of unlimited length, in English or French. *Comptes Rendus Géoscience* is published according to a virtuous policy of diamond open access, free of charge for authors (no publication fees) as well as for readers (immediate and permanent open access).

About the journal

All journal's information, including the text of published articles, which is fully open access, is available from the journal website at https://comptes-rendus.academie-sciences.fr/geoscience/.

Author enquiries

For enquiries relating to the submission of articles, please visit this journal's homepage at https://comptes-rendus.academie-sciences.fr/geoscience/.

Contact

Académie des sciences
23, quai de Conti, 75006 Paris, France
Tel: (+33) (0)1 44 41 43 72
CR-Geoscience@academie-sciences.fr

Comptes Rendus
Géoscience — Sciences de la Planète
2022, 354, nº S3

Contents / *Sommaire*

Comptes Rendus
Géoscience — Sciences de la Planète
2022, Vol. 354, Special Issue S3, p. 1-4
https://doi.org/10.5802/crgeos.197

Integrated stratigraphy of the Jurassic and the Cretaceous: a tribute to Jacques Rey /
Stratigraphie intégrée du Jurassique et du Crétacé : un hommage à Jacques Rey

Integrated stratigraphy of the Jurassic and the Cretaceous: a tribute to Jacques Rey (1940–2018)

Stratigraphie intégrée du Jurassique et du Crétacé : un hommage à Jacques Rey (1940–2018)

Joseph Canérot [a], Carine Lézin [*, b] and Thomas Saucède [c]

[a] 3, Chemin Cordeau, 31200 Toulouse, France

[b] Géosciences Environnement Toulouse (GET), UMR5563 Université de Toulouse/CNRS/IRD/Université Paul Sabatier, Observatoire Midi-Pyrénées, Toulouse, France

[c] Biogéosciences, UMR6282, CNRS, Université Bourgogne Franche-Comté, 6 boulevard Gabriel, 21000 Dijon, France

E-mails: jcanerot@live.fr (J. Canérot), carine.lezin@get.omp.eu (C. Lézin), thomas.saucede@u-bourgogne.fr (T. Saucède)

Published online: 13 January 2023, Issue date: 13 January 2023

The Groupe Français du Crétacé and Groupe Français d'étude du Jurassique are pleased to join and offer this thematic issue as a tribute to our colleague and friend, Professor Jacques Rey, for his remarkable career as a specialist of stratigraphy. Jacques Rey was a pioneer in Sequence Stratigraphy.

Jacques Rey passed away at home, in Toulouse, on March 5th, 2018. He had carried out his academic career at Paul Sabatier University of Toulouse. He began as a teacher in 1962 until he retired in 2002. During these forty years, he successively passed all academic degrees: laboratory assistant (1964), assistant lecturer (1967), lecturer (1975) and professor (1979), jumping up to the exceptional level (1993). Since 2002, he was professor emeritus.

1. Academic activities: *teaching, management, expert assessment*

Jacques Rey taught geology at all academic levels, undergraduate and graduate, but also for public administrations, secondary schools, or industrial managers. He also gave over 30 lectures on the evolution of life on Earth, and in the palaeontology, stratigraphy and geology of the Pyrenees in different towns and universities of southern France, Spain, Portugal and Morocco. In 1983, he published a book on stratigraphy (Technip). Finally, during 10 years long he taught sequence stratigraphy at the National High School for Oil and Motors in Paris.

* Corresponding author.

He directed nearly 30 PhD theses and took part in many doctoral boards in France, Portugal, Spain and Morocco. He also organized 14 scientific meetings and participated to 53 congresses, including the International Geological Congresses of Paris (1980), Moscow (1984) and Beijing (1996).

Jacques Rey has been involved in many administrative positions, at different levels:

- *International*: member of the International Subcommission on Stratigraphic Classification (IUGS, 1990–1998); member of the Valuation Committee of Earth and Space research Units of Portugal (1990–1998);
- *National*: President of Commission 2 within the 36th section of the National Committee of the Universities (1992–1995); President of the National French Committee of Stratigraphy (1990–1998) which published a book titled "Stratigraphie, terminologie française" [Rey, 1997]; Director of the Research Unit 1405 of the National Centre for Scientific Research (1990–1994); President of the French Group of the Cretaceous (1978–1982);
- *Local*: member of the Board of Directors of Paul Sabatier University (1986–1990); Provisional Administrator of the Research Formation, Unit "Life and Earth sciences" (1984–1987); President of the Commission for Teaching (1986–1990).

Finally, Jacques Rey has been involved as an expert in different fields such as the hydrogeology of the French departments of Lot, Tarn and Tarn-et-Garonne, the Administrative Tribunal of Toulouse, or the Scientific Council of the Regional Natural Parc of Quercy.

2. Geological research: *from biostratigraphy to sequence stratigraphy*

After a Master thesis dedicated to the geological study of the Northern part of the Arize Massif in the Central Pyrenees (1963), Jacques Rey moved to Portugal where he worked up to the last years of his life. His State Doctorate concerned the Lower Cretaceous of the Lusitanian Basin [Rey, 1972], then he carried out cooperative studies in a widened area involving different Atlantic-verging basins from France (Aquitaine Basin), Portugal (Lusitanian and Algarve basins) and Morocco (Essaouira Basin). All along these over 40 years of intense activity, he developed three main stratigraphic approaches regarding the Jurassic and Cretaceous infillings of the considered basins.

2.1. *Biostratigraphy*

In his doctorate thesis, Jacques carried out a detailed stratigraphic study of the Lower Cretaceous of the Estremadura Basin, defining different units and providing new data on their age and correlation, both for marine and terrestrial paleoenvironments. Age dating was based on micro-(foraminifera, algae) and macrofauna, especially echinoderms, one of his main palaeontologic specialities. This biostratigraphic approach led to the definition of different, newly correlated units, using sequence stratigraphy concepts and giving way to new palaeoenvironmental and palaeogeographic reconstructions.

A synthesis of his main results was published in 2002 and 2008 [Dinis et al., 2002, 2008]. In the same way, more studies were carried out in different Atlantic bordering basins such as the Algarve, Aquitaine and Essaouira ones.

2.2. *Sequence stratigraphy*

Since 1984, Jacques Rey took interest in the concepts and methods of sequence stratigraphy, the source documents being published by Vail et al. (American Association of Petroleum Geologists, [1977]). Following this new interpretation, "cycles of relative sea level changes on a global scale are evident throughout Phanerozoic time. The evidence is based on the facts that many regional cycles (third order sequences) developed on different continental margins are simultaneous and that the relative magnitudes of the changes are generally similar".

In the study area (Aquitaine, Portugal and Morocco), Jacques and his colleagues described all third order sequences (genetic sequences) developed in Jurassic and Early Cretaceous times. Detailed biostratigraphic, sedimentological and tectonic data were gathered within third order sequences made up of system tracts and separated by unconformities, providing good correlations at the scale of the different studied basins. The respective control of the relative sea-level change, subsidence and sedimentary supply was pointed out within the accumulation process. New data were provided in regional

studies: normal faulting may occur suddenly and provide more accommodation than eustatic sea level changes (Jurassic series from Quercy); third order sequences can be diachronous when they are included within basin infillings provided by different tectonic plates (Lusitanian and Moroccan basins).

2.3. *Relationship between system tracts and micropaleontological associations*

Considering that foraminifers and ostracods constitute good stratigraphical and palaeoenvironmental markers, Jacques Rey used these microfossils for his interpretations of variations in sea level change, palaeogeographic communications between basins, nourishing supplies and physicochemical properties impacting benthic communities. In turn, micropalaeontological associations could also help identify system tracts.

A first study concerning Toarcian Foraminifera from Northern Aquitania (Quercy, France) showed the existence of a close relationship between the composition of Nodosariidae communities and sea-level changes. Later on, working on Foraminifera from the Carixian and Domerian of Quercy and Grands Causses (France) he confirmed these interpretations and highlighted the contribution of quantitative methods to appreciate depth variations in platform environments. Other studies dealing with the factorial diversity of deposits and the factorial amplitude of species led Jacques Rey to draw three main conclusions: (i) microfossil associations allow identifying sedimentary system tracts even in homogeneous series (such as in marls, for example), low and high sea levels providing different biocoenotic signals; (ii) the statistical analysis of micropalaeontological communities can lead to "factorial correlations" at basin scale; (iii) sea level changes influence the species composition of assemblages and speciation processes.

In his last years, Jacques began new studies on the North Pyrenean foreland basin infilling but his declining health broke this new project.

Jacques Rey was the Fontannes (1975) and Bourcart (1990) prices winner given by the French Geological Society. He had a decoration (Palmes Académiques) given by the French Ministry of Education (1990) and was Doctor Honoris Causa of the Universidade Nova de Lisboa, Portugal (2012) (Figure 1).

Figure 1. Jacques Rey during his talk of "Doctor Honoris Causa" at the Universidade Nova de Lisboa (Portugal).

Jacques Rey was a great specialist of stratigraphy and developed an integrated stratigraphy approach in order to give a temporal framework to sedimentary series and reconstruct the evolution of paleoenvironments and sedimentary basins, particularly during Jurassic and Cretaceous periods.

The present thematic issue was an opportunity for his former students and colleagues to celebrate Professor Jacques Rey for his remarkable career and achievements in the promotion and development of integrated stratigraphy. We are deeply honoured and pleased to contribute to such a tribute to him in this thematic issue of *Comptes Rendus Geoscience* entitled "Integrated stratigraphy of the Jurassic and the Cretaceous".

Illustrating the value of integrated stratigraphic approaches to sedimentologists and paleontologists for high-resolution evaluation of past climatic, oceanographic, sedimentary, ecological and biogeographic processes in Earth history, the present issue includes six original contributions to the fields of sedimentology and palaeontology, based on original Jurassic and Cretaceous case studies. Two of them highlight the value of linking fossil and stratigraphic studies, not only in taxonomy, evolution, and biostratigraphy, but also in biogeography and for the reconstruction of paleoenvironments. Studying ammonites of the Lower Jurassic (Pliensbachian) series of Southern Vendée (France), Fauré and Bohain [2022] contribute to improving our understanding of

the paleobiogeography of the Lusitanian Basin and Southern Vendée, and more widely of the North-West European Bioprovince with regards to the dispersal of Tethyan marine fauna to the western Europe. Picollier [2022] explores the rich belemnite faunas of early Cretaceous deposits (Berriasian–Albian) of the Vocontian Basin (southeast of France) and reminds the value of well-delineated paleontological species in biostratigraphy based on quantitative and statistical approaches. The four other contributions show the interest of an integrated approach for determining the factors controlling sedimentation. Chemostratigraphic ($\delta^{13}C$) and biostratigraphic correlations between the Poigny borehole (Paris Basin) and other European sections, associated to other data (palynological assemblages, dinoflagellates, clay mineralogy), allow to recognize thirty-three palynological events and show the dominant role of sea-level variations in paleoenvironmental changes during the upper Coniacian-Campanian [Pearce et al., 2022]. The work by Ferry et al. [2022] contributes to demonstrate the tectonic control of the forced regression around the Aptian–Albian boundary recorded in the SE France basins, associated to the "Austrian" tectonic pulse. Duarte et al. [2022] present a sedimentological, organic, and isotopic study of the Upper Sinemurian of the S. Pedro de Moel section (Lusitanian Basin) that reveal the transgressive context of sedimentation and the impact of diagenetic transformations on $\delta^{13}C$ variations. Finally, the analysis of the organic fraction (Rock-Eval, Palynofacies…) in late Jurassic deposits of the Boulonnais (France) by Schnyder et al. [2022] highlights the importance of seawater warming for the occurrence of the Kimmeridgian Organic Rich Bands deposition in NW Europe.

Conflicts of interest

Authors have no conflict of interest to declare.

References

Dinis, J. L., Rey, J., Callapez, P. P., Cuneha, P. P., and Pena Dos Reis, R. (2008). Stratigraphy and allogenic controls of the western Portugal Cretaceous: an updated synthesis. *Cretac. Res.*, 29, 772–780.

Dinis, J. L., Rey, J., and de Graciansky, P. C. (2002). Le Bassin lusitanien (Portugal) à l'Aptien supérieur — Albien: organisation séquentielle, proposition de corrélations, évolution. *C. R. Géosci.*, 334, 757–764.

Duarte, L. V., Silva, R. L., Azerêdo, A. C., Comas-Rengifo, M. J., and Mendonça Filho, J. G. (2022). Shallow-water carbonates of the Coimbra Formation, Lusitanian Basin (Portugal): contributions to the integrated stratigraphic analysis of the Sinemurian sedimentary successions in the western Iberian margin. *C. R. Géosci.*, 354(S3), 89–106.

Fauré, P. and Bohain, P. (2022). Pliensbachian ammonites from Southern Vendée (France). Toward the individualization of an Atlantic paleobiogeographic region. *C. R. Géosci.*, 354(S3), 5–25.

Ferry, S., Grosheny, D., and Amédro, F. (2022). Sedimentary record of the "Austrian" tectonic pulse around the Aptian–Albian boundary in SE France, and abroad. *C. R. Géosci.*, 354(S3), 67–87.

Pearce, M. A., Jarvis, I., Monkenbusch, J., Thibault, N., Ullmann, C. V., and Martinez, M. (2022). Coniacian–Campanian palynology, carbon isotopes and clay mineralogy of the Poigny borehole (Paris Basin) and its correlation in NW Europe. *C. R. Géosci.*, 354(S3), 45–65.

Picollier, M.-C. (2022). Biometry and biostratigraphy of the Early Cretaceous belemnite genus Castellanibelus from the southeast of France. *C. R. Géosci.*, 354(S3), 27–43.

Rey, J. (1972). *State Doctorate thesis - Recherches géologiques sur le Crétacé inférieur de l'Estremadura (Portugal)*, volume 21. Mem. Serv. Geol. Portugal, N.S., Lisboa.

Rey, J. (1997). *Stratigraphie, terminologie française*. Elf Exploration Editions.

Schnyder, J., Baudin, F., and Jan du Chêne, R. (2022). The Oxfordian-Kimmeridgian transition in the Boulonnais (France) and the onset of organic-rich marine deposits NW Europe: a climatic control? *C. R. Géosci.*, 354(S3), 107–124.

Vail, P. R., Mitchum Jr., R. M., and Thompson, S. (1977). Seismic stratigraphy and global changes of sea level, part four: global cycles of relative changes of sea level. *AAPG mem.*, 26, 83–98.

Comptes Rendus
Géoscience — Sciences de la Planète
2022, Vol. 354, Special Issue S3, p. 5-25
https://doi.org/10.5802/crgeos.136

Integrated stratigraphy of the Jurassic and the Cretaceous: a tribute to Jacques Rey /
Stratigraphie intégrée du Jurassique et du Crétacé : un hommage à Jacques Rey

Pliensbachian ammonites from Southern Vendée (France). Toward the individualization of an Atlantic paleobiogeographic region

Philippe Fauré[*, a] **and Patrick Bohain**[b]

[a] Muséum d'Histoire naturelle de Toulouse, 35 allées Jules Guesde, 31000, Toulouse, France

[b] Impasse Clément Bertrand, 85100, Les Sables d'Olonne, France

E-mails: philipfaure@wanadoo.fr (Ph. Fauré), bohain.patrick@neuf.fr (P. Bohain)

Abstract. The Lower Pliensbachian series (Ibex Chronozone) of Southern Vendée (France) contains a unique mix of ammonites, with several Polymorphitidae, *Uptonia atlantica* Fauré and Bohain [2017], and *Dayiceras dayiceroides* Mouterde [1951], whose distribution till date seemed restricted to the Lusitanian Basin. As in Portugal, these taxa extend the linear evolutionary sequence of this family during the Masseanum and Valdani Subchronozones. Their discovery in Vendée enables qualifying the importance of the Lusitanian endemism. It allows integrating the Lusitanian Basin and Vendée, which paleogeographic reconstructions place closer, into the same Atlantic paleobiogeographic area. It can be extended to the western borders of the North-West European Bioprovince. During the Late Pliensbachian, it is probably through a diffusion within this paleogeographic area that the Tethyan taxa, which are very numerous in Portugal, would have reached Vendée and Western Europe in successive waves. It seems that this atlantic communication route was privileged, at least until the Early Toarcian.

Keywords. Jurassic, Pliensbachian, Ammonitina, *Dayiceras*, *Uptonia*, Vendée, Lusitanian Basin.

Published online: 29 July 2022, Issue date: 13 January 2023

1. Introduction

The Jurassic of Southern Vendée is a thin platform series which lies unconformably on the Paleozoic Armorican basement, of which it represents the southern cover (Figure 1). Its geographical position, near the Atlantic Coastline, makes it the westernmost sedimentary witness of the northern Aquitaine border. Thus, the associated ammonite faunas, are the westernmost representatives of the Western European faunal ensemble. The Pliensbachian deposits are privileged paleogeographical witnesses because of their proximity to the North-Western margin of the Bay of Biscay.

Located north of the Iberian plate, the Bay of Biscay is an essential structural element of the Iberia–Armorica–Newfoundland conjugate margin. The Rift

* Corresponding author.

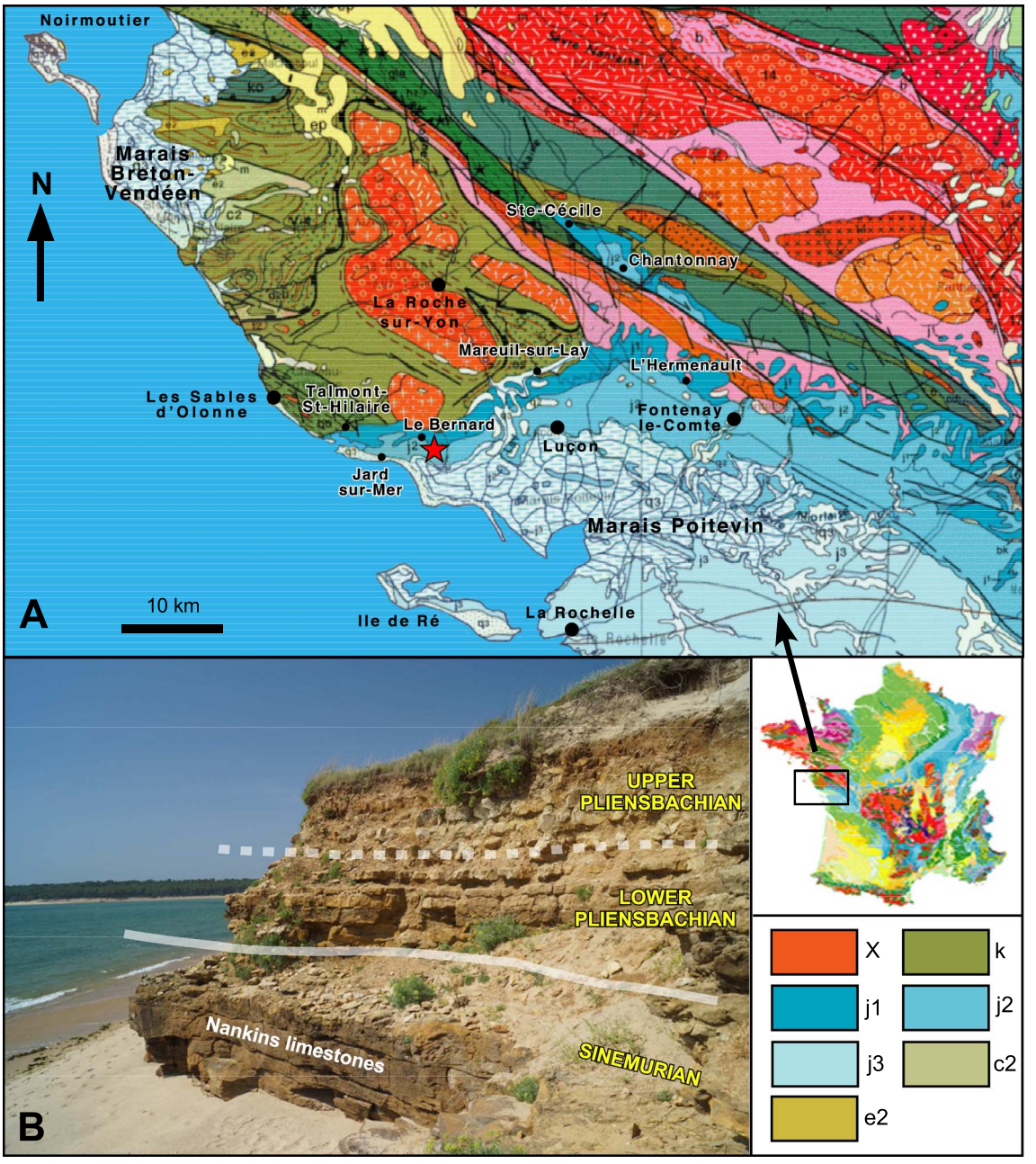

Figure 1. (A) Geographical and geological setting. Location of Southern Vendée. Simplified geological map (BRGM editions) and localities cited in the text. X: Metamorphic; k: Paleozoic; j1: Lower Jurassic (Lias); j2: Middle Jurassic; j3: Upper Jurassic; c2: Cretaceous; e2: Paleocene. Red star: Location of the Le Bernard section. (B) Photography of the Upper part of the Sinemurian "Nankins Limestones" and of the Pliensbachian clayed limestones and marls of the Payré Estuary (Jard-sur-Mer).

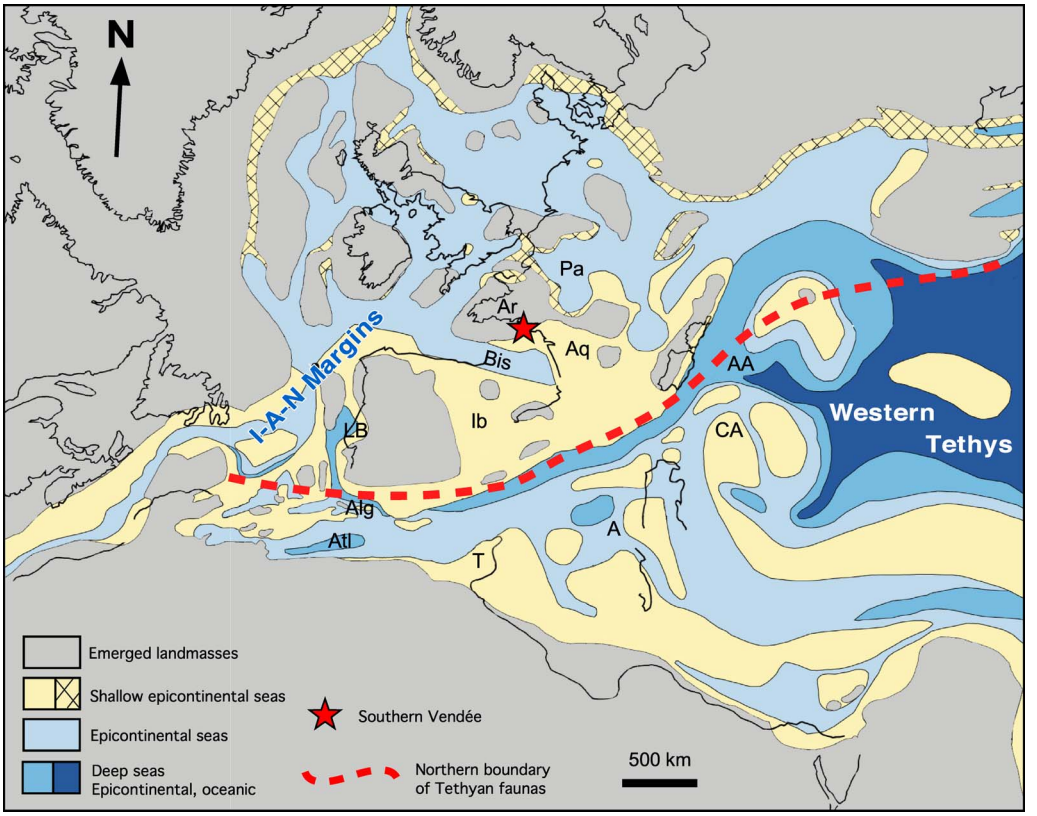

Figure 2. Paleogeographical framework for the Pliensbachian at the scale of Western Tethys [modified from Thierry et al., 2000]. Abbreviations. I-A-N Margin: Iberian-Armorica-Newfoundland Margins; Ar: Armorican Massif; Aq: Aquitaine Basin; Bis: Biscay Gulf; Pa: Parisian Basin; Ib: Iberian Basin; LB: Lusitanian Basin; Alg: Algarve; Atl: High Atlas; T: Tunisia; A: Apennines; AA: Austroalpine; CA: Calcareous Alps.

of Biscay was set up from the Triassic or the Lower Jurassic [Olivet, 1996, Rasmussen et al., 1998], at the same time as a mosaic of pre-drift basins which prefigured the North Atlantic Sea at the west of Iberia microplate (Figures 2, 8). In the absence of outcrop, we know nothing of the fauna of these essentially offshore basins, particularly of their macrofauna, and we have no element of comparison with the Jurassic of Vendée.

The Lusitanian Basin, located on the western Iberian margin (Figures 2, 8), is the only one to present rich Lower Jurassic onshore outcrops, whose ammonite faunas are now well known [Mouterde et al., 1983, 2007, Dommergues et al., 2010].

Belonging to the North-West European Type (Figure 2), these faunas are, on several occasions in the Upper Sinemurian, then in the Lower Pliensbachian, enriched by highly endemic faunas (genera, species). This remarkable endemism, although punctual and short, suggests a particular paleogeographical configuration of the conjugate "Iberia–Armorica–Newfoundland" passive margin of the Atlantic passive margin [Dommergues et al., 2010]. To date, its causes remain still poorly understood. It probably finds its origin in the relative isolation of the pre-existing Permian–Triassic west Iberian rift domain [Nirrengarten et al., 2018, Angrand et al., 2020]. Also, it has probably been favored by the early Jurassic first phase of rifting that created narrow and deep offshore basins, typically corresponding to asymmetric half grabens generated by tilted blocks tectonics (e.g. Lusitanian, Porto, Porcupine, Rockall Basins) [Olivet, 1996, Rasmussen et al., 1998] (Figures 2, 8). Despite the lack of data

about macrofauna in these offshore basins, it was very likely that all were interconnected, and that the Portuguese endemism was not restricted to the Lusitanian Basin alone, but could affect others neighbouring basins of "Iberia–Armoric–Newfoundland" [Dommergues et al., 2010].

The stratigraphic and taxonomic revision of the Pliensbachian ammonite faunas of Southern Vendée, that we have undertaken provides an element of response, by highlighting the presence, among the ammonites of the Vendean Lower Pliensbachian, of several taxa related to the Lusitanian endemism, of which the genus *Dayiceras* is the most emblematic element. The connection with the Lusitanian faunas is reinforced, in the Upper Pliensbachian, by the presence, in Vendée, of ammonites of Tethyan (Mediterranean) origin, abnormally numerous in North-Western Europe, but identical to those present in abundance at the same time, in the Lusitanian Basin.

This study presents the summary of a taxonomic revision of the Pliensbachian ammonite faunas of Southern Vendée based on material collected *in situ*, put in a rigorous biostratigraphic framework considering all paleobiogeographical and paleoecological aspects [Fauré and Bohain, 2017, Bohain and Fauré, 2022]. It offers a reliable spatio-temporal framework that we compare here with paleogeographic interpretations in the context of the pre-drift basins of the "Iberia–Armorica–Newfoundland" conjugate margins.

2. Stratigraphy

The Pliensbachian of Southern Vendée is a thin (4.5 m) condensed clayed limestone platform series, which overlies the "Sinémuro-Hettangian" dolomitic limestones called "Nankins Limestones", or overlaps directly the Paleozoic Armorican basement (Figure 1A). From Bourgenay (Talmond-Saint-Hilaire) to Saint-Nicolas Cove (Jard-sur-Mer), the layers of Pliensbachian age are known for their emblematic coastal outcrops, which can be followed for several kilometres of cliff or foreshore (Figure 1B). The hills of the Vendean hinterland (regions of Luçon, Chantonnay, Sainte-Cécile, and L'Hermenault) are much unfavourable for their study because of the rather flat topography where outcrops are rare and ephemeral (Figure 1A).

Although it has been already described by Péneau [1923], Butel [1951, 1953], Gabilly [1964], and Dubar and Gabilly [1964], the Vendean Pliensbachian remained little studied until recent stratigraphic revisions by Alméras et al. [2010a,b], based on the study of brachiopods, and those of Fauré and Bohain [2017] and Bohain and Fauré [2022], on ammonites, of which we summarize here some of the results.

The Pliensbachian sedimentary sequence is made of detrital silico-arkosic sandstones or microconglomerates (less than 0.5 m thick), followed by an alternation of clayed limestone and bioclastic marl beds rich in ferruginous oolites (3 to 4 m thick), particularly in the coastal part of Vendée where sedimentation rate decreases. The richness of these layers in fossils, such as brachiopods and ammonites, as well as corals, bivalves, gastropods, and echinoids, has proven to be remarkable and the specimens are particularly well preserved. Despite the low rate of sedimentation, the condensation (2 m thickness for the Lower Pliensbachian; 2.50 m thickness for the Upper Pliensbachian), and the disturbance caused by hydrodynamics and bioturbation, the succession of the ammonites has been found in conformity. We have been able to identify [Fauré and Bohain, 2017, Bohain and Fauré, 2022] all the standard chronostratigraphic divisions of the North-West European Pliensbachian [Dommergues et al., 1997, Page, 2003] (Figures 3, 4, 5).

3. Chronostratigraphic marks

The biostratigraphic precision offered by several sections of the Armorican occidental border, of which the Le Bernard, "Les Prés Noirs", section is the main one, allowed us to determine certain points of the ammonite succession. In the Lower Pliensbachian, from the Polymorphus Subchronozone to the Figulinum Subchronozone, 24 distinct chronostratigraphic divisions, standard zonules, or local biohorizons, could be separated [Fauré and Bohain, 2017] (Figures 3A, C). In the Upper Pliensbachian, 14 divisions could be separated thanks to Tethyan Hildoceratidae and Dactylioceratidae which offer the opportunity of a stratigraphic fineness that is not allowed by Amaltheidae alone [Bohain and Fauré, 2022] (Figures 3B, 4).

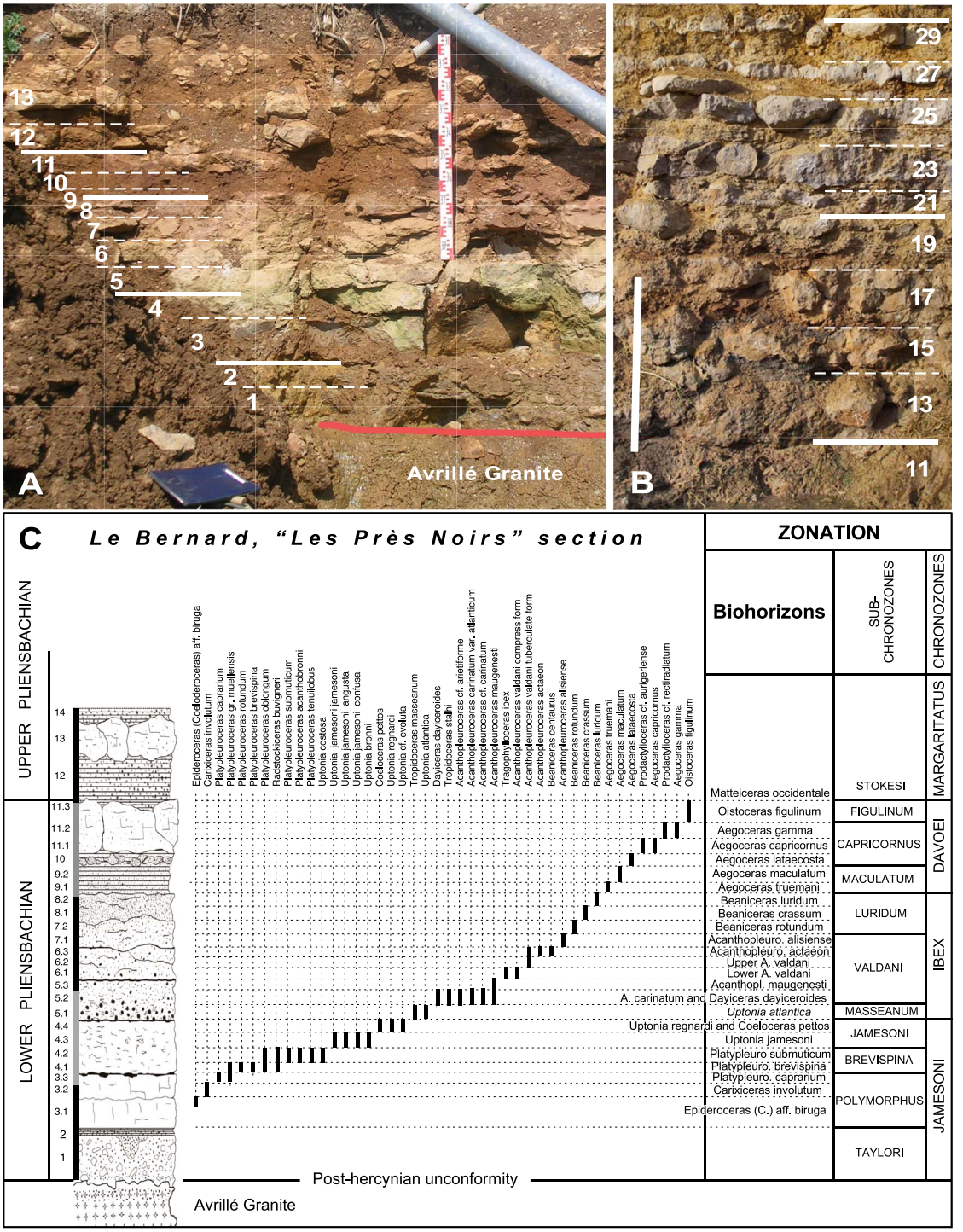

Figure 3. Le Bernard, "Les Prés Noirs" section. (A) Photography of the Lower Pliensbachian (scale: 1 m); (B) Photography of the Upper Pliensbachian (scale: 1 m); (C) Lithologic succession of the Lower Pliensbachian distribution of main ammonites (out of 87 taxa listed in this section. Complete inventory *in* Fauré and Bohain, 2017, Figure 9) and chronostratigraphic framework.

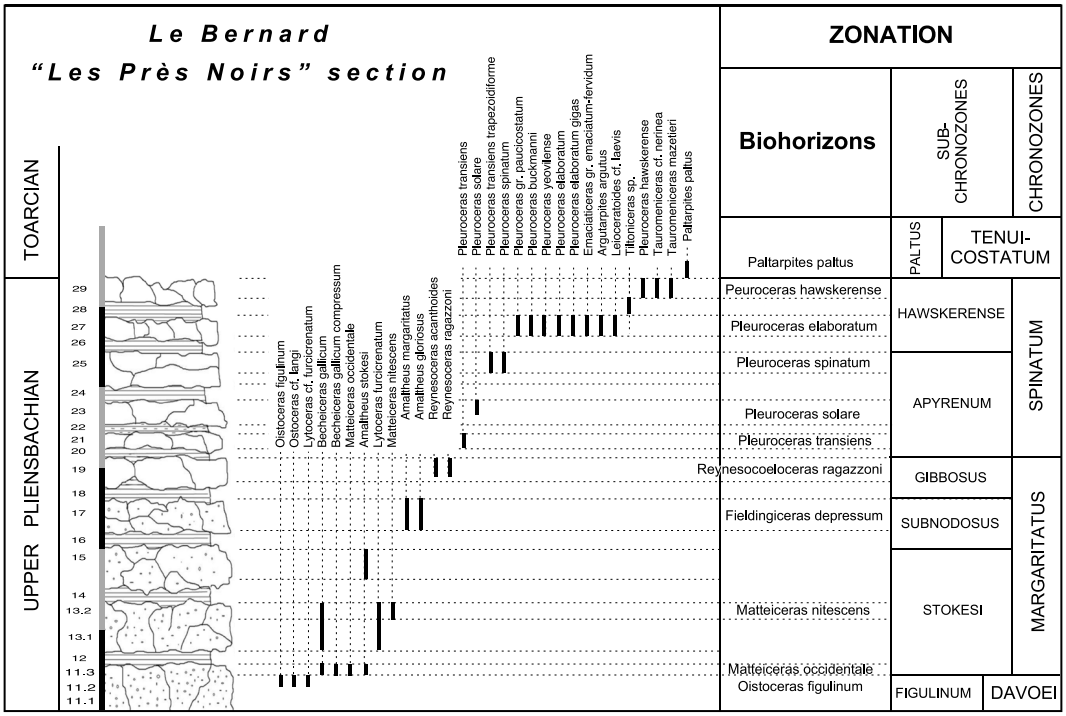

Figure 4. The Upper Pliensbachian of the Le Bernard, "Les Près Noirs" section. Lithologic succession, distribution of ammonites and chronostratigraphic framework.

3.1. *Lower Pliensbachian (Figure 3C)*

3.1.1. *Jamesoni Chronozone*

• Polymorphus Subchronozone: It has been divided into three distinct units, *Epideroceras* (*Coeloderoceras*) aff. *biruga* biohorizon, *Carixiceras involutum* biohorizon, and *Platypleuroceras caprarium* biohorizon; when the standard biozonation for North-Western Europe distinguishes only one (Polymorphus Zonule), and the Lusitanian standard two (Biruga and Costatus Zonules) [Page, 2003].

• Jamesoni Subchronozone: Its division into two units is modeled on the evolutionary sequence of the genus *Uptonia*, with the two successive species *Uptonia* gr. *jamesoni* [Sowerby, 1822] and *Uptonia regnardi* [Orbigny d', 1849] (Figure 6A):

– Jamesoni Zonule: Its limits are based on a new interpretation of the species *Uptonia jamesoni* and *U. lata* [Quenstedt, 1849], which we have already shown that they correspond, not to chronologically successive species, but to synonymous species [Fauré and Téodori, 2019].

– *Uptonia regnardi* and *Coeloceras pettos* biohorizon: The association in Vendée of the two taxa *Uptonia regnardi* [Orbigny d', 1849] and *Coeloceras pettos* [Quenstedt, 1849] allows us to integrate the Pettos Zonule of the standard divisions into the Jamesoni Chronozone (Figure 5).

3.1.2. *Ibex Chronozone*

• Masseanum Subchronozone: It corresponds to the acme of the species *Tropidoceras* gr. *masseanum* [Orbigny d', 1849]. In Vendée, it also contains the late *Uptonia*, *U. atlantica* Fauré and Bohain, 2017, allowing us to individualize *Tropidoceras masseanum* and *Uptonia atlantica* biohorizons (Figures 3, 5).

• Valdani Subchronozone: It could be divided into six successive units (Figure 3C):

– *Acanthopleuroceras carinatum* and *Dayiceras dayiceroides* biohorizons, equivalent to the Arietiforme Zonule of the standard; which combines primitive *Acanthopleuroceras* (*A. arietiforme* [Oppel, 1853], *A. carinatum* [Quenstedt, 1885], *A. carinatum atlanticum*

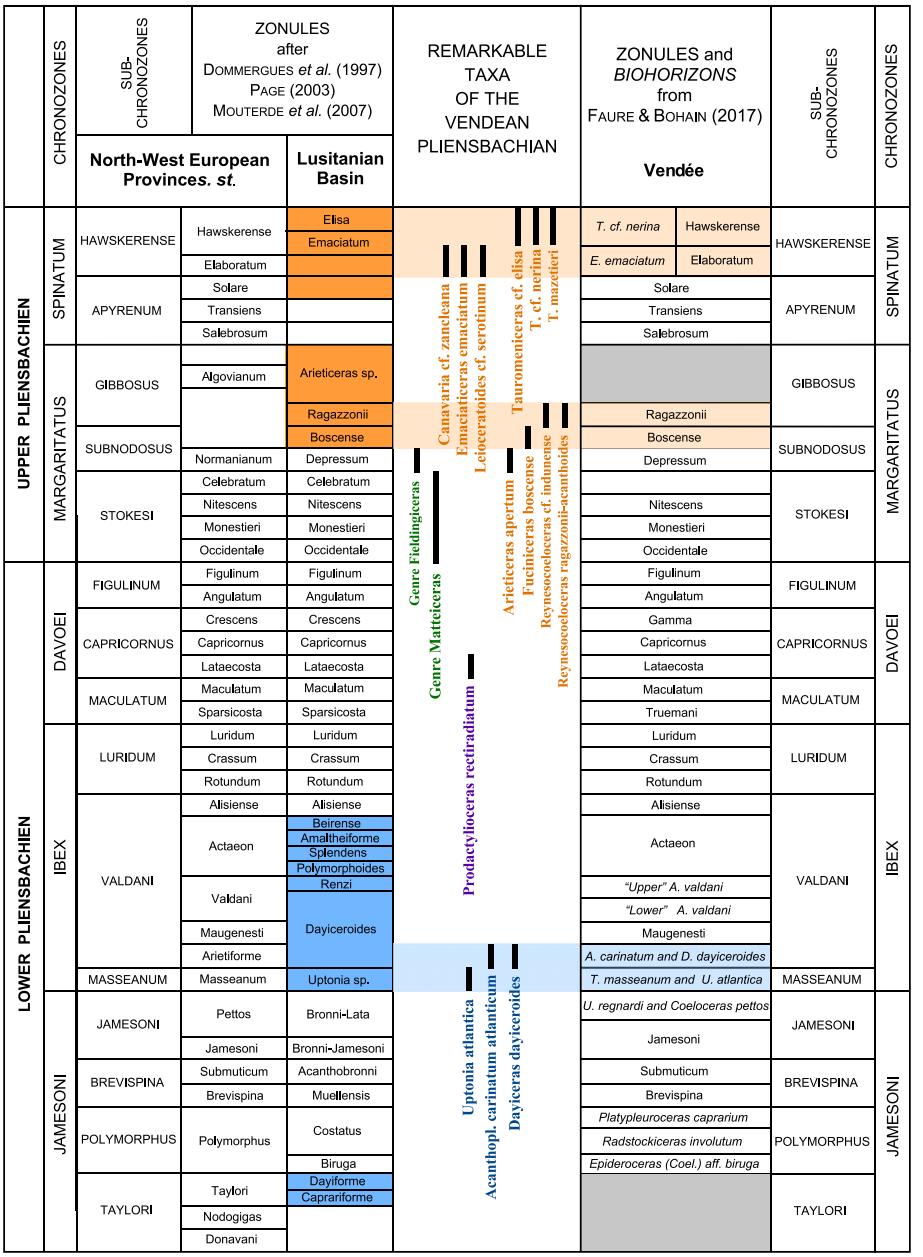

Figure 5. Ammonite standard zonation for the North-West European Province and the Lusitanian Basin [Dommergues et al., 1997, Page, 2003, Mouterde et al., 2007]. Comparison with the zonule and biohorizon (in italic) succession adopted in Southern Vendée [Fauré and Bohain, 2017]. In dark blue: periods of endemism of the Lusitanian faunas; in light blue: period of extension of Lusitanian endemism to the Vendée region; in dark orange: periods of expansion of Tethyan taxa in the Lusitanian Basin; in light orange: periods of Tethyan taxa presence in the Vendée Upper Pliensbachian; in grey: absence of fauna. Remarkable taxa column. Blue: species related to the Lusitanian endemism which are present in Vendée; purple: species common to Portugal, Vendée and Dorset; green: North-West European genera of "southern" affinity; orange: Tethyan taxa.

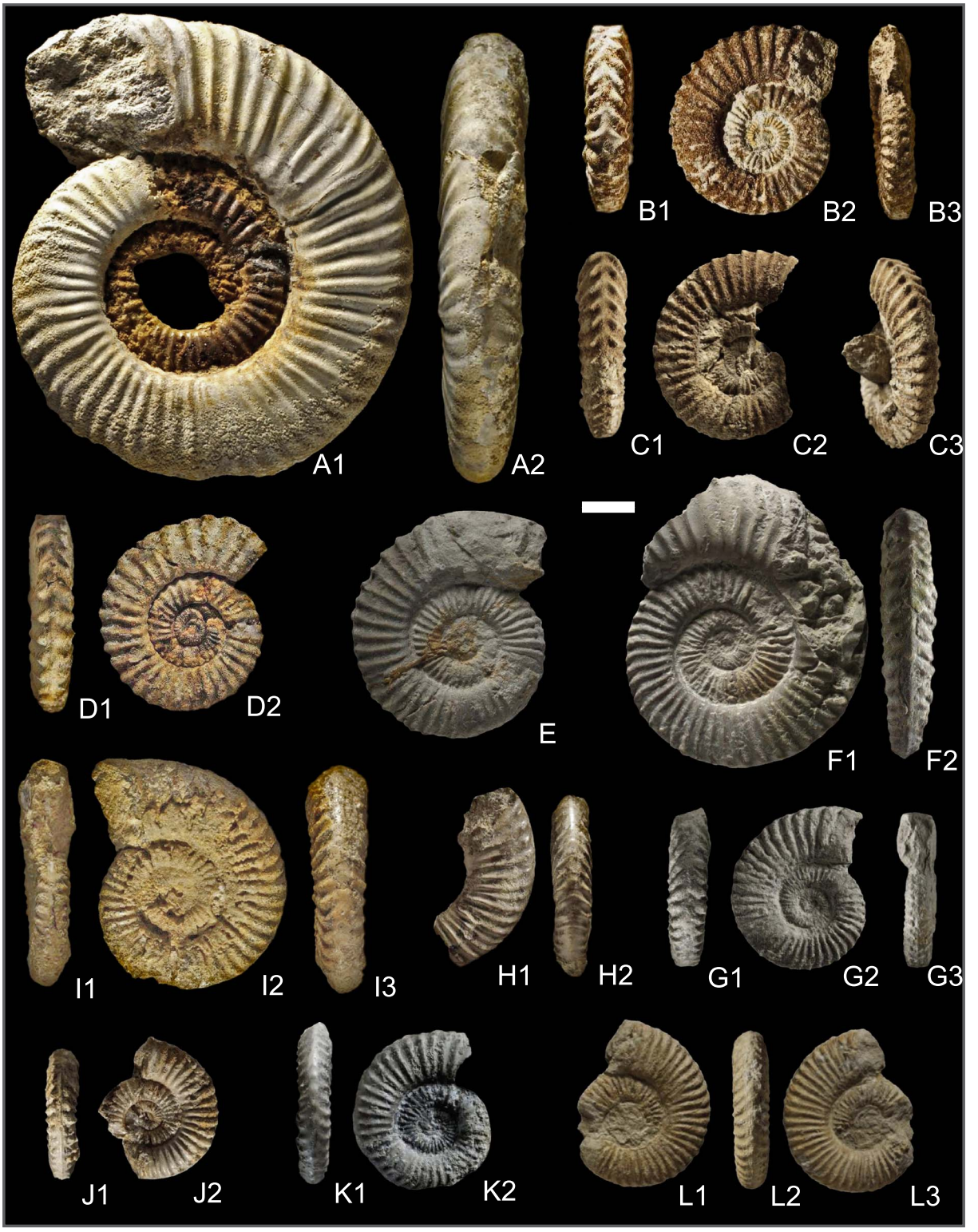

Figure 6. Caption continued on next page.

Figure 6 (cont.). A1–A2, *Uptonia regnardi* [Orbigny d', 1849], Jamesoni Chronozone and Subchronozone, *Uptonia regnardi* and *Coeloceras pettos* biohorizon, Le Bernard, niv. 4.4, Neotype designed by Fauré and Bohain [2017], X78; B, C, D, *Uptonia atlantica* Fauré and Bohain, 2017, Ibex Chronozone, Masseanum Subchronozone, *Tropidoceras masseanum* and *Uptonia atlantica* biohorizon, Le Bernard, niv. 5.1: B1–B3, Holotype, Y55; C1–3, Paratype, V70; D1–2, Z126; E, F, G, *Uptonia atlantica* Fauré and Bohain, 2017, Jamesoni Chronozone, Masseanum Subchronozone, Peniche (Portugal): E, V73; F1–2, V72; G1–3, V75; H, I, J, K, *Dayiceras dayiceroides* [Mouterde, 1951], Ibex Chronozone, Valdani Subchronozone, *Acanthopleuroceras carinatum* and *Dayiceras dayiceroides* biohorizon, Le Bernard, niv. 5.2: H1–2, Y58; I1–3, Z121; J1–2, Z122; K1–2, AU7; L1–3, *Dayiceras dayiceroid*es [Mouterde, 1951], Ibex Chronozone, Valdani Subchronozone, Dayiceroides Zonule, Peniche (Portugal): V84. The material belongs to the P. Bohain collection. It is kept in the collections of the Natural History Museum of Nantes (France). Scale bar 1 cm (all samples are natural size).

Dommergues and Mouterde, 1981) and the late Polymorphitidae *Dayiceras dayiceroides* [Mouterde, 1951].

– Maugenesti Zonule. *Dayiceras* is not seen in Vendée these days, while the genus remains abundant in the Lusitanian Basin.
– Valdani Zonule. It is subdivided into two distinct biohorizons based on the predominance of two morphotypes of the species *Acanthopleuroceras valdani* [Orbigny d', 1849], which were however not distinguished at a specific level [Fauré and Bohain, 2017].
– Actaeon Zonule and Alisiense Zonule, without local particularity.

3.1.3. *Davoei Chronozone*

• Maculatum Subchronozone: The two standard zonules are based on the evolution of primitive forms of the genus *Aegoceras* (Figures 3C, 5):

– Truemani Zonule. We substituted *Aegoceras truemani* Fauré and Bohain, 2017 (Figure 5) for the standard index ammonite "*Aegoceras sparsicosta*" [Trueman, 1919], because we consider the latter taxon as the peramorphic form ("*Androgynoceras*" form) of a *Beaniceras* from the Luridum Subchronozone.
– Maculatum Zonule. Without modification.

• Capricornus Subchronozone:

– Lataecosta Zonule. In Vendée, it is the level of *Prodactylioceras rectiradiatum* [Wingrave, 1916].
– Gamma Zonule. We have substituted *Aegoceras gamma* Dommergues, 1979 (Figure 5) for the standard index ammonites "*Aegoceras crescens*" (Hyatt, 1867 *in* Trueman, 1919), a species whose generic attribution (*Aegoceras* or *Oistoceras*) was ambiguous.

• Figulinum Subchronozone: Vendée data did not suggest any modification. It is limited at its top by the first concomitant appearance of the Amaltheidae [*Amaltheus stokesi* [Sowerby, 1822]] and Harpoceratinae (genus *Matteiceras*).

3.2. *Upper Pliensbachian (Figures 3B, 4)*

3.2.1. *Margaritatus Chronozone*

• Stokesi Subchronozone: Primitives *Amaltheus* [*Amaltheus stokesi, A. bifurcus* [Howarth, 1958], *A. wertheri* [Lange, 1932]] are associated with Harpoceratinae which are grouped in the subgenus, or genus, *Matteiceras* [Wiedenmayer, 1980] whose succession makes it possible to recognize, in Vendée, three standard zonules (Occidentale, Monestieri and Nitescens Zonules) for Southern Europe (Figures 4, 5).

• Subnodosus Subchronozone: It is the interval of existence of the group of *Amaltheus margaritatus* Montfort de, 1808, *A. gloriosus* [Hyatt, 1867] and *A. subnodosus* [Young and Bird, 1828]. The Harpoceratinae, grouped in the genus *Fieldingiceras* [Wiedenmayer, 1980], makes it possible to identify the Depressum Zonule in which appears the first Arieticeratinae of Tethyan affinity, *Arieticeras apertum* [Monestier, 1934] (Figure 4).

– Gibbosus Subchronozone: *Amaltheus gibbosus* [Schlotheim, 1820] is associated with *A. margaritatus*. Two standard zonules defined

in Southern Europe [Page, 2003] and based on taxa of Tethyan origin, are identified (Figures 4, 5):

– Boscense Zonule, with *Fuciniceras boscense* [Reynès, 1868].
– Ragazzonii Zonule, with the brief expansion of the genus *Reynesocoeloceras* [*R.* gr. *acanthoides* [Reynès, 1868]—*ragazzonii* [Hauer, 1856] and *R.* gr. *indunense* [Meneghini, 1881]], two Dactylioceratidae of Tethyan origin, which are a good time mark for the lower subchronozone. These taxa are present, at an identical level, in Portugal [Mouterde et al., 2007] and in Grands-Causses [Meister, 1989].

An important discontinuity marks a gap in the sedimentary record that lasts during the Middle et Upper part of the Gibbosus Subchronozone (Figure 5).

3.2.2. *Spinatum Chronozone*

• Apyrenum Subchronozone: The index *Pleuroceras apyrenum* [Buckman, 1930] is rare, so *P. solare* [Phillips, 1829] appears a better indicator of the subchronozone. The three standard Salebrosum, Transiens and Solare zonules are present (Figure 5). The last one contains *P. spinatum* [Bruguière, 1789] and *Amaltheus margaritatus* which persists up to the top of the zonule. Hildoceratidae of Tethyan origin are missing in Vendée.

• Hawskerense Subchronozone: The *Pleuroceras* are still very predominant, but the subchronozone is well marked by two waves of Arieticeratinae and Harpoceratinae belonging to Tethyan genera or species.

– Elaboratum Zonule, with the index species *Pleuroceras elaboratum* [Simpson, 1884], *P. gigas* Howarth, 1958, *P. buckmani* [Moxon, 1841], *P. yeovilense* Howarth, 1958 and *P. paucicostatum* Howarth, 1958. This is the level in Vendée of the Mediterranean taxa *Emaciaticeras emaciatum* [Catullo, 1853]—*fervidum* Fucini, 1931 (Figure 7B), *E.* cf. *archimedis* Fucini, 1931 (Figure 7F), *Canavaria* cf. *zancleana* [Fucini, 1931], *Leioceratoides* cf. *serotinum* [Bettoni, 1900] (Figure 7D) and *L.* cf. *laevis* [Haas, 1913] (Figure 7E).
– Hawskerense Zonule, with *Pleuroceras hawskerense* [Young and Bird, 1828] and the Tethyan taxa *Tauromeniceras* cf. *elisa* [Fucini, 1931] (Figure 7C), *T.* cf. *nerina* [Fucini, 1931] and *T. mazetieri* [Dubar, 1927] (Figure 7A).

We demonstrate here that the standard Elaboratum and Hawskerense zonules of the Northwestern European standard are respectively equivalent to the Emaciatum and Elisa zonules defined in Portugal, a region in which amaltheids are scarce [Page, 2003, Mouterde et al., 2007] (Figure 5).

4. Paleobiogeographic affinities of the Ammonites

The Pliensbachian Ammonitina under study are clearly related to the North-West European Paleobiogeographic Bioprovince (Figure 2) and the standard biozonation can be applied without amendment at the level of the chronozone and the subchronozone (Figure 5). The presence, in the Lower Pliensbachian, of taxa representative of the endemism prevailing in the Lusitanian Basin, then in the Upper Pliensbachian, of numerous Tethyan taxa, confers clear originality to the ammonite faunas of Southern Vendée.

4.1. *Vendean lower Pliensbachian*

In Vendée, the Lusitanian affinity ammonites are numerous within the lower part of the Ibex Chronozone (Masseanum and Valdani Subchronozones); a time-interval during which the endemism is precisely the most marked in the Lusitanian Basin [Phelps, 1985, Dommergues, 1987] (Figure 5). These taxa are for the first time brought to light outside the Lusitanian Basin:

• *Uptonia atlantica* Fauré and Bohain, 2017 (Figure 6B–G) (Polymorphitidae). It is the "*Uptonia* sp." of Mouterde et al. [1983], identified by these authors in the Masseanum Subchronozone of the Peniche section (Portugal) (Figure 5). In Vendée, this well-established species clearly succeeds to *U. regnardi* and, as in Portugal, extends the monophyletic clade of the genus *Uptonia*, into the Masseanum Subchronozone (Ibex Chronozone).

• *Dayiceras dayiceroides* [Mouterde, 1951] (Figure 6I–L) (Polymorphitidae). This is the first species belonging to the genus *Dayiceras*. This species, which still shows many characters of *Uptonia*, extends into the Valdani Subchronozone the lineage of the Polymorphitidae. In Vendée [Fauré and Bohain, 2017], as

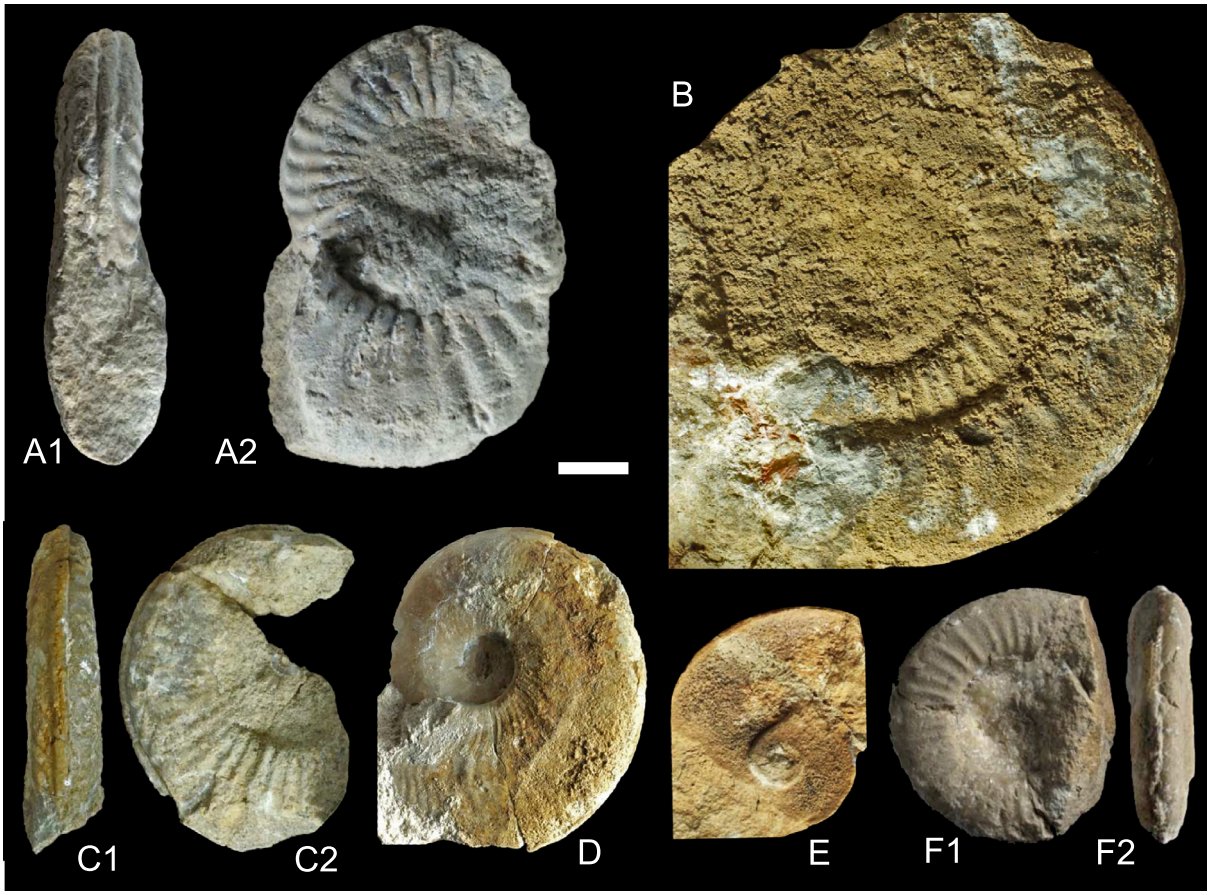

Figure 7. A1–A2, *Tauromeniceras mazetieri* [Dubar, 1927], Spinatum Chronozone, Hawskerense Subchronozone and Hawskerense Zonule, Le Bernard, niv. 29: AT9; B, *Emaciaticeras* gr. *emaciatum* [Catullo, 1853]—*fervidum* Fucini, 1931, Spinatum Chronozone, Hawskerense Subchronozone and Elaboratum Zonule, Talmont-Saint-Hilaire, Coteau des Draillards (=Le Bernard niv. 27): ER2 (×0.75); C1–C2, *Tauromeniceras* cf. *elisa* [Fucini, 1931], Spinatum Chronozone, Hawskerense Subchronozone and Zonule, Sainte-Cécile, La Maison Neuve: FR7; D, *Leioceratoides* cf. *serotinum* [Bettoni, 1900], Spinatum Chronozone, Hawskerense Subchronozone and Elaboratum Zonule, Sainte-Cécile, Coteau de Bellevue: EL8; E, *Leioceratoides* cf. *laevis* [Haas, 1913], Spinatum Chronozone, Hawskerense Subchronozone and Elaboratum Zonule, Talmont-Saint-Hilaire, Bas de la Brunetière (=Le Bernard, niv. 27): EW7; F1–F2, *Emaciaticeras* cf. *archimedis* Fucini, 1931, Spinatum Chronozone, Hawskerense Subchronozone, Elaboratum Zonule, Sainte-Cécile, Coteau de Bellevue: AG7. Scale bar 1 cm (all samples are natural size, except B).

in Portugal [Mouterde, 1951, 1967, Mouterde et al., 1983], it occurs at exactly the same level (Arietiforme Zonule) (Figure 5).

• *Acanthopleuroceras carinatum atlanticum* Dommergues and Mouterde, 1981 (Tropidoceratidae). First *Acanthopleuroceras* at the base of the Valdani Subchronozone. This micromorphic species is considered by Dommergues and Mouterde [1981] as a geographical subspecies of *A. carinatum* [Quenstedt, 1885], which would have undergone possible constraints specific to the Lusitanian Basin.

While in Western Europe (France, Germany, Spain, England), the Polymorphitidae lineage died out at the top of the Jamesoni Chronozone, in Southern Vendée, as in Portugal, it persists until the Masseanum Subchronozone and the lower part

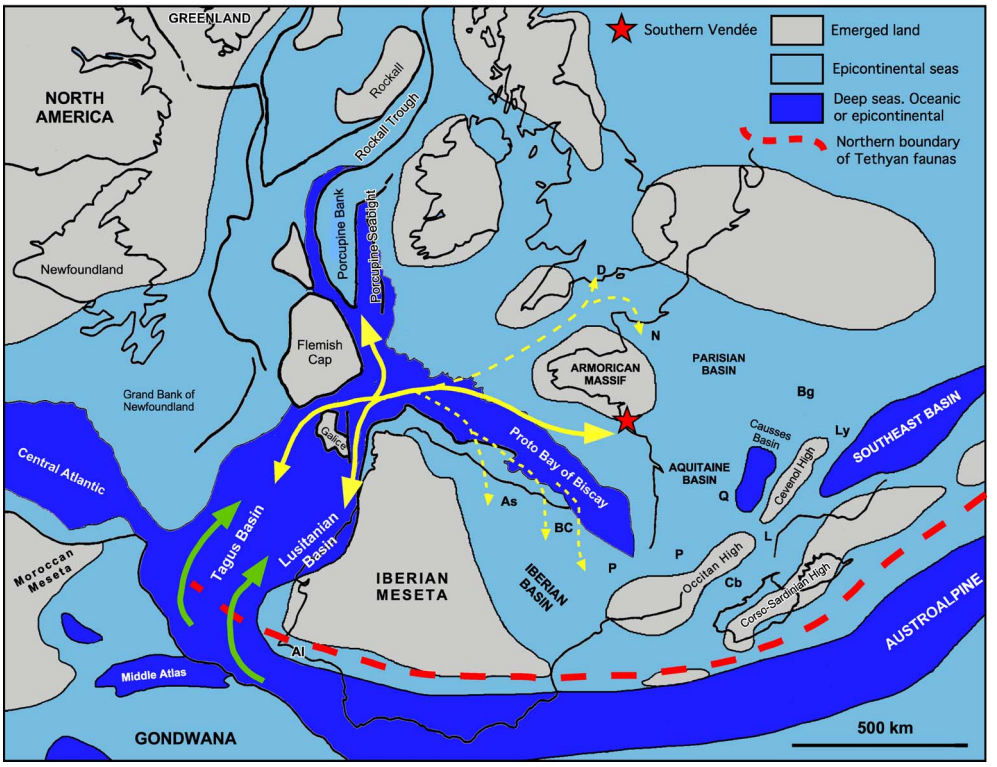

Figure 8. Paleogeographical reconstruction of the Atlantic region and western Tethys for the Jurassic and relative movements of Iberia and Europe. Example of partial closure of peri-Iberian oceanic basins with limited strike-slip movement between Europe and Iberia, according to Olivet [1996, Figure 12] under the assumption of basins inherited from either the Paleozoic or the Triassic. Green arrows: migration route of Upper Pliensbachian Tethyan taxa from the Mediterranean realm to the Atlantic area. Continuous yellow arrows: Lower Pliensbachian. Hypothetical main exchange route of *Uptonia atlantica* and *Dayiceras dayiceroides* between an Atlantic source of evolution, the Lusitanian Basin, and Southern Vendée (red star). Upper Pliensbachien: Same hypothetical migration route of Tethyan taxa inside the Atlantic area. Dotted yellow arrows: Lower and Upper Pliensbachian. Hypothetical way of dispersal of isolated individuals to the northern European platforms. Abbreviations. Al: Algarve; As: Asturias; BC: Basco-Cantabrian Basin; P: Pyrenees; Cb: Corbières; L: Languedoc; Q: Quercy; Ly: Lyon Area; Bg: Burgundy; D: Dorset; N: Normandy.

of the Valdani Subchronozone (Ibex Chronozone) with the two species *Uptonia atlantica* and *Dayiceras dayiceroides*. These two species were previously only known in the same stratigraphic level in the Peniche and São Pedro de Muel sections (Portugal) where they were considered to be particularly representative of the Lusitanian endemism [Mouterde et al., 1983, Phelps, 1985, Dommergues, 1987].

D. dayiceroides is however the only *Dayiceras* represented on the Armorican border whereas, in the Lusitanian Basin, the genus diversifies up to the top of the Actaeon Zonule. For reasons unknown, no ammonite relating to the Lusitanian endemism is recognized in Vendée after the Arietiforme Zonule while the endemic continues, very marked, in Portugal, until the top of the Actaeon Zonule (Figure 5).

4.2. *Vendean upper Pliensbachian*

Most of the Upper Pliensbachian ammonite assemblages of Southern Vendée are representative of the North-West European paleobiogeographic Province, but the presence of numerous Hildoceratidae

(Harpoceratinae, Arieticeratinae) and Dactylioceratidae of Tethyan origin, gives to the Vendean ammonite associations a very "southern" character. We find them, in greater or lesser abundance, at several stratigraphic levels (Figure 5):

During the Stokesi and the Subnodosus subchronozones, Harpoceratinae are represented by the genera, *Matteiceras* and *Fieldingiceras*. Although these taxa have a Tethyan origin, they are totally endemic to the North-West European Province. They, nevertheless, predominate in the southern part of the European platform, near the North Tethyan margin [Dommergues and Mouterde, 1980, Dommergues, 1987, Meister and Stampfli, 2000].

Within their maximum distribution area, we will first mention the Lusitanian Basin where they clearly outclass the Amaltheidae [Mouterde et al., 2007]. They are also very frequent in the meridional part of the European craton: Iberian Ranges [Comas-Rengifo, 1985], Basque-Cantabrian Basin, Asturias [Rodriguez-Luengo et al., 2012], Pyrenees [Fauré, 2002, Fauré and Téodori, 2019], Grands-Causses [Meister, 1989], Quercy [Fauré and Brunel, 2019], Corbières [Fauré, 2006], Languedoc and Cevenol Margin [Mattei et al., 1971, Cassel, 1997] and Provence [Lanquine, 1935]. They also reach the Lyonnais [Rulleau, 2007], Burgundy [Dommergues and Mouterde, 1980], Lorraine [Maubeuge, 1971], as well as England [Howarth, 1992] and Southern Germany [Fischer, 1975] where these are therefore few specimens, or even isolated individuals.

Their abundance in Vendée, away from the north Tethyan margin, must be emphasized.

During the Gibbosus and Hawskerense subchronozones, the genera *Leioceratoides* (Harpoceratinae), *Arieticeras*, *Emaciaticeras*, *Tauromeniceras* (Arieticeratinae), *Reynesocoeloceras* (Dactylioceratidae), and the species they represent, are this time authentically Tethyan taxa, recognized at an identical stratigraphic level in the Mediterranean Province such as the Maghrebian margin of Africa (Morocco, Algeria, Tunisia), the Betic Ranges, or the Apennines.

Their frequency in Southern Vendée, far from the north Tethyan margin, is remarkable. Except for the Lusitanian Basin which is occasionally, at the end of the Spinatum Chronozone, integrated into the Mediterranean Province [Mouterde et al., 2007], these ammonites are still few in the southern part of the North-West European platforms: Basque-Cantabrian Basin, Asturias [Comas-Rengifo et al., 2016], Iberian Ranges [Comas-Rengifo, 1985, Braga et al., 1982, Comas-Rengifo et al., 1999], Southern Pyrenees [Fauré, 2002], Corbières [Fauré, 2006] and Grands-Causses [Meister, 1989]. They are notably found in regions further north as Dorset [Howarth, 1992] and Normandy [Dubar, 1927].

This colonization movement of the South Armorican margin by Tethyan faunas goes on during the Paltus Subchronozone (Lower Toarcian). At that time, many Tethyan affinity ammonites (*Protogrammoceras, Eodactylites, Neolioceratoides,*...) will constitute, as in Portugal, most of the ammonite associations [Bécaud, 2005].

5. Discussion

5.1. *The expression of the lower Pliensbachian Lusitanian endemism*

It should be remembered that, during the Early Pliensbachian, the Lusitanian Basin was exclusively populated with genera and species of North-West European type. The paleogeographical configuration of this region has, however, on several occasions, been favourable to the development of endemic taxa (species and genera). These phases of endemism begin in Portugal as early as the Upper Sinemurian (Obtusum Chronozone), a time interval in which it only affects the Asteroceratinae Family, with the genera *Ptycharietites*, *Epophioceroides*, and *Pompeckioceras*, whose representatives are only known in Portugal [Dommergues et al., 2010].

• During the Taylori Subchronozone (Jamesoni Chronozone), targeted endemism phenomena affects the Phricodoceratidae with the presence of the endemic genus *Pseudophricodoceras* [Mouterde et al., 1983]. This genus has however been reported in the "Sierra de la Demanda" (Iberian Cordillera) by Comas-Rengifo et al. [1988] and in North-West Germany by Hoffmann [1982].

• With the Brevispina Subchronozone, the apparent endemism phenomena described by Mouterde et al. [1983] must be put into perspective. Two micromorphic Polymorphitinae, *Platypleuroceras muellensis* [Mouterde, 1951] and *P. acanthobronni* [Mouterde et al., 1983], said to be endemic to the Lusitanian Bassin, are respectively the microconch of two ammonites, *Playpleuroceras* gr. *brevispina*

[J. de C. Sowerby, 1846] and *P. submuticum* group [Oppel, 1853], whose paleogeographic range is much wider [Fauré and Téodori, 2019].

• With the Valdani Subchronozone (Ibex Chronozone), the endemism is the most pronounced (Figure 3). Indeed, while on the North-West European platform, the Polymorphitidae (genus *Uptonia*) are completely replaced at the top of the Jamesoni Subchronozone by the Tropidoceratidae (genera *Tropidoceras* and *Acanthopleuroceras*), in the Lusitanian Basin, the evolutionary sequence of the Polymorphitidae continues within the Ibex Chronozone with several taxa, such as *Uptonia atlantica* Fauré and Bohain, 2017 within the Masseanum Subchronozone and the genus *Dayiceras* within the Valdani Subchronozone [Mouterde et al., 1983, Dommergues, 1987].

In the lower part of the Valdani Subchronozone [Renzi Lusitanian subzone of Mouterde et al., 1983], there have been six successive species of *Dayiceras* as a result of processes of gradual evolution [Mouterde et al., 1983, Dommergues, 1987] (Figure 5): *D. dayiceroides* [Mouterde, 1951], *Dayiceras renzi* [Meister, 1913] [= *D. quiaosensis* Mouterde, 1967], *D. polymorphoides* Spath, 1920, *D. splendens* Mouterde, 1967, and *D. amaltheiforme* Mouterde, 1967 with *D. nanum* Mouterde, 1967.

The *Dayiceras* lineage disappears at a level equivalent to the upper part of the Actaeon Zonule of the North-West European zonal standard (Figure 5). Then, the Eoderoceratidae *Metaderoceras beirense* Mouterde, 1967, remains the only representative of Lusitanian endemism which definitively disappears at the top of the Actaeon Zonule.

• In the Capricornus Subchronozone, the case of *Prodactylioceras rectiradiatum* [Wingrave, 1916] should be mentioned (Figure 5). This taxon, known from the Lusitanian Basin and Dorset, is found at the same age in Vendée. Its "Atlantic" affinities had been emphasized by Dommergues et al. [1984].

5.2. *Worldwide distribution of the genus Dayiceras*

The *Dayiceras* genus is the emblematic ammonite of the Lusitanian endemism. It has nevertheless been reported, before us, by many authors outside Portugal:

5.2.1. *In the North-West European Province*

In the Dorset Coast (Great Britain), where the genus *Dayiceras* has been defined by Spath [1920], *Dayiceras polymorphoides* Spath, 1920 is precisely positioned stratigraphically by Phelps [1985] in the "Centaurus Zonule". One can draw a parallel between this level and the Actaeon Zonule of the standard (Valdani Subchronozone, Ibex Chronozone). We also point out to the unique specimen of *Dayiceras* [*D.* cf. *langi* Spath, 1920] reported by Hoffmann [1982] in the Masseanum Subchronozone of North-West Germany (Hannover) (Figure 8).

The age of these specimens is identical to that of the Portuguese *Dayiceras*, show the dispersal of isolated individuals at a distance from the Lusitanian Basin.

5.2.2. *In the Tethyan Realm*

Dayiceras has been so often reported in the Tethyan Realm that many authors have believed the ubiquitous nature of this genus [Taylor et al., 1984]. We propose here a critical review of all *Dayiceras*'s occurrences outside of the North-West European Province.

Occurrences in the Mediterranean Province.

• *In the "Tunisian Dorsale"*, by Rakús [1972], who describes the new species "*Dayiceras*" *balzeri* Rakús, 1972 in the Demonense Chronozone of Jebel Staa. But this generic attribution is questioned by Wiedenmayer [1977], who attributes this species, a homeomorph of *Dayiceras*, to an Eoderoceratidae. It will then be recombined by Rakús and Guex [2002] in the new genus *Balzerites* and placed, according to the suture lines, within the Ectocentritinae Subfamily. The taxon will then be placed in the Dubariceratinae Subfamily by Venturi et al. [2007].

• *In the Italian Calcareous Alps*, by Wiedenmayer [1977, pl. 15, figures 3–4], under the taxon "*Dayiceras* sp. nov. aff. *polymorphoides*", and placed in the Polymorphitinae. The species is reassigned to "*Dayiceras*" *bettonii* [Parona, 1897, pl. X, figure 1a–b] by Wiedenmayer [1980, p. 177], and placed in the Eoderoceratidae.

• *In the Apennines (Italy)*, by Faraoni et al. [1996, pl. 7, figure 3; pl. 10, figures 7, 8], under the names "*Dayiceras* sp." and "*Dayiceras* sp. aff. *D. dayiceroides*", from the lower part of the "Gemmellaroi Zone" (Tethyan equivalent of the Valdani Subchronozone).

A "*Dayiceras* sp." will later be figured by Venturi and Ferri [2001]. All these samples are reassigned to *Balzerites balzeri* [Rakús, 1972] by Venturi et al. [2010] and placed by these authors in the Dubariceratinae Subfamily. The genus *Balzerites* is now placed into the Ectocentritinae Subfamily by Dommergues and Meister [2017, p. 204].

East Pacific Domain (South America). In Chile and Argentina, Hillebrandt [1987, pl. 2, Figure 11–12] describes "tight-costulated specimens similar to *Dayiceras*, but without the crenulated keel" in the Meridianus Zone, associated with a closely related species, "*Polymorphites* (?) sp." [Hillebrandt, 1987, pl. 2, figures 6–10]. All these species will later be attributed to the taxon *Eoamaltheus multicostatus* [Hillebrandt, 2006, p. 143] whose age, specified to the Multicostatus Subzone, may be correlated with the lower part of the North-West European Davoei Chronozone.

The same is true for the "*Dayiceras*" described by Leanza and Blasco [1990], *Dayiceras pseudophylliticum* and *D. pleuriforme*, which Hillebrandt [2006, p. 174] compares, for the first one, to *Andidiscus multiforme* Hillebrandt, 2006, and for the second one, to *Andidiscus behrendseni* [Jaworski, 1926]. These two taxa originate from the Behrendseni Zone, which can be correlated with the upper part of the North-West European Davoei Chronozone (Figulinum Subchronozone).

All these genera and species are endemic to the Andean East Pacific Realm.

East Pacific Domain (North America). The first mention of "*Uptonia* cf. *U. dayiceroides*" is given in the Princess Charlotte Island Pliensbachian by Frebold [1970, p. 438, pl. 1, figure 9a–b] but the author specifies that "the absence of crenulation differentiates it from specimens from Mouterde, 1951". Smith [1983] gave the first detailed and well-argued description of numerous specimens of "*Dayiceras dayiceroides*" from the Outer Rocky Mountains (Nevada, Oregon, British Columbia, Alberta, Southern Alaska) and Princess Charlotte Island. Smith [1983], Taylor et al. [1984], then Thompson and Smith [1992], deduced that the genus "*Dayiceras*" was very common in the Tethyan Domain and would be a good marker of Tethyan fauna. According to Smith et al. [1988], all these specimens came from the base of the Freboldi Zone which can be correlated with the top of the Ibex Chronozone of the lower part of the Davoei Chronozone. "*Dayiceras* sp. [Thompson and Smith, 1992, pl. 4, Figures 3–5] from British Columbia is later clearly related to *Eoamaltheus multicostatus* by Hillebrandt [2006, p. 154]. Like the Andean Cordilleras "*Dayiceras*", the north American "*D. dayiceroides*" are more recent than the Lusitanian *Dayiceras*.

It is very likely that all of the East Pacific species reported as genus *Dayiceras* by the authors correspond in fact to primitive Dubariceratidae or Fanninoceratidae [*sensu* Venturi et al., 2007] and that they are endemic to the East Pacific Domain.

5.3. *Paleobiogeographic implications*

The genus *Dayiceras* is absent in the Tethyan Realm, Mediterranean Province, and East Pacific Domain (Chile, Argentina, Canada, United States), in which all of its mentions have since been recombined within the Ectocentritidae, Dubariceratidae or Fanninoceratidae families. It thus appears that the genus *Dayiceras* depends only on the North-West European Province and that, with the rare exceptions corresponding to the dissemination of isolated individuals in Dorset and North-Western Germany, its paleogeographic distribution is restricted to the Lusitanian Basin which is its evolutionary source.

The discovery, in Vendée, of a population of *Dayiceras dayiceroides* makes it possible to widen the paleogeographic distribution of the species, because the Vendean populations of this late Polymorphitidae are abundant and their lineage appears well established there. In Vendée, as in the Lusitanian Basin, the species extends the Polymorphitinae clade in the Ibex Chronozone and succeeds to *Uptonia atlantica*, a species which was also, to date, only known in Portugal. It cannot be a dispersion of isolated individuals, by an Atlantic route, at a distance from a Lusitanian pool, but rather a permanent installation, although of short duration, which makes it possible to significantly extend the paleogeographical distribution of Masseanum and Early Valdani Subchronozones Polymorphitinae. To these two emblematic species of Lusitanian endemism, we can add *Acanthopleuroceras carinatum atlanticum*.

These ammonites suggest integrating the Lusitanian Basin and Southern Vendée, which paleogeographic reconstructions place close to each other

(Figures 2, 8), in the same Atlantic paleobiogeographic area and demonstrate, despite their complexity, that there were connections between the predrift basins of the "Iberia–Armorica–Newfoundland" conjugate margin.

As in Vendée, the Lusitanian faunas are clearly dominated by North-Western European influences [Dommergues, 1987]. The North-West European polarity of Lusitanian faunas remains unexplained because all the paleogeographic reconstructions of the proto-Atlantic region currently available [Thierry et al., 2000] suggest a large structural opening of the western Iberian Basins towards the Mediterranean Basin of the western Tethys, and the absence of an obvious structural barrier (Figures 2, 8). The demonstration of the Tethyan (Mediterranean) affinities of the Algarve Basin faunas, the southernmost basins of the western Iberian margin (Figures 2, 8), could geographically precise the transition, but does not provide additional explanation for the structural and/or ecological nature of the barrier that separates the two faunal realms [Dommergues et al., 2011]. This barrier, whatever its nature, may have been particularly sealed during the Lower Pliensbachian, a time interval during which the provincialism of the ammonite faunas was the most pronounced [Dommergues, 1987]. It suggests a particular tectonic context which could also be the cause of the large proportion of endemic taxa in the Lusitanian Basin. Its attenuation in the Upper Pliensbachian allowed Tethyan taxa, which are numerous in the western Mediterranean Basins (Rif, Middle Atlas, High Atlas) to migrate north toward the "Iberia–Armorica–Newfoundland" conjugate margin. This is especially true for the Late Pliensbachian (Hawskerense Subchronozone), when several waves of Harpoceratinae (*Argutarpites*, *Leioceratoides*) and Arieticeratinae (*Arieticeras*, *Emaciaticeras*, *Canavaria*, *Tauromeniceras*), which are very common in the western Tethyan realm, reached northward the western Iberian Basins. Note that this interval also allowed various typically West European ammonites (Amaltheidae) such as *Pleuroceras* gr. *solare*, to reach the western Tethyan Basins and, beyond, part of the Mediterranean Province. The presence of Tethysian ammonites in the Upper Pliensbachian of Southern Vendée is related to this northward migration movement of Mediterranean ammonites. Despite the complexity of the "Iberia–Armorica–Newfoundland", no obstacle could limit the dispersion of the ammonites in an Atlantic marine area (Figure 8).

The reality of an Atlantic diffusion area is also attested in the Lower Pliensbachian, with an ammonite, *Prodactylioceras rectiradiatum* [Wingrave, 1916], common to the Lusitanian Basin, Southern Vendée, and Dorset [Dommergues et al., 1984]. *Argutarpites argutum* [Buckman, 1930], although not listed in Portugal, seemed to show the same Atlantic distribution area.

This marine area, where we demonstrate the presence, in the Lower Pliensbachian (Lower Ibex Chronozone) and in the Late Pliensbachian (Hawskerense Subchronozone), is from the Early Mesozoic, initiated by an important phase of rifting. It is established on a mosaic of basins, grabens or hemigrabens, linked to the "Iberia–Armorica–Newfoundland" passive conjugate margin, which also includes the Rift of Biscay (Figures 2, 8). Although located between stable western Europe and the Iberian micro-plate, the Rift of Biscay is at the origin of the proto-Gulf of Biscay, a narrow basin which is largely opened on this Atlantic domain (Figure 8). The crustal thinning that affects its margins is attested from the Hettangian in Southern Vendée [Montenat et al., 2003]. It makes the proto-Bay of Biscay and its margins a favored route for the diffusion of Atlantic fauna towards the western borders of the West European Domain (Figure 8).

6. Conclusions. Towards the individualization of an area of Atlantic paleobiogeographic influence

The Pliensbachian Ammonitina under study are clearly related to the North-West European paleobiogeographic Bioprovince (Figure 2). The presence, in the Lower Pliensbachian, of taxa representative of the endemism that trends in the Lusitanian Basin, then in the Upper Pliensbachian, of numerous Tethyan taxa, confers clear originality to the ammonite faunas of Southern Vendée.

The most outstanding result of this study is the demonstration of the persistence, in the Vendean Ibex Chronozone, of several Polymorphitidae whose distribution seemed until now restricted to the Lusitanian region. As in Portugal, these taxa extend the linear evolutionary sequence of Polymorphitidae into the Ibex Chronozone, while it died out

everywhere else in the summital Jamesoni Chronozone. It is possible in Vendée, as in Portugal, to study the complete evolutionary sequence between the genera *Uptonia* and *Dayiceras* (Figure 5):

• *Uptonia atlantica*, in the Masseanum Subchronozone, gradually succeeds to *U.* gr. *jamesoni* and *U. regnardi*.

• *Dayiceras dayiceroides*, first species of the genus, extend the Polymorphitidae lineage in the Valdani Subchronozone.

These two taxa, whose paleogeographic distribution seemed restricted to the Lusitanian Basin, till date, are representative of the endemism that developed during the same time (Masseanum and Valdani Subchronozones) in the Lusitanian Basin. Their discovery in Vendée allows to put into perspective the importance of the Lusitanian endemism at the base of the Ibex Chronozone because the Vendean populations of these late Polymorphitidae are not isolated individuals, but an abundant population that appears to be well settled. This makes it possible to integrate the Lusitanian Basin and Vendée, which paleogeographic reconstructions place close to each other (Figures 2, 8), in the same Atlantic paleobiogeographic area.

It is probably through a diffusion within this Atlantic paleogeographic area that the "southern" affinity taxa such as the genera *Matteiceras* and *Fieldingiceras*, but also Tethyan genera (genera *Reynesocoeloceras, Arieticeras, Emaciaticeras, Tauromeniceras, Leioceratoides*...), which are very numerous in the Upper Pliensbachian of Portugal, would reach Vendée in successive waves and would be able to reach, by this way, the western borders of the North-West European Bioprovince such as, for example, the Basque-Cantabrian region, Asturias, Iberian Ranges, Pyrenees and, to a lesser extent, Dorset and Normandy, as many regions where the Upper Pliensbachian also shows important supplies of Tethyan ammonites.

Without however denying the possibility of Tethyan influences coming from the faunal transition zones, which are well documented on the distant Alpine margins of the European craton [Meister and Stampfli, 2000], this Atlantic communication route seems to us to be privileged, at least until the Lower Toarcian.

Conflicts of interest

Authors have no conflicts of interest to declare.

Acknowledgements

We thank Ms. Aloé Hok-Schlagenhauf for checking the English translation. We sincerely thank the two anonymous reviewers and the editor Thomas Saucède for their valuable comments and their constructive suggestions on an earlier version of the article, which allowed a very significant improvement of the manuscript.

References

Alméras, Y., Bécaud, M., and Cougnon, M. (2010a). *Brachiopodes liasiques de la Bordure sud du Massif armoricain (Vendée, Deux-Sèvres; France): Paléontologie et chronostratigraphie. Bulletin de la Société des Sciences naturelles de l'Ouest de la France*. 1er supplément hors-série.

Alméras, Y., Cougnon, M., and Bécaud, M. (2010b). Les brachiopodes liasiques de la Bordure Sud du Massif Armoricain : succession des peuplements et environnements ; chronostratigraphie. *Rev. de Paléobiologie*, 29(2), 319–339.

Angrand, P., Mouthereau, F., Masini, E., and Asti, R. (2020). A reconstruction of Iberia accounting for Western Tethys-North Atlantic kinematics since the late Permian-Triassic. *Solid Earth*, 11, 1313–1332.

Bécaud, M. (2005). Ammonites peu connues du Toarcien inférieur du sud-ouest de la Vendée. *Le Naturaliste Vendéen*, 5, 45–48.

Bettoni, A. (1900). *Fossili Domeriani della Provincia di Brescia*, volume 28 of *Mémoires de la Société paléontologique suisse*.

Bohain, P. and Fauré, Ph. (2022). *Les ammonites du Pliensbachien supérieur de la Vendée méridionale (France). Étude taxonomique. Implications chronostratigraphiques et paléogéographiques*. Strata, série 2, coed Strata and Dédale Editions, Lyon. (in press).

Braga, J. C., Comas-Rengifo, M. J., Goy, A., and Rivas, P. (1982). Comparaciones faunisticas y correlaciones en el Pliensbachiense de la Zona Subbética y Cordillera Ibérica. *Bol. R. Soc. Esp. Hist. Nat.*, 80, 221–244.

Bruguière, J. G. (1789). *Histoire naturelle des vers*. Partie de l'encyclopédie méthodique, Paris I-XVIII.

Buckman, S. S. (1909–1930). *Yorkshire Type Ammonites*, volume I–ll. Welseyand Son ed., Londres. p. i–xvi et 1–121, pl. 1–130; *Type Ammonites*, volume III–VII. Weldon and Welsey ed., Londres.

Butel, P. (1951). Révision de la feuille des Sables-d'Olonne au 1/80000. Le Lias et le Jurassique du littoral. *Bulletin des Services de la Carte géologique de la France*, XLIX(232), 97–107.

Butel, P. (1953). Les formations d'âge secondaire dans le Sud de la Vendée, entre le massif ancien et l'océan (feuille des Sables d'Olonne au 80 000e). *Bulletin des Services de la Carte géologique de la France*, LI(239), 301–333.

Cassel, Y. (1997). *Évolution géodynamique de la marge cévenole entre Saint-Ambroix et Anduze (Gard septentrional) de l'Hettangien au Bajocien inférieur*, volume 144 of *Documents des laboratoires de géologie de Lyon*.

Catullo, T. A. (1853). *Intorno da una nuova classificazione delle Calcarie Rosse Ammonitiche della Alpi venete*. Memorie dell'I.R. Istitito Veneto du Scienze, Lettere ed Arti, volume 5.

Comas-Rengifo, M.-J. (1985). *El Pliensbachiense de la Cordillera Iberica*. Tesis doctoral, Universitad Complutense de Madrid.

Comas-Rengifo, M.-J., Duarte, L. V., Felix, F. F., Goy, A., Paredes, R., and Silva, R. L. (2016). Amaltheidae e Hildoceratidae (ammonitina) del Pliensbachiense Superior (Cronozona Spinatum) en las cuencas septentrionales de la Península Ibérica. In Meléndez, G., Núñez, A., and Tomás, M., editors, *Actas de las XXXII Jornadas de la Sociedad Española de Paleontología. Cuadernos del Museo Geominero*, volume 20, pages 47–52. Instituto Geológico y Minero de España, Madrid. ISBN 978-84-9138-016-0.

Comas-Rengifo, M.-J., Gomez, J. J., Goy, A., Herrero, C., Perilli, N., and Rodrigo, A. (1999). El Jurasico Inferior en la seccion de Almonacid de la Cuba (sector central de la Cordillera Ibérica, Zaragoza, España. *Cuadernos de Geologia Ibérica*, 25, 25–57.

Comas-Rengifo, M.-J., Goy, A., and Yébenes, A. (1988). El Lias en el sector suroccidental de la Sierra de la Demanda (Castrovido, Burgos). In *II Colloquio de Estratigrafia y Paleogeografia de Jurassica de España. Gruppo español del Mesozoico éd. Sciencias de la Terra. Geologia*, volume 11, pages 120–138. Instituto de Estudios Riojanos, La Rioja.

Dommergues, J.-L. (1979). *Le Carixien bourguignon. Biostratigraphie, paléogéographie, approche paléontologique et sédimentologique*. Thèse de doctorat, Université de Dijon.

Dommergues, J.-L. (1987). *L'évolution chez les Ammonitina du Lias moyen (Carixien, Domérien basal) en Europe occidentale*, volume 98 of *Documents des Laboratoires de Géologie de Lyon*.

Dommergues, J.-L., Fauré, Ph., and Mouterde, R. (1984). Le genre *Prodactylioceras* (Ammonitina, Pliensbachien inférieur); biostratigraphie, paléogéographie et modalités évolutives. Description d'une espèce nouvelle: *Prodactylioceras aurigeriense* nov. sp. *Géobios*, 17(1), 77–83.

Dommergues, J.-L. and Meister, C. (2017). Ammonites du Jurassique inférieur (Hettangien, Sinémurien, Pliensbachien) d'Afrique du Nord (Algérie, Maroc et Tunisie). Atlas d'identification des espèces. *Rev. de Paléobiologie*, 36(2), 189–367.

Dommergues, J.-L., Meister, C., and Mouterde, R. (1997). Pliensbachien. In *Biostratigraphie du Jurassique ouest-européen et méditerranéen: zonations parallèles et distribution des invertébrés et microfossiles*, volume 17 of *Bulletin des Centres de Recherche Elf, Exploration-Production*, pages 15–23. Groupe français d'étude du Jurassique, Pau. Cariou, E. and Hantzpergues, P., (coord.).

Dommergues, J.-L., Meister, C., and Rocha, R. (2010). The Sinemurian ammonites of the Lusitanian Basin (Portugal): an example of complex endemic evolution. *Palaeodiversity*, 3, 59–87.

Dommergues, J.-L., Meister, C., and Rocha, R. (2011). The Pliensbachian ammonites of the Algarve Basin (Portugal) and their paleobiogeographical significance for the "Iberia-Newfoundland" conjugate margin. *Swiss J. Geosci.*, 104, 81–96.

Dommergues, J.-L. and Mouterde, R. (1980). Modalités d'installation et d'évolution des Harpoceratinés (Ammonitina) au Domérien inférieur dans le sud-ouest de l'Europe (France, Portugal). *Géobios*, 13(3), 289–325.

Dommergues, J.-L. and Mouterde, R. (1981). Les Acanthopleurocératinés portugais et leurs relations avec les formes subboréales. *Ciênc. Terra*, 6, 77–100.

Dubar, G. (1927). Sur une nouvelle ammonite charmouthienne de Normandie. *Bull. Soc. Linn. Normandie*, 7(IX), 30–34.

Dubar, G. and Gabilly, J. (1964). Le Lias moyen

de Saint-Vincent-Sterlange et de Saint-Cyr-en-Talmondais (Vendée). *Comptes-rendus de l'Académie des Sciences de Paris*, 259, 2481–2483.

Faraoni, P., Marini, A., Pallini, G., and Venturi, F. (1996). New Carixian ammonite assemblages of Central Apennines (Italy), and their impact on Mediterranean Jurassic biostratigraphy. *Paleopelagos*, 6, 75–122.

Fauré, Ph. (2002). *Le Lias des Pyrénées*. Thèse de doctorat, l'Université Paul Sabatier, Toulouse. *Strata*, série II, 39.

Fauré, Ph. (2006). Le Pliensbachien supérieur des Corbières (Aude, France). Biostratigraphie, évolution sédimentaire et paléogéographie. *Bulletin de la société d'Études scientifiques de l'Aude*, CVI, 29–44.

Fauré, Ph. and Bohain, P. (2017). *Les ammonites du Pliensbachien inférieur de la Vendée méridionale (France). Étude taxonomique. Implications paléogéographiques et paléobiogéographie*, volume 54 of *Strata, série 2*. Coed Strata and Dedale Editions, Lyon.

Fauré, Ph. and Brunel, F. (2019). Le Pliensbachien supérieur du Quercy septentrional (environs de Gramat, Lot, Corrèze). Stratigraphie et paléontologie des ammonites. *Carnets natures*, 6, 15–34.

Fauré, Ph. and Téodori, D. (2019). Les Ammonites du Pliensbachien des Pyrénées ariégeoises (Zone nord-pyrénéenne, France) : taxonomie, stratigraphie et implications paléogéographiques. *Rev. de Paléobiologie*, 38(2), 269–361.

Fischer, R. (1975). Die deutschen Mittellias-Falciferen (Ammonoidea, *Protogrammoceras*, *Fuciniceras*, *Arieticeras*). *Palaeontographica A*, 15, 47–101.

Frebold, H. (1970). Pliensbachian Ammonoids from British Columbia and Southern Yukon. *Can. J. Earth Sci.*, 7, 435–456.

Fucini, A. (1931). Fossili domeriani dei dintorni di Taormina. *Palaeontographia Italica*, 31(1929–30), 93–149.

Gabilly, J. (1964). Le Jurassique inférieur et moyen sur le littoral vendéen. *Travaux de l'Institut de géologie et d'Anthropologie préhistorique de la Faculté des Sciences de Poitiers*, 5, 65–107.

Haas, O. (1913). Die Fauna des mittleren Lias von Ballino in Südtirol. *Beiträge zur Paläontologie und Geologie Österreich-Ungarns und des Orients*, 26, 1–161.

Hauer, F. (1856). Uber die Cephalopoden aus dem Lias der nordostlichen Alpen. *Denkschrift der Mathematisch-Naturwissenschaften Classe der Kaiserlichen Akademie der Wissenschaften*, 11, 1–86.

Hillebrandt, A. von. (1987). Liassic ammonites zones of South America and correlations with other Provinces. With description of new genera and species of Ammonites. In *Biostratigrafia de los Sistemas Regionales del Jurasico y Cretacico de America del Sur*, pages 111–197. Comité Sudamericano del Jurasico y Cretácico, Buenos Aires.

Hillebrandt, A. von. (2006). Ammoniten aus dem Pliensbachium (Carixium und Domerium) von Südamerika. *Rev. de Paléobiologie*, 25(1), 1–403.

Hoffmann, K. (1982). *Die Stratigraphie, Paläeogeographie und Ammonitenführung des Unter-Pliensbachium (Carixium, Lias gamma) in Nordwest-Deutschland*, volume 55 of *Geologisches Jahrbuch A*. Hannover.

Howarth, M. K. (1957–1958). *A Monograph of the Ammonites of the Liassic Family Amaltheidae in Britain*. Palaeontographical Society, London, UK. (Part 1) 111, 1–26; (Part 2) 112, 27–53.

Howarth, M. K. (1992). *The ammonite family Hildoceratidae in the Lower Jurassic of Britain*. Monograph of the Palaeontographical Society. Palaeontographical Society, London, UK. part 1: 1–106; part 2, 107–200.

Hyatt, A. (1867). The fossils cephalopods of the Museum of Comparative Zoology. *Bull. Mus. Comp. Zool.*, 3, 71–102.

Jaworski, E. (1926). La Fauna del Lias y Dogger de la Cordillera argentina en la parte meridional de la Provincia de Mendoza. In *Actas de la Academia Nacional de Ciencias en Cordoba*, volume IX, page 317.

Lange, W. (1932). Über ein *Hammatoceras* aund einen Amaltheenvorläufer (*Proamaltheus wertheri* gen. nov. sp. nov.) aus dem Lias gamma und delta von Werther in Westfalen. *Zeitschrift der Deutschen Geologischen Gesellschaft*, 84(4), 235–241.

Lanquine, A. (1935). *Le Lias et le Jurassique des Chaines Provençales. Recherches stratigraphiques et paléontologiques. 1er partie. Le Lias et le Jurassique inférieur*, volume 32, no. 173 of *Bulletin des Services de la Carte géologique de France*.

Leanza, H. A. and Blasco, G. (1990). Estratigrafia y ammonitas pliensbachianos del area des Arroyo

Ñireco, Neuquen, Argentina, con la descripcion de *Austromorphites* gen. nov. *Asociacion geologica argentina, revista*, XLV(1–2), 159–174.

Mattei, J., Elmi, S., Mouterde, R., Tintant, H., and Gabilly, J. (1971). Le domérien dans quelques régions du centre et du sud de la france. In *Colloque du Jurassique, Luxembourg, 1967*, volume 75 of *Mémoires du BRGM*, pages 567–580.

Maubeuge, P. L. (1971). Présence d'éléments méditerranéens dans la faune d'ammonites du Jurassique inférieur de la partie nord-est du bassin de Paris (Luxembourg belge et Lorraine septentrionale). *Académie royale de Belgique, Bulletin de la Classe des sciences*, 57, 422–426.

Meister, C. (1989). *Les ammonites du Domérien des Causses (France). Analyses paléontologiques et stratigraphiques. Cahiers de Paléontologie*. Éditions du CNRS.

Meister, C. and Stampfli, G. (2000). Les ammonites du Lias moyen (Pliensbachien) de la Néotéthys et de ses confins; compositions fauniques, affinités paléogéographiques et biodiversité. *Rev. de Paléobiologie*, 19(1), 227–292.

Meister, E. (1913). Zur kenntniss der Ammonitenfauna des portugiesischen Lias. *Zeitschrift der Deutschen Geologischen Gesellschaft*, 65, 518–586.

Meneghini, G. (1867–1881). In Stoppani, A., editor, *Monographie des fossiles appartenant au calcaire rouge ammonitique de Lombardie et de l'Apennin de l'Italie centrale*, Paléontologie Lombarde, page 242.

Monestier, J. (1934). *Ammonites du Domérien de la région au sud-est de l'Aveyron et de quelques régions de la Lozère, à l'exclusion des Amalthéidés*, volume 23 of *Mémoires de la Société géologique de France, NS*.

Montenat, C., Bessonnat, G., and Roy, C. (2003). Structuration cassante de la marge vendéenne au Lias inférieur. Exemple de l'estuaire du Payré, au sud de Talmont-Saint-Hilaire. *Le Naturaliste Vendéen*, 3, 29–37.

Montfort de, D. (1808). *Conchyliologie systématique et classification méthodique des coquilles*. Paris.

Mouterde, R. (1951). Ammonites du Lias moyen portugais. *Boletim da Societad Geologica Portugal*, 9, 175–190.

Mouterde, R. (1967). Le Lias du Portugal. Vue d'ensemble et division en Zones. *Comunicaçoes dos Serviços Geologicos de Portugal*, 52, 185–208.

Mouterde, R., Dommergues, J.-L., Meister, C., and Rocha, R. B. (2007). Atlas des fossiles caractéristiques du Lias portugais. IIIa Domérien (Ammonites). *Ciênc. Terra*, 16, 67–111.

Mouterde, R., Dommergues, J.-L., and Rocha, R. B. (1983). Atlas des fossiles caractéristiques du Lias portugais. II- Carixien. *Ciênc. Terra*, 7, 187–254.

Moxon, C. (1841). In *Illustration of the Characteristic Fossils of British Strata*, page 46. H. Baillère, J. Tennant and E. Ramsden, London.

Nirrengarten, M., Manatschal, G., Tugend, J., Kusznir, N., and Sauter, D. (2018). Kinematic evolution of the southern North Atlantic: Implications for the formation of hyperextended rift systems. *Tectonics*, 37, 89–118.

Olivet, J.-L. (1996). La cinématique de la plaque ibérique. *Bulletin des Centres de Recherche exploration-production d'ELF Aquitaine*, 20, 131–195.

Oppel, A. (1853). *Der Mittlere Lias Schwabens*, volume 10 of *Württemberg Naturwissenschaft Jahreshefte*.

Orbigny d', A. (1842–1849). *Paléontologie française. Terrains jurassiques*. Masson édit, Paris, I : Céphalopodes; texte.

Page, K. N. (2003). The Lower Jurassic of Europe: its subdivision and correlation. *Geol. Surv. Denmark Greenland Bull.*, 1, 23–59.

Parona, C. F. (1897). *Contribuzione alla conoscenza delle Ammoniti liassiche di Lombardia. II - di alcune ammoniti del Lias medio*, volume 24 of *Mémoires de la Société paléontologique suisse*.

Péneau, J. (1923). Observations géologiques sur la côte sud-vendéenne. *Bulletin de la Société de Sciences naturelles de l'Ouest de la France*, 4(3), 57–73.

Phelps, M. (1985). A refined ammonites biostratigraphy for the Middle and Upper Carixian (Ibex and Davoei zones, Lower Jurassic) in North-West Europe and stratigraphical details of the Carixian-Domérian boundary. *Géobios*, 18(3), 321–362.

Phillips, J. (1829). *Illustrations of the Geology of Yorkshire*. York.

Quenstedt, F. A. (1845–1849). *Petrefactenkunde Deutschlands. I: Die Cephalopoden*. Fuess édit, Tübingen.

Quenstedt, F. A. (1885). *Die Ammoniten des schwabischen Jura*, volume 3. Schweizerbart ed., Stuttgart.

Rakús, M. (1972). Sur la présence du genre *Dayiceras* Spath (Ammonoidea, Cephalopoda) dans le

Carixien de Tunisie. *Bulletin des Laboratoires de Géologie, Minéralogie, Géophysique et du Musée géologique de l'Université de Lausanne*, 195, 1–3.

Rakús, M. and Guex, J. (2002). Les ammonites du Jurassique inférieur et moyen de la dorsale tunisienne. *Mémoires de Géologie, Lausanne*, 39, 1–217.

Rasmussen, E. S., Lomholt, S., Andersen, C., and Vejbæk, O. V. (1998). Aspects of the structural evolution of the Lusitanian Basin in Portugal and the shelf and slope area offshore Portugal. *Tectonophysics*, 300(1–4), 199–225.

Reynès, P. (1868). *Essai de géologie et de paléontologie aveyronnaises*. Baillière, Paris.

Rodriguez-Luengo, E., Comas-Rengifo, M. J., and Goy, A. (2012). Caracterisacion de *Matteiceras* Wiedenmayer, 1980 (Ammonoidea, Hildoceratidae) en el Pliensbachiense superior de Cordillera Cantabrica. In Liao, J. C., Gamez Vintaned, J. A., Valenzuela-Rios, and Garcia-Forner, A., editors, *XXVIII Jornadas SEP 2012. Homenaje a Guillem Colom Casanovas (1900–1993). Libro de Resumenes*, pages 187–190.

Rulleau, L. (2007). *Biostratigraphie et paléontologie de la région lyonnaise*. Du socle au Lias moyen. Rulleau, ed.

Schlotheim, E. F. von. (1820). *Die Petrefactenkunde auf ihrem jetzigen Standpunkte dursch die beschreibung seimer Sammlug*. Gotha.

Simpson, M. (1884). *The Fossils of the Yorkshire Lias; Described from Nature*. Whittaker and Co, London, 2nd edition.

Smith, P., Tipper, H., Taylor, D., and Guex, J. (1988). An ammonite zonation for the Lower Jurassic of Canada and United States: the Pliensbachian. *Can. J. Earth Sci.*, 25(9), 1503–1523.

Smith, P. L. (1983). The Pliensbachian ammonites *Dayiceras dayiceroides* and Early Jurassic paleogeography. *Can. J. Earth Sci.*, 20(1), 86–91.

Sowerby, J. (1812–1822). *The Mineral Conchology of Great Britain; or coloured figures and descriptions of those remains of testaceous animals or shells, which have been preserved at various times and depths in the earth*. 1–3, 4 pars: 1–383 pl.

Sowerby, J. de C. (1823–1846). *The Mineral Conchiology of Great Britain*. 4 (end)-7, 384–648 pl.

Spath, L. F. (1920). On a new genus (*Dayiceras*) from the Lias of Charmouth. *Geol. Mag.*, LVII, 538–543.

Taylor, D. G., Callomon, J. H., Hall, R., Smith, P. L., Tipper, H. W., and Westermann, G. E. G. (1984). Jurassic ammonite biogeography of western north america: The tectonic implications. In Westermann, editor, *Jurassic-Cretaceous Biochronology and Paleogeography of North America*, volume 27 of *Geological Association of Canada, Special Paper*, pages 121–141.

Thierry, J. et al. (2000). Late Sinemurian (193-191 Ma). In Crasquins, S., editor, *Atlas Peri-Tethys, Paleogeographic Maps. Explanatory Notes*. CCGM-CGMV, Paris. map no 7.

Thompson, R. C. and Smith, P. L. (1992). *Pliensbachian (Lower Jurassic) biostratigraphy and ammonite fauna of the Spatsizi area, north-central British Columbia*, volume 437 of *Geological Survey of Canada, Paper*.

Trueman, A. E. (1919). The evolution of the Liparoceratidae. *Q. J. Geol. Soc. Lond.*, 74, 247–298.

Venturi, F. and Ferri, R. (2001). *Ammoniti Liassici dell'Appennino Centrale*. Citta di Castello ed.

Venturi, F., Nannarone, C., and Bilotta, M. (2007). Ammonites from the Early Pliensbachian from the Furlo Pass (Marche, Italy); biostratigraphic and paleobiogéographic implications. *Bolletino della Società Paleontologica Italiana*, 46, 1–31.

Venturi, F., Rea, G., Silvestrini, G., and Bilotta, M. (2010). *Ammoniti. Un viaggio nelle montagne appenniniche*. Porzi ed., Perugia.

Wiedenmayer, W. F. (1977). *Die Ammoniten des Besazio-kalks (Pliensbachian, Sud Tessin)*, volume 98 of *Mémoires suisses de Paléontologie*.

Wiedenmayer, W. F. (1980). *Die Ammoniten der mediterranen Provinz im Pliensbachian und unteren Toarcian aufgrund neuer Untersuchungen im Generoso-Becken (Lombardische Alpen)*, volume 43 of *Mémoires de la Société helvétique des Sciences naturelles*. Birkhäuser, Basel.

Wingrave, W. (1916). A new variety of the Ammonite *Coeloceras davoei* from the Lower Lias, Dorset. *Geol. Mag.*, 3, 196–198.

Young, G. M. and Bird, J. (1828). *A Geological Survey of the Yorkshire Coast: Describing the Strata and Fossils Occurring between the Humber and the Tees, from the German Ocean to the Plain of York*. Office of G. Clark, Whitby, 2nd edition. (enlarged).

Comptes Rendus
Géoscience — Sciences de la Planète
2022, Vol. 354, Special Issue S3, p. 27-43
https://doi.org/10.5802/crgeos.166

Integrated stratigraphy of the Jurassic and the Cretaceous: a tribute to Jacques Rey /
Stratigraphie intégrée du Jurassique et du Crétacé : un hommage à Jacques Rey

Biometry and biostratigraphy of the Early Cretaceous belemnite genus *Castellanibelus* from the southeast of France

Marie-Claire Picollier [a]

[a] 27 impasse des Iris, La Vitonie, 24160 St Pantaly d'Excideuil, France
E-mail: mc.picollier@wanadoo.fr

Abstract. Early Cretaceous deposits (Berriasian–Albian) crop out over large areas in the Vocontian Basin (VB, southeast of France). The important exposures have provided rich marine fossil faunas, including many specimens of ammonites and belemnites over the last 200 years. From the early 19th century onward, the definition of Lower Cretaceous belemnite species from the VB was essentially based on descriptive, qualitative approaches. This resulted in a variety of morphologically very closely related species, sometimes difficult to differentiate between each other. Biometric data and their statistical analysis offer a mathematical and objective framework to clearly delineate and define morphological species, especially when consecutive belemnite assemblages are continuously available from different stratigraphic levels. The present study is based on the analysis of 1762 specimens of *Castellanibelus* collected by ammonite zones and subzones across the entire Valanginian interval of the VB. Biometric data of this genus have been statistically analyzed and used to define four species, including one new to science: *Castellanibelus orbignyanus*, *Castellanibelus vaubellensis*, *Castellanibelus suborbignyanus*, and *Castellanibelus toucasi* sp. nov.

Keywords. Belemnites, Lower Cretaceous, Valanginian, Vocontian Basin, *Castellanibelus*, Taxonomy, Biostratigraphy.

Published online: 28 October 2022, Issue date: 13 January 2023

1. Introduction

The Early Cretaceous (Berriasian–Albian; 145.5–99.6 Ma) belemnite faunas of the Tethys have been the subject of numerous studies since the pioneering publications of the 19th century [e.g. Ducrotay de Blainville, 1827, Raspail, 1829, Duval-Jouve, 1841, d'Orbigny, 1847]. Since then, the rich faunas of the Vocontian Basin (VB; southeast of France) have been described in detail [e.g., Combémorel, 1972, 1973, Gayte and Combémorel, 1981, Janssen, 2007, 2009, 2018].

For defining taxa, the concepts used in these studies have, however, several set-backs. They suffer either from a limited number of specimens, or are only explained using a qualitative descriptive approach. Efforts for a more objective approach to define belemnite species using quantitative, biometric data go back to the second half of the twentieth century. Biometric data of rostra and their statistical evaluation have been successfully used for defining species and accomplishing phylogenies, particularly for Late Jurassic and Cretaceous species [e.g., Spaeth,

1971, Christensen, 1975, 2000, Challinor, 1979, 1999]. Till date, this biometric approach has not yet been applied to the study of the VB belemnite faunas.

A pre-requisite for such biometric studies is the availability of large belemnite assemblages (>30 specimens) of the conventionally defined species or genera, collected bed-by-bed from stratigraphically well-defined levels. A second step requires a time-consuming biometric analysis of specific features, and a subsequent statistical analysis of data in a third step.

The current study focuses, in the first instance, on a biometric and statistical analysis of 1762 rostra of the belemnite genus *Castellanibelus* (family Duvaliidae). These specimens have been collected following the standard ammonite zonation of the Valanginian–Hauterivian interval of the Early Cretaceous in the VB [Reboulet et al., 2014]. The data resulted in a taxonomic revision of the genus *Castellanibelus*. The individual species were then interpreted in their biostratigraphic context. Finally, the abundance patterns of *Castellanibelus* are compared to those of other co-occurring belemnite genera, in order to obtain quantitative distribution patterns for each ammonite zone.

2. Material

The specimens were collected from the upper surface of beds, following the standard ammonite zones of the standard Kilian group zonation [Reboulet et al., 2014], in the following Az stands for ammonite zones and Asz for ammonite subzones. Most of the specimens come from the departments of Alpes de Haute-Provence, Drôme and Hautes-Alpes. The reference specimens have been deposited in collections of the National Geological Reserve of Haute-Provence.

The genus *Castellanibelus*, which first appeared in the Tithonian [Combémorel, 1972], reached its acme in the Early Valanginian and disappeared subsequently in the latest Valanginian. The biometric analysis performed in this study was carried out on 1762 rostra collected in 112 outcrops exposing Valanginian strata. The investigated exposed surface area in the VB is estimated to be around 4500 km^2 based on data from the Geoportail website of Institut national de l'information géographique et forestière [IGN, 2022].

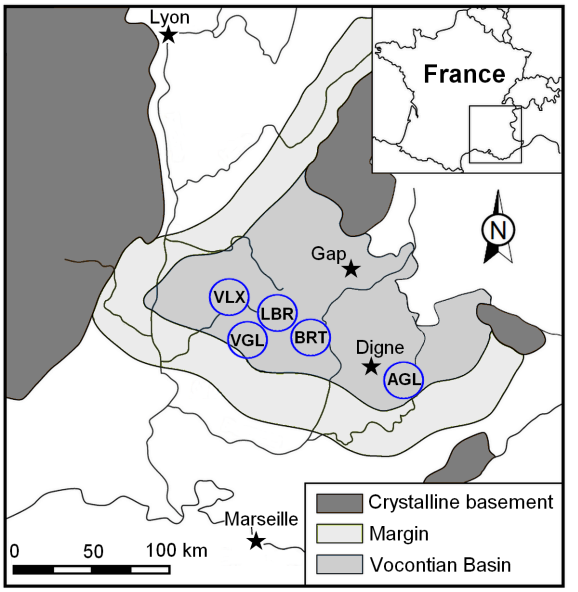

Figure 1. Distribution of study areas in the Vocontian Basin: AGL: Angles-Castellane; BRT: Barret/Méouge and Jabron valley; LBR: Laborel-Rosans; VGL: Montbrun-Vergol, VLX: Villeperdrix; [from Martinez, 2013, modified].

The statistical study required the grouping of outcrops into study areas around a reference section. The five selected areas are as follows (Figure 1):

- AGL: Angles-Castellane and Barrème-Moriez area ($n = 237$); n = number of *Castellanibelus* studied
- BRT: Barret/Méouge area and Jabron valley ($n = 235$);
- LBR: Laborel-Rosans and Haute-Ouvèze area ($n = 545$)
- VGL: Montbrun-Vergol area ($n = 593$)
- VLX: Villeperdrix-Col Lazarier area ($n = 136$).

Five isolated outcrops on the margins of the VB yielded 16 additional rostra. These were used in the biometric study but excluded from the biostratigraphic study.

Specimens of *Castellanibelus* are highly abundant throughout the Lower Valanginian *Thurmanniceras pertransiens* Az up to the basal Upper Valanginian *Saynoceras verrucosum* Az (Figure 2).

Out of a total of 9001 belemnites collected in this interval, in the study area, 1746 rostra were attributed to *Castellanibelus* (Figure 2a,b). Near the base of the

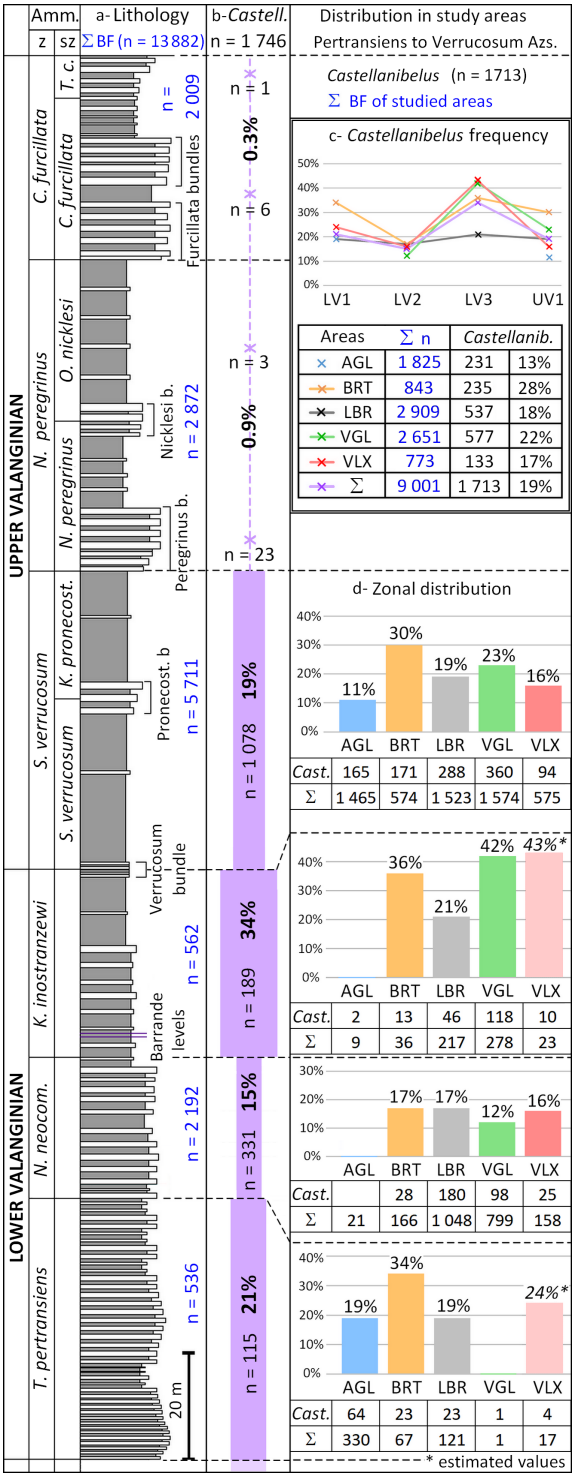

Figure 2. Biostratigraphic distribution of *Castellanibelus* spp. during the Valanginian by ammonite zone for the entire Vocontian Basin.

Figure 2. (**cont.**) (a) In blue: total number of rostra of BF per Az; (b) absolute numbers (=*n*) and relative numbers (%) of *Castellanibelus* spp. per Az; (c,d) Abundances of *Castellanibelus* spp. in the studied areas (Pertransiens Az—Verrucosum Az interval); codes for study areas as in Figure 1, [from the synthetic Valanginian lithographic section of Martinez, 2013].

Neocomites peregrinus Az, *Castellanibelus* suddenly became very scarce. A few specimens were still found in the Peregrinus bundle, above this level the genus becomes extremely rare (0.2% of the rostra). Out of the 4700 rostra collected in the Hauterivian not a single specimen has been attributed to *Castellanibelus*.

In the Valanginian, in its range of abundance from the Pertransiens Az to the Verrucosum Az, *Castellanibelus* is abundant and represents about one fifth (~19%) of the belemnite fauna (BF). It peaks at one third of the belemnite fauna in the Inostranzewi Az.

The spatial and stratigraphic distribution of the 1746 *Castellanibelus* rostra studied across the VB is congruent with our knowledge of the rest of the belemnite fauna (13,882 rostra in total) long collected in the study area under the same conditions (Figure 2c,d), despite outcrops sometimes being 150 km apart. Only a slight under-representation of the genus in the Laborel sector (LBR), Inostranzewi Az, must be mentioned.

3. Measurements and morphometric analysis

3.1. *Measurements*

Biometric data have been obtained from the 1762 specimens collected from the Valanginian of the VB. The measurements were made using a digital caliper to an accuracy of 0.01 mm. Each value was measured three times successively for assessment of measurement error.

In order to obtain statistically useful data, measurements of specific features must be linked to tie points. The position of the protoconch is one such tie point used in many studies [e.g. Christensen, 1975, 2000]. The position of the protoconch in *Castellanibelus* is easy to identify because of the regularity of its alveolar cavity. Its median position, relatively close to the apex but anterior to the maximum diameter of

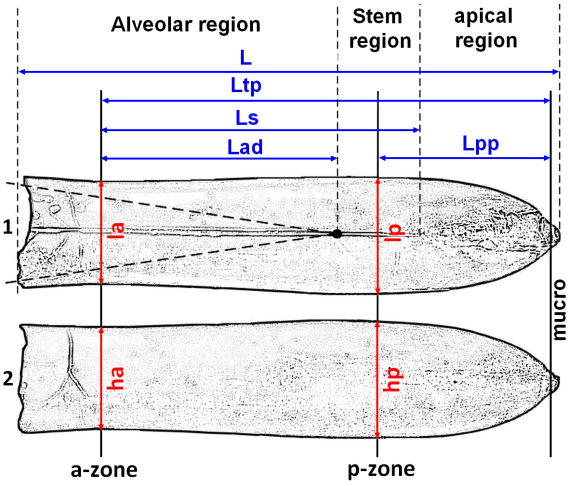

Figure 3. Dorsal (1) and lateral views (2) of a *Castellanibelus* rostrum, showing the measurements taken for the present study.

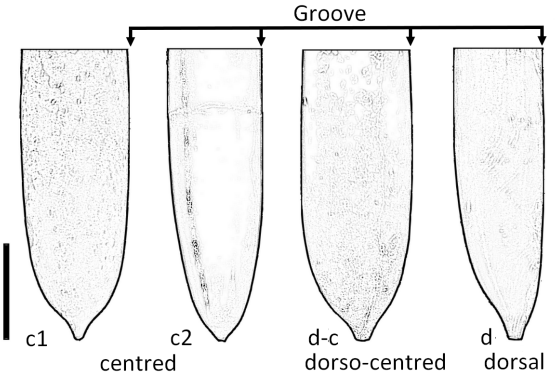

Figure 4. Position of the mucro in lateral view. (c1) centred, *C. orbignyanus*, no. 92234; (c2) centred, *C. suborbignyanus*, no. 3025; (d-c) dorso-centred, *C. vaubellensis*, no. 90872; (d) dorsal, *C. toucasi*, no. 48583. Scale bar = 1 cm.

the posterior part, does not allow an efficient use of the protoconch-apex length (Figure 3a). The mucro, often broken or incomplete, was excluded from the longitudinal measurements.

The slightly hastate or club-shaped rostra of *Castellanibelus* show two sectors of minimum and maximum diameters, both in dorsal and lateral views, which are here used as a reference for further measurements. The smallest lateral and dorsoventral diameter ∅, measured in the anterior or alveolar zone (a-zone), marks the first tie point (Figure 3). This definition allows to measure the length of the rostrum (a-zone–apex, $=L_{tp}$), excluding the mucro. The posterior zone (p-zone) corresponds to the maximum lateral and dorsoventral diameter ∅ of the rostrum. The resulting second tie point facilitates a second length measurement (p-zone–apex, $=L_{pp}$) excluding the mucro. A few rostra show a slight shift between the positions of posterior diameters. In this case, the p-zone retained is the one defined in dorsal view.

The following measurements were used in the current study:

Longitudinal measurements (in mm):

- L: Total length of rostrum.
- L_{tp}: Reference length (a-zone to apex excluding mucro).
- L_{pp}: Posterior part length (p-zone to apex excluding mucro).
- L_s: Groove length (a-zone to groove end).

Transverse measurements (in mm)

- ha: Anterior dorsoventral diameter
- la: Anterior lateral diameter
- hp: Posterior dorsoventral diameter
- lp: Posterior lateral diameter

Alveolar measurements

- L_{ad}: Alveolar depth (a-zone to protoconch, in mm).
- Angle of the alveolar cavity (in degrees).

In lateral view, the position of the mucro was assessed as follows: centred (c), dorsal (d) and dorso-centred (dc), (Figure 4).

3.2. *Morphometry and statistics*

Biometric data provide a quantitative means of comparing and statistically testing differences among individual rostra of a belemnite assemblage. Because belemnite rostra are subject to allometric growth, biometric ratios rather than raw measurement values are commonly used in statistical analyses of belemnite assemblages comprising individuals of different sizes and ages. Ratios of values taken at the same point on rostra are therefore widely used in belemnite biometry suggesting that they are reliable tools [e.g. Spaeth, 1971, Mutterlose et al., 1983].

The following ratios have been computed for the present study:

- **ica** (ha/la): anterior compression index
- **icp** (hp/lp): posterior compression index
- **iddv** (lp/la): dorsoventral dilation index
- **idlat** (hp/ha): lateral dilation index
- **Psr** (L_{pp}/lp): posterior shape ratio
- **apical angle** (INVTAN[(l_{max}/2)/L_{pp}]) × 2))
- **alveolar relative depth** (L_{ad}/L_{tp})

Calculations and graphs were accomplished with an Excel database. The arithmetic means and standard deviations were calculated to the nearest hundredth. Many graphics show a polynomial curve of degree 2, used to analyse variations in a large data set. The full data and calculations are available in the Supplementary Information.

3.3. *Belemnite populations and ontogeny*

In biology, the term "population" is defined as a group of organisms of a species co-existing in an area, i.e. organisms which reproduce sexually with each other. The usage of the term "population" is thus problematic when analysing a belemnite genus which may well consist of several species. Another problem is the duration of 0.6–0.8 Ma of individual Valanginian ammonite zones, and even 1.4 Ma in the case of the N. peregrinus Az. These long time intervals, which reflect our belemnite assemblages, are clearly excluding the use of the term "population". We therefore prefer the term "assemblage" when discussing the biometric data of specific, stratigraphically bounded rostra.

For the statistical analysis, the rostra have been grouped as assemblages in the following way. For each of the five studied areas, the available belemnites have been assigned to one of the 6 standard ammonite zones of the Valanginian zones [standard Kilian group zonation—Reboulet et al., 2014]. In this manner, five assemblages have been evaluated for each ammonite zone.

Daily increments of rostrum growth [Hoffmann and Stevens, 2019] can be observed in rostrum longitudinal sections (Supplementary Information, Plate S5, Figure S1). They show a continuous growth of the rostra which is not contradictory with potential allometric growth. For the ontogenetic study, the 1746 rostra assemblage was partitioned into five growth stages. The criteria used were rostra length (L) and/or cavity depth (L_{al}).

The shortest rostra correspond to shapes observed on the first growth increments. They are therefore comparable to the most juvenile individuals (mj) (mj: $L \approx 21$ mm, $L_{al} \approx 4.5$ mm). In contrast, the longest rostra are here interpreted as adult forms (a) of *Castellanibelus* (a: $L \approx 58$ mm, up to 70 mm [Combémorel, 1972], $L_{al} \approx 20.5$ mm). Three other categories present intermediate forms between these two extreme stages. They are named here very juvenile (vj) (vj: $L \approx 28$ mm, $L_{al} \approx 6.5$ mm), juvenile (j) (j: $L \approx 41$ mm, $L_{al} \approx 11.5$ mm) and subadult (sa) (sa: $L \approx 50$ mm, $L_{al} \approx 16$ mm). These last designations have no absolute biological meaning but only correspond to distinct growth stages in terms of size and shape.

4. Biometric results

4.1. *Ontogeny*

4.1.1. *Rostrum length and alveolar depth*

Measuring the length of rostra between the protoconch and the anterior extremity, and between the protoconch and the apex requires that rostra be complete, a requirement fulfilled by only 251 out of the 1746 studied rostra (=14%).

The shortest measured length of a complete specimen is 15.6 mm long (no. 98790, Verrucosum Az), the largest complete one 67.6 mm (no. 79022, Inostranzewi Az). Adults longer than 60 mm were found from the Pertransiens Az to the Verrucosum Az.

Alveolar depth changes during growth, from 37% on average for juveniles to over 50% for adults (extreme values are comprised between 17 and 67%, n = 875). The increase in alveolar depth is continuous in juvenile stages (mj–j), and it slows down strongly in subadult and adult stages, when the width of rostra is maximum.

4.1.2. *Compression indices*

The compression index (ic) describes the lateral compression in the anterior (ica = ha/la) or posterior part of the rostrum (icp = hp/lp). Three conditions can be met: laterally compressed (ic > 1), circular (ic ≈ 1), or dorsoventrally depressed (ic < 1).

Figure 5. Transverse section through the p-zone of one of the oldest adult rostrum showing growth increments and the progressive increase in width of the rostrum (icp = 0.84, no. 79759).

Overall, *Castellanibelus* rostra show a slight depression (mean ic = 0.92, n = 861). The degree of depression varies according to the region of the rostrum, the taxonomy (Supplementary Information 1.A) and the growth stage, with most juvenile rostra showing a sub-circular posterior cross-section.

Most juvenile rostra (mj) are sub-circular in the apical region (mean icp = 1) and slightly depressed in the alveolar region (mean ica = 0.92). Later ontogenetic stages (vj–a) show a steady shift to more depressed apical regions, due to an allometric increase of width with growth (Figure 6). The adult phase (a) is depressed in the apical region (icp = 0.89) and less so in the alveolar region (ica = 0.94). Throughout ontogeny, the area of maximum depression is shifting from its alveolar position in juvenile specimens to a more apical one in adults. These data document an allometric growth of *Castellanibelus* in width, the lateral growth rate obviously exceeding the dorsoventral one (Figure 5).

The degree of depression of the posterior part of the rostra decreased during the Valanginian. For adult specimens, the icp values increased from 0.85 in the Pertransiens Az (icp = 0.85) to 0.91 in the Verrucosum Az (icp = 0.91; n = 157).

This evolution towards more circular cross-sections is linked to a change in taxonomic composition: the dominant taxon at the base of the Valanginian, which is very depressed, tends to disappear progressively in favour of other, less depressed taxa of *Castellanibelus*.

4.1.3. *Dilation indices*

The dilation index (id) describes the shape of the rostrum in dorsoventral (dv) or lateral (lat) view.

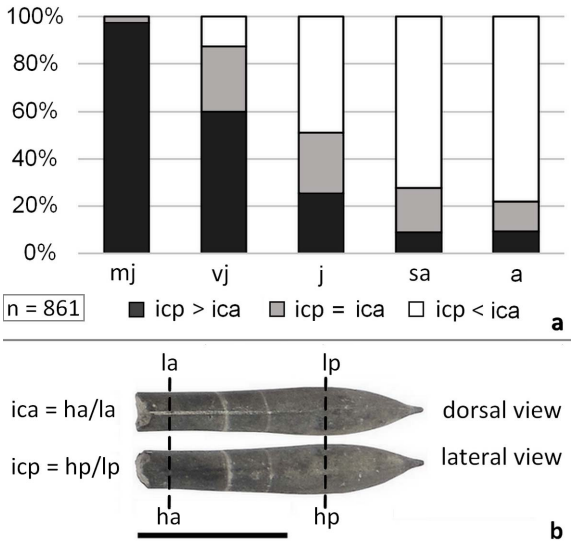

Figure 6. (a) Ontogenetic stages and compression index for *Castellanibelus*: icp > ica: rostrum more depressed anteriorly; icp = ica: rostrum depressed anteriorly as posteriorly; icp < ica → rostrum more depressed posteriorly. (b) One of the most juvenile rostrum, depressed anteriorly and sub circular posteriorly (ica = 0.97, icp = 1.03, no. 4924, scale bar = 1 cm).

Three conditions are possible: hastate, or club shaped rostra (id > 1); cylindrical rostra (id ≈ 1); conical rostra (id < 1).

The mean dilation indices of *Castellanibelus* document a slightly hastate shape in general (iddv = 1.12; idlat = 1.11, n = 861).

The mean dilation indices change with growth stages. They show a greater dilation in the early stages of growth (iddv = 1.15, idlat = 1.22). This dilation then evolves towards less dilated forms in the following growth stages (iddv = 1.11, idlat = 1.10). Finally, there is a further increase in the dilatation index in dorso-lateral view in the longest rostra (iddv = 1.13, idlat = 1.08; Figure 7, Supplementary Information 1.A).

The dilation of the rostra of *Castellanibelus* is therefore varying according to ontogenetic stages. Three phases can be distinguished. The rostra of very juvenile specimens are slightly hastate (mj/vj). This dilation phase is followed by an elongation of the rostra which corresponds to the juvenile stages (j/sa). The rostra then show a sub-cylindrical shape. Then,

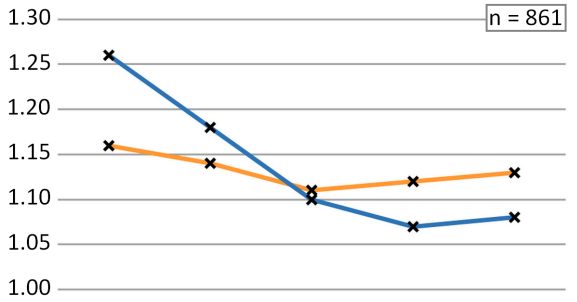

Figure 7. Distribution of mean values of dorsoventral (iddv) and lateral (idlat) dilation indices for the different ontogenetic stages.

with the thickening of the posterior part of the rostra, the mature rostra again show a slightly hastate outline in dorsolateral view.

No significant changes of shape have been observed throughout the Valanginian.

4.1.4. *Alveolar groove and position of mucro*

The alveolar groove, positioned dorsally, is narrow and long (mean L_s = 74% of L, n = 864). It never reaches the apex (maximum 92% of L). Its length increases with age from 65% in most juvenile forms to about 76% in adults.

The growth of the rostrum is asymmetrical in the apical region. The mucro gradually shifts with rostrum length to a more centred position: only 11% of the juveniles show a centred mucro compared to 42% of the adults (n = 1423, Supplementary Information 1.B).

4.1.5. *Growth key*

Using morphological features (e.g. shape, mucro, sulcus, lateral lines), previous authors concluded that there were no significant ontogenetic changes in *Castellanibelus* [e.g. Duval-Jouve, 1841, d'Orbigny, 1847, Combémorel, 1972, Janssen, 2018], an assessment based solely on qualitative observations.

Present biometric results document significant morphological changes of the rostrum with growth. These changes are summarised in Figure 8.

4.2. *Morphotypes and stratigraphy*

The following biometric indices of *Castellanibelus* show a significant variation across the Valanginian: the Posterior shape ratio (Psr), the apical angle and the Posterior compression index (icp) (Figure 9 and Supplementary Information 1.A, 1.B, 1.C).

4.2.1. *Posterior shape ratio and apical angle*

The Psr values are also controlled by ontogeny, the earliest ontogenetic stages (mj) having a higher relative posterior length than adults. The Psr ratio varies considerably between specimens and indicate for <1 a very short posterior length (<1), for a median posterior length (±1.50) and a very long posterior length (for >2). Extreme values of Psr range between 0.73 and 2.76.

Based on the examination of 1416 specimens, Psr values document three distinct morphotypes (A, B, C; Figure 9c; Supplementary Information 1.B). A fourth morphotype, D, differs significantly in its posterior compression index (icp), described in Section 4.2.2. The Psr values are closely related to the size of the apical angle, where a short posterior length is mirrored by a large apical angle.

- A: median length posterior, mean Psr = 1.57; extreme values between 1.99 (most juvenile) to 1.13 (adult), mean apical angle = 36°, n = 569;
- B: short posterior length, mean Psr = 1.20, extreme values between 1.66 (most juvenile) to 0.73 (adult), mean apical angle = 46°, n = 374;
- C: long posterior length, mean Psr = 2.00, extreme values between 2.76 (most juvenile) to 1.58 (adult), mean apical angle = 28°, n = 170;
- D: median posterior length, mean Psr = 1.45, extreme values between 1.94 (most juvenile) to 0.97 (adult), mean apical angle = 39°, n = 303.

4.2.2. *Compression indices*

The anterior (ica) and posterior (icp) compression indices show a steady decrease in depression during the Valanginian:

- Pertransian Az: mean ica = 0.89; mean icp = 0.89

Ontogeny	Length (mm) mean val.	Growth process	Cross section			Shape			Alveolar depth (% L)
			post. (p-zone)	mean values icp ica	ant. (a-zone)	dorsoventral view	mean values iddv idlat	lateral view	mean val.
mj	≈ 21	bulging posteriorly	sub circular	1.01 > 0.92	regular thickening	slightly hastate	1.16 < 1.26	slightly hastate	37%
vj	≈ 28	thrust in length	little depressed	0.95 > 0.92			1.14 ≤ 1.18		40%
j	≈ 41			0.92 ≈ 0.93		sub-cylindrical	1.11 = 1.10	sub-cylindrical	45.5%
sa	≈ 50	progressive thickening (width > height)	depressed	0.90 > 0.94		sub-cylindrical to slightly hastate	1.12 ≥ 1.07		49%
a	≈ 58			0.89 < 0.94			1.13 > 1.08		50.5%

Figure 8. Measurements of the five ontogenetic stages of *Castellanibelus*; icp, $n = 1416$; ica, iddv, idlat, $n = 861$; length and alveolar depth, $n = 875$.

- Verrucosum Az: mean ica = 0.93; mean icp = 0.93.

This decrease in depression is due to morphotype D that is more depressed than other morphotypes, especially posteriorly: mean icp D = 0.87; icp A, B and C = 0.93, Figure 9d).

Morphotype D is clearly dominant at the base of the Valanginian: from 76% of all *Castellanibelus* in the Pertransian Az, it decreases in abundance steadily and represents only 7% of *Castellanibelus* in the Verrucosum Az. This decreasing abundance of morphotype D explains the overall increase in compression indices observed due to morphotypes A, B and C.

The strong depression of D, both anteriorly and posteriorly, is a characteristic dorso-ventral flattening, which results in a sub-quadrangular to oval shape in cross-section. A trend towards dorso-ventral flat rostra was also observed for mature rostra of morphotypes A, B, C, where it is less distinctive and only developed in the posterior part.

4.2.3. *Mucro position*

The position of the mucro in lateral view has been quantified semi-quantitatively (mucro centred, dorso-centred, dorsal; Figure 4), based on 1423 rostra. The position also varies with ontogeny (Supplementary Information 1.B).

Two of the four morphotypes show a mucro in a centred position: C (77%, $n = 172$), B (67%, $n = 385$). The rostra of morphotype A have a dorso-centred mucro (85%, $n = 567$). Group D has a mucro between dorso-centred and dorsal, depending on the ontogenic stage (dorsal: 55%, dorso-centred 43% and 2% centred, $n = 299$).

4.3. *Biostratigraphy*

Specimens of *Castellanibelus* represent about one fifth of the belemnite fauna in the Pertransiens Az to Verrucosum Az interval (Figure 2). The four morphotypes (A, B, C, D) are not evenly distributed across this stratigraphic interval (Figure 9).

In the Lower Valanginian Pertransiens Az, morphotype D is very frequent (76% of all *Castellanibelus* specimens). Morphotypes A, B and C are present, but rather rare. The abundance of morphotype D gradually decreases in the Neocomiensiformis Az (46%) and Inostranzewi Az (26%), while morphotypes A and B become more common. The Verrucosum Az sees a peak of A and B (47%, 33%), while D is rare (7%). Morphotype C is stable throughout the entire Valanginian (≈12%).

Castellanibelus becomes very rare at the transition with the Peregrinus Az. A few rare resilient specimens of all four morphotypes are still present in the Peregrinus bundle (Figure 9). A single specimen of morphotype C was found at the top of the Valanginian stage in the *Teschenites callidiscus* Ammonite subzone.

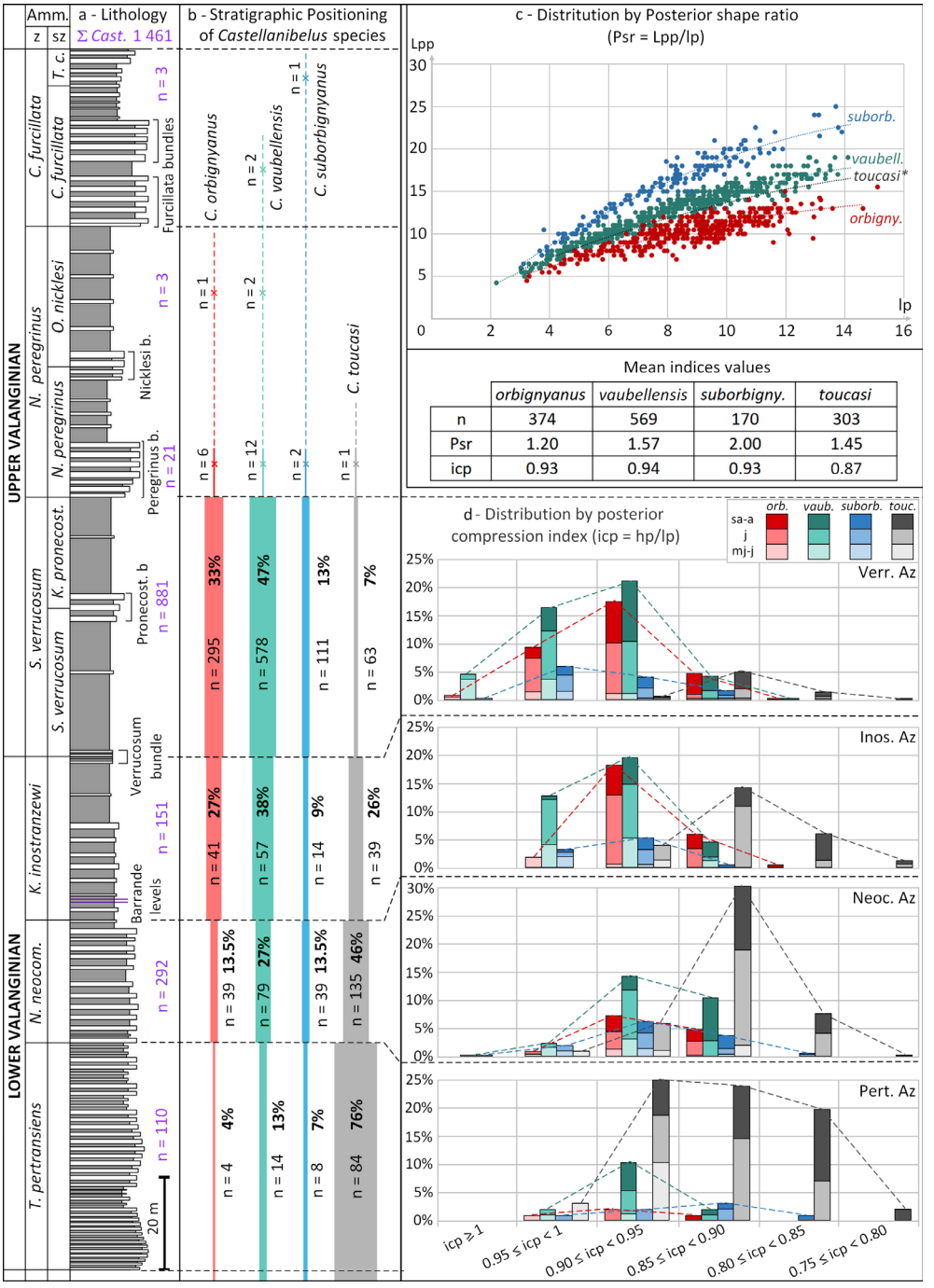

Figure 9. Stratigraphic distribution (a–b) and biometric indices (c–d) of *Castellanibelus* species during the Valanginian [from Martinez, 2013]; (a) number of *Castellanibelus* specimens collected per Az; (b) absolute number (*n*) and percentage (%) of specimens for each *Castellanibelus* species: red = *C. orbignyanus*, green = *C. suborbignyanus*, blue = *C. vaubellensis* and grey = *C. toucasi*; (c) distribution of posterior shape ratio for each species, polynomial curves give the general trend for each species (**C. toucasi* is only represented by its polynomial curve for a better readability); (d) distribution of the posterior compression index values by ammonite zone in the *Castellanibelus* abundance interval (Pertransiens Az – Verrucosum Az); for each species, colour intensity refers to the different ontogenetic stages: light (mj–vj), medium (j), dark (sa–a).

5. Taxonomy

5.1. *Species concept in the genus Castellanibelus*

Toucas [1890] proposed two varieties of the species created by Duval-Jouve [1841]: *Belemnites orbignyanus* var. *jouvei* and *Belemnites orbignyanus* var. *suborbignyi*. These creations were not taken up subsequently. When the genus *Castellanibelus* was created, Combémorel [1972] considered it to be a mono-specific genus. All rostra in this genus were attributed to the species *Castellanibelus orbignyanus* until the subsequent revisions and creations by Janssen [1997, 2003, 2007, 2018] and Janssen and Clément [2002].

In the present study, biometric data demonstrate the existence of four distinct species within the genus *Castellanibelus*, three were attributed to earlier creations (morphotypes A, B and C), the fourth (morphotype D) requiring the erection of a new species.

5.1.1. *Type species*

The short, obtuse apical part, the centred or slightly eccentric mucro and the slight depression of the rostra assigned to morphotype B are consistent with the diagnosis of the species *Castellanibelus orbignyanus* [Duval-Jouve, 1841]. The type figure is a juvenile and not an adult specimen as thought by Duval-Jouve [1841] (L = 46 mm). The juvenile rostrum no. RHP.04236-026.AA.516 (Figure 10B2), figured here, is very close.

Castellanibelus (*Belemnites*) *picteti* [Mayer, 1866] shows the same characters and corresponds to the type species *orbignyanus*.

5.1.2. *Variety suborbignyi Toucas, 1890*

Morphotype C is characterized by a minor depression, an elongation of the apical part which ends in a mostly centred mucro (Figures 10C1–C3). These criteria are similar to those of the *Castellanibelus* variety *suborbignyi* [Toucas, 1890], which is thus raised to the species status under the name *Castellanibelus suborbignyanus* [Toucas, 1890].

5.1.3. *Morphotypes A and D*

Morphotype A has an apical part of medium length, a mucro in intermediate position associated with a weak posterior depression (mean icp = 0.94). The intermediate positioning of the mucro is correlated with a more flattened dorsal surface in dilated adults and a characteristic posterior bulge in lateral view (Figure 10A3).

While these criteria match with those of the holotype of *Castellanibelus vaubellensis* Janssen, 2018, some elements of the diagnosis of this species require revision (sub-hastate form and dorso-ventral flatness). The dilation of the rostra of *Castellanibelus* is variable and cannot be used as a determination criterion. This variability is due to ontogeny (see Section 4.1.3) and to a more or less strong growth in width of the adult rostrum according to the individuals, inducing shapes going from nearly subcylindrical to sub-hastate in all morphotypes (Supplementary Information 1.A, 1.C).

Janssen [2018] reports a dorso-ventral flattening in *C. vaubellensis*. Adult rostra of all morphotypes tend towards a posterior dorso-ventral flattening due to the increase in width with age. When this flattening occurs all along the rostrum and appears in juvenile stages, it induces the significant depression characteristic of morphotype D. The juvenile paratype of *C. vaubellensis* [Janssen, 2018] (Jans. Figures 7.3–4) shows such a depression, accompanied by the dorso-ventral flattening attributable to D.

Morphotype D is characterised by its strong depression, its dorso-ventral flatness inducing an oval to sub-quadrangular cross-section, its predominantly dorsal mucro, and its stratigraphic peak in the Lower Valanginian (Figures 10D1–D3). The distinctive depression of this morph group is mentioned by Pictet and de Loriol [1858, ic = 0.81] and Combémorel [1972, ic ≈ 0.85]. A sub-quadrangular section or a flattening of the sides is also indicated by Janssen and Clément [2002, *Castellanibelus* sp. B] and Janssen [2003, *Castellanibelus* sp. A]. No valid species exhibiting the characters of morphotype D, it is assigned to a new species, *Castellanibelus toucasi* sp. nov.

5.1.4. *Comparison with other species*

Janssen [2003] proposed the classification of *Conobelus triquetus* Weiss, 1991, in the genus *Castellanibelus*. If the depression (0.73) of the rostrum of Weiss would tend to bring it closer to *Castellanibelus*, the shallow depth of the alveolus strongly eccentric, the groove reaching the apex, the absence of lateral lines, the absence of a mucro are incompatible with a positioning within the genus *Castellanibelus*. *C. triquetus* should therefore be returned to its original

Figure 10. *Castellanibelus* species from the Valanginian of the Vocontian Basin. Scale bar 1 cm. (A) *C. vaubellensis* [Janssen, 2018], (B) *C. orbignyanus* [Duval-Jouve, 1841], (C) *C. suborbignyanus* [Toucas, 1890], (D) *C. toucasi* sp. nov.. Very juvenile (1), juvenile (2) and adult (3) forms for each of the 4 species. References: A1 (no. RHP.04236-026.AA518), A2 (no. RHP.04204-024.AA522), A3 (no. RHP.26018-001.AA514), B1 (no. RHP.04236-026.AA517), B2 (no. RHP.04236-026.AA516), B3 (no. RHP.26018-001.AA513), C3 (no. RHP.30173-001.AA515)—Upper Val., Verrucosum Asz.; C2 (no. RHP.05135-002.AA521), D1 (no. RHP.26153-001.AA523)—Lower Val., Neocomiensiformis Az.; C1 (no. RHP.04210-001.AA519), D2 (no. RHP.04210-001.AA520), D3 (no. RHP.04179-026.AA524)—Lower Val., Pertransiens Az.

genus, *Conobelus*.

Castellanibelus? *bonti* Janssen, 2007, was created from a single specimen showing characters contradictory with the diagnosis of the genus (very shallow alveolar cavity, very dilated asymmetric shape, prominent alveolar groove…). Its leaf-like shape allows a very probable attribution to a malformed specimen of *Duvalia emerici* [Raspail, 1829]. The organ responsible for the presence of the alveolar groove has slipped laterally, inducing a flattening of one face and a bulging of the other [forma aegra *dissulcata* Keupp, 2012].

5.2. *Revision of the genus Castellanibelus*

Order Belemnitida Zittel, 1895
Suborder Belemnopseina Jeletzky, 1966
Family Duvaliidae Pavlow, 1914

Genus *Castellanibelus* [Combémorel, 1972]

Type species: *Belemnites orbignyanus* Duval-Jouve, 1841, Plate 8, Figures 4–9.

Diagnosis: Rostrum slender, up to 68 mm long; dorsoventrally depressed, except for very juvenile stages, which are sub cylindrical; anteriorly less depressed than posteriorly; slightly hastate in outline

and profile; dorsal alveolar groove narrow, not reaching mucronate apex; alveolus circular, reaching half of the rostrum in adult stage, ~18°; double lateral lines faint, sometimes reduced to simple flat surfaces.

Discussion: Combémorel [1972] established the genus *Castellanibelus* and assigned it to the family Duvaliidae. This classification was based on 3 rostra showing a dorsal position of the groove, opposite to the siphuncle. This observation is here confirmed for 62 studied specimens (Supplementary Information 3, Plate S5; Figures 1–6).

Castellanibelus differs from the other genera of Valanginian Duvaliidae (*Duvalia*, *Berriasibelus*, *Pseudobelus*) by its depression, which can be observed on the whole rostrum, more or less important depending on the area of the rostrum, the species and the ontogenic stage. Other characteristic features of the genus are the mucronate apex, the alveolar depth (18°, centred, 1/2 of the adult rostrum), the long narrow groove not reaching the apex and the presence of lateral lines.

Stratigraphic distribution: *Castellanibelus* is reported as soon as the Tithonian [Combémorel, 1972], it is common throughout the Lower Valanginian and basal Upper Valanginian (Verrucosum Az) where it represents about 20% of the total belemnite fauna (BF). Abundance decreases dramatically near the boundary of the Verrucosum Az/Peregrinus Az, only very rare specimens have been observed in the Peregrinus Az and Furcillata Az (0.4% of BF).

Geographical distribution: Southeast of France, the type species coming from the Castellane region which gave its name to the genus. Common in the Vocontian Basin (Alpes-de-Haute-Provence, Drôme, Hautes-Alpes, Ardèche, Gard). Reported from Switzerland [Ooster, 1857, Pictet and de Loriol, 1858, Mayer, 1866], Czech Republic [Vaňková, 2015] and Spain [Janssen, e.g. 1997, 2003].

Castellanibelus orbignyanus [Duval-Jouve, 1841]

Figures 10.B1–B3; Appendix 3, Plate S1, Figures 1–22

1841 *Belemnites orbignyanus* Duval-Jouve, p. 64–65, Plate 8, Figures 4–9.
non 1847 *Belemnites orbignyanus* Duval: Orbigny, p. 8–9, Plate 4, Figures 10–16.
1857 *Belemnites orbignyanus* Duval-Jouve: Ooster, p. 23, Plate 1, Figures 9–10.
non 1858 *Belemnites orbignyanus* Duval-Jouve: Pictet and Loriol, p. 8–9, Plate 1, Figures 6–7.
1866 *Belemnites picteti* Mayer, p. 366.
non 1867 *Belemnites orbignyanus* Duval-Jouve: Pictet, p. 54, Plate 8, Figure 2.
non 1868 *Belemnites orbignyanus* Duval-Jouve: Pictet, p. 217–218, Plate 36, Figure 3.
non 1873 *Belemnites orbignyanus* Duval: Gilliéron, p. 204–205, Plate 8, Figure 11.
1878 *Hibolites orbignyi* Duval: Bayle, atlas Plate 31, Figures 9–12.
non 1890 *Belemnites orbignyi* Duval: Toucas, p. 587–588, Plate 15, Figures 1–3.
? 1920 *Conobelus orbignyanus* Duval-Jouve: Bulow-Trummer, p. 177–178.
? 1963 *Curtohibolites orbignyanus* (Duval-Jouve): Stoyanova-Vergilova, p. 214–215, Plate 1, Figure 1.
pars 1972 *Castellanibelus orbignyanus* (Duval-Jouve, 1841): Combemorel, p. 75–77, Plate A, non Figures 12–14.
non 1988 *Curtohibolites orbignyanus* (Duval-Jouve): Ali-Zade, p. 394–395, Plate 1, Figure 4.
pars 2003 *Castellanibelus orbignyanus* (Duval-Jouve): Janssen, p. 142–143, Plate 2, Figures 11–12, non Figures 6–7, 13–14.
pars 2018 *Castellanibelus orbignyanus* (Duval-Jouve): Janssen, p. 175, Figures 7: 7–9, ?18–21, non 10–11.

Type: Type-species of the genus, introduced by Duval-Jouve [1841]. One adult and two juvenile specimens are designated here as paratypes (Figures 10B1–B3).

Material: 386 rostra, Valanginian, Southeast France.

Measurements: adult mean values ($n = 44$)

ica = 0.95; icp = 0.90; iddv = 1.12; idlat = 1.06; apex angle = 52°.

Diagnosis: Rostra medium size, maximum observed length 60 mm; slightly depressed anteriorly and posteriorly, increasing posteriorly with age (icp mean: juveniles' 0.97 to adults' 0.90); dorsal side tending to flatten with age; moderate dilatation; long alveolar groove extending into apical region, not reaching the apex; apical region short to very short, becoming obtuse, apical angle increasing with age (juveniles' mean 39°, adults' mean 52°, up to 68°); mucro centred or slightly offset dorsally.

Differential diagnosis: *C. orbignyanus* differs from related species (*C. suborbignyanus*, *C. vaubel-*

lensis) by its short apical region and its very obtuse apex and from *C. toucasi* by its lesser depression and its obtuse apex and its more centred mucro.

Stratigraphic distribution: Reported by authors in the Berriasian [Pictet, 1867, Toucas, 1890]; rare at the base of the Valanginian (Pertransian Az 14% of all *Castellanibelus* specimens), getting common in the Neocomiensiformis Az and Inostranzewi Az. *C. orbignyanus* reaches its acme in the Verrucosum Az (33%) and is very rare from the Peregrinus Az onwards. The last occurrence is found in the Nicklesi Asz.

Geographic distribution: Common in the Vocontian Basin (Southeast France), reported from Switzerland [Ooster, 1857, Pictet and de Loriol, 1858, Mayer, 1866], Czech Republic [Vaňková, 2015] and Spain [Janssen, e.g. 1997, 2003].

***Castellanibelus suborbignyanus* [Toucas, 1890]**
Figures 10.C1–C3; Appendix 3, Plate 2, Figures 1–23.

? 1847 *Belemnites orbignyanus* Duval: Orbigny, Plate 4, Figure 15.
1867 *Belemnites orbignyanus* Duval-Jouve: Pictet, p. 54, Plate 8, Figure 2.
1868 *Belemnites orbignyanus* Duval-Jouve: Pictet, p. 217–218, Plate 36, Figure 3.
? 1873 *Belemnites orbignyanus* Duval: Gillieron, p. 204–205, Plate 8, Figure 11.
1890 *Belemnites orbignyi* Duval-Jouve var. *surborbignyi* Toucas, p. 588, Plate 15, Figure 2.
1997 *Castellanibelus* sp. A Janssen, p. 6, 8, Plate 3, Figures 7–8.
pars 2003 *Castellanibelus orbignyanus* [Duval-Jouve, 1841]: Janssen, Plate 2, Figures 13–14.

Type: Variety of *Belemnites orbignyanus* introduced by Toucas [1890], raised to the species status here. One adult and two juvenile specimens are designated here as paratypes (Figures 10C1–C3).

Material: 174 rostra, Valanginian, Southeast France.

Measurements: adult mean values ($n = 17$)
ica = 0.94; icp = 0.90; iddv = 1.09; idlat = 1.07; apex angle = 31°.

Diagnosis: Rostra maximum observed length 60 mm; slight depression anteriorly and posteriorly; increasing posteriorly with age (icp mean: juveniles' 1.00 to adults' 0.90); very moderate dilation (around 1.08 in dorsal and lateral views) shape tending towards sub-cylindrical; distinctive dorsal alveolar groove, slightly shorter than in other *Castellanibelus*; apical region elongate, with very acute (juveniles, mean 21°) to acute (adults, mean 31°) apical angle; mucro centred or slightly dorsally offset.

Differential diagnosis: *C. suborbignyanus* differs from other species of *Castellanibelus* by the greater length of its posterior part. This gives it an acute alveolar angle and an elongated outline/profile, more sub cylindrical, and by its slightly shorter dorsal groove.

Stratigraphic distribution: Reported by Pictet [1867] and Toucas [1890] in the Berriasian. Present from the base of the Valanginian [Janssen, 1997, this study], in the Pertransiens Az (7% of all *Castellanibelus* specimens), its population remains around 12% up to the top of the Verrucosum Az., very rare above. One specimen found at the top of the Valanginian (Callidiscus Asz).

Geographic distribution: Southeast of France [Pictet, 1867, Toucas, 1890; this study], Switzerland [Pictet, 1868] and southeast of Spain [Janssen, 1997, 2003].

***Castellanibelus vaubellensis* Janssen, 2018**
Figures 10.A1–A3; Appendix 3, Plate 3, Figures 1–20.

1890 *Belemnites orbignyi* Duval-Jouve var. *jouvei* Toucas, p. 588, Plate 15, Figure 3.
1972 *Castellanibelus orbignyanus* (Duval-Jouve): Combemorel, Plate A, Figures 12–14.
pars 2018 *Castellanibelus vaubellensis* Janssen, p. 175–176, Figures 7.5–6, non 1–4.

Type: The holotype of Janssen, 2018 is here supplemented by three paratypes: one adult and two juvenile specimens (Figures 10A1–A3).

Material: 579 rostra, Valanginian, Southeast France.

Measurements: Adult mean values ($n = 77$)
ica = 0.94; icp = 0.91; iddv = 1.14; idlat = 1.11; apex angle = 41°.

Diagnosis: Rostra as long as 68 mm and slightly depressed anteriorly and posteriorly; the depression increases with age (icp mean: juveniles 1.01, adult 0.91), the flattening of the dorsal side being compensated by a characteristic bulge of the ventral side; the dilation is moderate (mean 1.13) but can be more accentuated (up to 1.39) giving individuals a more hastate outline/profile, both dorsoventrally and laterally; dorsal furrow long, fading at the maximum width, apical part of median size (juv. 31°, adult

41°); mucro intermediate in position, between centred and dorsal.

Differential diagnosis: *C. vaubellensis* is distinguished by the median length of its posterior part, between the obtuse part of *C. orbignyanus* and the acute part of *C. suborbignyanus*. It differs from *C. toucasi* by its less pronounced depression and swollen ventral side in the posterior part.

Stratigraphic distribution: Reported by Toucas [1890] from the Berriasian and by Janssen [2018] from the Lower Valanginian (Neocomiensisformis Az), *C. vaubellensis* is common from the base of the Valanginian (Pertransiens Az, ~13% of all *Castellanibelus* specimens) and becomes the dominant species from the Inostranzewi Az. Abundance of *C. vaubellensis* peak in the Verrucosum Az (~47% of all *Castellanibelus* specimens) before declining abruptly at the transition with the Peregrinus Az. Very rare above the Peregrinus bundle, the last occurrences were found in the Furcillata Asz.

Geographic distribution: Southeast of France [Toucas, 1890, Janssen, 2018; this study].

***Castellanibelus toucasi* sp. nov.**

Figures 10.D1–D3, Appendix 3, Plate 4, Figures 1–22

? 1858 *Belemnites orbignyanus* Duval-Jouve: Pictet and Loriol, p. 8–9, Plate 1, Figures 6–7.
? 1972 *Castellanibelus orbignyanus* (Duval-Jouve): Combemorel, p. 81, Plate 3.
2002 *Castellanibelus* sp. B sp. nov. Janssen and Clement, p. 520
2003 *Castellanibelus* sp. A Janssen, p. 144, Plate 2, Figures 3–7.
pars 2018 *Castellanibelus orbignyanus* [Duval-Jouve, 1841]: Janssen; Figures 7.10–11.
pars 2018 *Castellanibelus vaubellensis* nov. sp. Janssen, Figures 7.3–4.

Locus typicus: 04200 Saint-Geniez, Alpes-de-Haute-Provence.

Stratum typicum: base of the Pertransiens Az.

Derivatio nominis: in homage to Aristide Toucas [1843–1912] who was the first to observe the variability within the genus *Castellanibelus*.

Type series: Adult holotype (Figure 10D3, no. 3028), Pertransiens Az, Lower Valanginian, Saint-Geniez locality. Paratypes: very juvenile (Figure 10D1, no. 43568), Neocomiensiformis Az, lower Valanginian, Laborel locality; juvenile (Figure 10D2, no. 88233), Pertransiens Az, Lower Valanginian, Soleilhas locality.

Material: 319 rostra, Valanginian, Southeast France.

Measurements: Adult mean values ($n = 23$)

ica = 0.91; icp = 0.83; iddv = 1.15; idlat = 1.04; apex angle = 45°.

Diagnosis: Rostra with a maximum length of 63 mm; markedly depressed anteriorly and more posteriorly (mean icp 0.87, up to 0.75 for adults); dorsal and ventral sides flattening, inducing an oval to sub quadrangular posterior cross-section; moderate dilation, especially in lateral view (mean idlat 1.09); long dorsal groove, extending apically without reaching apex; apical part of median size, apical angle increasing with age (juveniles' mean: 32°, adults' mean: 45°, up to 50°); mucro dorsally offset in juvenile stage, dorso-centred thereafter.

Differential diagnosis: *C. toucasi* differs from other species of *Castellanibelus* by its anteriorly and posteriorly more marked depression (*C. toucasi* mean icp = 0.87; other *Castellanibelus* mean icp ≈ 0.94), its dorso-ventral flatness and its mucro tending towards a more dorsal position. Showing an apical angle close to that of *C. vaubellensis*, it differs in its posterior sub-quadrangular cross-section and in the absence of the ventral bulge observed in *C. vaubellensis*.

Stratigraphic distribution: *C. toucasi* occurs from the Berriasian to the mid-Valanginian. The species is frequent at the base of the Valanginian, in the Pertransiens Az (~76% of all *Castellanibelus* specimens). Its abundance gradually decreases and shows a clear decline from the Inostranzewi Az onwards. *C. toucasi* is rare in the Verrucosum Az (~7% of all *Cast.* specimens) and disappears in the Peregrinus Az (last occurrence at the base of the Peregrinus bundle).

Geographic distribution: Southeast of France [Combémorel, 1972; this study], Switzerland [Pictet and de Loriol, 1858] and southeast of Spain [Janssen, 2003].

Taxonomic key: The Figure 11 summarizes the different taxonomic variations.

6. Conclusions

A biometric study of 1762 rostra of the belemnite genus *Castellanibelus*, collected in the Valanginian marls of the Vocontian Basin (VB; Southeast France),

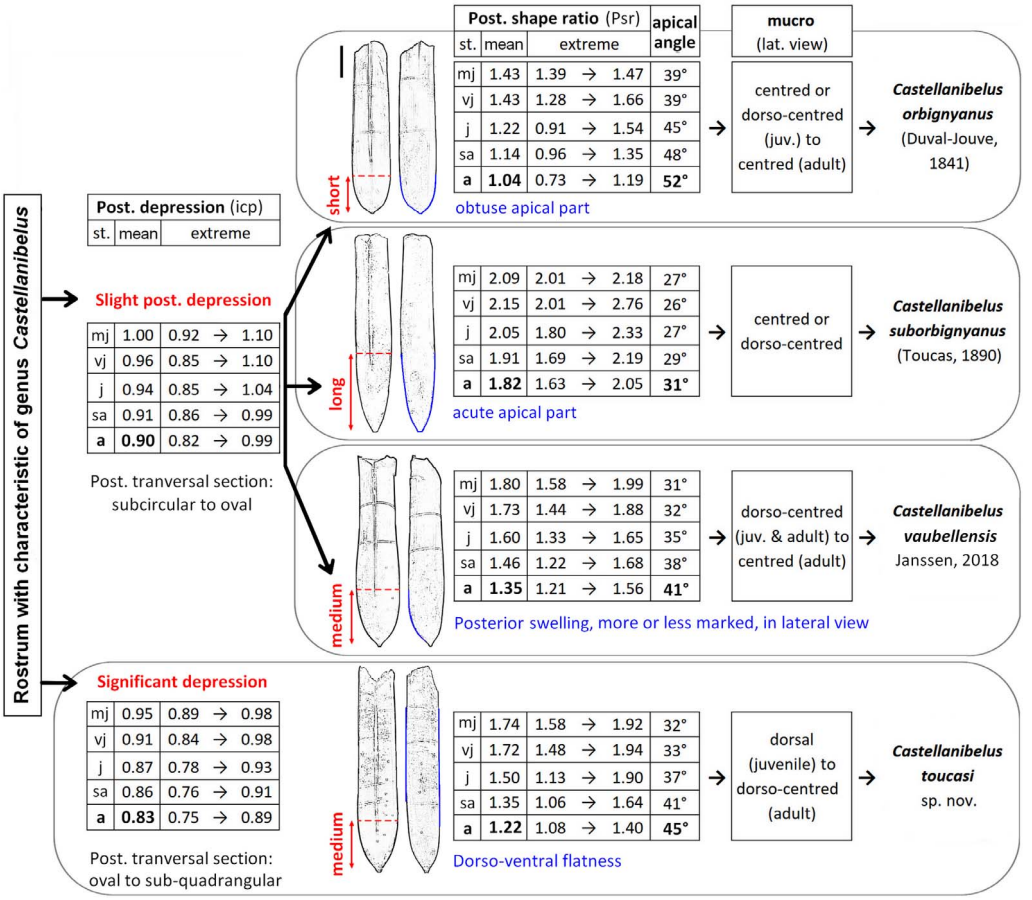

Figure 11. Taxonomic key of *Castellanibelus* species based on index values for the different ontogenetic stages.

has provided insights into the ontogeny, evolution and phylogeny of this group of cephalopods. In the VB, throughout the Valanginian, the genus *Castellanibelus* is common and evenly distributed in all five study areas and in stratigraphy, implying a cohesive distribution of belemnite faunas across the VB. In terms of abundance, *Castellanibelus* specimens represent about 1/5th of the entire Valanginian belemnite faunas in the Lower Valanginian-Upper Valanginian interval (from the *Thurmaniceras pertransiens* to the *Saynoceras verrucosum* ammonite zone). The genus becomes very rare from the middle Upper Valanginian onwards (base of the *Neocomites peregrinus* ammonite zone), with only a few occurrences in the Uppermost Valanginian. It disappears at the top of the stage.

Species of the genus *Castellanibelus* show an allometric growth. Juvenile forms have a sub-circular cross-section and an elongated shape. Adult forms show a depressed cross-section and a sub-cylindrical to slightly hastate shape.

Biometric data enable differentiation of four species of *Castellanibelus* varying by the degree of depression and shape of the apical part of the rostrum. The taxonomy of the species *Castellanibelus orbignyanus* [Duval-Jouve, 1841] and *Castellanibelus vaubellensis* [Janssen, 2018] has been revised. *Castellanibelus surborbignyanus* [Toucas, 1890] has been raised to the species level and one new species, *Castellanibelus toucasi* sp. nov. is proposed.

Conflicts of interest

The author has no conflict of interest to declare.

Acknowledgements

I would like to thank my husband, Patrick, for his unfailing support and involvement, my father, Gérard Thomel, who collected half of the specimens, Jörg Mutterlose and Thomas Saucède for their precious help and encouragement, and Didier Bert, curator of the Haute-Provence Geological Reserve, for his kind permission to carry out research.

Supplementary data

Supporting information for this article is available on the journal's website under https://doi.org/10.5802/crgeos.166 or from the author.

References

Challinor, A. B. (1979). The succession of Belemnopsis in the Heterian stratotype, Kawhia Harbour, New Zealand. *New Zealand J. Geol. Geophys.*, 22(1), 105–123.

Challinor, A. B. (1999). Belemnite biostratigraphy of the New Zealand Late Jurassic Mangaoran (Early Puaroan) Substage and the Puaroan Stage revisited. *New Zealand J. Geol. Geophys.*, 42(3), 369–393.

Christensen, W. (1975). Upper Cretaceous belemnites from the Kristianstad area in Scania. *Foss. Strat.*, 7, 1–69. Plate 1–12.

Christensen, W. (2000). Gradualistic evolution in Belemnitella from the middle Campanian of Lower Saxony, NW Germany. *Bull. Geol. Soc. Denmark*, 47, 135–163.

Combémorel, R. (1972). Position systématique de *Castellanibelus* nov. gen. et de trois espèces de bélemnites du Crétacé inférieur français. *Geobios*, 5(1), 67–81.

Combémorel, R. (1973). Les Duvaliidae Pavlow (Belemnitida) du Crétacé inférieur français. *Doc. Lab. Géol. Fac. sci. Lyon*, 57, 131–185.

d'Orbigny, A. (1847). *Paléontologie française, supplément : Terrains crétacés.* Arthus-Bertrand, Paris, France.

Ducrotay de Blainville, H.-M. (1827). *Mémoire sur les bélemnites, considérées zoologiquement et géologiquement.* Levrault ed., Strasbourg. Plate 1–5.

Duval-Jouve, J. (1841). *Bélemnites des terrains crétacés inférieurs des environs de Castellane (Basses-Alpes).* Fortin, Masson et Cie, Paris, France.

Gayte, D. and Combémorel, R. (1981). Vaunagites pistilliformis (Blainville) n. gen. Et V. nemausina n. sp., deux bélemnites remarquables du Crétacé inférieur du sud-est de la France. *Geobios*, 14(1), 105–113.

Hoffmann, R. and Stevens, K. (2019). The palaeobiology of belemnites - foundation for the interpretation of rostrum geochemistry. *Biol. Rev.*, 95(1), 94–123.

IGN (2022). Géoportail. https://www.geoportail.gouv.fr [accessed 21/02/2022].

Janssen, N. M. M. (1997). Mediterranean neocomian belemnites, part 1: Rio Argos sequence (Province of Murcia, Spain): the Berriasian-Valanginian and the Hauterivian-Barremian boundaries. *Scr. Geol.*, 114, 1–55.

Janssen, N. M. M. (2003). Mediterranean neocomian belemnites, part 2: the Berriasian-Valanginian boundary in southeast Spain (Río Argos, Cañada Lengua and Tornajo). *Scr. Geol.*, 126, 121–183.

Janssen, N. M. M. (2007). Records of new species of Duvaliidae Pavlow, 1914. *Scr. Geol.*, 135, 275–282.

Janssen, N. M. M. (2009). Mediterranean Neocomian belemnites, part 3 : Valanginian-Hauterivian belemnites. *Carnets de Géol.*, 09/01.

Janssen, N. M. M. (2018). Valanginian belemnites: New taxonomical and stratigraphical observations. *Carnets Geol.*, 18(7), 167–181.

Janssen, N. M. M. and Clément, A. (2002). Extinction and renewal patterns among Tethyan belemnites in the Verrucosum Subzone (Valanginian) of southeast France. *Cretac. Res.*, 23, 509–522.

Keupp, H. (2012). *Atlas zur Paläophatologie der Cephalopoden, Berliner Paläobiolog. Abh.* Inst. für Geologische Wiss., Fachrichtung Paläontologie, Berlin. t. 12.

Martinez, M. (2013). *Calibration astronomique du Valanginien et de l'Hauterivien (Crétacé inférieur): Implications paléeoclimatiques et paléeocéanographiques.* PhD thesis, Sciences de la Terre. Université de Bourgogne, https://tel.archives-ouvertes.fr/tel-00906955v2.

Mayer, Ch. (1866). Diagnoses de bélemnites nouvelles. *J. Conchyliol.*, 14, 358–369. 3ème série, t. 6.

Mutterlose, J., Schmid, F., and Spaeth, C. (1983). Zur Paläobiogeographie von Belemniten der Unter-Kreide in NW-Europa. *Zitteliana*, 10, 293–307.

Ooster, W. A. (1857). Céphalopodes acétabulifères. In *Catalogue des céphalopodes fossiles des Alpes suisses, 1ère partie*, pages 5–34. Société Helvétique des Sciences naturelles, Zurich, CH.

Pictet, F.-J. (1867). Etudes paléontologique sur la faune à Terebratula diphyoides de Berrias (Ardeche). In *Mélanges paléontologiques*, Mémoires de la SPHN, Ch, t. 1, pages 43–130. SPHN, Genève.

Pictet, F.-J. (1868). Etude provisoire des fossiles de la Porte-de-France, d'Aizy et de Lémenc. In *Mélanges paléontologiques*, Mémoires de la SPHN, CH, 1,4, pages 207–220. SPHN, Genève.

Pictet, F.-J. and de Loriol, P. (1858). Description des fossiles contenus dans le terrain néocomien des Voirons. Vol. 2. Description des animaux invertébrés. In Pictet, F.-J., editor, *Matériaux pour la paléontologie Suisse*, pages 1–64. Kessman, Geneve. 2ème série.

Raspail, F.-V. (1829). Histoire Naturelle des Bélemnites. In *Annales des Sciences d'Observation, tome I, Paris*.

Reboulet, S., Szives, O., Aguirre-Urreta, B., Barragán, R., Company, M., Idakieva, V., Ivanov, M., Kakabadze, M. V., Moreno-Bedmar, J. A., Sandoval, J., Baraboshkin, E. J., Çaglar, M. K., Fözy, I., González-Arreola, C., Kenjo, S., Lukeneder, A., Raisossadat, S. N., Rawson, P. F., and Tavera, J. M. (2014). Report on the 5th International Meeting of the IUGS Lower Cretaceous Ammonite Working Group, the Kilian Group (Ankara, Turkey, 31th August 2013). *Cretac. Res.*, 50, 126–137.

Spaeth, C. (1971). *Untersuchungen an Belemniten des Formenkreises um Neohibolites minimus (Miller 1826) aus dem Mittel- und Ober-Alb Nordwestdeutschlands*, volume 100 of *Beihefte zum Geologischen Jahrbuch*. German Geological Survey BGR, Hannover, Germany.

Toucas, A. (1890). Faune des couches tithoniques de l'Ardèche. *Bull. Soc. Géol. De France*, 14, 560–629. 3ème série, t. 18.

Vaňková, L. (2015). *Belemniti spodní křídy lokality Štramberk: taxonomie, stratigrafie, paleoekologie, paleobiogeografie*. PhD thesis, Univerzita Karlova v Praze, Přírodovědecká fakulta, Ústav geologie a paleontologie.

Weiss, A. F. (1991). Krevizii belemnitov roda Conobelus Stolley, 1919. *Paleontol. Ž.*, 2, 18–33.

Comptes Rendus
Géoscience — Sciences de la Planète
2022, Vol. 354, Special Issue S3, p. 45-65
https://doi.org/10.5802/crgeos.118

Integrated stratigraphy of the Jurassic and the Cretaceous: a tribute to Jacques Rey /
Stratigraphie intégrée du Jurassique et du Crétacé : un hommage à Jacques Rey

Coniacian–Campanian palynology, carbon isotopes and clay mineralogy of the Poigny borehole (Paris Basin) and its correlation in NW Europe

Martin A. Pearce [a, b], **Ian Jarvis** [*, b], **Johannes Monkenbusch** [c], **Nicolas Thibault** [c], **Clemens V. Ullmann** [d] **and Mathieu Martinez** [e]

[a] Evolution Applied Limited, 33 Gainsborough Drive, Sherborne, Dorset DT9 6DS, UK

[b] Department of Geography, Geology and the Environment, Kingston University London, Penrhyn Road, Kingston-upon-Thames KT1 2EE, UK

[c] Department of Geosciences and Natural Resource Management, University of Copenhagen, Øster Voldgade 10, DK-1350, Copenhagen C., Denmark

[d] Camborne School of Mines and the Environment and Sustainability Institute, University of Exeter, Penryn Campus, Penryn, Cornwall TR10 9FE, UK

[e] CNRS, Géosciences Rennes, Université de Rennes, UMR 6118, 35000 Rennes, France

E-mails: info@evolutionapplied.com (M. A. Pearce), i.jarvis@kingston.ac.uk (I. Jarvis), johannes.monkenbusch@web.de (J. Monkenbusch), nt@ign.ku.dk (N. Thibault), c.ullmann@exeter.ac.uk (C. V. Ullmann), mathieu.martinez@univ-rennes1.fr (M. Martinez)

Abstract. The Poigny borehole near Provins (Seine-et-Marne) provides the most complete single pristine section through the Upper Cretaceous Chalk of the Paris Basin. A well preserved and diverse palynoflora including 236 species and subspecies of organic-walled dinoflagellate cysts (dinocysts) is documented from the borehole, together with a high-resolution carbon-isotope curve ($\delta^{13}C_{carb}$) for the Coniacian–Campanian interval. Integration of the palynological and $\delta^{13}C_{carb}$ data provides a basis for a chemostratigraphic and biostratigraphic correlation to England and Germany. Carbon isotope events (CIEs) are used to refine the placement of sub-stage boundaries in the core, and to calibrate and correlate distinctive palynological events with those from other European sections. Thirty-three palynological events in the upper Coniacian–Campanian, judged to be of biostratigraphic significance, are described. Palynological assemblages, the peridinioid/gonyaulacoid (P/G) dinocyst ratio and clay mineralogy are compared to depositional sequences and implicate sea-level as a major driver of palaeoenvironmental change.

Keywords. Poigny borehole, Dinoflagellate cysts, Biostratigraphy, Santonian, Campanian, Carbon isotopes, Sea-level change.

Published online: 23 May 2022, Issue date: 13 January 2023

* Corresponding author.

1. Introduction

The Upper Cretaceous Chalk of the eastern Paris Basin close to Provins (Seine-et-Marne) was cored at Poigny and Sainte-Colombe by the Craie 700 programme in 1999 [Figure 1; Mégnien and Hanot, 2000]. The objective was to provide regional reference sections for the Chalk where the succession approaches its maximum preserved thickness in the Basin (>600 m, Figure 1), and to characterise large-scale diagenetic patterns that affect seismic wave velocity, variations in which had remained unexplained despite more than 50 years of petroleum exploration.

The Poigny area (Figure 1) displays "normal" Chalk seismic velocities while the Sainte-Colombe area was chosen to represent an area of anomalous fast velocities [Mégnien and Hanot, 2000]. These were shown to be caused by local bodies of dolomitized chalk: the Sainte-Colombe borehole includes a dolostone interval in the mid-Campanian and the underlying Campanian–Turonian chalks display pervasive diffuse (<15% dolomite) dolomitization [Gély and Blanc, 2004, Thiry et al., 2003]. By contrast, dolomite is absent from the Campanian at Poigny, and occurs as only a minor accessory mineral below, despite the site being located <3 km to the east of Sainte-Colombe.

The Poigny and Sainte-Colombe cores have been correlated and dated using a combination of lithostratigraphy and benthic foraminifera biostratigraphy, supplemented by macrofossil, calcareous nannofossil and organic-walled dinoflagellate cysts (dinocyst) records [Robaszynski et al., 2005], although the exact placement of stage boundaries has remained uncertain. Studies of the clay mineralogy, stable-isotope geochemistry, and sequence stratigraphy of the Upper Cretaceous succession in the Provins area have been largely confined to the Poigny core [Chenot et al., 2016, 2018, Deconinck et al., 2000, Lasseur, 2007, Le Callonnec et al., 2021], due to the diagenetic overprint at Sainte-Colombe.

2. Study succession

The Poigny Craie 701 borehole (48.5350° N, 3.2925° E) was continuously cored with a recovery approaching 98%; coring stopped in the lower Cenomanian at a depth of 700 m [Robaszynski et al., 2005]. The Coniacian–Campanian succession between 400–50 m depth is the focus of the present study. It comprises six lithostratigraphic units [Figure 2; Robaszynski, 2000, Robaszynski et al., 2005], from base to top:

(1) indurated white chalk with black and grey flints; abundant platyceramid bivalve debris occurs towards the top (427.6–371 m);
(2) flintless indurated bioturbated white chalk; numerous inoceramid fragments [*Platyceramus* gr. *mantelli*? (de Mercey), ?*Cladoceramus undulatoplicatus* (Roemer)] at the base are indicative of the lower Santonian (371–345 m);
(3) indurated greyish white chalk with scattered flints, becoming increasingly common with thin tabular flints towards the top; between 345–320 m the chalk is very poor in flint and has been fragmented into 3–5 cm thick "biscuits" by coring; a flaser marl is present around 310 m and a 3–4 cm marl at 285 m (345–285 m);
(4) flinty white chalk with grey bioturbation, becoming significantly less indurated upwards, soft and friable above 250–200 m; *Zoophycos* flints and inoceramid debris abundant towards the summit, the lower third includes small ?paramoudra flints (285–164 m);
(5) soft flintless white chalk with grey bioturbation bounded by two pairs of omission surfaces at its bottom (164.2–164.0, 162.6 m) and top (142.0, 140.0–139.9 m), and a bed of "brecciated" intraclastic chalk at 158.3 m (164–140 m);
(6) soft white bioturbated chalk with few flints; very rare black flints in the lower half, scattered black flints in the upper half; a fossiliferous interval from 106–92 m with fragments of oysters, bryozoa, sponges, a hexacoral and fish scales, includes numerous *Magas chitoniformis* (Schlotheim) (= *M. pumilus* of literature) brachiopods—*Magas* beds (140–34.75 m).

Between 600–317 m depth some beds contain dispersed (<2%) small dolomite rhombs [Blanc and Gély, 2000, Thiry et al., 2003]. Chalks above 60 m display increasing yellowish to brown discolouration and altered flints towards the Eocene unconformity at 34.75 m, particularly in the top 10 m. This is interpreted to represent the product of meteoric weathering below the unconformity.

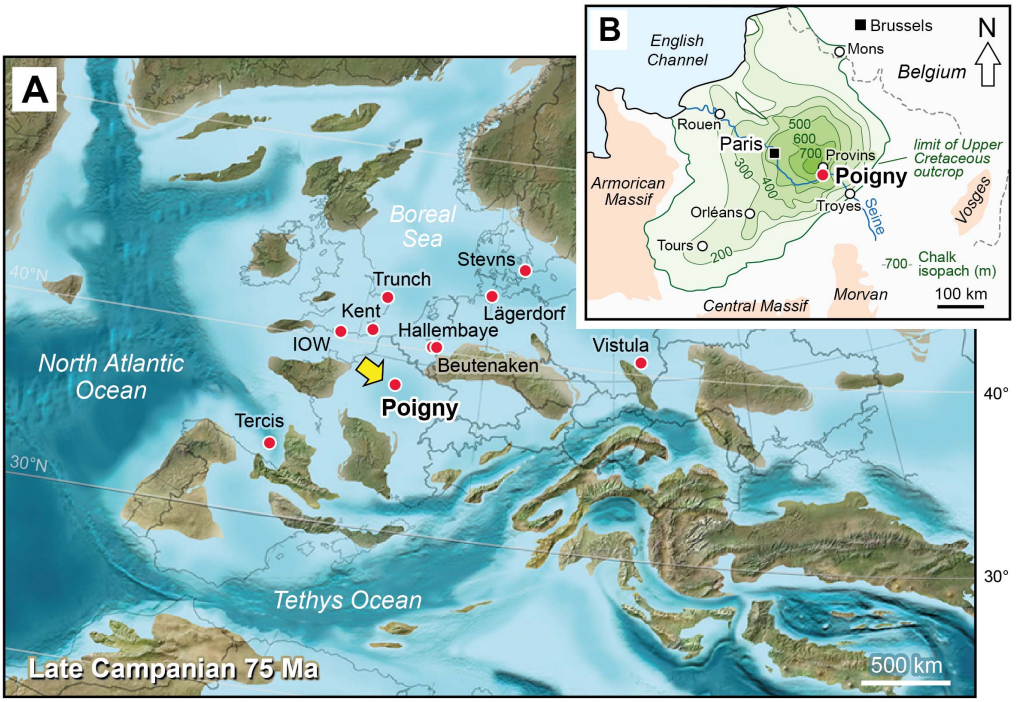

Figure 1. Campanian palaeogeography of Europe and geographic location of the Poigny borehole and comparative study sections. (A) Palaeogeographic map [modified from Blakey, 2012] with the location of sections discussed in this paper. Poland palaeogeography after Niechwedowicz et al. [2021]. IOW, Isle of Wight, Whitecliff; Vistula, Middle Vistula River. (B) Chalk isopach map of the Paris Basin [modified from Robaszynski et al., 2005].

3. Material and methods

3.1. *Carbon isotopes*

A total of 763 bulk sediment samples (50 g) were taken between 399.65–59.20 m depth (average spacing 45 cm) for stable isotope analysis from the Poigny core. Analytical methods are summarised in Supplemental Material A.

3.2. *Palynology*

For palynological analysis, 73 samples were selected from the carbon isotope sample set at approximately 5 m intervals (Figures 2, 3). Analytical methods are described in Supplemental Material A.

4. Carbon isotope stratigraphy

Chenot et al. [2016] presented carbon and oxygen isotope curves for the upper Santonian–Campanian of Poigny based on bulk carbonate samples taken at 1 m intervals between 309 m and 50 m depth (Figure 2). The new higher resolution $\delta^{13}C_{carb}$ curve for the upper Coniacian–Campanian (400–58.5 m) obtained during the present study is plotted in Figure 2, together with the data of Chenot et al. [2016]. Excellent agreement exists for the overlapping upper Santonian–Campanian section.

Correlation of the Poigny $\delta^{13}C_{carb}$ profile with carbon isotope curves for equivalent aged successions from the southern North Sea Basin at Trunch, eastern England [Figure 1; Jarvis et al., 2002, 2006, Jenkyns et al., 1994, Linnert et al., 2018], and from Lägerdorf in the North German Basin [Voigt and Schönfeld, 2010] shows remarkably similar trends and $\delta^{13}C_{carb}$ values (Figure 2). This enables the correlation of the overall long-term trends and short-term positive and negative excursions, with the recognition of all previously named carbon isotope events (CIEs) defined for the upper Coniacian–Campanian [Jarvis

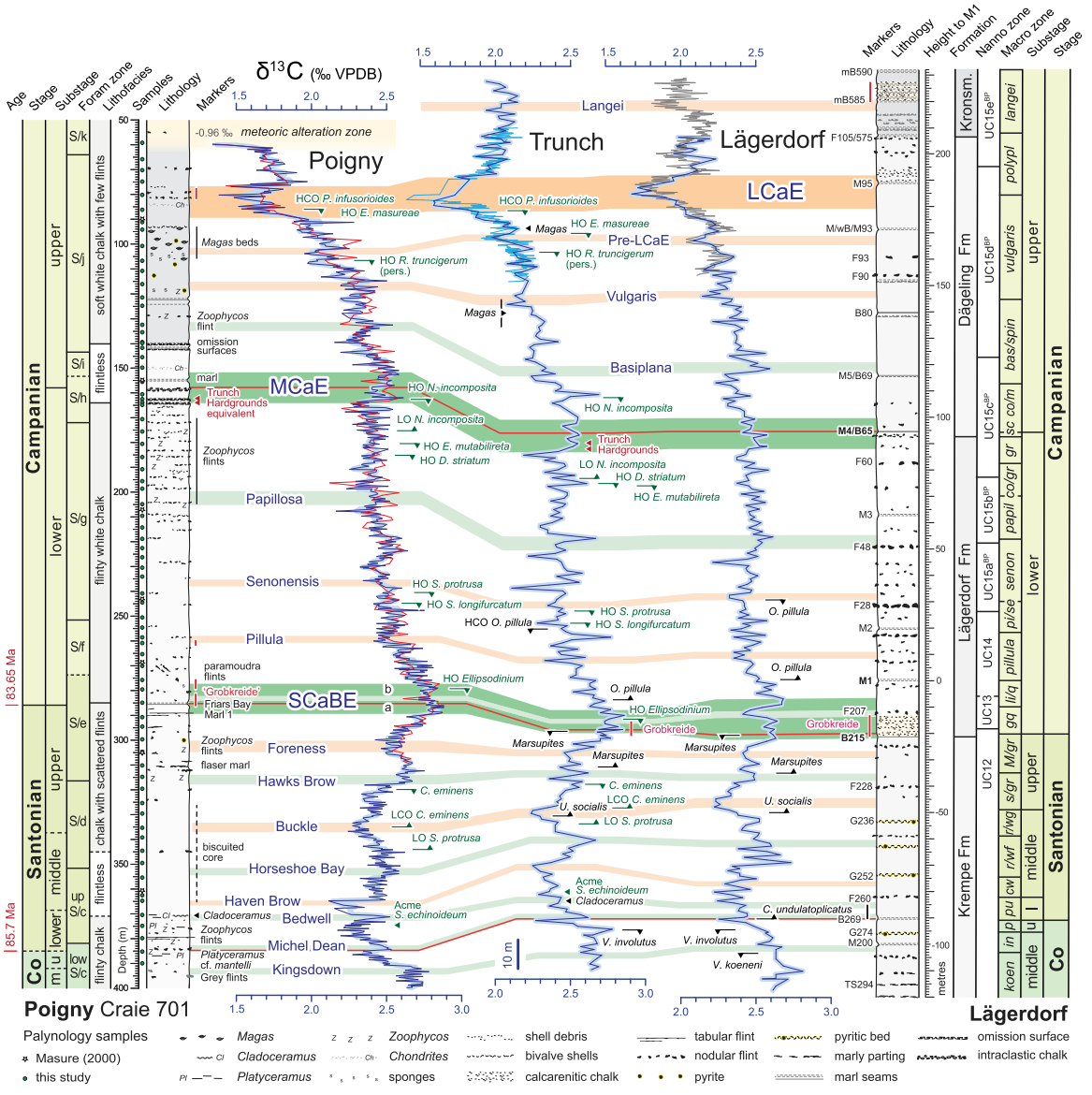

Figure 2. Coniacian–Campanian stratigraphy and carbon isotope event correlation of the Poigny borehole with the English Chalk Trunch borehole and Lägerdorf quarries, north Germany. Carbon isotope event terminology modified after Jarvis et al. [2002, 2006], Linnert et al. [2018], Perdiou et al. [2016], and Thibault et al. [2016]. Ages from GTS2020 [Gale et al., 2020]. Poigny benthic foraminifera zonation and stratigraphy from Robaszynski et al. [2005] with revisions based on this study; $\delta^{13}C$ data from Chenot et al. [2016, thin red line] and this study (blue curves; thick pale blue curve is 3-point moving average). Selected dinocyst datum levels (this study, green text and symbols) are indicated. Trunch data compiled from Jarvis et al. [2002, 2006], Jenkyns et al. [1994], and Linnert et al. [2018, medium blue curve]; macrofossil datum levels (black symbols and text) from Morter et al. [1975], Pearce et al. [2020] and Wood et al. [1994]. Lägerdorf carbon isotope data from Voigt et al. [2010, grey curve is Lägerdorf–Heidestrasse]. Calcareous nannofossil zones after Burnett et al. [1998]. Lägerdorf macrofauna datum levels from Schulz et al. [1984]; zone terminology, abbreviations and relative thicknesses of units after Voigt et al. [2010]. Co, Coniacian; l, lower; m, middle; u, upper; Kronsm., Kronsmoor Formation.

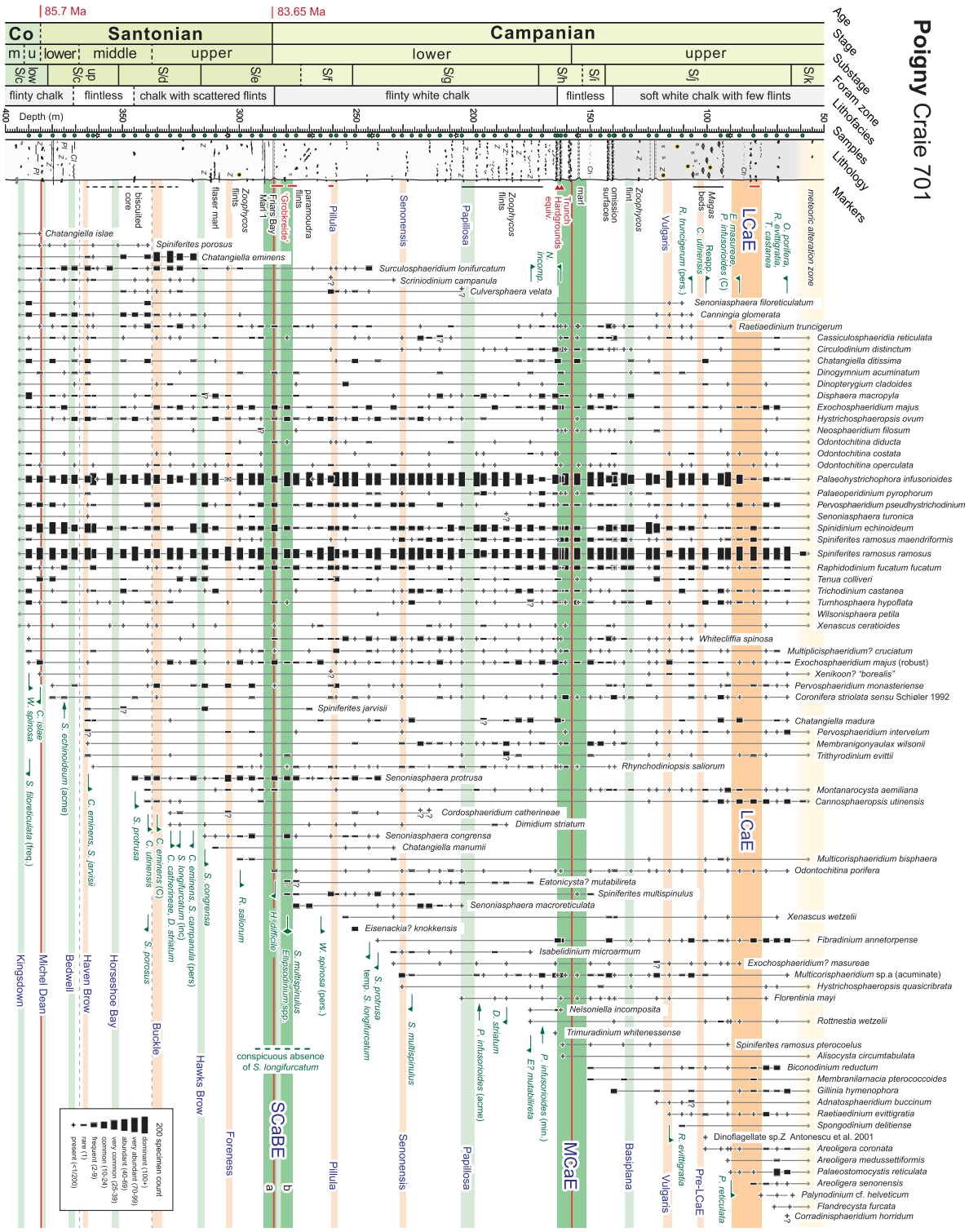

Figure 3. Range chart of stratigraphically significant dinocysts for the Coniacian–Campanian of the Poigny borehole. Stratigraphy after Figure 2.

et al., 2002, 2006, Linnert et al., 2018, Perdiou et al., 2016, Thibault et al., 2016]. The three most significant CIEs: Santonian–Campanian Boundary Event (SCaBE); Mid-Campanian Event (MCaE); and Late Campanian Event (LCaE), are named by reference to their subage positions [cf. Chenot et al., 2016, Cramer and Jarvis, 2020, Jarvis et al., 2002]. Subsidiary Coniacian–Santonian events are named principally after English Chalk marker beds, following Jarvis et al. [2006]. Secondary Campanian events are named by reference to their stratigraphic position within the macrofossil biozonation at Lägerdorf [Figure 2; cf. Thibault et al., 2016].

The top of the Poigny core above 61 m displays anomalous large negative excursions in $\delta^{13}C_{carb}$ and $\delta^{18}O_{carb}$, with values falling to −0.96‰ and −2.6‰ respectively at 54–55 m; these values are 2.4‰ $\delta^{13}C_{carb}$ and 1.1‰ $\delta^{18}O_{carb}$ lower than the immediately underlying succession and clearly separated from other samples on a $\delta^{13}C_{carb}$ vs. $\delta^{18}O_{carb}$ cross plot [Chenot et al., 2016, figure 6]. The excursions are attributed to meteoric alteration below the Eocene unconformity, further evidenced by yellow and brown staining and Mg- and Sr-depletion of the chalks above 60 m [Le Callonnec et al., 2000]. Our single palynological sample from this interval at 59.2 m yielded a very low abundance (<1 palynomorph per gram; ppg) and highly impoverished assemblage (Figure 3), consistent with partial oxidation of the organic fraction.

The bases of the Santonian, lower Campanian, and upper Campanian in the Poigny succession, estimated to be between 380–371 m, 290–285 m and 197–165.2 m, respectively by Robaszynski et al. [2000, 2005], are placed here using correlation of the CIE stratigraphy at: 385 m, 285 m, and 158 m (Figure 2). Overall, a succession of 17 CIEs is recognised in the middle Coniacian–upper Campanian at Poigny, offering a substantial improvement in stratigraphic resolution. Limited macrofossil records and key dinocyst marker levels occurring at both Poigny and Trunch (Figure 2) are fully consistent with the carbon isotope stratigraphy. Of note are: (1) records of *Cladoceramus undulatoplicatus* attributed to the level of the Bedwell CIE; (2) the presence of coarse-grained calcarenitic chalks within the SCaBE interval, noted by Lasseur [2007] at Poigny (red bars in Figure 2), and typified by the Grobkreide at Lägerdorf [Niebuhr, 2006]; (3) paired omission surfaces at the base of the MCaE at Poigny correlative to the Trunch Hardgrounds; (4) records of *Magas chitoniformis* brachiopods at the level of the Pre-LCaE at both Poigny and Trunch.

Based on our carbon isotope correlation (Figure 2), the base of the upper Coniacian is tentatively placed at the top of the Kingsdown CIE at 392 m, the base of the middle Santonian at 368 m, midway between the Bedwell and Haven Brow CIEs, and the base of the upper Santonian is equated to the base of the Buckle CIE at 347 m. The marl seam at 285 m, situated within the SCaBE, is correlated to Friars Bay Marl 1 in southern England [cf. Thibault et al., 2016] rather than the Old Nore Marl, as proposed by Robaszynski et al. [2005].

5. Palynology results

A summary relative abundance range chart of selected taxa is presented in Figure 3; the entire data set is provided in Supplemental Materials B–D. Absolute abundance, specific diversity profiles and stratigraphic changes in the palynological assemblage are presented in Figure 4. Species occurrences from the preliminary palynological study of the middle Santonian to upper Campanian section by Masure [2000, seven samples at an average spacing of ~40 m] are indicated on Figure 3 by pale green filled stars.

The palynoflora is diverse with a total of 236 species and subspecies of dinocysts recorded through the section (Supplemental Material B; taxa grouped in undifferentiated genera—i.e., *Alterbidinium* spp.—and the probable ecdysal pellicles of the Dinogymnioideae are included in the sum; questionable specimens are counted separately—Supplemental Material C). Assemblages are dominated by subequal amounts of *Palaeohystrichophora infusorioides* and *Spiniferites ramosus* (typical of the *Spiniferites–Palaeohystrichophora* (S–P) assemblage; [Jarvis et al., 2021, Pearce et al., 2003, 2009, Prince et al., 2008]), although some significant fluctuations exist in the former.

Palynomorph abundance, dinocyst species richness and diversity, and acritarch and algae abundances all generally decrease upwards through the Santonian. An abundance minimum occurs in the mid-upper Santonian and a diversity minimum coincident with a maximum in the

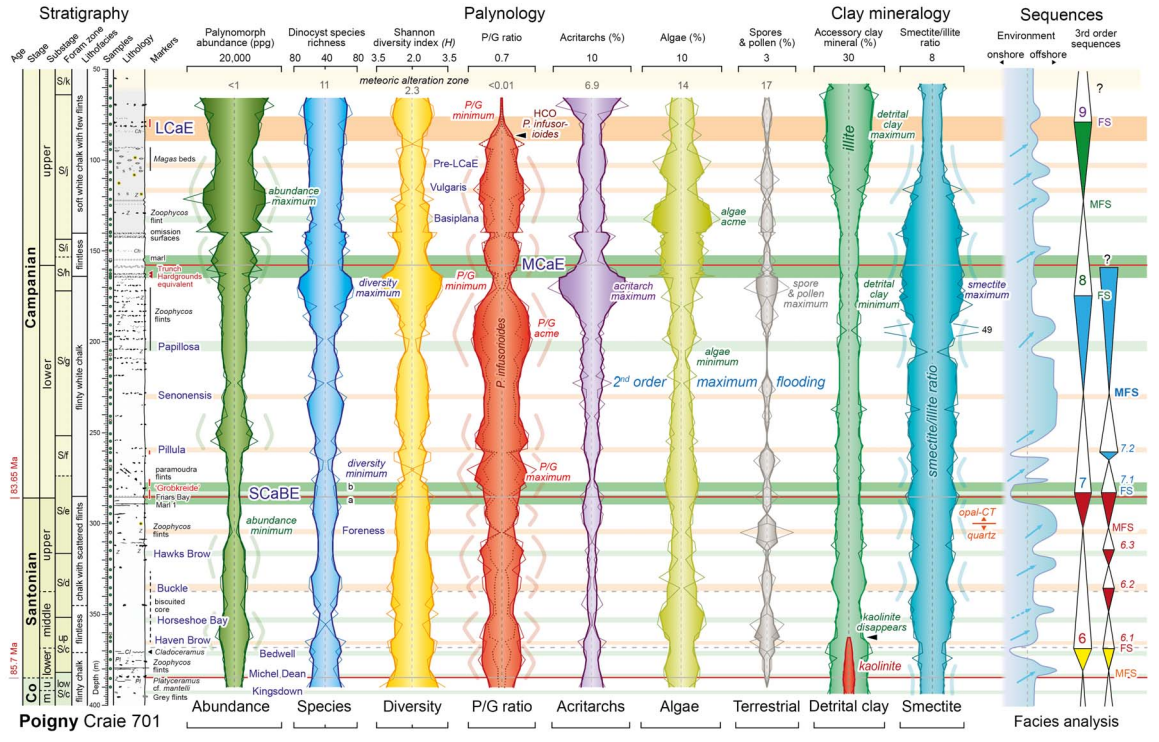

Figure 4. Stratigraphy, palynomorph abundance, dinocyst assemblage parameters and clay mineral assemblage plots, and third-order sequences for the Coniacian–Campanian of the Poigny borehole. P/G ratio = species number of peridinioid/gonyaulacoid cysts. Stratigraphy and carbon isotope events (coloured horizontal bars with blue annotation) follow Figure 2. Shaded areas and thick coloured lines are 3-point moving averages of individual sample data (thin lines; Supplemental Material C). Grey numerals in the meteoric alteration zone are for sample at 59.20 m. Clay mineralogy from Deconinck et al. [2000]. Sequences from Lasseur [2007] based on sediment microfacies analysis.

peridinioid/gonyaulacoid (P/G) dinocyst ratio occurs in the lowest Campanian, immediately above the SCaBE.

Abundance, species richness and diversity generally increase through the lower Campanian with a diversity maximum accompanying acritarch and terrestrial palynomorph maxima and a marked P/G ratio minimum at the top of the substage, immediately below the MCaE. An algae minimum and subsequent P/G acme, dominated by high numbers of *P. infusorioides* (Figures 3, 4), precede the diversity maximum.

A palynomorph abundance maximum occurs in the upper Campanian around the level of the Vulgaris CIE, above an algae acme centred on the Basiplana CIE, below. A crash in numbers of *P. infusorioides* at the base of the LCaE leads to a marked P/G minimum spanning the LCaE, despite significant increases in palynomorph abundance.

In addition to the long-term trends summarised above, many of the parameters show a cyclic pattern at a decametre scale. This is particularly evident in the P/G ratio, which is controlled largely by variation in the abundance of *P. infusorioides* (Figure 4). This is discussed further below (Section 8).

6. Dinocyst biostratigraphy of the Coniacian–Campanian

Results from the Poigny borehole may be compared to similar high-resolution palynology data from key European sites (Figure 1), in Belgium (Hallembaye quarry), Denmark (Stevns-1 borehole),

England (Whitecliff outcrop, Isle of Wight; Kent outcrops; Trunch borehole), France (Tercis outcrop), The Netherlands (Beutenaken quarry), and Poland (Middle Vistula River outcrops) that are constrained by CIE chemostratigraphy and/or, macro- or microfossil biostratigraphy. Following a brief description of the comparable sections, stratigraphically significant events are discussed.

6.1. *Summary of comparable stratigraphic sections*

6.1.1. *Belgium and the Netherlands*

Slimani [2001] carried out a sub-1 m resolution study of 21 samples through ~20 m of the uppermost lower Campanian to upper Campanian of Beutenaken quarry (The Netherlands). A slightly lower resolution study was undertaken through the uppermost lower Campanian to upper Maastrichtian section of Hallembaye quarry (Belgium) located 15 km to the west (Figure 1). At Hallembaye, 26 samples were studied at an average spacing of ~3 m through the ~80 m uppermost lower Campanian to upper Maastrichtian section, with 11 samples restricted to the Campanian. Both quarries benefit from a belemnite biozonation for calibration. Only relative abundance data were presented by Slimani [2001]; however, the assemblages are very diverse and some subtle changes in relative abundance are clearly recognisable.

6.1.2. *Denmark*

Surlyk et al. [2013] carried out a multidisciplinary study of the Stevns-1 core containing one of the most expanded upper Campanian–Maastrichtian successions worldwide. Among other disciplines, nannofossil and dinocyst palaeontology, and $\delta^{13}C_{carb}$ data were provided; $\delta^{13}C_{carb}$ correlations to Lägerdorf–Kronsmoor [Thibault et al., 2012, figure 8] and to Gubbio [Surlyk et al., 2013, figure 3] indicate that the base of the Stevns-1 core lies some distance above the LCaE, and is therefore above the top of the Poigny core. However, the presence, absence, or relative abundance of dinocyst species in Stevns-1 have important implications for the palynostratigraphy.

6.1.3. *England*

Prince et al. [1999] presented a ~1 m scale palynology study of 98 samples from the lower Santonian to lower Campanian (upper *Offaster pillula* Zone) outcrop section at Whitecliff (Isle of Wight). The section is calibrated by macrofossil zones and benefits from a previous $\delta^{13}C_{carb}$ study by Jenkyns et al. [1994].

Prince et al. [2008] documented the results of a study of dinocysts from the entire Coniacian–Santonian Chalk succession in Kent based on 139 1-m spaced samples from six overlapping outcrop sections. Results of a study of the Coniacian succession at Whitecliff (70 samples) supplemented the data obtained from the higher section by Prince et al. [1999]. Jenkyns et al. [1994] summarised the stratigraphy and presented stable isotope curves for a composite Kent section, constructed using data from the same localities as Prince et al. [2008].

Pearce et al. [2020] studied 267 samples from the lower Cenomanian to mid-lower Campanian (lowermost *Gonioteuthis quadrata* Zone) of the Trunch borehole (Norfolk) also at ~1 m resolution. A palynological study of the remaining Campanian to lowermost Maastrichtian is ongoing, although preliminary ranges of new species were reported by Pearce [2010] and some significant events are documented here as personal observations (pers. obs.). Jenkyns et al. [1994] presented $\delta^{13}C_{carb}$ data for the Campanian of the Trunch borehole, which was extended to the lower Cenomanian by Pearce et al. [2020].

6.1.4. *France*

The quarry at Tercis-les-Bains near Dax in Landes, SW France, is the Global Boundary Stratotype Section and Point (GSSP) for the Campanian–Maastrichtian boundary [Figure 1; Gale et al., 2020]. Antonescu et al. [2001a] provided presence/absence palynology information for 39 samples (with 31 in the upper Campanian) at an average sampling spacing of ~4 m from the section, while Schiøler and Wilson [2001] presented full quantitative counts at an average spacing of ~12 m (with eight in the upper Campanian). Collectively, these studies span a total of ~160 m (with ~115 m in the upper Campanian). Multidisciplinary biostratigraphic analyses (ammonites, benthic and planktonic foraminifera, calcareous nannofossils, ostracods, spores and pollen) were also conducted [see Odin, 2001]. Walaszczyk et al. [2002] subsequently erected an inoceramid zonation and of particular interest is the recognition of the "*Inoceramus*" *redbirdensis* Zone that spans the Campanian–Maastrichtian boundary.

A $\delta^{13}C_{carb}$ record for Tercis les Bains was presented by Voigt et al. [2012]. Although Voigt et al. [2012] recognised many of the sampled horizons used by Odin [2001], the direct placement of their $\delta^{13}C_{carb}$ samples in the biostratigraphic framework had to be estimated from their position relative to marker beds. We interpret the broad positive excursion in $\delta^{13}C_{carb}$ values from 6–14 m [Voigt et al., 2012, figure 3] to be the MCaE, as proposed previously by Perdiou et al. [2016].

6.1.5. *Poland*

Niechwedowicz et al. [2021] and Niechwedowicz and Walaszczyk [2022] presented a detailed palynology and inoceramid biostratigraphy of the Middle Vistula River composite outcrop section. Samples (182) from seven sections across an ~80 m upper Campanian to lower Maastrichtian composite section were analysed at <1 m resolution, producing the most detailed palynological study of the boundary interval to date. From five of the sections (Piotrawin, Raj, Raj North, Podole and Kłudzie North) 138 samples are from the upper Campanian with one sample taken from the distinctive Campanian–Maastrichtian "boundary marl" that occurs within the "*I.*" *redbirdensis* inoceramid Zone.

The stratigraphically lowest sample in the composite succession (Piotrawin) was assigned to the "*Inoceramus*" *altus* Zone, defined by the lowest stratigraphic occurrence of the nominate species. The lowest occurrence of "*I.*" *altus* at Tercis [Walaszczyk et al., 2002] was placed at the minimum of the LCaE by Voigt et al. [2012]. The LCaE occurs close to the top of the Poigny core (Figure 2) so there may be a small stratigraphic overlap between Poigny and the Middle Vistula River composite section.

6.2. *Dinocyst and acritarch biostratigraphic events*

Biostratigraphically significant dinocyst and acritarch events from the Aquitaine Basin (Tercis), Anglo-Paris Basin (Poigny, Whitecliff Isle of Wight, Kent), North Sea Basin (Beutenaken, Hallembaye, Stevns-1, Trunch) and Mid-Polish Basin (Middle Vistula River) are discussed below, from the stratigraphically lowest occurrence (LO) to highest occurrence (HO), and are summarised in Supplemental Material D. For the uppermost Coniacian to lower Campanian, only the Whitecliff and Kent composite outcrops, and the Trunch borehole have overlapping sections with Poigny. For the remainder of the Campanian, comparable sections from Beutenaken, Hallembaye, Stevns-1, Middle Vistula River, and personal observations from the Trunch borehole are available.

6.2.1. *Upper Coniacian events*

(1) LO of *Whitecliffia spinosa:* Pearce et al. [2020, section 7.5.1] described the temporal and spatial distribution of *W. spinosa* and stated that the LO has been recorded in the Coniacian. *Whitecliffia spinosa* is rare and sporadic in the Santonian but a specimen in the lowest studied sample from Poigny at 390 m between the Kingsdown and Michel Dean CIEs (Figure 3), confirms its presence in the upper Coniacian.

(2) Increase in *Senoniasphaera filoreticulata*: This species was described by Slimani [1994, as *Cyclonephelium filoreticulatum*] from the upper Campanian at Beutenaken quarry. Very rare specimens were recorded in the upper Campanian at Poigny at 116.2 m and 110.8 m within and above the Vulgaris CIE.

Pearce et al. [2020, figure 18, section 7.4.3.1] suggested that the temporary disappearance of persistently occurring *S. filoreticulata* within the lower Santonian could be a locally significant event. A highest persistent occurrence is not apparent at Poigny; however, the largest number of recorded specimens occurs in the lowest studied sample at 390 m (between the Kingsdown and Michel Dean CIEs) in the upper Coniacian (Figure 3). This is consistent with the highest abundant occurrence in the upper Coniacian at Whitecliff [Prince, 1997, sample 58] and in Kent [Kingsdown; Prince, 1997; Iain Prince pers. comm., sample 17].

Through the Coniacian to middle Santonian at Whitecliff and in Kent, the proximal *Circulodinium–Heterosphaeridium* (C–H) assemblage (i.e., that characterised by areoligeracean dinocysts such as *Senoniasphaera*) dominates, enabling the clear recognition of the HO of abundant *S. filoreticulata* specimens. At Trunch, this same interval is overwhelmingly dominated by the more distal S–P assemblage, which heavily dilutes the relative proportion of C–H assemblage species. Nevertheless, at Trunch a very slight increase in the relative abundance of *S. filoreticulata*

is still apparent in the upper Coniacian at 375 m [Pearce et al., 2020, supplementary table 2], also between the Kingsdown and Michel Dean CIEs. Therefore, the observation of frequently occurring specimens of *S. filoreticulata* in our lowest sample from Poigny is a good indication for the marked higher relative abundance expected in the upper Coniacian.

(3) HO of *Chatangiella islae*: This species is taken in the biostratigraphy industry to have a highest common occurrence (HCO) at the top of the Coniacian and a HO in the Santonian. In the Norwegian Sea, the HO of *C. islae* occurs close to the HO of *Heterosphaeridium difficile* [see Pearce et al., 2019, figure 2, note that rare occurrences of *C. islae* illustrated above 2700 m are probably reworked]. At Poigny, the HO of *H. difficile* occurs at 285 m (lowermost Campanian), and of *C. islae* at 385.35 m, immediately below the Michel Dean CIE, in the uppermost Coniacian (Figure 3). As these events are separated by over 100 m, the HO of *C. islae* at Poigny may be related to the HCO of the species elsewhere.

6.2.2. *Lower Santonian events*

(4) Acme of *Spinidinium echinoideum*: At Poigny, a pronounced acme of *S. echinoideum* occurs at 374.9 m (reaching 30% of the dinocyst assemblage), immediately below the Bedwell CIE. In the Trunch borehole, common–abundant specimens span the Bedwell CIE with an acme immediately above it. The acme interval therefore approximates the Bedwell CIE (Figures 2, 3). Azema et al. [1981] similarly recorded a bloom of *S. echinoideum* in the "Senonian" (?Santonian) of the Duttières 3 borehole, Vendée, western France; further study is required to determine if this bloom is the lower Santonian acme.

6.2.3. *Middle Santonian events*

(5) LO of *Chatangiella eminens*: Pearce et al. [2020, figure 18] recorded the lowest stratigraphic occurrence of *C. eminens* at 346 m in the Trunch borehole, at the base of the Horseshoe Bay CIE. At Poigny, the same event is recorded at 364.85 m, within the Haven Brow CIE, extending the range of the species lower in the middle Santonian (Figure 3). According to Pearce et al. [2020] the LO at Whitecliff also occurs in the middle Santonian, but slightly higher again at the level of the n1 CIE (i.e., between the Horseshoe Bay and Buckle CIEs).

(6) LO of *Spiniferites jarvisii*: Pearce et al. [2020, figure 18, section 7.4.15] suggested that the species (described from the Trunch borehole) could be a potentially useful marker for the middle–upper Santonian boundary, but that more records were required to establish this. At Trunch the event falls immediately below the Buckle CIE, while at Poigny, the LO was found at 364.85 m at the top of the Haven Brow CIE (Figure 3), extending the range lower in the middle Santonian.

(7) First Appearance Datum level (FAD) of *Senoniasphaera protrusa*: Records of the distribution of *S. protrusa* may be unreliable prior to the emendation of the species by Prince et al. [1999]; see Pearce et al. [2020, section 7.4.8] for a brief discussion. The lowest stratigraphic occurrence of *S. protrusa* in the middle Santonian is consistent at Whitecliff, in Kent and at Trunch. At Trunch, the LO occurs at 339 m [Pearce et al., 2020, figures 6, 18] between the Horseshoe Bay and Buckle CIEs. At Poigny, the LO of *S. protrusa* occurs at 344.65 m and is apparently synchronous with Trunch (Figures 2, 3). At Whitecliff, the event occurs 3 m above the Barrois Sponge Bed [Prince et al., 1999, figure 2, sample 90] within the Horseshoe Bay CIE [Jarvis et al., 2006, figure 11], while at Whiteness [Kent, Prince et al., 2008, figure 7, sample 4] it occurs within the Barrois Sponge Bed. At Dover (Kent), where a $\delta^{13}C_{carb}$ record is available [Jarvis et al., 2006, figure 11], the Barrois Sponge Bed occurs above the m2 CIE and below the Horseshoe Bay CIE.

The LO of *S. protrusa* at Whiteness in the Barrois Sponge Bed was suggested by Pearce et al. [2020] to represent the FAD of the taxon, and this appears to be correct.

(8) LO of *Senoniasphaera congrensa*: Of the sections considered here, *S. congrensa* has only been recorded at Poigny and in Kent [where it was described by Prince et al., 2008 from Foreness Point, as *Senoniasphaera protrusa congrensa*]. In Kent, the LO of *S. congrensa* occurs at the summit of the middle Santonian at Whiteness, in Rowe's Echinoid Band [= *Conulus albogalerus* band; Prince et al., 2008, figure 7, sample 6], ~2 m above *S. protrusa* (sample 4) and below the Horseshoe Bay CIE and presumably above the m2 CIE. At Poigny, the LO of *S. congrensa* occurs at 314.8 m in the upper Santonian, immediately above the Hawks Brow CIE (Figure 3), and therefore stratigraphically higher than at Whiteness.

(9) FAD of *Dimidium striatum*: Pearce et al. [2020, figure 18, section 7.4.14] discussed the temporal and spatial distribution of *D. striatum* and suggested that the stratigraphically lowest record found at Whitecliff by Prince et al. [1999, figure 2] could tentatively be taken to represent the FAD of the species. The event at Whitecliff occurs in the middle Santonian, above the Horseshoe Bay CIE. At Poigny, the LO of *D. striatum* occurs at 329.6 m, in the upper Santonian, above the Buckle CIE (Figure 3), close to the suggested FAD.

(10) Last Appearance Datum (LAD) of *Spiniferites porosus*: Pearce et al. [2020, figure 18, section 7.4.9] discussed the distribution of *S. porosus* and suggested that the LAD occurs in the mid-Santonian in the Northern Hemisphere and placed it at the isotope peak immediately above the m2 CIE. At Poigny, a HO of the species was recorded at 339.25 m (Figure 3), immediately below the Buckle CIE, therefore, extending the range upwards slightly.

(11) LO of *Cannosphaeropsis utinensis*: The LO of *C. utinensis* in the sections considered here, appears to occur in the Poigny core at 339.25, in the uppermost middle Santonian, immediately below the Buckle CIE (Figure 3). Moving progressively northwards, the LO occurs in the upper Santonian, *Uintacrinus socialis* Zone at Whitecliff [Prince et al., 1999, figure 2], and in the *Marsupites* Zone, below the SCaBE at Trunch [Pearce et al., 2020, figure 18]. This suggests a diachronous northward migration of the species, possibly associated with progressive Late Cretaceous cooling.

6.2.4. *Upper Santonian events*

(12a, b) Lowest Common Occurrence (LCO) and HO of *Chatangiella eminens*: At Poigny the LCO of *C. eminens* occurs at 335.35 m, in the lowermost upper Santonian, within the Buckle CIE. The HO occurs at 319.7 m, immediately below the Hawks Brow CIE. These events appear to be synchronous in the Trunch borehole [Pearce et al., 2020, figure 18] and at Whitecliff [see Pearce et al., 2020, section 7.4.10], making it an extremely useful species (Figures 2, 3).

(13) LO of *Cordosphaeridium catherineae*: In the type material from the Trunch borehole, the LO of *C. catherineae* was recorded at 323 m [Pearce et al., 2020, figure 18] in the upper Santonian, *U. socialis* Zone, base of the Hawks Brow CIE. At Poigny, the LO was recorded at 329.6 m, above the Buckle CIE (Figure 3), thereby extending the event downwards slightly.

(14) Increase in *Surculosphaeridium longifurcatum*: At Trunch [Pearce et al., 2020, supplemental table 2, at 335 m], Whiteness [Kent, Prince, 1997, enclosures 7, 8, in sample 14] and Whitecliff [Prince et al., 1999, figure 2, in sample 114] a clear highest stratigraphic occurrence of common specimens of *S. longifurcatum* is observed in the *O. pillula* Zone. At Trunch, this event occurs within the Buckle CIE, while at Whitecliff and in Kent, we estimate it occurs slightly higher between the Buckle and Hawks Brow CIEs. At Poigny, this prominent HO of frequent specimens occurs at 325.45 m, also between the Buckle and Hawks Brow CIEs (Figure 3).

(15) HO of persistent *Scriniodinium campanula*: Despite two sporadic occurrences of *S. campanula* in the lower Campanian of the Poigny borehole (260.9 m, 234.1 m), a clear HO of persistent specimens in the upper Santonian may be significant (Figure 3). At Poigny, this event occurs at 319.7 m, immediately below the Hawks Brow CIE. At Whitecliff, a HO event was recorded by Prince et al. [1999, figure 2, sample 122] in the upper Santonian, high *U. socialis* Zone, ~4 m below the Hawks Brow Flint and immediately below the Hawks Brow CIE [Jarvis et al., 2006, figure 11]. In the Kent composite section, Prince et al. [2008, figure 3] only recorded rare specimens in a single sample from the mid-Coniacian. This is predictable because the S–P assemblage, of which *S. campanula* is presumed to be a member, is very poorly represented in Kent. However, at Trunch (where the S–P assemblage dominates), *S. campanula* is recorded up to 322 m in the *U. socialis* Zone [Pearce et al., 2020, figure 18], within the Hawks Brow CIE.

(16) LO of *Rhynchodiniopsis saliorum*: In the Trunch borehole, the lowest stratigraphic occurrence of *R. saliorum* was recorded at 312 m in the *Marsupites* Zone by Pearce et al. [2020, figure 18], between the q1 and SCaBE CIEs. At Foreness Point (Kent), Prince et al. [2008, figure 8] also recorded the event in the *Marsupites* Zone from their lowermost sample 1 (Palm Bay Echinoid Band), ~1 m below the Foreness Flint; this level approximates the Hawks Brow CIE at Dover [Kent; Jarvis et al., 2006, figure 11]. At Whitecliff, Prince [1997] recorded the species as *Rhynchodiniopsis* sp. A in sample 126 at the *O. pillula–Marsupites* Zone boundary, also within

the Hawks Brow CIE [Jarvis et al., 2006, figure 11]. At Poigny the LO of *R. saliorum* occurs at 299.75 m in the upper Santonian, immediately above the Foreness CIE (Figure 3), and therefore slightly higher than at Foreness Point and Whitecliff.

6.2.5. *Lower Campanian events*

(17) LAD of *Heterosphaeridium difficile*: Pearce et al. [2020, figure 18, section 7.4.20] suggested that the LAD of *H. difficile* occurs in the low upper Santonian (mid-*U. socialis* Zone). At Poigny, generally rare and sporadic specimens occur to a highest level of 285 m, raising the LAD to the base of the lower Campanian, at the top of SCaBE peak a (Figure 3).

(18) HO of *Ellipsodinium* spp.: At Poigny, Whitecliff [Prince et al., 1999], Trunch [Pearce et al., 2020] and the composite section for Kent [Prince et al., 2008], a distinctive HO of *Ellipsodinium membraniferum* or *E. rugulosum* occurs within the SCaBE. Excluding *E. tenuicinctum* He Chengquan from the Eocene (where we are unaware of any published occurrences outside of China), this may be broadly considered as a HO *Ellipsodinium* spp. event.

Prince [1997] recorded the HO of *E. membraniferum* in the lower Campanian, low *O. pillula* Zone at Whitecliff (sample c7), although the species was not mentioned in the biostratigraphic study of that section by Prince et al. [1999], and was only formally described by Prince et al. [2008]. In Kent and at Trunch, the HOs of *E. membraniferum* and *E. rugulosum* occur in the uppermost upper Santonian (top *Marsupites* Zone) and within SCaBE peak a, respectively. At Poigny, the HO of *E. membraniferum* occurs at 279.9 m in lower Campanian SCaBE peak b (Figures 2, 3).

(19a, b) LO and HO of *Spiniferites multispinulus*: Pearce et al. [2020, figure 21, section 7.5.4] suggested that the LO of *S. multispinulus* may be a potentially useful bioevent for the lower Campanian (upper *O. pillula* Zone). At Poigny, the LO occurs at 279.6 m in SCaBE peak b, supporting that suggestion. The HO of the species in the Trunch borehole was recorded by Pearce [2010, figure 2] in the lower *G. quadrata* Zone. At Poigny, this event occurs at 226.3 m, immediately above the Senonensis CIE, marginally higher than at Trunch (Figure 3).

(20) LO of persistently occurring *Whitecliffia spinosa*: Pearce et al. [2020, section 7.5.1] regarded a LO of persistently occurring specimens of *W. spinosa* in the lower Campanian to be significant. At Poigny, this event occurs at 265.65 in the lower Campanian below the Pillula CIE (Figure 3). Pearce et al. [2020] reported that at Whitecliff, the lowest persistent occurrence of *W. spinosa* occurs in the lower Campanian in the middle of the SaCBE. However, if this lowest persistent occurrence event is moved slightly upwards to where specimens are consecutively recorded [Prince et al., 1999, figure 2, sample c7], this occurs 1 m above the Old Nore Marl, which lies at the base of the Pillula CIE [Thibault et al., 2016].

(21) Temporary HO of *Surculosphaeridium longifurcatum*: The species *S. longifurcatum* has been recorded as high as the upper Maastrichtian of Hallembaye quarry by Slimani [2001, figure 7] and from the lower Maastrichtian of the Middle Vistula River composite section [Dziurków; Niechwedowicz et al., 2021]. It is also well distributed through the upper Campanian at Beutenaken quarry [Slimani, 2001, figure 6], and has been recorded in a single sample from the upper Campanian at Tercis [Schiøler and Wilson, 2001]. However, a clear HO of *S. longifurcatum* occurs in the low Campanian of southern Germany [Kirsch, 1991], in the lower Campanian at Trunch (pers. obs.), and close to the top of the lower Campanian at Whitecliff [Prince et al., 1999]. At Poigny, the HO of *S. longifurcatum* occurs at 244.6 m, midway between the Pillula and Senonensis CIEs (Figure 3), and this may be a useful local event for the Anglo-Paris Basin and southern North Sea Basin.

(22) HO of *Senoniasphaera protrusa*: At Poigny, the HO of *S. protrusa* was recorded at 240.9 m between the Pillula and Senonensis CIEs (Figures 2, 3). Pearce et al. [2020] recorded the HO in their highest sample from the Trunch borehole (270 m); however, personal observations indicate that specimens continue up to 266 m in the lower *G. quadrata* Zone.

Slimani [2001] recorded rare and sporadic specimens of *S. protrusa* in the upper Campanian of Beutenaken and rare to common specimens in the upper Campanian of Hallembaye. According to the emended species description [Prince et al., 1999, p. 162]: "*Senoniasphaera protrusa* differs from all other *Senoniasphaera* species by having an elongated inner and outer body which possess two antapical horns of unequal size, giving the cyst its characteristic elongate and asymmetrical shape".

Photographs of *S. protrusa* from Hallembaye [in Slimani, 2000, plate 5, figures 9, 10] that conform

to the original description of the species, illustrate a bilaterally symmetrical specimen of subequal width and length that we would now include in *Canningia glomerata*. We exclude records of *S. protrusa* by Slimani [2001], as he may have been unaware of the emendation. It is notable that the species has not been recorded from the upper Campanian of the Meer borehole [northern Belgium; Slimani et al., 2011] or at Tercis.

(23) HO of *Dimidium striatum*: Pearce [2010, figure 2] indicated that the HO of *Dimidium striatum* occurs in the upper *G. quadrata* Zone in the Trunch borehole [i.e. below the MCaE, see Jarvis et al., 2002]. This appears to be consistent with the record from Poigny, where the HO occurs at 185.9 m, between the Papillosa CIE and the MCaE (Figure 2).

(24) LO of *Nelsoniella incomposita*: The lowest stratigraphic occurrence of *N. incomposita* from the Trunch borehole occurs at 220 m [Pearce, 2010, figure 2], below the MCaE [Jarvis et al., 2002, figure 3]. This appears to be synchronous in the Poigny borehole, where the event occurs at 175.6 m (Figures 2, 3).

(25) HO of *Eatonicysta*? *mutabilireta*: At Poigny, *E.*? *mutabilireta* was recorded persistently in the lower Campanian from 175.6 m (below the MCaE) to 214.3 m (between the Senonensis and Papillosa CIEs; Figure 2). Pearce [2010, figure 2] demonstrated that the range is restricted to the stratigraphically equivalent *G. quadrata* Zone in the Trunch borehole type material. Rare and sporadic occurrences of the species at Poigny from 275.75 m and 279.6 m, around the top of the SCaBE, indicate that the species may have an inception in the lower *O. pillula* Zone (Figure 3).

6.2.6. *Upper Campanian events*

(26) HO of *Nelsoniella incomposita*: Pearce [2010, figure 2] recorded the HO of *N. incomposita* at 192 m in the Trunch borehole, immediately above the MCaE [Jarvis et al., 2002, figure 3]. At Poigny, the same event occurs at 162.6 m, slightly lower, within the uppermost lower Campanian portion of the MCaE (Figures 2, 3).

(27) LO of *Raetiaedinium evittigratia*: The LO of *R. evittigratia* occurs at 116.2 m at Poigny within the Vulgaris CIE (Figure 3). It was persistently recorded but always rare (<0.5%) and only encountered during scanning after the main count. The species was found in the Piotrawin opoka (siliceous chalk) at 1.5 m by Niechwedowicz and Walaszczyk [2022], close to the base of their composite Middle Vistula River section in Poland, and within the "*I.*" *altus* Zone. It was also recorded by Schiøler and Wilson [2001, figure 1] at 15.8 m in their lowest sample at Tercis, but not in the deeper samples studied by Antonescu et al. [2001a]. According to the inoceramid zonation at Tercis by Walaszczyk et al. [2002], the position recorded by Schiøler and Wilson [2001] occurs in an unzoned interval, but stratigraphically lower than at Piotrawin, and according to Voigt et al. [2012], to a level well below the LCaE. Our preliminary estimation suggests that the LO of *R. evittigratia* occurs within the MCaE at Tercis, therefore stratigraphically lower than at Poigny.

(28) HO of persistent *Raetiaedinium truncigerum*: This species is typically rare in all the sections compared here and appears to have a HO "just below" the Boundary Marl, within the "*I.*" *redbirdensis* Zone of the Middle Vistula River succession [Kłudzie North section, Niechwedowicz and Walaszczyk, 2022]. It is worth noting that from other sections containing the "*I.*" *redbirdensis* Zone, the species was absent at Kłudzie South and Raj North, and extremely rare at Podole. It is rare and sporadic in the mid-*Belemnitella langei* Zone at Beutenaken [Slimani, 2001] and was not recorded at Stevns-1 (Poul Schiøler pers. comm.).

A HO of persistently occurring *R. truncigerum* occurs in the mid-*Belemnitella mucronata* Zone at Beutenaken [Slimani, 2001, text-figure 3, figure 6a] that is apparently synchronous with the HO event in the *Belemnitella woodi* Zone at Hallembaye [Slimani, 2001, text-figure 2, figure 7a] and Trunch (pers. obs.). At Poigny, we recorded the HO of *R. truncigerum* at 106.8 m, immediately below the Pre-LCaE (Figures 2, 3). Masure [2000] recorded *R. truncigerum* slightly higher at 90 m, above the Pre-LCaE, but she did not record *R. evittigratia*, making it possible that specimens of the latter species may have been grouped in *R. truncigerum*. The precise relationship between the Upper Cretaceous belemnite zonation and the carbon isotope stratigraphy is currently uncertain, but our preliminary estimation places the Pre-LCaE within the *B. woodi* Zone.

At Tercis, the HO of arguably persistently occurring specimens of *R. truncigerum* occurs at 23.8 m [Antonescu et al., 2001a, table 1] below the LCaE

[Voigt et al., 2012, figure 3] and probably well below the level at Poigny.

(29) LO of *Palaeostomocystis reticulata*: Marheinecke [1992] stated that the known range of this acritarch is Turonian to Danian. The species is rare and sporadic at Tercis and was recorded by Antonescu et al. [2001a, table 1] down to 80.6 m, within the "*I.*" *altus* Zone according to Walaszczyk et al. [2002]. We estimate that this horizon occurs above the LCaE [see Voigt et al., 2012, figure 3]. Niechwedowicz and Walaszczyk [2022] found the species to be particularly common in their lowest Middle Vistula River composite section (Piotrawin) and abundant in their lowest sample, also within the "*I.*" *altus* Zone.

The LO of *P. reticulata* at Poigny occurs at 90 m [Masure, 2000; we recorded it at 86.2 m in the next sample above] immediately below the LCaE (Figure 3) and therefore, stratigraphically slightly lower than at Tercis. Slimani [2001] found the species in the *B. mucronata* Zone in the upper Campanian of Beutenaken quarry (that would presumably contain the Langei CIE and LCaE), together with the LO of *Biconodinium reductum*. At Tercis, the LO of *B. reductum* was recorded at 86.2 m, immediately above the LO of *P. reticulata*, indicating a close correlation [Antonescu et al., 2001a]. Consequently, the LO of *P. reticulata* appears to be broadly synchronous at Beutenaken, Poigny, Tercis and in the Middle Vistula River succession around the LCaE.

(30) HCO of *Palaeohystrichophora infusorioides*: At Poigny, a very prominent HCO of *P. infusorioides* occurs at 86.2 m in the lower LCaE and is believed to be synchronous in the Trunch borehole (Figures 2, 3, pers. obs.). No quantitative data for this species at Tercis were provided by Antonescu et al. [2001a], while Schiøler and Wilson [2001] show the species to be extremely rare throughout. In the palynological synthesis of the Tercis data, Antonescu et al. [2001b, p. 256] stated that the "last common occurrence" occurs between 34.8 m and 39.5 m, at a level we estimate to lie below between the MCaE and LCaE CIEs, and therefore slightly lower than at Poigny and Trunch.

The discrepancy in the position of the HCO of *P. infusorioides* at Poigny and Tercis may be the result of a palaeoenvironmental control. Two distinct dinocyst assemblages in the European chalks: *Circulodinium–Heterosphaeridium* (C–H) and *Spiniferites–Palaeohystrichophora* (S–P), are well known [Jarvis et al., 2021, Pearce et al., 2003, 2009, Prince et al., 2008]. The S–P assemblage is found to occupy more distal water masses, presumably receiving nutrients only from upwelling. For example, Pearce et al. [2009] argued that the catastrophic decline in relative numbers of *P. infusorioides* at the Cenomanian–Turonian boundary was the result of the shutdown of the Anglo-Paris Basin upwelling system due to thermal stratification.

Interestingly, three spot palynofacies samples at Tercis [Schiøler and Wilson, 2001, table 1] indicate that black and brown wood comprises >44% of the total assemblage, outnumbering dinocysts, with <4% spores and pollen. This suggests a significant proximity to the shoreline, and the rarity of *P. infusorioides* further suggests relatively oligotrophic conditions due to a minimum in the runoff of continental nutrients [see Pearce et al., 2003, 2009, section 3.1].

(31) HO of *Exochosphaeridium*? *masureae*: This distinctive species was described by Slimani [1996] from the Campanian of the Turnhout borehole, Belgium. In macrofossil-calibrated material from Hallembaye, the HO was recorded in the *B. woodi* Zone by Slimani [2001, text-figure 2, figure 7b]. At Beutenaken, Slimani [2001, text-figure 3, figure 6a] recorded the HO in the uppermost *B. mucronata* (of conventional usage) and therefore, comparable with the event at Hallembaye. Personal observations from the Trunch borehole, place the HO at 136 m also in the *B. woodi* Zone, below the LCaE. Our observations at Poigny place the HO at 86.2 m (Figure 3), in the lower LCaE; therefore, slightly above that at Trunch, but still highly comparable. However, the HOs at Tercis at 23.8 m [Antonescu et al., 2001a, table 1] above the MCaE [cf. Voigt et al., 2012, figure 3] to the south, and Stevns-1 in the uppermost Campanian, *B. langei* Zone [Surlyk et al., 2013, appendix 1] to the north, indicate a pronounced diachroniety.

7. Clay mineralogy

The clay mineralogy of the Poigny core, plotted in Figure 4, has been documented by Deconinck et al. [2000, 2005] and was interpreted in a regional context by Chenot et al. [2016, 2018]. The clay mineral assemblage in the Coniacian–upper Campanian interval is dominated by smectitic minerals including R0 random illite/smectite mixed-layers and

smectite (75–98%), with minor illite (2–25%) and accessory kaolinite (<5%). Chlorite is absent. The smectite/illite ratio generally ranges from 2 to 10.

The maximum burial depth of 500 m estimated for the top Chalk at Poigny [Brunet and Le Pichon, 1982] and the high proportion of smectites, which transform into illite from 60 °C [Środoń, 2009], indicate that the clay mineral assemblages of the Poigny core are primary [Chenot et al., 2016]. Oxygen stable isotope values of −2.7‰ to −1.5‰ $\delta^{18}O_{carb}$ in a rising trend and through the Campanian at Poigny [Chenot et al., 2016] are comparable to other shallow buried chalk successions with minimal diagenetic overprint [e.g. Jenkyns et al., 1994]. However, the chalks become noticeably more indurated below 250 m and a mineralogical transition downwards from opal-CT to quartz as the dispersed silica phase occurs at 300 m depth [Figure 4; Deconinck et al., 2000]. Nonetheless, smectite continues to be the dominant mineral through most of the section down to the core base at 700 m depth.

Stratigraphic trends in the clay mineral assemblage, summarised in Figure 4, are: (1) kaolinite occurs as a minor phase at the section base in the Coniacian–lower Santonian, and is absent above 365.9 m; (2) the proportion of illite decreases upwards with an associated increasing smectite/illite ratio that reaches a broad maximum from 180 to 120 m, spanning the lower–middle Campanian boundary and the MCaE (Figure 4); (3) the illite content increases rapidly above 120 m with declining smectite/illite ratios and displays a maximum spanning the LCaE, above which illite attains a maximum of 25% before falling slightly in the meteoric alteration zone at the section top.

The smectitic fraction constitutes the background sediment of a low-terrigenous supply, attributable to the absence of significant near-by land masses and topography (Figure 1A), regional volcanic activity, and the warm humid climate and high sea level that prevailed during the Late Cretaceous in the region [Deconinck et al., 2005, Jeans, 2006]. Increased proportions of illite, considered to be sourced by erosion of igneous or metamorphic continental basement rocks, represent pulses of enhanced terrigenous supply, potentially associated with climate cooling, tectonism and/or sea-level fall. Kaolinite may have a pedogenic origin or be reworked, but its close coupling with illite at Poigny and in the Campanian elsewhere favour the latter origin [Chenot et al., 2018]. It is notable that the increase in detrital clay below the Pre-LCaE is coincident with an inflection point in the Sr isotope curve towards more steeply rising $^{87}Sr/^{86}Sr$ ratios at Lägerdorf [McArthur et al., 1993], consistent with an increase in the continental weathering flux at that time.

A detrital clay maximum immediately preceding and spanning the LCaE is also seen at Tercis [Chenot et al., 2016, figure 3] where increased illite is accompanied by increasing chlorite and a large pulse of kaolinite. This evidences a regional phase of increased continental erosion accompanying the LCaE with a mineral assemblage at Poigny characteristic of semi-humid conditions contrasting to a more humid tropical climate at Tercis [Chenot et al., 2018]. A diachronous regional increase in detrital input through the Campanian has been linked to local tectonic pulses that led to the emergence of shelf areas and increased siliciclastic supply. However, additionally, there is regional evidence for a significant sea-level fall during the late Campanian—the *polyplocum* Regression of northern Germany [Niebuhr et al., 2000].

The associated increase in silicate weathering, driving atmospheric CO_2 drawdown, may have contributed to the accelerated long-term Campanian cooling trend evidenced by rising bulk sediment $\delta^{18}O_{carb}$ values at Poigny [Chenot et al., 2016, figure 4] and, more generally, widespread rising planktonic and benthic foraminifera $\delta^{18}O_{carb}$ and falling TEX_{86} values through the stage [O'Brien et al., 2017].

8. Sequences and sea-level change

Lasseur [2007] undertook a facies analysis of the Poigny core based on sediment fabric, composition, and texture, incorporating thin section analysis of 95 samples from the upper Coniacian–Campanian. The coarsest grained wackestone–packstone facies were assigned to more nearshore environments and regression, with lime mudstones representing the most offshore conditions and peak transgression. An onshore–offshore relative sea-level curve was generated from these data (Figure 4).

Lasseur [2007] additionally distinguished a succession of two second-order and nine major

third-order sequences through the Cenomanian–Campanian at Poigny, with the recognition of flooding "surfaces" (FS) corresponding to levels of maximum regression, and maximum flooding "surfaces" (MFS) associated with maximum transgression. It should be noted, however, that visible omission or erosion surfaces have not been documented at the designated levels in the upper Coniacian–Campanian core at Poigny, although the "Trunch Hardground equivalent" omission surfaces provide a potential level for the Sequence 8 FS. The FS and MFS might better be considered therefore as "zones" of maximum regression and maximum transgression. The Coniacian–Campanian comprises third-order sequences 5–9 (Figure 4).

It is notable that the interval of second-order maximum flooding at the Senonensis CIE lies within a long-term interval of relatively low palynomorph abundance, low dinocyst diversity, moderate P/G ratio, low algae and terrestrial palynomorph numbers, and low illite content, consistent with a deeper water more offshore setting.

The onshore–offshore sea-level curve of Lasseur [2007] correlates with variation in many of the palynological parameters. The relationship that is most strongly expressed is a positive correlation between major episodes of short-term sea-level rise (blue arrows in Figure 4) and intervals of elevated P/G ratio (highlighted by the pale red curved lines in Figure 4). A cyclic pattern at a decametre scale is evident and approximates to a 400 kyr periodicity in the Santonian (five cycles in 2.05 Myr—Figure 4). A general positive correlation also exists between cycles of high P/G ratio and episodes of increased palynomorph abundance and decreased dinocyst species richness and diversity.

The P/G ratio is generally regarded as a proxy for nutrient availability and palaeoproductivity [see discussion in Jarvis et al., 2021, p. 24], suggesting a link between sea-level rise and increased nutrient supply. The cause of this is uncertain but nutrients might be supplied, for example, by their release from coastal plain sediments and soils during flooding [cf. Jarvis et al., 2002, p. 237], and/or by the landward movement of a marine high-productivity zone supported by marine upwelling [cf. Pearce et al., 2009]. Some intervals of high P/G ratio correspond to levels with lower smectite/illite ratios (pale blue curves in Figure 4) suggesting a relationship with periods of enhanced terrestrial clay input, favouring a terrestrial nutrient source, but the relationship is not universal.

The third-order sequences of Lasseur [2007] do not correspond consistently with specific changes in the palynomorph assemblage. However, prominent changes occur particularly around the Sequences 7, 8 and 9 flooding surfaces and the SCaBE, MCaE and LCaE carbon isotope excursions (Figure 4). Flooding surfaces of third-order sequences have been identified at the upper two levels at Tercis [Chenot et al., 2016, figure 3], and the three CIEs correspond to the levels of the *Marsupites* Transgression, the *mucronata* Transgression and *polyplocum* Regression in Germany [Niebuhr et al., 2000].

It can be envisaged that sea-level change will significantly impact palynomorph assemblages via changes in, for example, shoreline proximity, nutrient supply, water mass distribution and sea-surface temperature. Additional quantitative palynological records are required to further address relationships between variations in assemblage composition, CIEs, sea-level and climate change in the Santonian–Campanian.

9. Conclusions

A diverse and well-preserved palynological assemblage, including 236 species and subspecies of dinocysts, is documented from the upper Coniacian to upper Campanian of the Poigny Craie 701 borehole, constituting the most detailed dataset of its kind in France. The palynoflora is dominated by dinocysts of the S–P assemblage, with low algae and terrestrial palynomorph numbers suggesting a relatively distal open-marine setting. A low terrigenous influence and semi-humid climate is indicated by a clay mineral assemblage in which smectite predominates.

New $\delta^{13}C_{carb}$ data from the upper Coniacian to upper Campanian improves the resolution of the existing uppermost Santonian–Campanian curve and extends the carbon isotope profile downwards into the middle Coniacian. A succession of 17 named CIEs is identified and correlated between France (Poigny), England (Trunch borehole) and Germany (Lägerdorf quarries). The bases of the Santonian, lower and upper Campanian are specifically picked at Poigny based on the correlation of CIEs, constrained by limited available biostratigraphy, to other European sections.

A total of 33 palynological events from 24 dinocyst and one acritarch species, considered to have biostratigraphic significance, are recognised through the Coniacian to Campanian: three in the upper Coniacian; one in the lower Santonian; seven in the middle Santonian; six in the upper Santonian; ten in the lower Campanian; and six in the upper Campanian. These offer considerable potential for improving inter-regional correlation of the European Upper Cretaceous.

An association between elevated P/G dinocyst ratios and episodes of sea-level rise is apparent and indicates episodic pulses in surface water productivity triggered by the recycling of continental nutrients during flooding, or the shoreward movement of offshore upwelling zones. Coincident changes in clay mineral assemblages, with lower smectite/illite ratios accompanying P/G ratio increases, support a terrestrial nutrient source, but the relationship is not universal.

Conflicts of interest

Authors have no conflict of interest to declare.

Acknowledgements

NT and MM thank Francois Guillocheau (University of Rennes) for granting access to the Poigny core, and Damien Gendry for their help in the management of core boxes and access to laboratory facilities that greatly facilitated the sampling. Chris Mitchell (University of Exeter, Penryn Campus) supported the C and O isotope analysis. Malcolm Jones (Palynological Laboratory Services Limited, PLS) is thanked for the preparation of the palynological samples. We are particularly grateful to Mariusz Niechwedowicz and Poul Schiøler for sharing their palynology data from the Middle Vistula River and the Stevns-1 sections. Carlsbergfondet CF16-0456 funded travel expenses, sampling, and geochemical analysis by NT and JM. Support by Evolution Applied Limited to MAP and Equinor Energy AS (previously Statoil ASA) to IJ (contract 4502311303) is gratefully acknowledged. We thank the reviewers, Ligia Castro and an anonymous referee, for their useful suggestions that improved the manuscript.

Supplementary data

Supporting information for this article is available on the journal's website under https://doi.org/10.5802/crgeos.118 or from the author.

References

Antonescu, E., Foucher, J.-C., and Odin, G. S. (2001a). Les kystes de dinoflagellés de la carrière de Tercis les Bains (Landes, France). In Odin, G. S., editor, *The Campanian–Maastrichtian Boundary. Characterisation at Tercis les Bains (France) and Correlation with Europe and other Continents*, pages 235–252. Elsevier, Amsterdam.

Antonescu, E., Foucher, J.-C., Odin, G. S., Schiøler, P., Siegl-Farkas, A., and Wilson, G. J. (2001b). Dinoflagellate cysts in the Campanian–Maastrichtian succession of Tercis les Bains (Landes, France), a synthesis. In Odin, G. S., editor, *The Campanian–Maastrichtian Boundary. Characterisation at Tercis les Bains (France) and Correlation with Europe and other Continents*, pages 253–264. Elsevier, Amsterdam.

Azema, C., Fauconnier, D., and Viaud, J. M. (1981). Microfossils from the upper Cretaceous of Vendée (France). *Rev. Palaeobot. Palynol.*, 35, 237–281.

Blakey, R. (2012). Paleogeography of Europe series, Cretaceous ca. 75 Ma. Colorado Plateau Geosystems (now DeepTimeMaps™), Flagstaff AZ.

Blanc, P. and Gély, J. P. (2000). Etude pétrographique et minéralogique de la diagenèse carbonatée de la craie du Crétace supérieur des forages profonds 701 (Poigny) et 702 (Sainte-Colombe) (région de Provins, Seine-et-Marne). *Bull. Inf. Géol. du Bassin Paris*, 37, 87–100.

Brunet, M. F. and Le Pichon, X. (1982). Subsidence of the Paris Basin. *J. Geophys. Res.*, 87, 8547–8560.

Burnett, J. A., Gallagher, L. T., and Hampton, M. J. (1998). Upper Cretaceous. In Bown, P. R., editor, *Calcareous Nannofossil Biostratigraphy*, pages 132–199. Kluwer, Dordrecht.

Chenot, E., Deconinck, J. F., Puceat, E., Pellenard, P., Guiraud, M., Jaubert, M., Jarvis, I., Thibault, N., Cocquerez, T., Bruneau, L., Razmjooei, M. J., Boussaha, M., Richard, J., Sizun, J. P., and Stemmerik, L. (2018). Continental weathering as a driver of Late Cretaceous cooling: new insights from clay mineralogy of Campanian sediments from the southern

Tethyan margin to the Boreal realm. *Glob. Planet. Change*, 162, 292–312.

Chenot, E., Pellenard, P., Martinez, M., Deconinck, J. F., Amiotte-Suchet, P., Thibault, N., Bruneau, L., Cocquerez, T., Laffont, R., Puceat, E., and Robaszynski, F. (2016). Clay mineralogical and geochemical expressions of the "Late Campanian Event" in the Aquitaine and Paris basins (France), Palaeoenvironmental implications. *Palaeogeog. Palaeoclimatol. Palaeoecol.*, 447, 42–52.

Cramer, B. S. and Jarvis, I. (2020). Carbon isotope stratigraphy. In Gradstein, F., Ogg, J. G., and Ogg, G., editors, *The Geologic Time Scale 2020*, pages 309–343. Elsevier, Amsterdam.

Deconinck, J. F., Amédro, F., Baudin, F., Godet, A., Pellenard, P., Robaszynski, F., and Zimmerlin, I. (2005). Late Cretaceous palaeoenvironments expressed by the clay mineralogy of Cenomanian–Campanian chalks from the east of the Paris Basin. *Cret. Res.*, 26, 171–179.

Deconinck, J. F., Amédro, F., Robaszynski, F., Pellenard, P., and Recourt, P. (2000). Influences détritiques et volcaniques sur la minéralogie de la fraction argileuse des formations crayeuses traversées par le forage de Poigny (project Craie 700). Résultats préliminaires. *Bull. Inf. Géol. du Bassin Paris*, 37, 107–111.

Gale, A. S., Mutterlose, J., Batenburg, S., Gradstein, F. M., Agterberg, F. P., Ogg, J. G., and Petrizzo, M. R. (2020). Chapter 27—The Cretaceous Period. In Gradstein, F. M., Ogg, J. G., Schmitz, M. D., and Ogg, G. M., editors, *Geologic Time Scale 2020*, pages 1023–1086. Elsevier, Amsterdam.

Gély, J. P. and Blanc, P. (2004). Evolution diagénétique dans la craie pélagique dolomitisée du Crétacé supérieur du bassin de Paris (région de Provins, France). *Eclog. Geol. Helv.*, 97, 393–409.

Jarvis, I., Gale, A. S., Jenkyns, H. C., and Pearce, M. A. (2006). Secular variation in Late Cretaceous carbon isotopes: a new δ^{13}C carbonate reference curve for the Cenomanian–Campanian (99.6–70.6 Ma). *Geol. Mag.*, 143, 561–608.

Jarvis, I., Mabrouk, A., Moody, R. T. J., and De Cabrera, S. (2002). Late Cretaceous (Campanian) carbon isotope events, sea-level change and correlation of the Tethyan and Boreal realms. *Palaeogeogr. Palaeoclimatol. Palaeoecol.*, 188, 215–248.

Jarvis, I., Pearce, M., Püttman, T., Voigt, S., and Walaszczyk, I. (2021). Palynology and calcareous nannofossil biostratigraphy of the Turonian–Coniacian boundary: the proposed boundary stratotype at Salzgitter-Salder, Germany and its correlation in NW Europe. *Cret. Res.*, 123, 1–32.

Jeans, C. V. (2006). Clay mineralogy of the Cretaceous strata of the British Isles. *Clay. Miner.*, 41, 47–150.

Jenkyns, H. C., Gale, A. S., and Corfield, R. M. (1994). Carbon- and oxygen-isotope stratigraphy of the English Chalk and Italian Scaglia and its palaeoclimatic significance. *Geol. Mag.*, 131, 1–34.

Kirsch, K.-H. (1991). Dinoflagellatenzysten aus der Oberkreide des Helvetikums und Nordultrahelvetikums von Oberbayern. Münch. geowiss. Abh: Reihe A. *Geol. Paläontol.*, 22, 1–306.

Lasseur, E. (2007). *La Craie du Bassin de Paris (Cénomanien–Campanien, Crétacé supérieur). Sédimentologie de faciès, stratigraphie séquentielle et géométrie 3D.* Phd thesis, Géosciences Rennes, Université Rennes 1, https://tel.archives-ouvertes.fr/tel-00350422. p. 409.

Le Callonnec, L., Briard, J., Boulila, S., and Galbrun, B. (2021). Late Cenomanian–Turonian isotopic stratigraphy in the chalk of the Paris Basin (France): a reference section between the Tethyan and Boreal realms. *BSF Earth Sci. Bull.*, 192, article no. 14.

Le Callonnec, L., Renard, M., Pomerol, B., Janodet, C., and Caspard, E. (2000). Données géochimiques préliminaires sur la série Cénomanien–Campanienne des forages 701 & 702 du programme Craie 700. *Bull. Inf. Géol. du Bassin Paris*, 37, 112–119.

Linnert, C., Robinson, S. A., Lees, J. A., Perez-Rodriguez, I., Jenkyns, H. C., Petrizzo, M. R., Arz, J. A., Bown, P. R., and Falzoni, F. (2018). Did Late Cretaceous cooling trigger the Campanian–Maastrichtian Boundary Event? *Newsl. Strat.*, 51, 145–166.

Marheinecke, U. (1992). Monographie der dinozysten, acritarcha und chlorophyta des Maastrichtian von Hemmoor (Niedersachsen). *Palaeontogr. Abt. B*, 227, 1–173.

Masure, E. (2000). Les kystes de dinoflagellés en matière organique des forages du programme Craie 700, étude préliminaire. *Bull. Inf. Géol. du Bassin Paris*, 37, 44–51.

McArthur, J. M., Thirlwall, M. F., Chen, M., Gale, A. S., and Kennedy, W. J. (1993). Strontium isotope stratigraphy in the Late Cretaceous: numerical cal-

ibration of the Sr isotope curve and intercontinental correlation for the Campanian. *Paleoceanography*, 8, 859–873.

Mégnien, C. and Hanot, F. (2000). Deux forages scientifiques profonds pour étudier les phénomènes diagénétiques de grande ampleur dans la craie du bassin de Paris. *Bull. Inf. Géol. du Bassin Paris*, 37, 3–7.

Morter, A. A., Gallois, R. W., and Clark, R. D. (1975). *Record of the IGS Trunch borehole*. Institute of Geological Sciences, London.

Niebuhr, B. (2006). Multistratigraphische Gliederung der norddeutschen Schreibkreide (Coniac bis Maastricht), Korrelation von Aufschlüssen und Bohrungen. *Z. Dtsch. Ges. Geowiss*, 157, 245–262.

Niebuhr, B., Wood, C. J., and Ernst, G. (2000). Isolierte Oberkreide—vorkommen zwischen Wiehengebirge und Harz. In Hiss, M., Schönfeld, J., and Thiermann, A., editors, *Stratigraphie von Deutschland III. Die Kreide der Bundesrepublik Deutschland*, pages 101–109. Cour. Forsch.-Inst. Senckenberg, 226.

Niechwedowicz, M. and Walaszczyk, I. (2022). Dinoflagellate cysts of the upper Campanian–basal Maastrichtian (Upper Cretaceous) of the Middle Vistula River section (central Poland): stratigraphic succession, correlation potential and taxonomy. *Newsl. Strat.*, 55, 21–67.

Niechwedowicz, M., Walaszczyk, I., and Barski, M. (2021). Phytoplankton response to palaeoenvironmental changes across the Campanian–Maastrichtian (Upper Cretaceous) boundary interval of the Middle Vistula River section, central Poland. *Palaeogeog. Palaeoclimatol. Palaeoecol.*, 577, article no. 110558.

O'Brien, C. L., Robinson, S. A., Pancost, R. D., Damste, J. S. S., Schouten, S., Lunt, D. J., Alsenz, H., Bornemann, A., Bottini, C., Brassell, S. C., Farnsworth, A., Forster, A., Huber, B. T., Inglis, G. N., Jenkyns, H. C., Linnert, C., Littler, K., Markwick, P., McAnena, A., Mutterlose, J., Naafs, B. D. A., Puttmann, W., Sluijs, A., van Helmond, N., Vellekoop, J., Wagner, T., and Wrobel, N. E. (2017). Cretaceous sea-surface temperature evolution: constraints from TEX86 and planktonic foraminiferal oxygen isotopes. *Earth Sci. Rev.*, 172, 224–247.

Odin, G. S. (2001). *The Campanian–Maastrichtian Stage Boundary. Characterisation at Tercis les Bains (France) and Correlation with Europe and other Continents*. Elsevier, Amsterdam.

Pearce, M. A. (2010). New organic-walled dinoflagellate cysts from the Cenomanian to Maastrichtian of the Trunch borehole, UK. *J. Micropalaeontol.*, 29, 51–72.

Pearce, M. A., Jarvis, I., Ball, P. J., and Laurin, J. (2020). Palynology of the Cenomanian to lowermost Campanian (Upper Cretaceous) Chalk of the Trunch Borehole (Norfolk, UK) and a new dinoflagellate cyst bioevent stratigraphy for NW Europe. *Rev. Palaeobot. Palynol.*, 278, article no. 104188.

Pearce, M. A., Jarvis, I., Swan, A. R. H., Murphy, A. M., Tocher, B. A., and Edmunds, W. M. (2003). Integrating palynological and geochemical data in a new approach to palaeoecological studies, Upper Cretaceous of the Banterwick Barn Chalk borehole, Berkshire, UK. *Mar. Micropaleontol.*, 47, 271–306.

Pearce, M. A., Jarvis, I., and Tocher, B. A. (2009). The Cenomanian–Turonian boundary event, OAE2 and palaeoenvironmental change in epicontinental seas: new insights from the dinocyst and geochemical records. *Palaeogeog. Palaeoclimatol. Palaeoecol.*, 280, 207–234.

Pearce, M. A., Stickley, C. E., and Johansen, L. M. (2019). *Chatangiella islae* and *Trithyrodinium zakkii*, new species of peridinioid dinoflagellate cysts (Family Deflandreoideae) from the Coniacian and Campanian (Upper Cretaceous) of the Norwegian Sea. *Rev. Palaeobot. Palynol.*, 271, article no. 104080.

Perdiou, A., Thibault, N., Anderskouv, K., van Buchem, F., Buijs, G. J. A., and Bjerrum, C. J. (2016). Orbital calibration of the late Campanian carbon isotope event in the North Sea. *J. Geol. Soc. Lond.*, 173, 504–517.

Prince, I. M. (1997). *Palynology of the Upper Turonian to Lower Campanian Chalks of Southern England*. Phd thesis, Institute of Earth Studies, University of Wales, Aberystwyth. p. 334.

Prince, I. M., Jarvis, I., Pearce, M. A., and Tocher, B. A. (2008). Dinoflagellate cyst biostratigraphy of the Coniacian–Santonian (Upper Cretaceous): new data from the English Chalk. *Rev. Palaeobot. Palynol.*, 150, 59–96.

Prince, I. M., Jarvis, I., and Tocher, B. A. (1999). High-resolution dinoflagellate cyst biostratigraphy of the Santonian–basal Campanian (Upper Cretaceous): new data from Whitecliff, Isle of Wight, England. *Rev. Palaeobot. Palynol.*, 105, 143–169.

Robaszynski, F. (2000). Le forage de Poigny (701) : description lithologique. *Bull. Inf. Géol. du Bassin Paris*, 37, 18–26.

Robaszynski, F., Pomerol, B., Masure, E., Bellier, J. P., and Deconinck, J. F. (2005). Stratigraphy and stage boundaries in reference sections of the Upper Cretaceous Chalk in the east of the Paris Basin: the "Craie 700" Provins boreholes. *Cret. Res.*, 26, 157–169.

Robaszynski, F., Pomerol, B., Masure, E., Janin, M. C., Bellier, J. P., and Damotte, R. (2000). Corrélations litho-biostratigraphiques et position des limites d'étages dans le Crétacé des sondages de Poigny et de Sainte-Colombe : une synthèse des premiers résultats. *Bull. Inf. Géol. du Bassin Paris*, 37, 74–85.

Schiøler, P. and Wilson, G. J. (2001). Dinoflagellate biostratigraphy around the Campanian–Maastrichtian boundary at Tercis les Bains, southwest France. In Odin, G. S., editor, *The Campanian–Maastrichtian Boundary. Characterisation at Tercis les Bains (France) and Correlation with Europe and other Continents*, pages 221–234. Elsevier, Amsterdam.

Schulz, M. G., Ernst, G., and Weitschat, W. (1984). Stratigraphie und fauna der Ober-Kreide (Coniac–Maastricht) von Lägerdorf und Kronsmoor (Holstein). In Degens, E. T., Hillmer, G., and Spaeth, C., editors, *Exkursionsführer Erdgeschichte des Nordsee- und Ostseeraumes*, pages 483–517. Geologisch-Paläontologisches Institut, Hamburg.

Slimani, H. (1994). Les dinokystes des craies du Campanien au Danien à Halembaye, Turnhout (Belgique) et à Beutenaken (Pays-Bas). *Mém. Explic. Cart. Géol. Min. Belg.*, 37, 1–107.

Slimani, H. (1996). Les dinokystes des craies du Campanien–Danien à Hallembaye et Turnhout (Belgique) et à Beutenaken (Pays-Bas) : supplément de systématique. *Ann. Soc. Géol. Belg.*, 117, 371–391.

Slimani, H. (2000). Nouvelle zonation aux kystes de dinoflagellés du Campanien au Danien dans le nord et l'est de la Belgique et dans le sud-est des Pays-Bas. *Mem. Geol. Surv. Belg.*, 46, 1–88.

Slimani, H. (2001). Les kystes de dinoflagellés du Campanien au Danien dans la région de Maastricht (Belgique, Pays-Bas) et de Turnhout (Belgique) : biozonation et corrélation avec d'autres régions en Europe occidentale. *Geol. Palaeontol.*, 35, 161–201.

Slimani, H., Louwye, S., Dusar, M., and Lagrou, D. (2011). Connecting the Chalk Group of the Campine Basin to the dinoflagellate cyst biostratigraphy of the Campanian to Danian in borehole Meer (northern Belgium). *Neth. J. Geosci.*, 90, 129–164.

Środoń, J. (2009). Quantification of illite and smectite and their layer charges in sandstones and shales from shallow burial depth. *Clay. Miner.*, 44, 421–434.

Surlyk, F., Rasmussen, S. L., Boussaha, M., Schioler, P., Schovsbo, N. H., Sheldon, E., Stemmerik, L., and Thibault, N. (2013). Upper Campanian–Maastrichtian holostratigraphy of the eastern Danish Basin. *Cret. Res.*, 46, 232–256.

Thibault, N., Husson, D., Harlou, R., Gardin, S., Galbrun, B., Huret, E., and Minoletti, F. (2012). Astronomical calibration of upper Campanian–Maastrichtian carbon isotope events and calcareous plankton biostratigraphy in the Indian Ocean (ODP Hole 762C): implication for the age of the Campanian–Maastrichtian boundary. *Palaeogeog. Palaeoclimatol. Palaeoecol.*, 337, 52–71.

Thibault, N., Jarvis, I., Voigt, S., Gale, A. S., Attree, K., and Jenkyns, H. C. (2016). Astronomical calibration and global correlation of the Santonian (Cretaceous) based on the marine carbon isotope record. *Paleoceanography*, 31, 847–865.

Thiry, M., Hanot, F., and Pierre, C. (2003). Chalk dolomitization beneath localized subsiding Tertiary depressions in a marginal marine setting in the Paris Basin (France). *J. Sediment. Res.*, 73, 157–170.

Voigt, S., Friedrich, O., Norris, R. D., and Schönfeld, J. (2010). Campanian–Maastrichtian carbon isotope stratigraphy: shelf-ocean correlation between the European shelf sea and the tropical Pacific Ocean. *Newsl. Strat.*, 44, 57–72.

Voigt, S., Gale, A. S., Jung, C., and Jenkyns, H. C. (2012). Global correlation of Upper Campanian–Maastrichtian successions using carbon-isotope stratigraphy: development of a new Maastrichtian timescale. *Newsl. Strat.*, 45, 25–53.

Voigt, S. and Schönfeld, J. (2010). Cyclostratigraphy of the reference section for the Cretaceous white chalk of northern Germany, Lägerdorf-Kronsmoor: a late Campanian–early Maastrichtian orbital time scale. *Palaeogeog. Palaeoclimatol. Palaeoecol.*, 287, 67–80.

Walaszczyk, I., Cobban, W. A., and Odin, G. S. (2002). The inoceramid succession across the Campanian–Maastrichtian boundary. *Bull. Geol. Soc. Denmark*, 49, 53–60.

Wood, C. J., Morter, A. A., and Gallois, R. W. (1994). Appendix 1. Upper Cretaceous stratigraphy of the Trunch borehole. In Arthurton, R. S., Booth, S. J., Morigi, A. N., Abbott, M. A. W., and Wood, C. J., editors, *Geology of the Country around Great Yarmouth. Memoir for 1:50,000 Sheet 162 (England and Wales) with an Appendix on the Trunch Borehole by Wood and Morter*, pages 105–110. HMSO, London.

Comptes Rendus
Géoscience — Sciences de la Planète
2022, Vol. 354, Special Issue S3, p. 67-87
https://doi.org/10.5802/crgeos.121

Integrated stratigraphy of the Jurassic and the Cretaceous: a tribute to Jacques Rey /
Stratigraphie intégrée du Jurassique et du Crétacé : un hommage à Jacques Rey

Sedimentary record of the "Austrian" tectonic pulse around the Aptian–Albian boundary in SE France, and abroad

Enregistrement sédimentaire de la pulsation tectonique autrichienne vers la limite Aptien–Albien dans le sud-est de la France, et à plus grande échelle

Serge Ferry[*, a, b], **Danièle Grosheny**[c] **and Francis Amédro**[d, e]

[a] 6D avenue Général de Gaulle, 05100 Briançon, France

[b] Université de Lyon (retired), France

[c] Université de Lorraine, Ecole Nationale Supérieure de Géologie, UMR CNRS 7359 GeoRessources, BP 10162, F-54506 Vandoeuvre-lès-Nancy cedex, France

[d] 26 rue de Nottingham, 62100 Calais, France

[e] Université de Bourgogne - Franche-Comté, UMR 6282, CNRS Biogéosciences, 6 boulevard Gabriel, 21000 Dijon, France

E-mails: serge.ferry@yahoo.fr (S. Ferry), daniele.grosheny@univ-lorraine.fr (D. Grosheny), francis.amedro@free.fr (F. Amédro)

Abstract. A tectonically-controlled forced regression occurred on the western margin of the French subalpine basin around the Aptian–Albian boundary. It nearly emptied the western part of the Vocontian Trough during the early and middle Albian. A compressional pulse associated with vertical movements along the Cevennes fault row and its satellites is inferred. This forced regression is correlated with an inverse transgressive trend, both in the Paris Basin and the northern subalpine chains. The black shales of the early Aptian OAE1a and Albian OAE1b of the Vocontian Trough succession occur within opposite regional sea level trends, transgressive for the former, regressive for the latter. The inferred tectonic pulse is also recorded on a broader scale from literature data. The overall picture also shows outphasings in relative sea level changes on a large scale, likely controlled by tectonics.

Résumé. Une régression forcée d'origine tectonique s'est produite sur la marge occidentale de la mer subalpine au passage Aptien–Albien. Elle a vidangé presque complètement la partie ouest de la fosse vocontienne pendant l'Albien inférieur et moyen. Une pulsation tectonique en régime compressif

* Corresponding author.

associée à des mouvements verticaux est suggérée le long du couloir de failles cévenol et satellites. La régression forcée est corrélée avec une tendance inverse transgressive dans le Bassin de Paris et dans les Chaines Subalpines nord. Les black shales vocontiens des événements anoxiques océaniques globaux OAE1a (Aptien) et OAE1b (Albien) s'inscrivent dans des tendances opposées en termes de variations du niveau marin relatif, largement transgressive pour le premier, fortement régressive pour le second. La pulsation tectonique déduite se manifeste à plus grande échelle d'après les données de la bibliographie. Elle est également responsable des déphasages constatés dans les variations locales du niveau marin à grande échelle.

Keywords. French Alps, Paris Basin, Lower Cretaceous, Sequence stratigraphy, OAE1a, OAE1b.

Mots-clés. Alpes françaises, Bassin de Paris, Crétacé inférieur, Stratigraphie séquentielle, OAE1a, OAE1b.

Published online: 12 May 2022, Issue date: 13 January 2023

1. Introduction

This paper is part of a broader research aimed at understanding the progressive closure of the Vocontian Trough (VT) in the French Subalpines Chains during the Cretaceous. The VT (Figure 1A) is a narrow basin oriented approximately perpendicular to the Alpine belt, but connected to the Pyrenean basin through the SW–NE "Rhodanian saddle" [Porthault, 1974], whose subsidence was controlled by the sedimentary play of the Cévennes fault row (Figure 1B). The geodynamic significance of the highly-subsiding VT remains poorly-understood between the Pyrénées and the Alps.

The work is accomplished by the analysis of the sedimentary record, through depositional facies analysis and stratigraphic correlation. A similar research was performed earlier in this basin for another short time interval spanning the Cenomanian–Turonian boundary [Grosheny et al., 2017]. In contrast to the marine flooding generally found elsewhere during the boundary event, the deposition of the OAE2 black shale occurred within a regressive context in the subalpine basin. This is why the present work aims at also integrating two of the other Vocontian black shale beds, namely the lower Aptian Goguel Level (OAE1a) and the lower Albian Paquier Level (OAE1b) into a regional sequence stratigraphic framework, including the Paris Basin on the stable European plate, outside the Alpine margin.

In addition to the data available in the literature, new subalpine sections have been logged and dated by planktic foraminifer assemblages and ammonites. This biostratigraphic control is indicated close to the logs in the figures hereafter. For abbreviations, symbols and significance of background colours, see Figure 2.

2. Stratigraphy

For convenience, we rely on the local substages that were once commonly used in France for the Aptian and the Albian. The Aptian is divided, in ascending order, into Bedoulian (lower Aptian), Gargasian (upper Aptian) and Clansayesian (uppermost Aptian). For the Albian, the upper part of the stage is divided into upper Albian *sensu stricto* and uppermost Albian or Vraconnian, the latter beginning with the Fallax ammonite zone [Kilian Group (Reboulet S. et al.), 2018]. In the following text, "upper Albian" will always refer to upper Albian *sensu stricto*.

The Aptian–Cenomanian succession in the VT is as follows (Figure 3). Lower Bedoulian deposits are a bed-scale limestone–marl alternation which is the basinal equivalent of the last sequences of the Urgonian platformal carbonates surrounding the basin. Uppermost Bedoulian beds are a marlstone layer hosting the Goguel black shale (a lateral equivalent of the Selli Level in Italy), overlain by a double limestone bed ["Niveau Blanc" of Friès and Parize, 2003] which marks the lower to upper Aptian boundary. Within the upper Aptian, Gargasian deposits are almost uniformly made of blue grey marlstone, which have given the Formation name "Marnes Bleues" (Blue Marls). The Clansayesian is mostly represented by a laterally-continuous bed bundle, the Fromaget Beds [Bréhéret, 1995] bearing a rich *Hypacanthoplites* ammonite fauna. In the eastern VT another bed bundle (Nolan Beds, from the *Nolaniceras* ammonites found in it) is found under the Fromaget bundle [Bréhéret, 1995] but it is less prominent or almost completely subdued in western sections. The

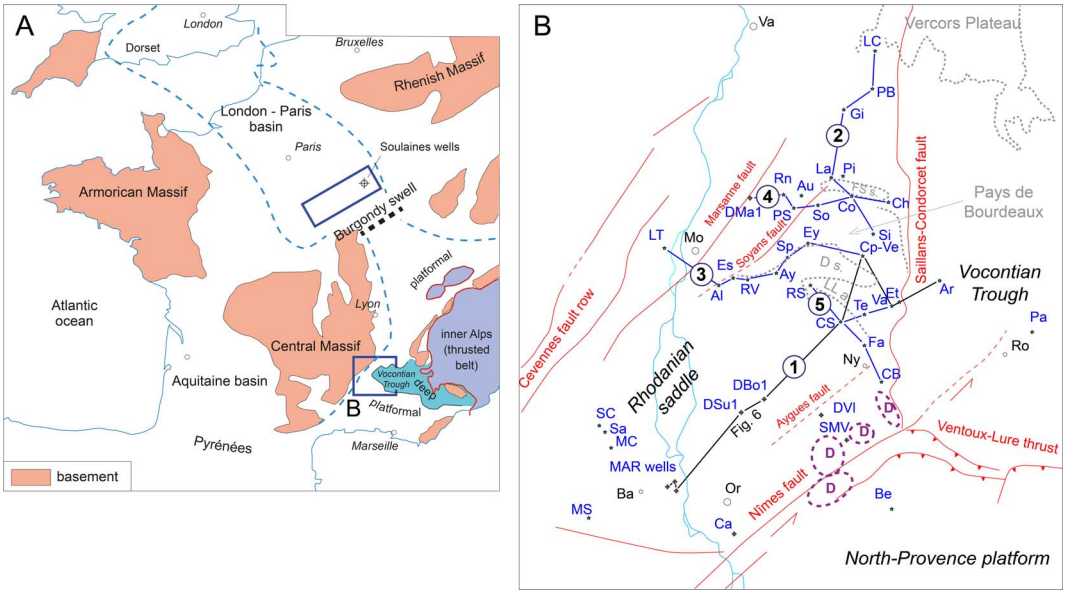

Figure 1. Location maps. (A) the two areas studied (boxed). Dotted, maximal areal extension of the connection between the Alpine sea and the London–Paris basin over the Burgondy swell. (B) detailed map of the subalpine margin. 1 to 5, correlation transects described. Abbreviations, see Figure 2.

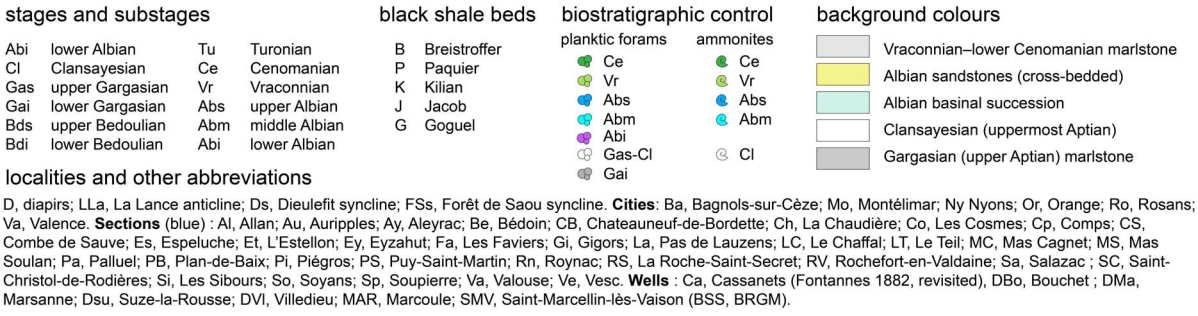

Figure 2. Abbreviations and biostratigraphic symbols used, and significance of background colours in figures.

first 70 m of the thick marlstone succession overlying the Fromaget beds comprises three black shale levels, i.e. in ascending order the Jacob, Kilian and Paquier levels [Bréhéret, 1995]. The Aptian–Albian boundary has been recently fixed on top of the Kilian level [Kennedy et al., 2000, 2014, Petrizzo et al., 2012], which leaves about 35 m of marlstone above the Fromaget bed bundle to be ascribed a latest Aptian age. The Albian marlstone succession is not perfectly uniform as it comprises several bundles of argillaceous limestone beds and other black shale layers [Paquier and Breistroffer levels, Bréhéret, 1995]. The Cenomanian succession is an alternation of well-marked bed bundles and marlstone-dominated intervals. The Albian–Cenomanian boundary was fixed by the first occurrence of the planktic *Thalmaninella globotruncanoides* in the Vocontian reference section of the Palluel Pass [Kennedy et al., 2014], within the upper part of the "Albian" marlstone succession, or about a few tens of metres below the first Cenomanian bed bundle.

Vocontian successions comprise numerous slump layers, and sandstone turbidite bodies, most of them channelled. The latter have been numbered from G1

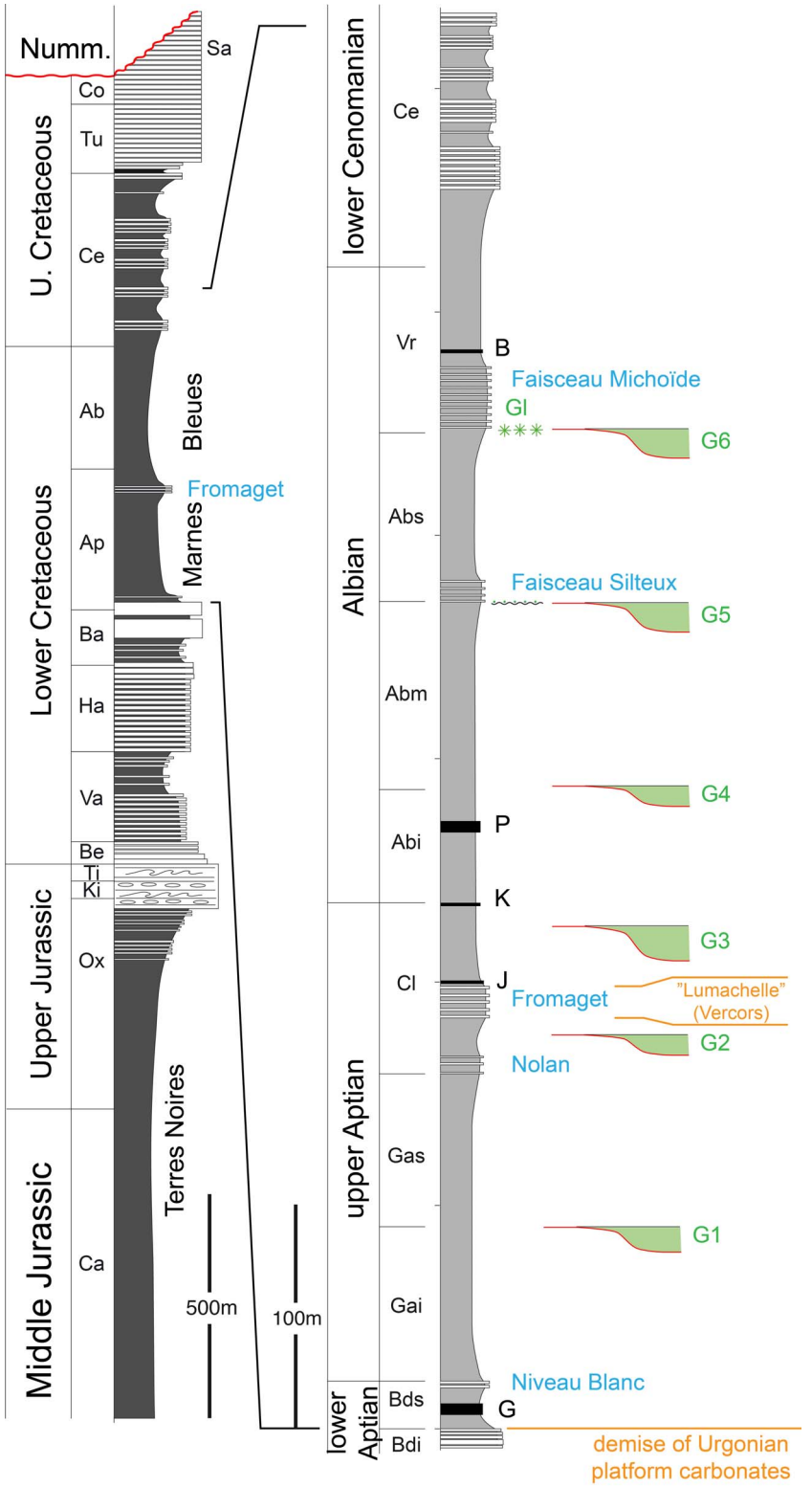

Figure 3. Caption continued on next page.

Figure 3 (cont.). The Vocontian stratigraphic succession with enlargement for the Aptian–Cenomanian. Abbreviations, see Figure 2. In blue, laterally-continuous limestone bed bundles as named by Bréhéret [1995]. G1 to G6, sandstone turbidite bed bundles. The "faisceau michoïde" was dated by Gale et al. [2011] and also by a glauconite bed bearing ammonites of the Fallax zone [lowermost Vraconnian, Kilian Group (Reboulet S. et al.), 2018] at its base [Vincent et al., 2020]. Correspondences with some peripheral platformal carbonates are indicated. Thicknesses are approximate.

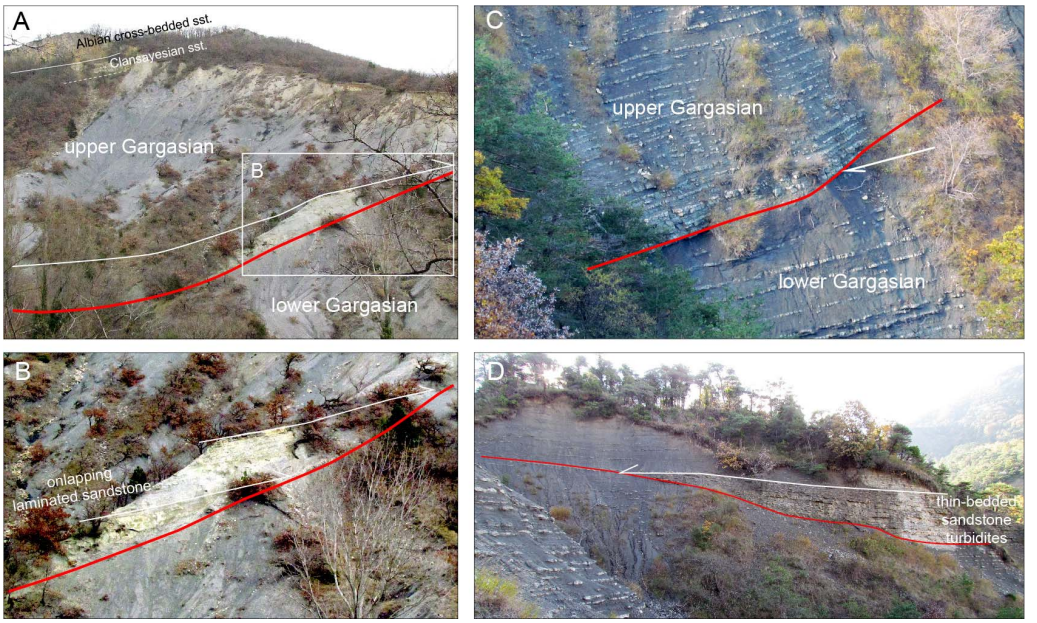

Figure 4. The mid-Gargasian regional erosional surface in slope deposits on the north-western Vocontian margin. (A, B), Roynac; (B, C), Gigors (for location, see Figure 1B).

to G6 (from the mid-Gargasian to the uppermost Albian) by Rubino [1989] but later studies identified more levels from T1 (G1) to G9, within the same stratigraphic range [Bréhéret, 1995, Friès and Parize, 2003]. The lower to upper Bedoulian and Bedoulian–Gargasian transitions are marked by mass-transport deposits covering large areas in the western VT (respectively the CL3 and CL4 debris flow beds of Ferry and Flandrin [1979]. Several bundles of thin-bedded turbidites (Pl for "plaquettes rousses", or red slabs) with reddish patina also occur within the black shale bearing upper Bedoulian sequence and in the lower part of the Gargasian marlstone. The G1–G2 turbidites are associated with a laterally-continuous erosional surface on the basin slope (Figure 4). This surface correlates with the mid-Gargasian [Conte, 1985] "Grès à Discoidea" found in the Rhodanian saddle, and which likely represents an incised valley fill (Figure 5).

The exact stratigraphic position of turbidites "G" versus limestone bed bundles in Albian Blue Marls is approximate. In the model proposed by Rubino [1989], limestone bundles were thought to represent the basinal expression of lowstand deposits, therefore lined at the base by the so-called basin floor fan ("G" beds, here), in accordance with the Vail et al. [1977] sequence stratigraphy model, widely used in the eighties. But the limestone bed bundles and the turbidite "G" beds do not occur in superimposition in most real sections, so the sequence stratigraphic interpretation remains somewhat speculative.

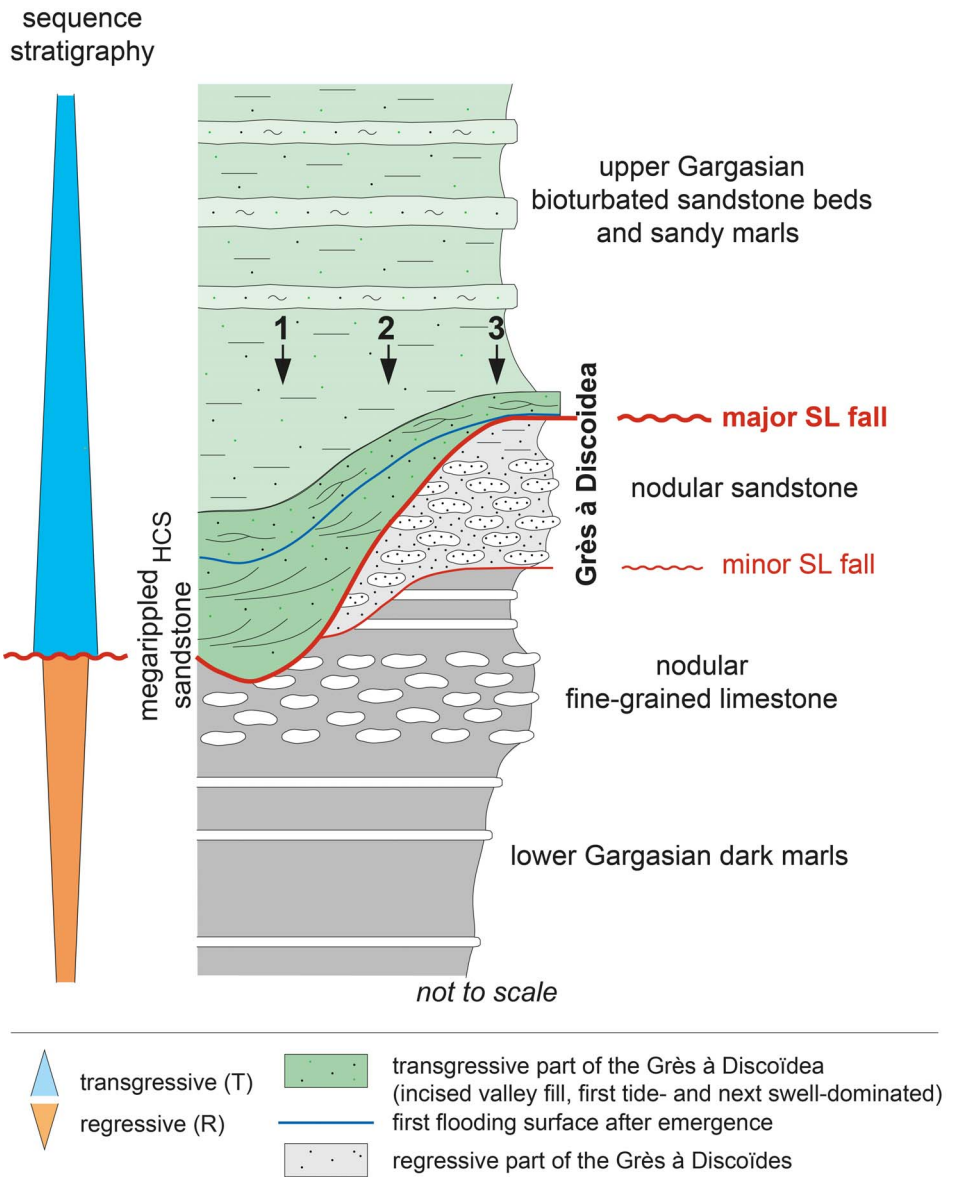

Figure 5. Sequence stratigraphic analysis of the mid-Gargasian Grès à Discoïdea in the Gard Department (Rhodanian saddle, Figure 1B). Type sections: 1, Salazac village; 2, Mas Cagnet ravine; 3a, Saint-Christol-de Rodières; 3b, Mas Soulan (Saint-Laurent-la Vernède road). From Ferry [1997, unpublished ANDRA Report]. For location of type sections, see Figure 12.

3. Description of the stratigraphic transects across the VT western margin

Five transects are described (Figure 1B). Transect T1 goes from the Rhodanian saddle to the VT proper. It integrates the results of the ANDRA exploration works in the early nineties in search for a suitable location for a repository of nuclear waste close to the Marcoule plant. Detailed analysis is mostly available in unpublished reports but a short synthesis was published later [Ferry, 1999]. Transects T2 goes across the northern margin from the Vercors platform to the Pays de Bourdeaux which geographically

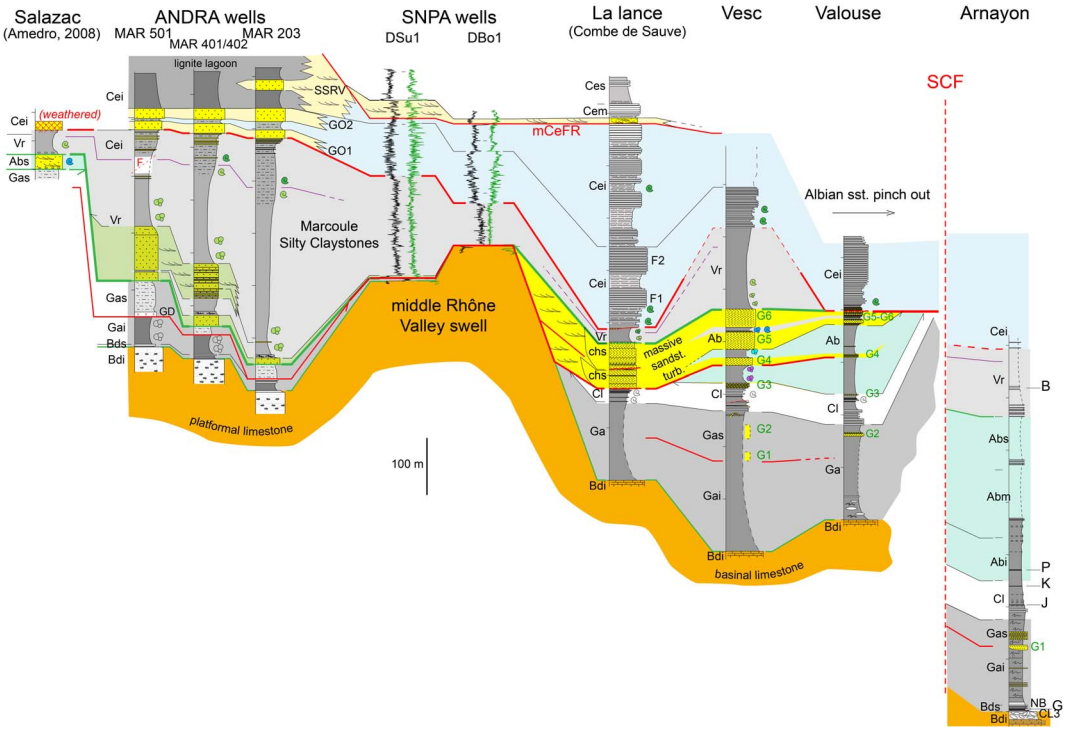

Figure 6. Transect 1 across the western Vocontian margin (upper–lower Aptian to mid-Cenomanian). Slightly modifed from Ferry [2017]. Location on Figure 1B. Chs, channelled massive sandstone; GD, mid-Gargasian "Grès à Discoidea"; GO, lower Cenomanian "Grès à orbitolines"; mCeFR, mid-Cenomanian forced regression; SSRV, lower to middle Cenomanian sandstone spit.

corresponds to what is called here the western VT. Transects T3 to T5 depict more detailed correlations on the western border of the western VT. Transect T5, along the La Lance anticline, is specially devoted to the relationships between cross-bedded Albian sandstones and massive turbidites, which cannot be understood along transect T3.

The narrow corridor between the Nîmes and Nyons faults is poorly-known due to the occurrence of salt diapirs (featured "D", Figure 1B). Ancient exploration wells (mostly by the SNPA company) have been used in areas covered by Miocene deposits of the Comtat basin (Middle Rhône valley). These deposits have prevented for long the reliance on the deposits of the Gard Department (also known as the Cèze River basin) and those of the VT.

3.1. *Transect T1*

Figure 6 summarizes the main stratigraphic results acquired after the ANDRA works in the Gard Department. It shows how the basinal Gargasian marlstone "pinches" out against Barremian slope limestone. The marsltone unit reappears modified west of the major hiatus of the middle Rhône Valley as a thin succession, where deposits of the upper Gargasian sequence are shallower than those of the first one, and fills a nested lowstand to transgressive estuarine sandstone system (Grès à Discoidea, GD, see also Figure 5). The most striking feature is the shift of cross-bedded Albian sandstone units to the east, where they appear "anchored" against a domal feature judged responsible for the Albian stratigraphic hiatus of the Middle Rhône Valley [Ferry, 1999]. Two superposed megarippled sandstone units have been described on the external platform by Rubino [1989]. Massive sandstones develop basin-

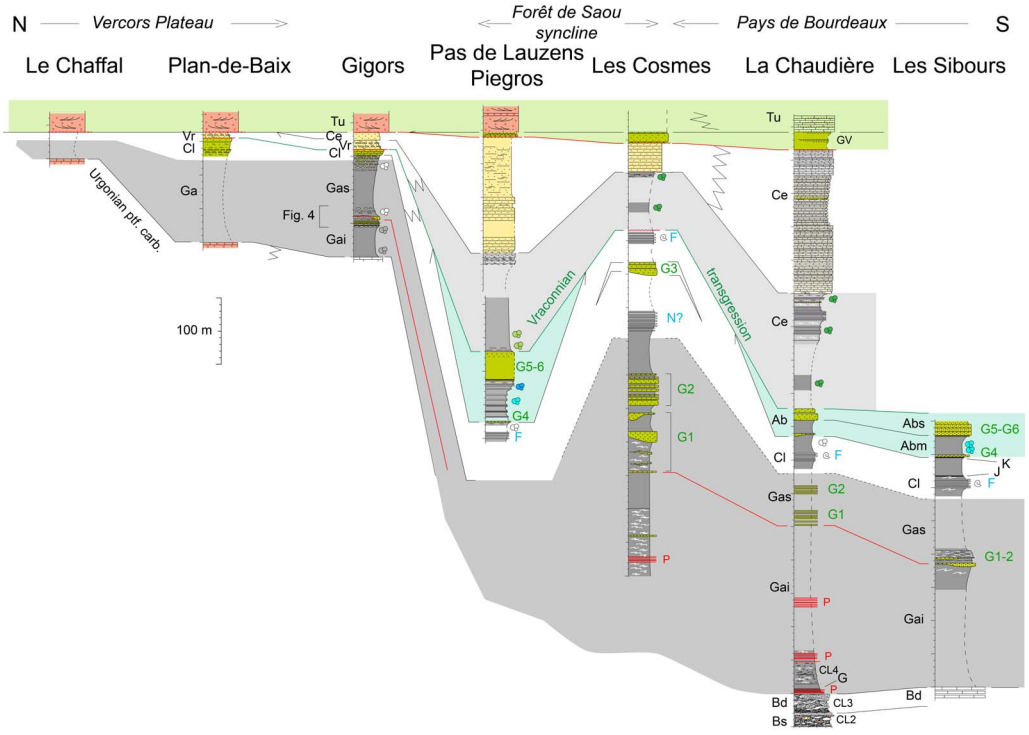

Figure 7. Transect 2 across the northern margin. For location, Figure 1B.

wards with all characteristics of turbidites. What is intriguing is that these massive turbidite deposits are rooted within (interfinger with) the megarippled sandstones of this margin [Rubino, 1989]. Albian deposits are lacking in ancient exploration wells of the Middle Rhône Valley where deposition resumes in the Vraconnian or the Cenomanian. Megarippled sandstone do reappear west of the hiatus area, but as a single sequence of late Albian age [Amédro, 2008] resting on the upper Gargasian sequence. A second striking feature is the large thickness of the Vraconnian sequence on the western part of the transect, suggesting a sharp increase in subsidence after the Albian hiatus. The Vraconnian sequence begins with a thick package of transgressive gravelly sandstone passing upward to a thick silty claystone (called "Couche Silteuse de Marcoule" in the ANDRA works). Ammonites found in the fully-cored wells show that the Albian–Cenomanian boundary [Amédro and Robaszynski, 2000] occur within a regressive trend leading to the two successive sequences of sandstone shore facies of the lower Cenomanian "Grès à Orbitolines" (GO1, GO2, Figure 6). The Grès à Orbitolines passes slopeward to a double thick package of evenly-bedded sandy limestone (F1 and F2, Figure 6). Their thickness reaches a maximum in La Lance anticline where F1 and F2 fills a large erosional surface lined at the base with superimposed shifting channels filled with fine to medium-grained sandstone. The slope erosional surface passes to a correlative conformity basinward (Valouse), which becomes strongly erosive again when approaching the N–S Saillans–Condorcet fault (SCF, Figure 6). This fault is a major lineament implying the basement according to a gravimetric survey [Flandrin and Weber, 1966]. Recent field work shows that, close to the fault (see further transect T3, Figure 8), the lower Cenomanian limestone rests directly on the lower part of the upper Gargasian marlstone. Also, the Albian G5 and G6 turbidite bundles thin before toplapping the erosional surface. East of the fault, a thick Albian marlstone succession occurs, devoid of turbidites, suggesting that the SCF fault uplifted the western part of the VT, and that the turbidite currents coming from the west waned against a relief.

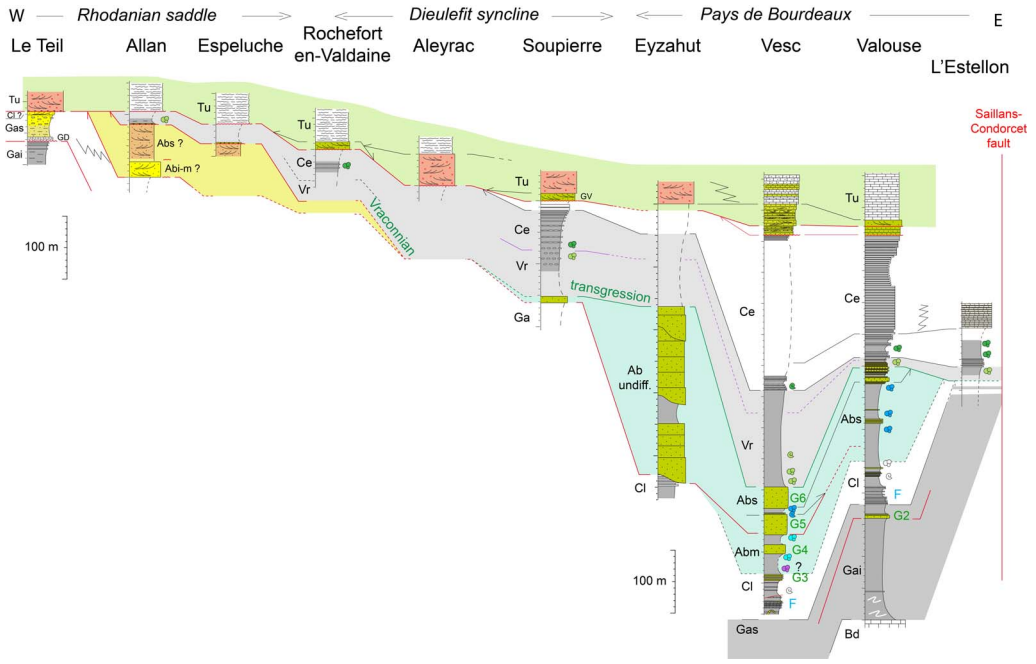

Figure 8. Transect 3 along the northern edge of the Dieulefit syncline. For location, Figure 1B.

3.2. *Transect T2*

This transect (Figure 7) is designed for imaging the pinching of the two gargasian marlstone sequences on the Vercors platform edge. The sequence boundary at the base of the upper sequence (Gas) shows the relationship between the slope channel of Gigors (Figure 4) and the G1 to G2 turbidite systems basinward. The sequence boundary is dated by planktic foraminifers to occur around the boundary between the *Martini* and *Nuttfieldensis* ammonites zones. The Clansayesian bed bundles and marlstone interbeds are laterally continuous. *Hypacanthoplites* ammonites of the Fromaget beds have been reported [Sibours, Bréhéret, 1995] or newly found (Les Cosmes section). The basinal fine-grained facies passes upslope to a bioturbated sandstone in the Gigors section and to cross-bedded sandstone a short distance to the north. Albian deposits are very thin. Turbidites are mostly represented by a sandstone package attributed to G5–G6 sandstone beds. A new discovery is the hiatus occurring along the southern flank of the Forêt de Saou syncline (Les Cosmes section) where the fine-grained limestone beds of the Fromaget bundle are directly overlain by Vraconnian to lowermost Cenomanian marlstone dated by planktic foraminifers. This is reminiscent of the uplift that occurred in the Middle Rhône Valley. The Vraconnian–lowermost Cenomanian marlstone passes upslope to a bioturbated sandstone bearing calcareous diagenetic nodules in the Gigors section, as for the Clansayesian deposits. Cenomanian deposits are represented here by shelfal to shore sandstones bearing wave features (HCS). They thin on the southern flank of the Forêt de Saou syncline (Les Cosmes) suggesting they onlap onto a swell. They pass to thicker finely-laminated, more or less bioturbated sandy limestone basinward (La Chaudière). The non-dated yellowish sandstone occurring under the transgressive Turonian calcarenite at Gigors and Plan-de-Baix were ascribed an Albian age until now [Porthault, 1974]. The strong areal restriction of Albian deposits in our correlation suggests they could either be the upslope facies of the Cenomanian sandy wedge called “Grès d’Auripples” by Porthault [1974].

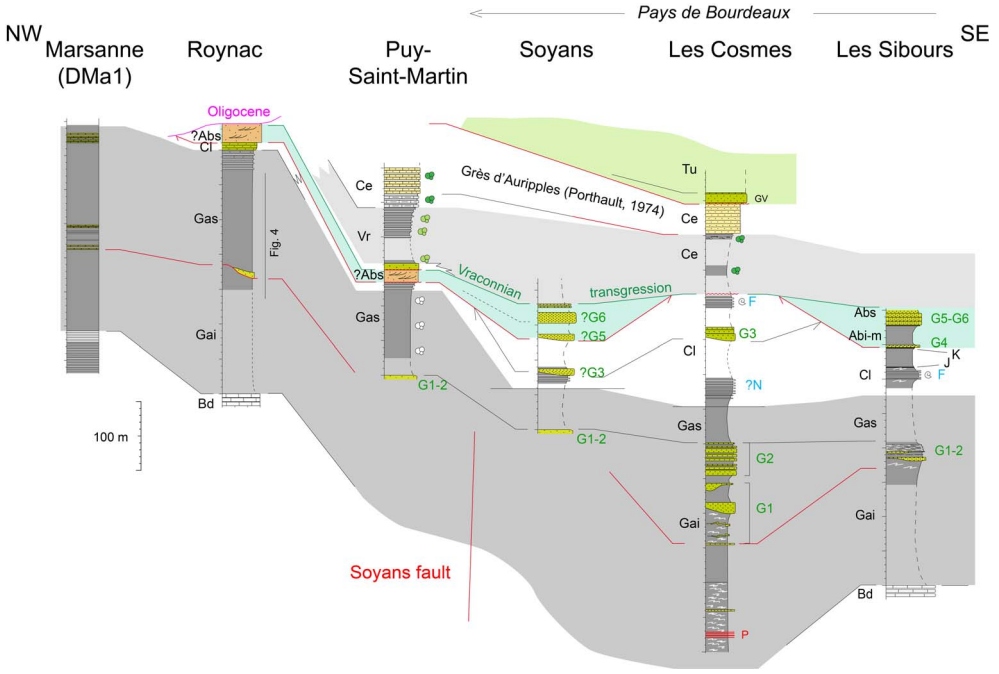

Figure 9. Transect 4 across the Pays-de-Bourdeaux. For location, Figure 1B.

3.3. *Transect T3*

This transect (Figure 8) runs along the edge of the restricted Albian basinal area NE of the Middle Rhône Valley hiatus area, which is represented by a sharp contact in Figure 6. To the west, the two Albian sequences of cross-bedded sandstone occur, from Allan to the NW termination of La Lance anticline, south of the Dieulefit syncline (resp. Al and RSS sections, Figure 1B), where their interfingering with massive sandstone beds occurs (see further transects T5 and T6, Figures 10 and 11 for details). Along transect T3, this interfingering is not visible. Massive sandstone turbidites suddenly appear on the northern flank of the Dieulefit syncline (Eyzahut). As shown on transect T1, these massive beds thin basinward where they interfinger (G4 to G6) with dark-grey marlstone beds, which have given middle to upper Albian pyritous ammonites [Moullade, 1966], in accordance with our findings on foraminiferal assemblages. As on transect T1, Gargasian to lower Cenomanian deposits toplap the erosional surface sealed by lower Cenomanian limestone when approaching the SCF. Well-dated by planktic foraminifers all along, the Vraconnian to lowermost Cenomanian marlstone is laterally-continous and transgressive on Albian deposits, either cross-bedded or turbiditic. As in the Rhodanian saddle (transect T1), its base is often lined by a lag of quartz gravels and coarse-grained sandstone, which may be given a regional stratigraphic value, as Albian sandstones are always fine-to medium grained everywhere. As in the Rhodanian Saddle (transect T1), the Albian–Cenomanian boundary lies within the upper part of the marsltone wedge. The transect also shows the truncation of the succession by the transgressive Turonian calcarenite [Porthault, 1974] after the major regional sea level fall that occurred around the Cenomanian–Turonian boundary [Grosheny et al., 2017]. The Venterol Sandstone [Porthault, 1974; GV, Figure 8] at the base of the calcarenite represents the lowstand deposit of the forced regression. At the western termination of the transect (Le Teil section, Figure 8), the Grès à Discoidea allows to identify the two Gargasian sequences, below and above. The full sandy facies of the upper one indicates it is closer to the shore than in the Rhodanian saddle. By comparison with transect T2, the overlying cross-

bedded sandstone under the transgressive Turonian calcarenite could be assigned a Clansayesian age (shore facies of the basinal bed bundles and marlstone). This would be a rare case where Clansayesian deposits are preserved in the Rhodanian saddle where all Clansayesian ammonites cited in the literature are reworked in transgressive lags of later sequences.

3.4. *Transect T4*

This transect (Figure 9) runs perpendicular to the SW–NE Marsanne and Soyans faults. It is designed to show again the thinness of Albian deposits versus Gargasian ones in the Pays de Bourdeaux. There is only one unit of cross-bedded Albian sandstone (? the upper one) in this transect versus the two units occurring in transects T3 and T1. The cross-bedded sandstone is directly overlain by the characteristic transgressive gravelly sandstone of the Vraconnian sequence. The succession is perfectly dated by planktic foraminifers in the Puy-Saint-Martin section, except for the Albian sandstone whose likely age will be discussed further. The transition between the cross-bedded sandstone and the massive turbidite beds of the Soyans section is not visible, and therefore their sequence stratigraphic relationships, if any, are also hidden. The facies change was likely controlled morphologically by the Soyans fault.

3.5. *Transect T5*

The transition between Albian cross-bedded and massive turbiditic sandstones is best understandable along the SW flank of La Lance anticline (Figure 10). The figure shows two subtransects roughly perpendicular, one upslope in cross-bedded deposits, the other alongslope in turbidite deposits. The Tour d'Alençon-Le Brut subtransect shows that the two Albian cross-bedded units are nested in an incised valley likely perpendicular to the SW–NE fault row of the Middle Rhône Valley. Both the overall geometry and the cross-bedding suggest an elongated estuarine deposit. The Célas to Chateauneuf-de-Bordette subtransect shows both the interfingering of cross-bedded and massive sandstones, earlier described by Rubino [1989], and the progressive thinning downslope of the massive sandstone beds over rather short distances. Regarding the sequence stratigraphic relationships between the likely estuarine deposits and the massive turbidites between the two close sections of Le Célas, there are two possibilities *a-priori*. Either the cross-bedded deposits are transgressive over the massive turbidites, or on the contrary, turbidites are transgressive over cross-bedded ones. The most likely explanation is the reworking of backstepping transgressive estuarine sands by storm rip currents when sea level rose in a narrow lowstand valley. Vegetation cover and recent alluvial deposits between the two Célas section do not allow to obtain better field data. The exact age (? middle–upper Albian, Figure 10) of the two Albian sequences cannot be determined because of the absence of marlstone interbeds able to give micropaleontologic data. The sandstone wedge is sandwiched between the Clansayesian Fromaget bed that has given a rich *Hypacanthoplites* ammonite fauna, and the Vraconnian marlstone dated by planktic foraminifers. The evenly-bedded, coarse to gravelly sandstone of the Vraconnian transgression seals the lateral facies change in Albian deposits. The transect also pictures the large erosional channel evoked above at the base of the lower Cenomanian limestone bed bundles F1 and F2 (transect T1).

An additional correlation (Figure 11) is given between La Lance and Valouse (for location, Figure 1B) just to enlighten how channeled were Albian deposits in the western part of the Vocontian Basin. A similar channelled pattern was suggested by Friès and Parize [2003] at a larger scale in the basin for Gargasian turbidites.

4. Gargasian and Albian subalpine palaeogeographies compared

4.1. *Gargasian palaeogeography*

From the transects described above and also sections published by Friès and Parize [2003], the Gargasian marsltone succession is on average 200 to 250 m thick but may reach 350 m in the Pays de Bourdeaux. The succession pinches progressively on Urgonian platformal carbonates of the Vercors to the north (Figure 7), as well as on those of the Bas-Vivarais across the present-day middle Rhône valley to the west, or those of the Provence platform to the south. The palaeogeographic picture (Figure 12) is that of

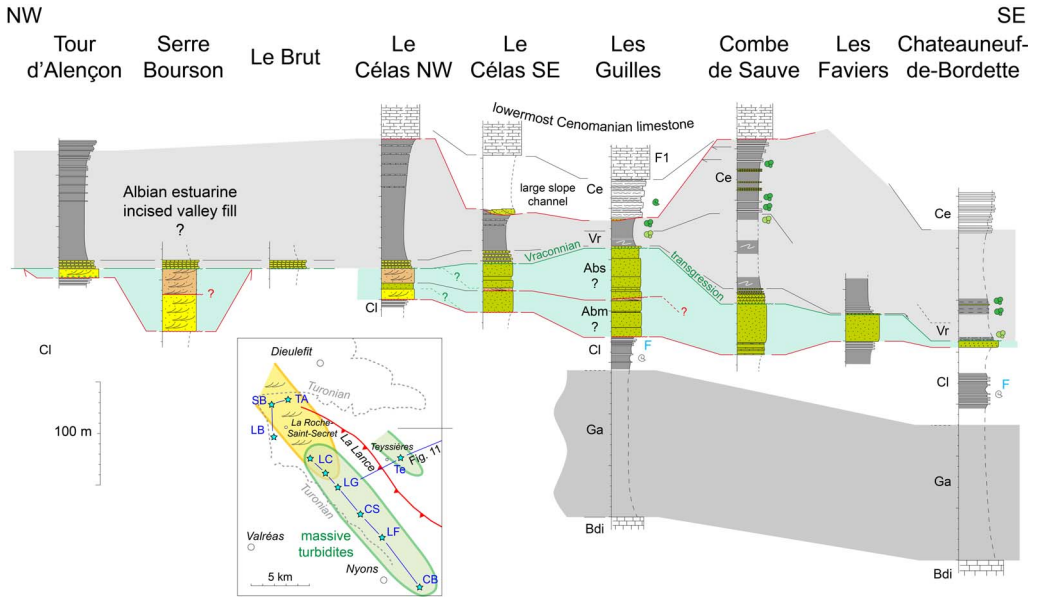

Figure 10. Detailed transect 5 along La Lance anticline. For location, Figure 1B.

a large basin including the platformal areas flooded after the demise of Urgonian shallow water carbonates surrounding the VT. The change from carbonate- to marlstone-dominated deposition is likely tied to a climate change, as suggested in other locations [Mutterlose et al., 2009]. The overall picture is complicated in the Rhodanian saddle by what will occur there around the Aptian–Albian boundary, as will be explained in detail in the next paragraph. These Gargasian marlstones may therefore be lacking but were probably present before Albian erosion. This is also true south of the Ventoux-Lure chain on what is known as the Albian Durancian Isthmus *auct.* [Masse and Philip, 1976] which separates the Vocontian domain and the south Provence basin to the south.

Vocontian Gargasian marls are interrupted in their middle part by a laterally continuous sandstone turbidite system [G1 of Rubino, 1989; G1/G2 of Bréhéret, 1995; T1a/T1b of Friès and Parize, 2003]. Later turbidite systems (Clansayesian to Albian) are more geographically restricted. The middle Gargasian turbidite system correlates to a major erosional surface in slope marls of the western margin (Figures 4 and 5), which allows to define two major Gargasian sequences. Into the Rhodanian saddle, this slope erosional surface correlates to a large incised valley hosting a probable estuarine system oriented to the NE (Figure 12). In the Rhodanian saddle, the lower Gargasian sequence is made of deeper marsltone than the upper Gargasian one which is more sandy (Figure 5), and accordingly shallower [Ferry, 1999]. This is not the case in the two slope valleys on the northwestern margin (Figure 4), where there are no differences in both facies and planktic foraminiferal abundances between the marls of the two sequences.

4.2. *Albian palaeogeography*

From the stratigraphic data presented above, the areal extension of Albian deposits in the western VT (Figure 13) is strongly restricted compared to that of Gargasian ones (Figure 12). The SCF played a major role in isolating, within the basinal environment, an upper terrace corresponding to the Pays de Bourdeaux, with rather thin successions, and a deeper eastern basin with expanded sections and very few turbidites. The change occurred after the deposition of the Clansayesian G3 turbidite system. The SCF is lined on its western side by a N–S anticline, the Montagne de Couspeau. Most Albian turbidites did not cross it, suggesting the occurrence of a submarine relief, by which they quickly decelerated and waned onto. Albian stratigraphy on the margins of the upper terrace is difficult to understand and interpret. The Clansayesian system underneath follows that of the

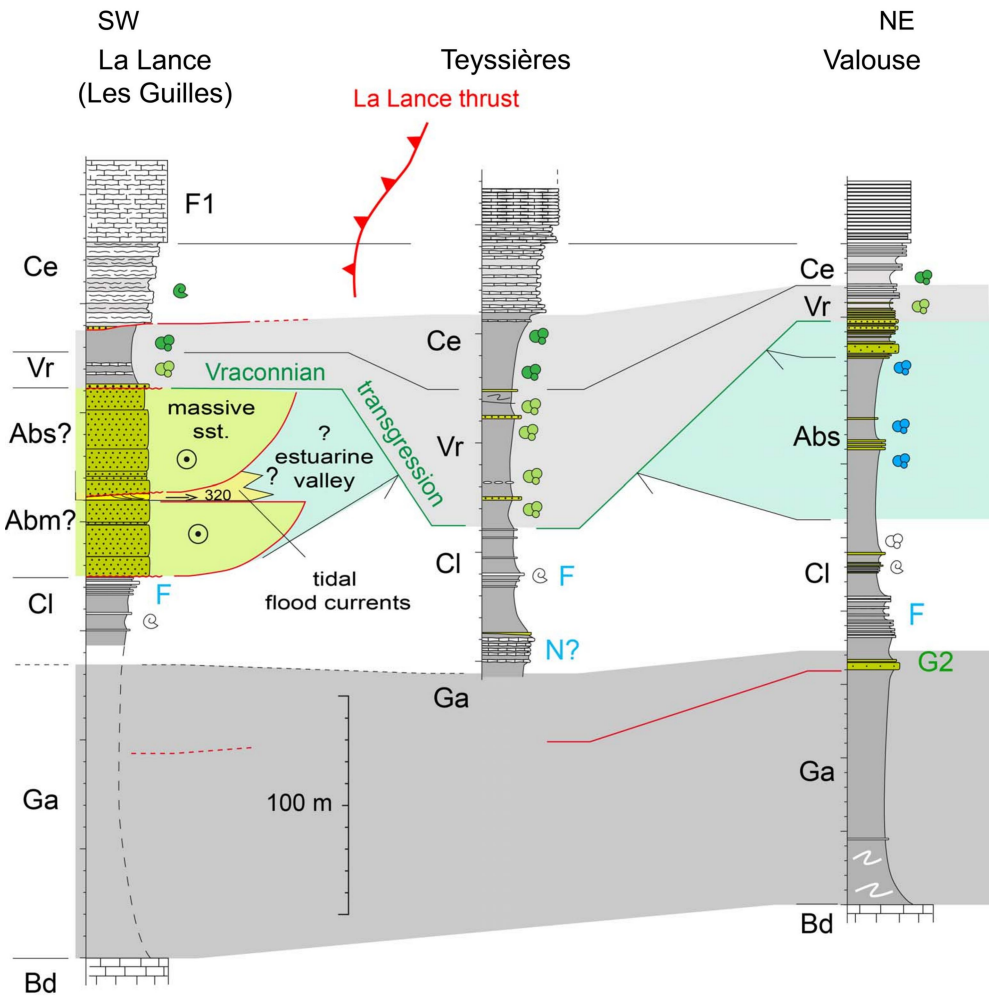

Figure 11. Correlation from La Lance to Valouse. For location, Figure 1B.

Gargasian one. Its marginal cross-bedded sandy deposits are recorded in the T1 to T4 transects. Vraconnian overall transgressive deposits seal everything. Of the two Albian cross-bedded units, the upper one is the most widely represented and dated upper Albian at Salazac [Amédro, 2008], on the North Provence platform [Joseph et al., 1987b,a], as on many other places of the VT margin according to Bréhéret [1995]. This is the reason why we ascribe a late Albian age to the second cross-bedded unit of La Lance anticline. This unit is clearly overall transgressive both in the Rhodanian saddle west of the hiatus of the Middle Rhône Valley and on the North Provence platform (Figure 13B). The areal extension of the mid-Albian marginal sandstone looks narrower but these deposits may have been truncated by the late (and especially the latest) Albian transgressions. The peculiar relationships between the first Albian cross-bedded unit and turbidites along transect T5 suggest that the lower to middle Albian shoreline may have been close to the limit of the light blue area in Figure 13A. Its shore facies may have been very narrow, even restricted to channelled estuarine deposits, as suggested in Figure 13A. Their extension along the Soyans fault may also have been eroded by the late Albian transgression. In the diapirs region (D, Figure 13), data are sparse. Outcrops [Masse et al., 1990] as well as well data allow to draw a

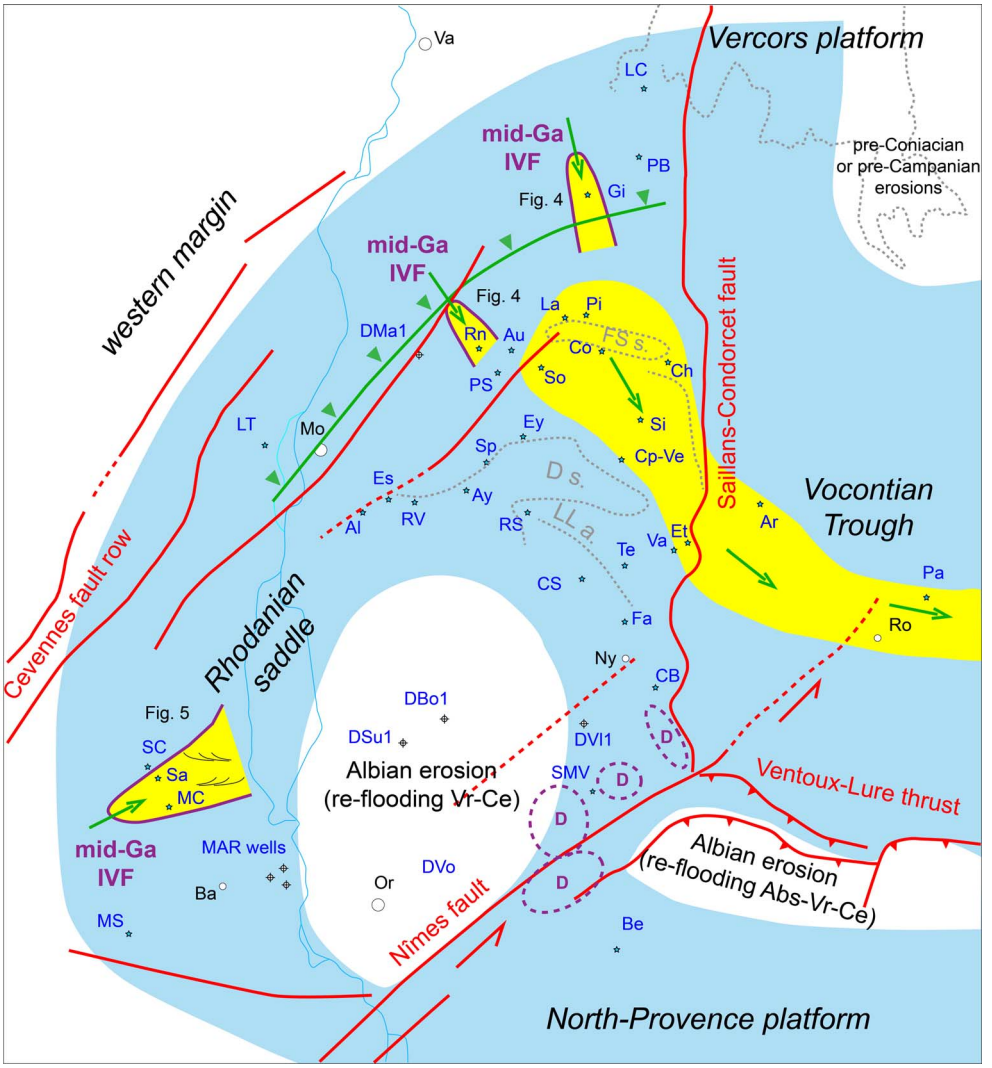

Figure 12. Gargasian facies map.

narrow band where a probably upper Albian cross-bedded sandstone unit is sandwiched between Gargasian and Vraconnian to lower Cenomanian marlstones (Figure 13B). Lower to middle Albian deposits are lacking.

The Middle Rhône Valley hiatus (Figures 6 and 13) is explained by an uplift that occurred around the Aptian–Albian boundary, as on the Durancian Isthmus on the Provence platform. Most of the western margin of the VT was then exposed during the early to middle Albian. This is consistent with other data from the Albian bauxites of southern France, which support a strong denudation of the sedimentary cover of the Variscan basement of the Massif Central [Marchand et al., 2021]. Deposits of later transgressions (late Albian, Vraconnian, Cenomanian) onlapped in a stepped way the Middle Rhône Valley swell.

In front of the Ventoux-Lure thrust, upper Albian breccias were described [Moullade and Porthault, 1970, Montenat et al., 2004] suggesting the occurrence of a rocky shore. Parts of the thrust emerged during the Albian [Montenat et al., 1986], with Cenomanian deposits resting directly on Bedoulian limestones.

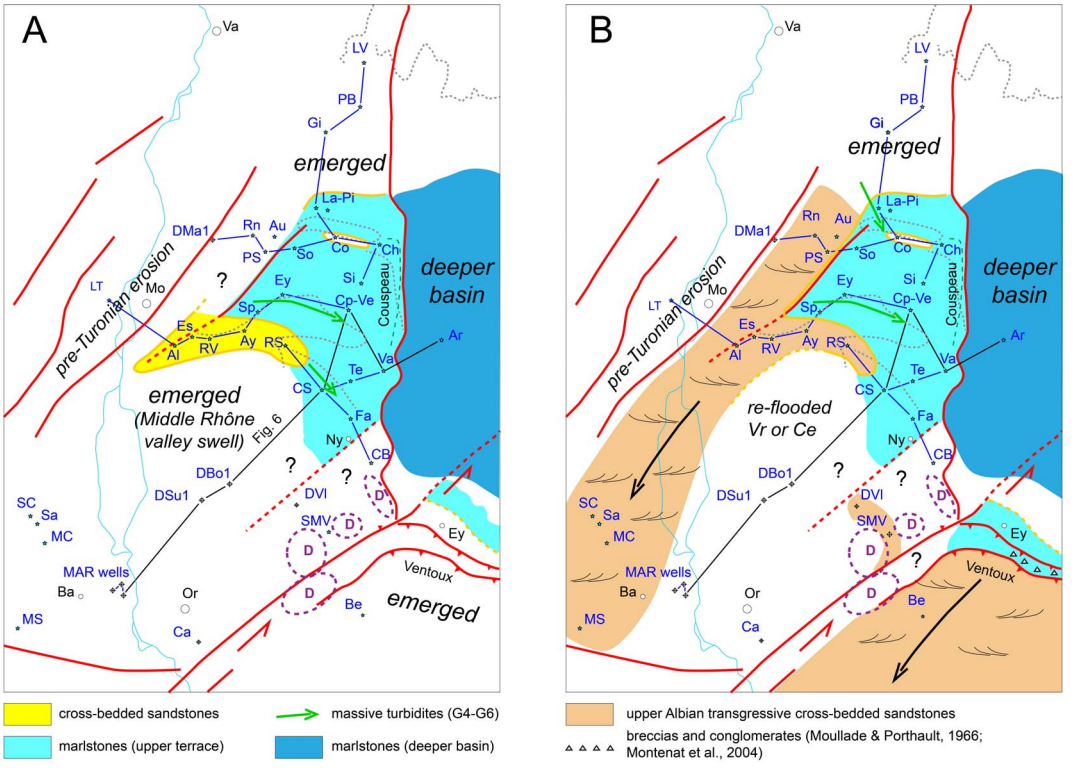

Figure 13. Albian facies maps.

Cross-bedded Albian sandstones were interpreted as relatively deep shelfal deposits under a north-Thetyan peri-Vocontian contour current [Delamette, 1988, Rubino and Delamette, 1988]. Newly acquired stratigraphic data hardly support such an interpretation. The new picture proposed is that of a restricted basin instead.

5. Connection with the Paris Basin

Figure 14 shows the correlation that can be done from the Alpine margin to the eastern border of the Paris Basin (Figure 1A). If the Vocontian margin experienced an uplift, the story is not the same on the European craton in front of the Alpine domain, according to the stratigraphic synthesis of Aptian–Albian deposits in the Paris Basin [Amédro et al., 2021]. In the ANDRA site of Soulaines (Figure 1A), which was cored extensively, the uppermost Bedoulian Argiles à Plicatules rest on a weathering profile covering at least the early Bedoulian and affecting underlying (? upper) Barremian sandstone and claystone [Ferry, 1997, unpublished ANDRA report]. The correspondence of the Argiles à Plicatules with the OAE1a Vocontian black shale is supported by δ^{13}C data [Deconinck et al., 2021]. Although the detail of upper Bedoulian transgressive tract may be somewhat complex (Figure 14), the picture is therefore that of a quick late Bedoulian transgression on a large regional scale after the demise of the Barremian–lower Bedoulian Urgonian carbonate platform on the Alpine margin. Should a cold snap [Mutterlose et al., 2009, Khunt et al., 2011, Millan et al., 2014] and a possible short-lived sea-level fall due to polar ice cap growth had occurred during OAE1a, the largely transgressive event recorded in front of the Alpine belt during the upper Bedoulian sequence did likely hide it.

The Argiles à Plicatules are sharply covered (sequence boundary) by a Gargasian glauconite-rich sandstone unit, next by a marlstone succession bearing lowermost Albian ammonites at its base. The whole Albian marlstone succession looks like com-

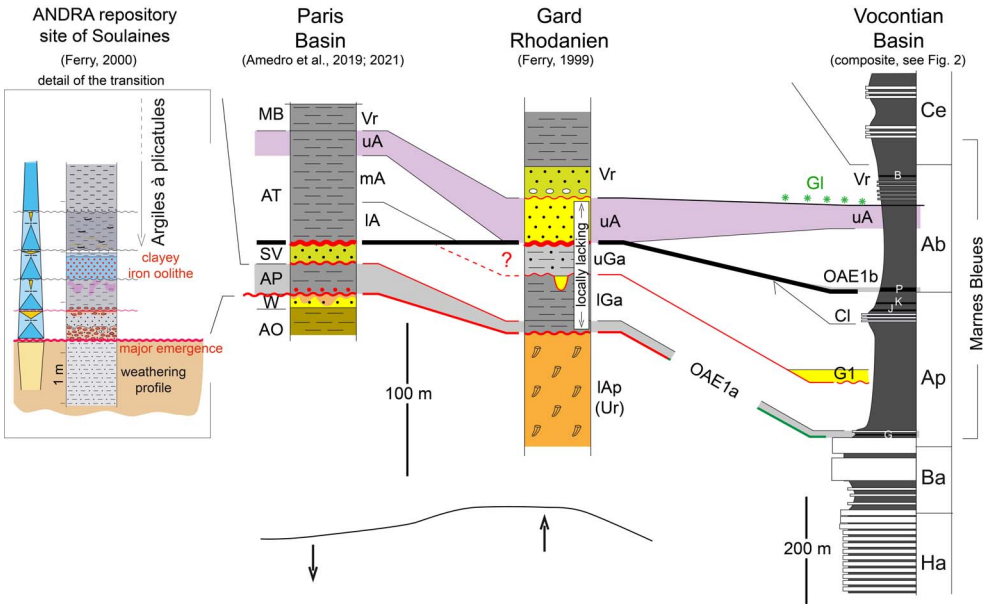

Figure 14. Stratigraphic correspondence between the Alpine margin and the Paris Basin around the Aptian–Albian boundary. For stage names abbreviations, see Figure 2. Formation names in the London–Paris Basin (in ascending order): AC, Atherfield Clay; AO, Argiles ostréennes; HB, Hastings Beds; W, Wealden deposits; AP, Argiles à plicatules; SV, Sables verts; AT, Argiles tégulines; MB, Marnes de Brienne.

plete from the ammonite record, notwithstanding the significance of the discontinuities lined by phosphatic nodules found in it. Without ammonites it is not possible to link the Gargasian sandstone unit to one of the two Gargasian sequences recorded in the Vocontian margin. As the deposits of the upper Gargasian sequence are shallower on the Alpine margin, the second sequence is likely lacking in the Paris Basin. The sea level changes recorded in the Paris Basin in the early to middle Albian are therefore exactly opposite tothose of the VT margin, i.e. emergence on the Alpine margin, submergence in the Paris Basin (Figure 14).

Regarding the OAEs recorded in the VT (Figure 3), the upper Bedoulian OAE1a is clearly within a large transgressive trend. But the three next ones (Jacob, Kilian and especially the lowermost Albian Paquier) are within an opposite regional sea level trend. The basin areal restriction during the deposition of these black shales is in accordance with the results of Heimhofer et al. [2006] and Okano et al. [2008] that suggest an increased riverine input during their deposition. Therefore Vocontian black shales do not occur as a result of increased organic matter production during transgressions as often proposed in the literature. The Vocontian case rather suggests an occurrence related to a global phenomenon but not linked to local relative sea level. The same is also found for the younger OAE2 in the VT [Grosheny et al., 2017].

6. Discussion

From the above, the emergence of the Rhodanian margin of the VT, as well as the near emptying of thebasin west of the SCF during early to middle Albian times is explained by a tectonic uplift along the Cevennes fault row. This uplift is likely related to a N–S contraction of the Provence domain (the Durancian Isthmus *auct.*) likely triggered by the Iberian plate rotational move during the Albian, as shown by earlier works [Hibsch et al., 1992, Montenat et al., 1997]. Gindre et al. [2002] even suggested that the South Provence Basin, until then judged extensional, could have been instead a compressional foreland basin, and the Durancian Isthmus some kind of forebulge. In this respect, what is described here along

the westen margin of the subalpine basin would appear as the result of a transpressional regime involving the Cevennes fault row and its satellites (Nîmes fault, for instance).

In the northern subalpine chains, the story is different, as a thin, channelled sequence of lower to middle Albian marlstone to sandstone is transgressive on condensed upper Aptian deposits [Delamette, 1986]. There, the early Albian transgression correlates to that of the Paris Basin which was flooded in the early Albian after an emergence that possibly spanned the latest Gargasian (the missing Gargasian sequence, see above). The story is therefore more or less similar along the large seaway that connected both areas (Figure 1). The Rhodanian uplift peaked later.

The occurrence of upper Albian breccias along the front of the Ventoux-Lure thrust (Figure 13), was interpreted by Moullade and Porthault [1970] as the result of a tectonic event they related to the early compression recorded in the eastern Alps, although such a connection still remains elusive in terms of a stress field on such a scale within the context of the overal convergence between Africa and Europe. We therefore use the term "Austrian tectonic phase" mainly on a historical basis.

Work in progress also shows that W–E Vocontian folds may have formed as early as the Turonian as a consequence of such a compressive context. The Albian crisis would just be a precursor. It should also be remembered that the local sedimentary record of the Cenomanian–Turonian Boundary Event [Grosheny et al., 2017] looks like very similar to what is recorded around the Aptian–Albian boundary, with also a short-lived, but stronger and larger, areal reduction of the Vocontian basin and the deposition of the OAE2 black shale within a regressive context, like the Albian OAE1b.

On a larger scale, other data are in accordance with the outphasing of ups and downs of the ground we see in France. Some, among many others, are listed hereafter.

On the Iberian Atlantic margin [Rey et al., 2009, and other references therein], Albian aggrading fluvial deposits suddenly occur, after a short-lived hiatus, on Aptian marine ones, implying a strong seawardshift of the facies belt, likely as a result of a long-lasting uplift of the margin. Nothing such is recorded on shelfal deposits of the Moroccan margin to the south [Jaillard et al., 2019]. In the western Pyrenean basin, the Aptian–Albian transition corresponds to the breaking of the Clansayesian platform, and the progressive onlap of breccia-lined Albian carbonate sequences onto the Iberian margin [Canerot et al., 2012, and other references therein], as a result of the opening of the Biscay Bay "rift" and Iberia rotation.

On the southern shores of the Tethys, work in progress in correlating well logs of the so-called "Continental Intercalaire" across the Saharan craton supports the early views of Busson [1970]. It shows that Panafrican arches were reactivated around the Aptian–Albian boundary, that is what is kown among local oil geologists as the "Austrian phase". In the Saharan Atlas, the unconformity is dated around the Aptian–Albian boundary [Emberger, 1960]. The lower Aptian carbonate unit (the "Aptian bar") on Barremian sandstones is lacking on arches due to an Albian erosion that may locally cut down to Hauterivian sandstones. This carbonate bar is also eroded close to the major Gafsa–Jeffara lineament (southern Tunisia), which was likely uplifted at that time. But in Central Tunisia, the story is somewhat different. The platform carbonate Serdj Formation spans the whole latest Aptian [Ben Chaabane et al., 2019]. It is covered by a thin marlstone to platformal carbonate of lower Albian age. The major hiatus is here dated to middle Albian [Jaillard et al., 2013].

On the Arabian plate, a progressive nesting to the north of uppermost Aptian to lowermost Albian platformal carbonates wedges is recorded [Greselle and Pittet, 2005, Rameil et al., 2012], associated with incised valleys [Raven et al., 2010] indicating a stepped relative sea level fall, which was interpreted by Maurer et al. [2013] as a result of glacio-eustasy. Given the whole context, a purely tectonic explanation is more likely.

This short and incomplete survey shows that the local Aptian–Albian boundary tectonic event in France is part of a widespread tectonic event that spanned the latest Aptian to the middle Albian. The outphasing of relative sea level changes during this time span, as quoted above, casts some doubts about a eustatic component in controlling depositional sequences. Or extracting a eustatic component from such a complex stratigraphic record would be difficult.

7. Conclusions

A strong contraction of the western part of the VT, associated with an uplift of the western and southern margin occurred around the Aptian–Albian boundary. This western VT was restricted during the early to middle Albian to a narrow gutter that channelled massive sandstone turbiditic units. These were rooted in a rather elusive marginal megarippled sandstone wedge, perhaps restricted to narrow estuaries. In contrast to the Gargasian turbidite system that was emplaced within a larger basin, most of the Albian massive sandstone beds never reached the eastern part of the basin that remained deep. This was due to an uplift along a major N–S fault crossing the VT that blocked their spreading. This uplift also resumed around the Albian–Cenomanian boundary.

The overall regressive trend recorded on the alpine margin correlates with an inverse trend in the Paris Basin, where one of the two Gargasian depositional sequences (probably the upper one) is lacking, and where lower Albian marlstones are transgressive instead. These data suggest that tectonic deformation occurred on a large scale in front of the French Alps. A sinistral transpressional movement implying the SW–NE faults of the Cevennes fault row is inferred along the alpine margin, associated with uplift.

While the deposition of the Aptian Goguel black shale (OAE1a) is associated with a "flash" marine transgression on a lateritic weathering profile in the Paris Basin, the Jacob, Kilian and Paquier (OAE1b) black shales of the VT were deposited in a basin restricted by the tectonic pulse.

This short-lived tectonic event, which is clearly compressive in SE France, is also recorded on a larger scale along the Atlantic margin, on the North African craton and the Arabian platform, as suggested by the analysis of both literature and work in progress. It is responsible for the outphasings in relative sea level changes depending on location.

Conflicts of interest

Authors have no conflict of interest to declare.

Acknowledgements

The authors warmly thank the comments of an anonymous reviewer and of E. Jaillard (Univ. Grenoble) who carefully corrected the manuscript both in the form and on the content.

References

Amédro, F. (2008). Support for a Vraconnian Stage between the Albian *sensu stricto* and the Cenomanian (Cretaceous System). *Carnets Géol. Mem.*, (CG2008_M02), 1–83.

Amédro, F., Matrion, B., and Deconinck, J.-F. (2021). Stratigraphie et corrélation de l'Albien (Crétacé inférieur) du Sud-Est du Bassin de Paris. *Bull. Inf. Géol. Bass. Paris*, 58(1), 2–28.

Amédro, F. and Robaszynski, F. (2000). La formation des argiles silteuses de Marcoule dans les sondages ANDRA du Gard Rhodanien (SE France) : la limite Albien terminal ("Vraconnien")-Cénomanien au moyen des ammonites et comparaison avec les affleurements de Salazac. *Géol. Médit.*, XXVII(3–4), 175–201.

Ben Chaabane, N., Khemiri, F., Soussi, M., Latil, J.-L., Robert, E., and Belhajtaher, I. (2019). Aptian-Lower Albian Serdj carbonate platform of the Tunisian Atlas: Development, demise and petroleum implication. *Mar. Pet. Geol.*, 101, 566–591.

Bréhéret, J.-G. (1995). *L'Aptien et l'Albien de la fosse vocontienne (des bordures au bassin). Evolution de la sédimentation et enseignements sur les événements anoxiques.* Thèse de doctorat, Université François Rabelais - Tours, https://tel.archives-ouvertes.fr/tel-00805488/.

Busson, G. (1970). *Le Mésozoïque saharien, 2 : Essai de synthèse des données des sondages algéro-tunisiens.* Editions du CNRS, Paris, France.

Canerot, J., Debroas, E.-J., and Bilotte, M. (2012). Le bassin crétacé de mauléon. création, évolution, intégration dans la chaîne pyrénéenne. pages 1–94. Livret-Guide excursion GFC, https://hal.archives-ouvertes.fr/hal-01236469 .

Conte, G. (1985). Découverte d'ammonites du Gargasien dans les "Grès et Calcaires à Discoïdes et Orbitolines" du Synclinal de la Tave (Gard, France). *Geobios*, 18, 203–213.

Deconinck, J.-F., Boué, D., Amédro, F., Baudin, F., Bruneau, L., Huret, E., Landrein, P., Moreau, J.-D., and Santoni, L. (2021). First record of early Aptian Oceanic Anoxic Event 1a from the Paris Basin (France)—climate signals on a terrigenous shelf. *Cretac. Res.*, 125, article no. 104846.

Delamette, M. (1986). *L'évolution du domaine helvétique entre Bauges et Morcles de l'Aptien au Turonien*. Thèse, University of Geneva.

Delamette, M. (1988). Relation between the condensed Albian deposits of the Helvetic domain and the oceanic current-influenced continental margin of the northern Tethys. *Bull. Soc. Géol. Fr. (8)*, IV(5), 739–745.

Emberger, J. (1960). Esquisse géologique de la partie orientale des monts des ouled nail (atlas saharian, algérie). volume 27 of *Bull. Serv. Carte Géol. Algérie, Alger*, page 399.

Ferry, S. (1997). Gard rhodanien. Géologie du Crétacé - Synthèse sédimentologique et stratigraphique. Rapport ANDRA BRP1UCB97-001/A (unpublished).

Ferry, S. (1999). Apports des forages ANDRA de Marcoule à la connaissance de la marge crétacée rhodanienne. In *Actes des Journées scientifiques CNRS-ANDRA, Bagnold-sur-Cèze, 20–21 octobre 1997*, pages 63–91. EDP Sciences, Paris, France, https://hal.archives-ouvertes.fr/hal-02445564 .

Ferry, S. (2017). Summary on Mesozoic carbonate deposits of the Vocontian Trough (Subalpine Chains, SE France). In Granier, B., editor, *Some key Lower Cretaceous sites in Drôme (SE France)*, volume CG2017_Bo1, pages 9–42. Carnets de Géologie, Madrid, Spain.

Ferry, S. and Flandrin, J. (1979). Mégabrèches de resédimentation, lacunes mécaniques et pseudo-"hard-grounds" sur la marge vocontienne au Barrémien et à l'Aptien inférieur (Sud-Est de la France). *Géol. Alp., Mém. HS*, 55, 75–92.

Flandrin, J. and Weber, C. (1966). Données géophysiques sur la structure profonde du Diois et des Baronnies. *Bull. Soc. Géol. Fr., (7)*, VIII, 387–392.

Friès, G. and Parize, O. (2003). Anatomy of ancient passive margin slope systems: Aptian gravity-driven deposition on the Vocontian palaeomargin, western Alps, south-east France. *Sedimentology*, 50, 1231–1270.

Gale, A. S., Bown, P., Caron, M., Crampton, J., Crowhurst, S. J., Kennedy, W. J., Petrizzo, M. R., and Wray, D. S. (2011). The uppermost Middle and Upper Albian succession at the Col de Palluel, Hautes-Alpes, France: An integrated study (ammonites, inoceramid bivalves, planktonic foraminifera, nannofossils, geochemistry, stable oxygen and carbon isotopes, cyclostratigraphy). *Cretac. Res.*, 32, 59–130.

Gindre, L., Rubino, J.-L., Machhour, L., Malartre, F., Soudet, H., and Landais, P. (2002). Architecture, systèmes de dépôts et stratigraphie séquentielle du Cénomanien de Basse Provence (Cassis — La Bédoule) : caractérisation des cortèges de bas niveau marin. *Doc. Lab. Géol. Lyon*, 56, 122–123.

Greselle, B. and Pittet, B. (2005). Fringing carbonate platforms at the Arabian Plate margin in northern Oman during the Late Aptian–Middle Albian: Evidence for high-amplitude sea-level changes. *Sediment. Geol.*, 175, 367–390.

Grosheny, D., Ferry, S., Lécuyer, C., Thomas, A., and Desmares, D. (2017). The Cenomanian-Turonian Boundary Event (CTBE) on the southern slope of the Subalpine Basin (SE France) and its bearing on a probable tectonic pulse on a larger scale. *Cretac. Res.*, 72, 39–65.

Heimhofer, U., Hochuli, P. A., Herrle, J. O., and Weissert, H. (2006). Contrasting origins of Early Cretaceous black shales in the Vocontian basin: Evidence from palynological and calcareous nannofossil records. *Palaeogeogr. Palaeoclimatol. Palaeoecol.*, 235, 93–109.

Hibsch, C., Kandel, D., Montenat, C., and Ott d'Estevou, P. (1992). Evénements tectoniques crétacés dans la partie méridionale du bassin subalpin (massif Ventoux-Lure et partie orientale de l'arc de Castellane, SE France. Implications géodynamiques. *Bull. Soc. Géol. Fr.*, 163(2), 147–158.

Jaillard, E., Dumont, T., Ouali, J., Bouillin, J.-P., Chihaoui, A., Latil, J.-L., Arnaud, H., Arnaud-Vanneau, A., and Zghal, I. (2013). The Albian tectonic "crisis" in Central Tunisia: Nature and chronology of the deformations. *J. African Earth Sci.*, 85, 75–86.

Jaillard, E., Kassab, W. H., Giraud, F., Robert, E., Masrour, M., Bouchaou, L., El Hariri, K., Hammed, M. S., and Aly, M. F. (2019). Aptian–early Albian sedimentation in the Essaouira-Agadir basin, Western Morocco. *Cretac. Res.*, 102, 59–80.

Joseph, P., Cabrol, C., and Fries, G. (1987a). Blocs basculés et passes sous-marines dans le champ de Banon (France S.E.) à l'Apto-Albien : une paléotopographie directement contrôlée par la tectonique synsédimentaire décrochante. *C. R. Acad. Sci. Paris*, 304 (II)(9), 447–452.

Joseph, P., Cabrol, C., and Fries, G. (1987b). Le champ

de Banon à l'Apto-Albien : contrôle de la sédimentation argilo-sableuse par la tectonique synsédimentaire. *Géol. Alp., Mém. HS*, 13, 227–234.

Kennedy, W. J., Gale, A. S., Bown, P. R., Caron, M., Davey, R. J., Gröcke, D., and Wray, D. S. (2000). Integrated stratigraphy across the Aptian-Albian boundary in the Marnes Bleues, at the Col de Pré-Guittard, Arnayon (Drôme), and at Tartonne (Alpes-de-Haute-Provence), France: a candidate Global Boundary Stratotype Section and Boundary Point for the base of the Albian Stage. *Cretac. Res.*, 21, 591–720.

Kennedy, W. J., Gale, A. S., Huber, B. T., Petrizzo, M. R., Bown, P., Barchetta, A., and Jenkyns, H. C. (2014). Integrated stratigraphy across the Aptian/Albian boundary at Col de Pré-Guittard (southeast France): A candidate Global Boundary Stratotype Section. *Cretac. Res.*, 51, 248–259.

Khunt, W., Holbourn, A., and Moullade, M. (2011). Transient global cooling at the onset of early Aptian oceanic anoxic event (OAE) 1a. *Geology*, 39(4), 323–326.

Kilian Group (Reboulet S. et al.) (2018). Report on the 6th International Meeting of the IUGS Lower Cretaceous Ammonite Working Group, the Kilian Group (Vienna, Austria, 20th August 2017). *Cretac. Res.*, 91, 100–110.

Marchand, E., Séranne, M., Buguier, O., and Vinches, M. (2021). LA-ICP-MS dating of detrital zircon grains from the Cretaceous allochthonous bauxites of Languedoc (south of France): Provenance and geodynamic consequences. *Basin Res.*, 33, 270–290.

Masse, J.-P., Masse, P. J.-L., and Tronchetti, G. (1990). Variations sédimentaires sous contrôle tectonique durant l'Aptien supérieur - Cénomanien moyen à l'articulation des blocs provençal et languedocien (SE de la France) : cadre paléocéanographique et implications paleogéographiques. *Bull. Soc. Géol. Fr.*, VI(6), 963–971.

Masse, J.-P. and Philip, J. (1976). Paléogéographie et tectonique du Crétacé moyen en Provence : révision du concept d'isthme durancien. *Rev. Geogr. Phys. Geol. Dyn. 2*, XVIII(1), 49–66.

Maurer, F., van Buchem, F. S. P., Eberli, G. P., Pierson, B. J., Raven, M. J., Larsen, P.-H., Al-Husseini, M. I., and Vincent, B. (2013). Late Aptian long-lived glacio-eustatic lowstand recorded on the Arabian Plate. *Terra Nova*, 25, 87–94.

Millan, M. I., Weissert, H. J., and Lopez-Horgue, M. A. (2014). Expression of the late Aptian cold snaps and the OAE1b in a highly subsiding carbonate platform (Aralar, northern Spain). *Palaeogeogr. Palaeoclimatol. Palaeoecol.*, 411, 167–179.

Montenat, C., Hibsch, C., Perrier, J.-C., Pascaud, F., and de Bretzel, P. (1997). Tectonique cassante d'âge crétacé inférieur dans l'arc de Nice (Alpes Maritimes, France). *Géol. Alp., Mém. HS*, 73, 59–66.

Montenat, C., Janin, M.-C., and Barrier, P. (2004). L'accident du Toulourenc : une limite tectonique entre la plate-forme provençale et le Bassin vocontien à l' Aptien–Albien (SE France). *C. R. Geosci.*, 336, 1301–1310.

Montenat, C., Ott d'Estevou, P., and Saillard, M. (1986). Sur la tectonique anté-cénomanienne du fossé de Sault-de-Vaucluse (Chaînes subalpines méridionales). *C. R. Acad. Sci. Paris*, 303 (II)(7), 609–612.

Moullade, M. (1966). *Etude stratigraphique et micropaléontologique du Crétacé inférieur de la "fosse vocontienne"*. Thèse, Université de Lyon, https://tel.archives-ouvertes.fr/tel-00814787.

Moullade, M. and Porthault, B. (1970). Sur l'âge précis et la signification des grès et conglomérats crétacés de la vallée du Toulourenc (Vaucluse). Répercussions de la phase orogénique " autrichienne" dans le Sud-Est de la France. *Géol. Alp., Mém. HS*, 46, 141–150.

Mutterlose, J., Bornemann, A., and Herrle, J. (2009). The Aptian–Albian cold snap: Evidence for "mid" Cretaceous icehouse interludes. *Neues. Jahrb. Geol. Palaontol. Abh.*, 252(2), 217–225.

Okano, K., Sawada, K., Takashima, R., Nishi, H., and Okada, H. (2008). Depositional Environments Revealed From Biomarkers in Sediments Deposited During the Mid-Cretaceous Oceanic Anoxic Events (OAEs) in the Vocontian Basin (SE France). In *Proceedings of the International Symposium "The Origin and Evolution of Natural Diversity", 1–5 October 2007, Sapporo*, pages 233–238.

Petrizzo, M. R., Huber, B. T., Gale, A. S., Barchetta, A., and Jenkyns, H. C. (2012). Abrupt planktic foraminiferal turnover across the Niveau Kilian at Col de Pré-Guittard (Vocontian Basin, southeast France): new criteria for defining the Aptian/Albian boundary. *Newsl. Stratigr.*, 45, 55–74.

Porthault, B. (1974). *Le Crétacé supérieur de la Fosse vocontienne et des régions limitrophes :*

(France sud-est), micropaléontologie, stratigraphie, paléogéographie. Thèse, Université de Lyon, https://tel.archives-ouvertes.fr/tel-00802577.

Rameil, N., Immenhauser, A., Csoma, A. E., and Warlich, G. (2012). Surfaces with a long history: the Aptian top Shu'aiba Formation unconformity, Sultanate of Oman. *Sedimentology*, 59, 212–248.

Raven, M. J., van Buchem, F. S. P., Larsen, P.-H., Surlyk, F., Steinhardt, H., Cross, D., Klem, N., and Emang, M. (2010). Late Aptian incised valleys and siliciclastic infill at the top of the Shu'aiba Formation (Block 5, offshore Qatar). *GeoArabia Sp. Pub.*, 4(2), 469–502.

Rey, J., Caetano, P., Callapez, J., and Dinis, J. (2009). Le Crétacé du Bassin Lusitanien (Portugal). https://hal.archives-ouvertes.fr/hal-00452152 . Livret-Guide Excursion GFC-AGSE, 11–13 septembre 2009.

Rubino, J.-L. (1989). Introductory remarks on the Gargasian/Albian mixed carbonate/siliciclastic system. In Ferry, S. and Rubino, J.-L., editors, *Mesozoic Eustacy Record on Western Tethyan Margins, Post-meeting field-trip in the Vocontian Trough*, pages 28–45. https://hal.archives-ouvertes.fr/hal-02013144 .

Rubino, J.-L. and Delamette, M. (1988). The Albian shelf of south-east France: an example of clastic sand distribution dominated by oceanic currents. In *6th Intern. Assoc. Sedim. Europ. Reg. Meeting Abstract Book*, pages 399–402.

Vail, P. R., Mitchum, R. M., and Thompson III, S. (1977). Seismic stratigraphy and gGobal changes of sea level, Part 3: relative changes of sea level from coastal onlap. *AAPG Mem.*, 26, 63–81.

Vincent, P., Grosjean, A.-S., Bert, D., Ferreira, J., Suchéras-Marx, B., Suan, G., Guinot, G., Perrier, V., Janneau, K., Brazier, J.-M., Sarroca, E., Guiomar, M., and Martin, J. E. (2020). Paleoenvironmental context and significance of a partial elasmosaurid skeleton from the Albian of Haute-Provence, France. *Cretac. Res.*, 108, article no. 104293. 1–20.

Comptes Rendus
Géoscience — Sciences de la Planète
2022, Vol. 354, Special Issue S3, p. 89-106
https://doi.org/10.5802/crgeos.144

Integrated stratigraphy of the Jurassic and the Cretaceous: a tribute to Jacques Rey /
Stratigraphie intégrée du Jurassique et du Crétacé : un hommage à Jacques Rey

Shallow-water carbonates of the Coimbra Formation, Lusitanian Basin (Portugal): contributions to the integrated stratigraphic analysis of the Sinemurian sedimentary successions in the western Iberian Margin

Luís Vítor Duarte *, [a], **Ricardo Louro Silva** [b], **Ana Cristina Azerêdo** [c], **María José Comas-Rengifo** [d] and **João Graciano Mendonça Filho** [e]

[a] Universidade de Coimbra, MARE and Departamento de Ciências da Terra, Rua Sílvio Lima, Polo II, 3030-325 Coimbra, Portugal

[b] Department of Earth Sciences, University of Manitoba, 230 Wallace Building, 125 Dysart Road, Winnipeg, Manitoba, R3T 2N2, Canada

[c] Universidade de Lisboa, Faculdade de Ciências, Departamento de Geologia and Instituto Dom Luiz (IDL), Campo Grande, Ed. C6, 4° piso, 1749-016 Lisboa, Portugal

[d] Departamento de Geodinámica, Estratigrafía y Paleontología, Universidad Complutense de Madrid, José Antonio Novais, 12, 28040, Madrid, Spain

[e] Geosciences Department and LAFO, Federal University of Rio de Janeiro, Rio de Janeiro, Brazil

E-mails: lduarte@dct.uc.pt (L. V. Duarte), ricardo.silva@umanitoba.ca (R. L. Silva), acazeredo@fc.ul.pt (A. C. Azerêdo), mjcomas@ucm.es (M. J. Comas-Rengifo), graciano@geologia.ufrj.br (J. G. Mendonça Filho)

Abstract. An integrated stratigraphic analysis of the Coimbra Formation was performed in the S. Pedro de Moel outcrops of the Lusitanian Basin (Portugal). This unit is dated from the lower–upper (Oxynotum Chronozone) Sinemurian and is subdivided into eight informal subunits. Except for its base, consisting of dolostones and microbialites, much of the succession consists of bioclastic and bioturbated micritic centimetric–decimetric limestones (sometimes rich in benthic macrofauna) alternating with millimetric–centimetric marly layers, all deposited in shallow-water carbonate ramp environments. Organic-rich sediments occur throughout, with total organic carbon reaching up to 12 wt%. At a broader scale, the Coimbra Formation is transgressive and part of a long-lasting 2nd-order transgressive–regressive facies cycle ending around the Sinemurian–Pliensbachian boundary. The vertical variation of $\delta^{13}C$ determined in bulk carbonate is characterized by relatively normal marine values (0–2.5‰); however, several negative shifts are associated with the organic-rich sediments,

* Corresponding author.

with a maximum amplitude of ~8‰ in the Obtusum Chronozone. These shifts in bulk carbonate $\delta^{13}C$ are interpreted to be of diagenetic origin and, therefore, of local significance. However, it cannot be discarded that a regional/global signal is imprinted on the observed trends.

Keywords. Sinemurian, Shallow-water carbonates, Organic-rich deposits, Stratigraphy, Stable carbon isotopes, Lusitanian Basin.

Published online: 13 October 2022, Issue date: 13 January 2023

1. Introduction

The Lower Jurassic of the Lusitanian Basin (Western Portugal) shows a distinctive succession of carbonate deposits that are a stratigraphic reference at a global scale [e.g. Duarte et al., 2017, Hesselbo et al., 2007, Rocha et al., 2016]. Much of the research interest arises from the preferred palaeogeographic location of these deposits between the Tethyan and pre-Atlantic realms [Thierry and Barrier, 2000], thus relevant for regional and global biostratigraphic correlations and palaeogeographic and palaeobiogeographic reconstructions [e.g. Ferreira et al., 2019, Rocha et al., 2016, Silva et al., 2021]. Except for its base, dated from the Sinemurian, the majority of the Lower Jurassic is composed of hemipelagic marly limestones with abundant benthic and nektonic macrofauna, formally organised in several lithostratigraphic units [e.g. Duarte and Soares, 2002, Duarte et al., 2010, Silva et al., 2015]. These formations are biostratigraphically well constrained (ammonites, calcareous nannofossils and dinoflagellates biostratigraphy) and dated from the uppermost Sinemurian to the upper Toarcian [e.g. Correia et al., 2018, Dommergues, 1987, Ferreira et al., 2019, Rocha et al., 2016]. In addition, a set of reference stable carbon isotopic curves, covering the Upper Sinemurian to Middle Toarcian, reinforces detailed regional and global correlation [e.g. Duarte et al., 2014a, Hesselbo et al., 2007, Oliveira et al., 2006, Silva et al., 2011, 2021, Suan et al., 2010].

A significant part of the Sinemurian is represented by the Coimbra Formation (Fm), a unit that integrates the lexicon of Portuguese stratigraphy since the late 19th century; the so-called "Couches de Coimbra" [Choffat, 1880]. The Coimbra Fm is individualised on its dominant dolostone component, particularly evident towards the east, and represents the first evidence of sustained marine influence in the Lusitanian Basin. However, and despite its widespread cartographic distribution, a detailed stratigraphic analysis of this lithostratigraphic unit is lacking [e.g. Azerêdo et al., 2010, Dimuccio et al., 2016].

The most complete section of the Coimbra Fm crops out in the S. Pedro de Moel region (Figure 1A,B). It is dominantly calcareous [Figure 1C,D; Azerêdo et al., 2010, Duarte et al., 2014b] and contains organic-rich facies [Duarte et al., 2013, Poças Ribeiro et al., 2013] and few levels with ammonites [e.g. Dommergues et al., 2004, 2010]; therefore, this section holds great potential to perform an integrated stratigraphic analysis of the lowermost Sinemurian in the Lusitanian Basin.

This paper, based on the analysis of the Lower Jurassic outcrops at S. Pedro de Moel, has three main goals: (i) to improve the lithostratigraphy and biostratigraphy of the Coimbra Fm, (ii) to perform a chemostratigraphic analysis of the studied sections based on stable carbon isotopes from bulk carbonates and total organic carbon (TOC), and (iii) to contribute to a better understanding of the Portuguese sedimentary record potentially associated with the hyperthermal Liasidium Event, such as recently recognised by Hesselbo et al. [2020], Munier et al. [2021] and Riding et al. [2013]. According to these authors, this hyperthermal event is characterised by an abundant record of the marine dinoflagellate cyst *Liasidium variabile* and the pollen grain *Classopollis classoides*, associated with a negative carbon isotope event.

2. Geological setting

The Lusitanian Basin, located in the western Iberian Margin, hosts a thick sedimentary succession dated from the Middle (?) Triassic to the Upper Cretaceous [e.g. Hiscott et al., 1990, Kullberg et al., 2013]. Except for the Hettangian lutitic and evaporitic deposits of the Dagorda Fm, the Lower Jurassic is represented by a thick succession of dolostones, limestones, and calcareous mudstones (up to 500 m thick), where several lithostratigraphic units are formalised [e.g. Dimuccio et al., 2016, Duarte and Soares, 2002]. Framed

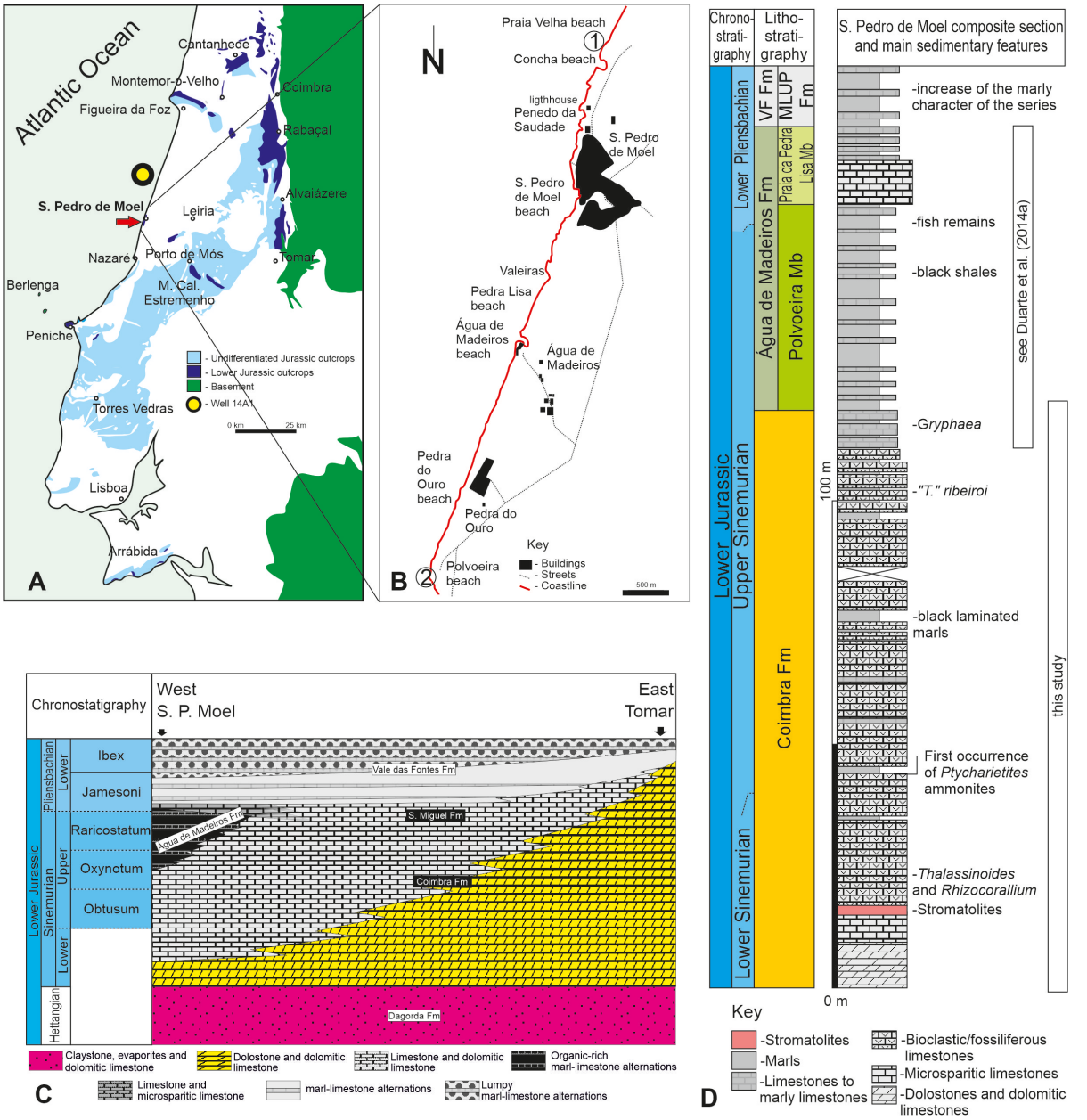

Figure 1. (A) Location of the S. Pedro de Moel region in the Lusitanian Basin (central Portugal), showing the main Lower Jurassic outcrops. (B) Studied area and location of the two sections: 1. Praia Velha-Lighthouse; 2. Polvoeira. (C) Lithostratigraphic chart of the Sinemurian for the Lusitanian Basin [modified from Duarte et al., 2010, 2012]. (D) Synthetic stratigraphic log of the Sinemurian–lower Pliensbachian succession in S. Pedro de Moel [modified from Azerêdo et al., 2010, Duarte et al., 2012, 2014a]. VF—Vale das Fontes Fm; MLUP—Marls and limestones with *Uptonia* and *Pentacrinus* member [see Duarte et al., 2010].

between the Hettangian Dagorda Fm and Pliensbachian hemipelagic marls and marly limestones, the base of the Sinemurian marks the beginning of carbonate deposition in the Lusitanian Basin in a shallow-water carbonate ramp [Azerêdo et al., 2010, Dimuccio et al., 2016, Duarte et al., 2014b, Sêco et al., 2018, Soares et al., 1993]. These carbonates belong to the Coimbra Fm, consisting mainly of dolostones and dolomitic limestones to the east and is dominated by limestone in the westernmost sectors of the basin [Dimuccio et al., 2016, Duarte et al., 2010; Figure 1C,D], including some thick marly intervals. Here, the Coimbra Fm is overlain by an upper Sinemurian–lowermost Pliensbachian marl–limestone unit rich in organic matter, the Água de Madeiros Fm [Duarte et al., 2010]. The Água de Madeiros Fm is particularly well exposed in the S. Pedro de Moel region and is the most representative of the latest Sinemurian age in Portugal [Duarte et al., 2014a,b; Figure 1C,D].

The most complete Sinemurian succession of the Lusitanian Basin crops out at S. Pedro de Moel. In this region, the Coimbra Fm is visible on both flanks of a fractured km-scale syncline exposed along the coastline (Figure 1B). At the Praia Velha Beach, located to the north of the S. Pedro de Moel Village and at the northern cropping out edge of the syncline, the base of the Coimbra Fm is highly fractured and folded, in a succession dipping towards the west [see Azerêdo et al., 2010, Cabral et al., 2015, Dommergues et al., 2004, 2010, Duarte et al., 2014b]. In the southern part of the syncline, at the Polvoeira Beach, the uppermost part of the Coimbra Fm is continuous [Figures 1B and 2; see also Duarte et al., 2012, 2014b, Paredes et al., 2013, 2016] and includes the transition to the overlying Água de Madeiros Fm [Duarte et al., 2010, 2012, 2014a].

The base of the Coimbra Fm was previously described by Azerêdo et al. [2010], who identified four subunits (UA to UD). Later, in a preliminary work, Duarte et al. [2014b] described the upper part of the formation and identified four other units (UE to UH). Units UA to UG are observed from the Concha Beach to the S. Pedro de Moel Lighthouse (the latter also known as Penedo da Saudade) section (coordinates: 39° 46′ 11.12″ N; 9° 1′ 38.70″ W), whereas UH occurs only at Polvoeira Beach (coordinates: 39° 43′ 8.74″ N; 9° 3′ 0.10″ W) (Figures 1B and 2). According to the ammonite record [see Dommergues et al., 2004, 2010, Duarte et al., 2014b], the Coimbra Fm in this region is dated from the lower to upper Sinemurian. Previous studies in this region have also focused on ostracod assemblages [Cabral et al., 2013, 2015], organic and petrographic geochemistry [Brito et al., 2017, Duarte et al., 2013, Poças Ribeiro et al., 2013] and gamma-ray analysis [Sêco et al., 2018].

3. Material and methods

This study focuses on the stratigraphic, sedimentologic and geochemical analysis of the Coimbra Fm at S. Pedro de Moel, through the examination of the Praia Velha and Polvoeira sections [Figures 1B and 2; see Azerêdo et al., 2010, Duarte et al., 2014b].

3.1. *Stratigraphy and sedimentology*

This study expands the sedimentological and lithostratigraphic description of the Coimbra Fm previously addressed in Azerêdo et al. [2010] and Duarte et al. [2014b]. This was achieved through new stratigraphic and sedimentological observations from the middle–upper part of the Coimbra Fm in the upper part of the Praia Velha-Lighthouse and Polvoeira sections. Field observation and sedimentological descriptions were complemented by microfacies synthetic characterization of 77 thin sections using a Nikon Eclipse polarised light microscope coupled with a Nikon digital microscope camera at the Department of Earth Sciences of the University of Coimbra. In addition, new ammonites were collected and identified.

3.2. *Total organic carbon (TOC) and total sulphur (ST)*

Insoluble residue (IR), total organic carbon (TOC) and total sulphur (TS) content were measured in 67 samples of grey to dark grey to black mudstone/marlstone (black shales) using a Leco-SC144 analyser and following the standard laboratory protocols of the Palynofacies and Organic Facies Laboratory of the Federal University of Rio de Janeiro [e.g. Mendonça Filho et al., 2012]. A higher resolution sampling scheme was used where the black shale lithology was more evident.

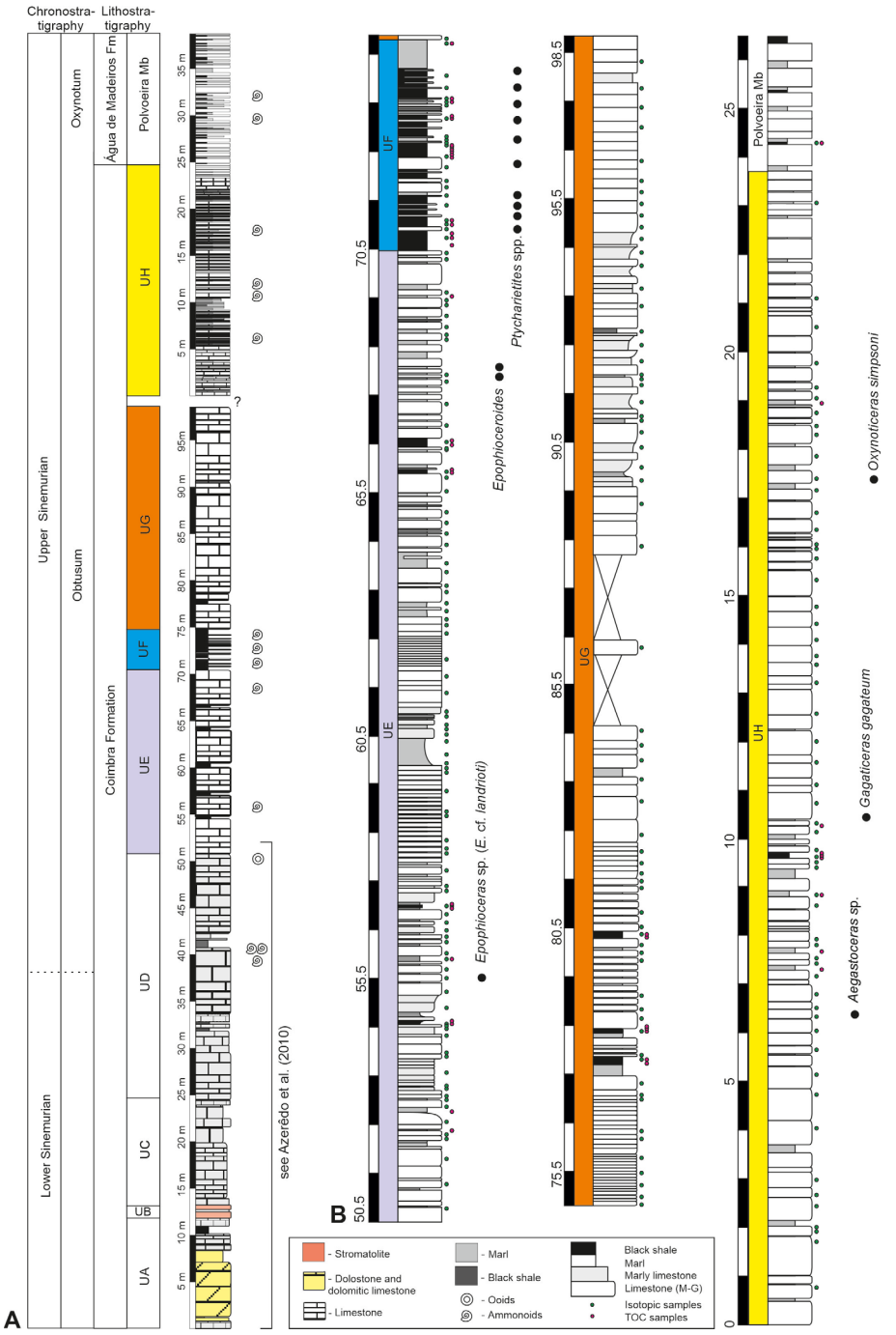

Figure 2. (A) General composite section of the Coimbra Fm (lower to upper Sinemurian) in the S. Pedro de Moel region. (B) Detailed stratigraphic columns of UE to UG (Lighthouse section) and UH (Polvoeira section). For more information about UA–UD, see Azerêdo et al. [2010]. *Epophioceroides* occurrences from Dommergues et al. [2010].

3.3. *Carbon and oxygen stable isotopes*

Carbon ($\delta^{13}C_{carb}$) and oxygen ($\delta^{18}O_{carb}$) stable isotopes ratios were analysed on 292 bulk carbonate samples. Due to the thickness of the studied succession and facies heterogeneity, samples were collected from micritic sediments and with an average sampling resolution of about one (1) meter, reduced to about 0.3 to 0.5 m in the middle to upper part of the series. Sample aquilots were selected to avoid shell fragments and hand-drilled in the laboratory to avoid sparitic cement. Stable oxygen and carbon isotopes were analysed at Iso-Analytical (UK). Isotopic results are presented in per mil (‰) standard notation (δ) relative to the Vienna PeeDee Belemnite (V-PDB). Reproducibility based on standards is better than 0.2‰ for both $\delta^{18}O_{carb}$ and $\delta^{13}C_{carb}$. The reference materials used during analysis were IAR022 (Iso-Analytical working standard calcium carbonate, $\delta^{13}C = -28.63$‰ and $\delta^{18}O = -22.69$‰), NBS-18 (carbonatite, $\delta^{13}C = -5.01$‰ and $\delta^{18}O = -23.2$‰) and IA-R066 (chalk, $\delta^{13}C = +2.33$‰ and $\delta^{18}O = -1.52$‰). IA-R022 was calibrated against and is traceable to NBS-18 and NBS-19 (limestone, $\delta^{13}C = +1.95$‰). IA-R066 was calibrated against and is traceable to NBS-18 and IAEA-CO-1 (Carrara marble, $\delta^{13}C = +2.5$‰). NBS-18, NBS-19 and IAEA-CO-1 are inter-laboratory comparison standard materials distributed by the International Atomic Energy Agency (IAEA).

4. Results

4.1. *Stratigraphy and sedimentary characterisation*

Integration of the two studied sections from S. Pedro de Moel allows inferring a minimum thickness of about 125 m (~100 m thick in the Praia Velha - Lighthouse section and ~25 m in the Polvoeira section) for the Coimbra Fm in this area of the Lusitanian Basin. The limitations to this observation refer to the fact that the boundary with the underlying Dagorda Fm is not visible here and there is a gap of observation between the two sections (Figure 2). In this region, the Coimbra Fm is subdivided into eight units (UA to UH; Figure 2). The main stratigraphic and sedimentological characteristics are described below. For more detail about units UA to UD see Azerêdo et al. [2010] (Figure 3A,B).

UA (~12 m)

Comprises a large diversity of dolomitic and limestone facies and textures (mudstone to grainstone), locally fossiliferous, including mainly bivalves and gastropods. Organic-rich marly intervals occur at the top of UA, alternating with laminated calcareous-dolomitic centimetric beds (Figure 3A).

UB (1.5 m)

Mainly composed of decimetric- to metric-scale domiform stromatolites, including centimetre micritic limestones and marly limestones (mudstones and wackestones) and a few centimetre-thick intervals of wacke-packstones (Figure 3A).

UC (11.3 m)

Alternation of marly, micritic, and bioclastic limestones, with rare levels of ostracod-rich marls, sometimes intensely bioturbated by *Rhizocorallium* and *Thalassinoides*. Some grainstone levels, generally thin (centimetric-scale), are enriched in *Unicardium* sp. and ostreids (Figure 3A,B).

UD (25.7 m)

With a facies arrangement similar to UC, UD includes rare marly levels (with ostracods) and fossiliferous limestones and coquinas of *Unicardium costae* and gastropods (Figure 3B). Some levels are intensely bioturbated with *Thalassinoides* and *Rhizocorallium* (*Rhizocorallium commune* var. *irregulare* [Knaust, 2013]; Figure 4A). The first ammonoids occur at around 40 m [*Asteroceras* sp. and some species of the *Ptycharietites* genus, see Dommergues et al., 2004, 2010] (Figures 3B and 4B), associated with an organic-rich marly interval. This unit ends with decimetric limestone beds of oosparites/grainstone.

UE (~20 m)

This unit mainly comprises limestone, generally composed of centimetric and irregular beds, locally intensely bioturbated and bioclastic, sporadically alternating with marly interbeds that can reach few decimeters in thickness, some corresponding to black shales (Figure 3C,D). Limestone lithotypes range from fossiliferous micrites to biopelsparites/grainstone. Despite occurrences of gastropods and echinoids, fossil macrofauna is dominated by bivalves (*Unicardium costae*, ostreids)

Figure 3. (A) Base of the Coimbra Fm at Praia Velha with stromatolites (UB), see also Azerêdo et al. [2010]. (B) Panoramic view of UC and UD at Concha Beach (white arrow: first level with *Ptycharietites*). (C) Base of UE showing a discrete level of black shale (white arrow). (D) Panoramic view of the thick black shale interval of UF, framed by UE and UG (just north of Lighthouse). (E) Uppermost part of UG around the Lighthouse, and location of Polvoeira Beach (red arrow). (F) Limestones enriched in brachiopods and bivalves of the base of UH at Polvoeira Beach.

forming several levels of coquinas. Bioturbation is a constant feature of this unit with *Rhizocorallium* and *Thalassinoides*. Two horizons with rare ammonoids [including *Epophioceroides apertus in* Dommergues et al., 2010] were identified in this unit.

UF (4.4 m)

Corresponds to the marliest part of the Coimbra Fm and includes well defined laminated organic-rich facies (black shales) alternating with centimetric

Figure 4. Relevant sedimentary and stratigraphic aspects of the Coimbra Fm at S. Pedro de Moel: (A) Intense bioturbated level of UD with *Rhizocorallium commune* var. *irregulare* [Knaust, 2013]. (B) Surface with a high concentration of *Unicardium* sp. and *Ptycharietites* sp. (see text). (C) Sharp transition between UE and UF (white arrow). Noteworthy are the decimetric levels of organic-rich marls of the base of UF. (D) The most organic-rich horizons observed in UH.

bioclastic limestone beds (biomicrites to pelsparites, packstone–grainstone) (Figures 3D and 4C). Similarly to the previous units, benthic macrofauna is dominated by bivalves (*Unicardium costae*, ostreids), although restricted to some of the limestone beds. This interval of the Coimbra Fm is particularly rich in ammonoids, including several species of the genus *Ptycharietites* [Dommergues et al., 2010].

UG (>24 m)

Composed of metric sets of centimeter layers of micritic and bioclastic limestones interbeded at the base with centimetric dark grey, organic-rich, marly limestones. The microfacies vary from grainstones, fossiliferous and intraoosparite micrites with different textures to mudstones. Fossiliferous and bioclastic facies (essentially bivalves) and bioturbated levels (mainly *Rhizocorallium*) are of less importance when comparing with the previous units. The intermediate portion of this unit is of difficult access (Figure 3D,E).

UH (>25 m)

This unit is restricted to the Polvoeira Beach (Figure 3E,F) and is composed of decimetric micritic limestone (fossiliferous micrites/mudstone to biomicrites/packstones)/millimetric-centimetric marl (sometimes organic-rich; Figure 4D) alternations. This succession contrasts with previous units of the Coimbra Fm because of its greater diversity of benthic macrofauna and the first record of brachiopods. Faunal assemblages include bivalves (some species of *Pholadomya*, *Mactromya*, *Unicardium*), brachiopods (specimens of "*Terebratula" ribeiroi* and the genus *Zeilleria* and *Cincta*), gastropods, crinoids, and rare ahermatypic corals [see also Paredes et al., 2013, 2016, Vitón et al., 2020].

Although less frequent than in other units (e.g. Units C to E), bioturbation is sometimes intense, consisting mainly of *Thalassinoides*, *Rhizocorallium* and *Diplocraterium*. Although extremely rare, ammonites occur according to the sequence of the following genus *Aegasteroceras*, *Gagaticeras* and *Oxynoticeras* (Figure 2).

4.2. *Total organic carbon and ST*

Total organic carbon contents determined in 67 marly horizons show that several levels of the Coimbra Fm are rich in organic matter. Except for UC, all units have TOC contents above 1 wt% (Figure 5 and Supplementary Table 1). In UA and UF (Figures 3A,C,D and 4C), TOC contents reach up to 6 wt% (~10.6 m) and 9 wt% (~72.9 m), respectively. The highest TOC contents were determined in discrete levels of the thicker UG and UE, reaching up to ~12 wt% (~77.7 m) and ~10 wt% (~65.87 m), respectively. The highest TS contents were determined in UF (3.0 wt%) and at the base of UG (2.8 wt%). Total sulfur contents of the remaining units are generally below 1 wt%. The carbonate content of the marly intervals is variable across the succession (Table 1 in Supplementary Material). The marly intervals of UA are those with lower carbonate content, where the siliciclastic contribution reaches up to 70% (insoluble residue). Insoluble residue contents decrease upwards, with the marly intervals of UH presenting contents generally below 20%.

4.3. *C and O stable isotopes in bulk carbonate*

$\delta^{13}C_{carb}$ from the Coimbra Fm ranges from −5.8‰ (73.21 m) to 2.8‰ (60.46 m) (Table 1 in Supplementary Material). The carbon-isotope curve shows little variation (around 2‰) except for a high amplitude negative excursion in UF (Figure 5). The lower (UA to middle part of UE) and upper (UG and UH) parts of the isotope curve are largely characterised by positive $\delta^{13}C_{carb}$ values, around 2‰. The most pronounced negative excursion, with an amplitude of ~8‰ (Figure 5), is observed in the organic-rich marly interval of UF. Less expressive is the negative excursion of ~6‰ at the top of unit G (~92.65 m) (IP1; Figure 5). Another very singular small negative peak in $\delta^{13}C_{carb}$ is associated to the enriched organic horizons observed in UH (IP2; Figures 4D and 5).

$\delta^{18}O_{carb}$ values are quite negative, ranging from −7.5‰ to −2.6‰, but with less significant fluctuations than those of carbon isotopes. The most negative values of $\delta^{18}O_{carb}$ are mainly within the microbialites of UB and in some parts of the UD units. On the other hand, at the top of the Coimbra Fm (UH) $\delta^{18}O_{carb}$ values are more homogeneous and considerably higher than in the rest of the stratigraphic succession (Table 1 in Supplementary Material). Despite the low values of $\delta^{18}O_{carb}$, quite negative, there is no correlation with the $\delta^{13}C_{carb}$ data, as confirmed by the Pearson R2 = −0.094 (Figure 1 in Supplementary data).

5. Discussion

5.1. *Biostratigraphic additions and thickness of the Coimbra Fm*

The lithological and facies succession of the Coimbra Fm in the S. Pedro de Moel area is unique within the Lusitanian Basin [e.g. Azerêdo et al., 2010, Duarte, 2004, Duarte et al., 2014b]. The vertical facies variation allows for a detailed palaeoenvironmental assessment and sequence stratigraphic interpretation. In addition, and despite the rarity of age-diagnostic ammonites, this is the only basin area where the biostratigraphic record allows dating the Coimbra Fm, although a large part of the ammonite record is endemic [Dommergues et al., 2004, 2010, Mouterde and Ruget-Perrot, 1975]. This work is the first to present a detailed stratigraphic analysis of the entire succession, allowing us to add new ammonite data and improve the upper Sinemurian biostratigraphic scheme for the western Iberian margin.

This work confirms the previous studies of Dommergues et al. [2004, 2010], indicating that a large part of the Coimbra Fm in the study area is dated from the Obtusum Chronozone. Ammonites, also the oldest occurrence in the Lusitanian Basin, are mainly restricted to the top of UD [*Asteroceras* sp. and *Ptycharietites* species; see Dommergues et al., 2010] and the UF (*Ptycharietites* species). Except for one horizon of UE (with *Epophioceras* sp. (*E.* cf. *landrioti*)), all taxa are endemic, making it difficult to draw correlations with the northwestern European basins [e.g. Corna et al., 1997, Page, 2003]. However, according to the standard zonation, the new found specimen of *Epophioceras* sp. (*E.* cf. *landrioti*) in the lower part of

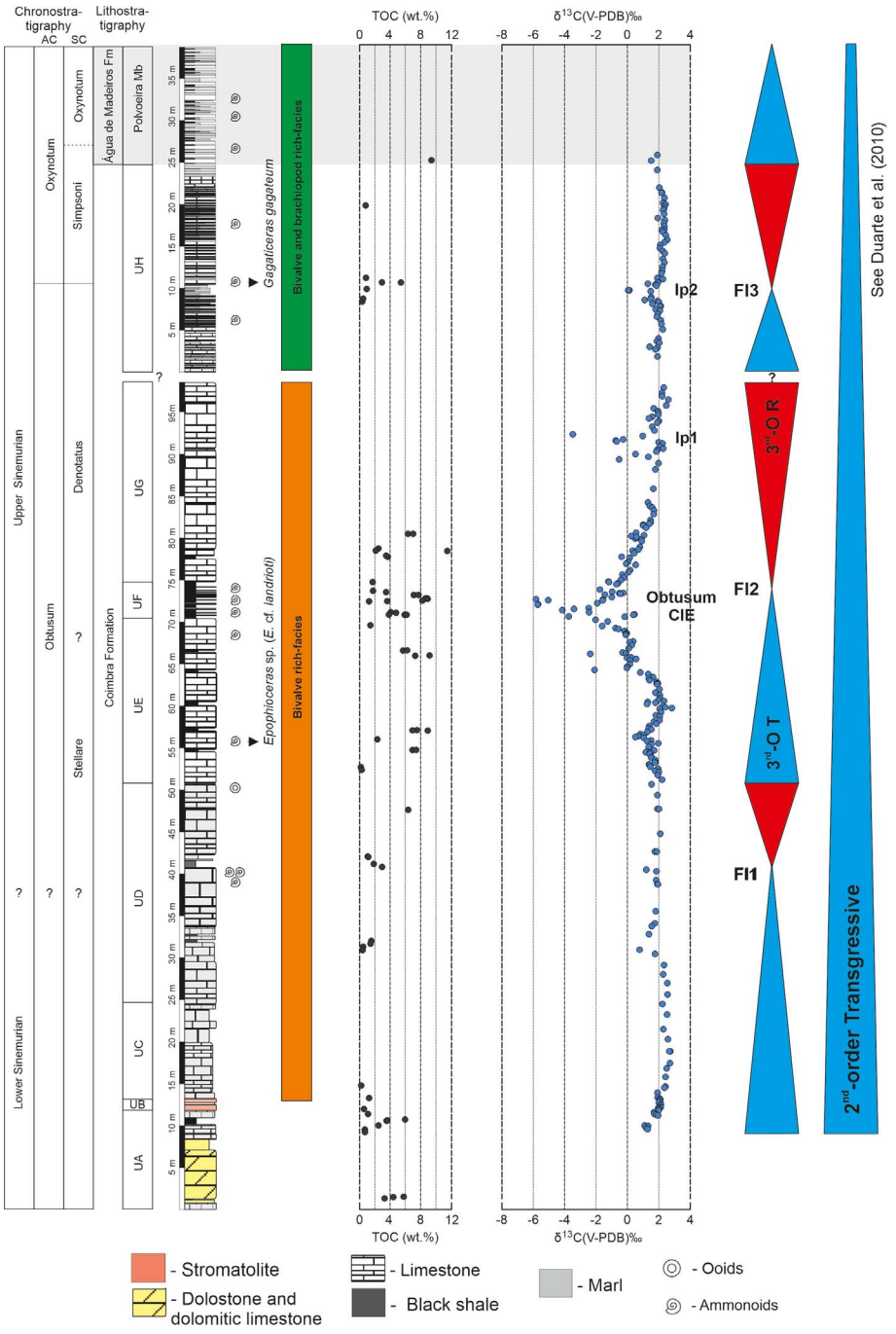

Figure 5. TOC variation, bulk carbonate carbon isotopic curve, and sequential interpretation [2nd and 3rd-order transgressive (3rd O T) and regressive (3rd O R) cycles] across the Coimbra Fm cropping out at S. Pedro the Moel. AC—Ammonite Chronozone; AS—Ammonite Subchronozone.

UE (at 56 m in Figures 2 and 5) indicates the middle part of Stellare Subchronozone.

Occurrence of *Aegasteroceras*, *Gagaticeras*, and *Oxynoticeras* [Figure 3; genus characteristic of the northwestern European basins, Comas-Rengifo et al., 2021, Hesselbo et al., 2020, Howarth, 2002] in UH allows assigning the top of the Coimbra Fm to the transition between the Obtusum and Oxynotum (Simpsoni Subchronozone) chronozones, as also recently noted by Comas-Rengifo et al. [2021] for the Asturias Basin, northern Spain. The presence of *Oxynoticeras simpsoni* undoubtedly marks the Simpsoni Subchronozone of the Oxynotum Chronozone. Comas-Rengifo et al. [2013] and Duarte et al. [2014a] noted that this ammonite Subchronozone extends to the basal part of the overlying Água de Madeiros Fm. In fact, the Oxynotum Chronozone shows Oxynoceratidae (*O.* gr. *oxynotum*, *C.* cf. *accipitris*), Eoderoceratidae (*B. bifer*) and Echioceratidae, an association that is recognised in the Oxynotum Subcrhonozone of Asturias [Comas-Rengifo et al., 2013, 2021, Duarte et al., 2014a].

Despite the overall uncertainty, the available biostratigraphic data show some important issues: firstly, the unusual thickness of the Obtusum Chronozone in S. Pedro de Moel. Considering the biostratigraphic uncertainty associated with the basal part of the succession and the lack of observation between UG and UH, the Obtusum Chronozone would be estimated to be about 90 m thick, much thicker when comparing with all other Lower Jurassic ammonite zones defined for the Lusitanian Basin [e.g. Duarte and Soares, 2002] and the thickness of the same zone in other European basins [e.g. Comas-Rengifo et al., 2021, and references therein]; secondly, and according to the two main intervals with ammonites, and following Dommergues et al. [2010], the middle–upper part of the UD may be limited to the Stellare Subchronozone; this Subchronozone extends to the base of the UE (with the occurrence of *Epophioceras* sp. (*E.* cf. *landrioti*)).

The age of the lower part of Coimbra Fm, i.e., from UA to UC and base of UD (~40 m), is unknown and is here informally assigned to the lower–initial upper Sinemurian. However, according to the recent stratigraphic reinterpretation based in gamma-ray spectrometry of the offshore well 14A1, located close to the studied outcrop (Figure 1A), the base of the succession at the Praia Velha Beach may correspond to the base of the Coimbra Fm [see Sêco et al., 2018]. In well 14A1, the Coimbra Fm is 150 m thick [Sêco et al., 2018]. This value contrasts with the approximately 125 m measured at S. Pedro de Moel, predicting that the gap observed between the top of the Praia Velha-Lighthouse succession and the base of the Polvoeira section may be important. However, and as indicated by the low gamma-ray values observed across UG and UH [see Sêco et al., 2018], carbonate sedimentation should characterise this interval, and lithologies should be very similar to the two units (UG and UH) mentioned above. Another unanswered issue is the location and nature of the boundary with the Dagorda Fm, which is not visible in the area.

5.2. *Organic matter deposition*

The new geochemical data presented here substantiate the high TOC contents previously determined in some parts of the Coimbra Fm at S. Pedro de Moel [e.g. Brito et al., 2017, Duarte et al., 2013, Poças Ribeiro et al., 2013]. It is important to point out that both the Sinemurian and Pliensbachian of the Lusitanian Basin are known for the occurrence of organic-rich deposits, i.e. the Água de Madeiros and Vale das Fontes formations (Figure 1C), both potential hydrocarbon source rocks [e.g. Brito et al., 2017, Duarte et al., 2010, 2012, 2013, Oliveira et al., 2006, Poças Ribeiro et al., 2013, Silva and Duarte, 2015, Silva et al., 2011, 2015, 2021, Sêco et al., 2018]. With the high TOC values (maximum of 12 wt%) determined in the present study, especially in the UA and UF (Figure 5), the importance of Coimbra Fm in this sector of the LB as a potential source rock, is also confirmed.

It is demonstrable that the characteristic Sinemurian shallow-water and relatively high-energy carbonate deposition in the area [see also Azerêdo et al., 2010, Cabral et al., 2015] was interrupted by brief episodes of deposition under lower energy conditions, favouring the accumulation of argillaceous sediments and preservation of organic matter, sometimes with high concentrations of S and pyrite. Organic matter accumulation probably resulted from increased productivity and poorly oxygenated bottom water conditions that had their climax in UA and UF; the latter is the thickest black shale interval in the studied succession, with organic rich facies devoid of benthic macrofauna and ichnofossils (Figures 3A,

3C,D, 4C and 5). These two intervals were also identified in well 14A1 [see Sêco et al., 2018]. The organic-rich intervals, combined with other sedimentological attributes, are essential criteria in the sequence stratigraphic interpretation of the succession (see below).

Regarding the organic matter content and its characterization, Poças Ribeiro et al. [2013] presented an analysis of palynofacies and biomarkers that, despite being based on a small number of samples (nine from UE, UF and UH), allows a better understanding of the depositional environment. First, the kerogen assemblages of the samples rich in organic matter (with TOC values between 3 and 9 wt%) are dominantly composed of amorphous organic matter (generally above 80%) and only with a residual contribution of particles belonging to the Phytoclast Group (<3 wt%). According to Poças Ribeiro et al. [2013], deposition of the organic-rich facies occurred in a relatively restricted and low-energy shallow-water carbonate ramp. By opposition, samples with the lowest TOC contents (<0.5 wt%) are associated with a higher content of phytoclasts (>56%), indicating relatively more proximal deposition under oxidising conditions and with strong continental influence [see Poças Ribeiro et al., 2013]. These facies are an essential argument in the sequential interpretation of the entire Sinemurian succession (see below). The occurrence of marine palynomorphs (acritarchs, prasinophytes, etc.), despite a slight increase in the upper part of the Coimbra Fm, is of little relevance when looking at the overall sequential organisation. In the limited number of samples analyzed in terms of palynofacies in Poças Ribeiro et al. [2013] no reference is made to the occurrence of dinoflagellate cyst *Liasidium variabile*.

5.3. *Palaeoenvironment and sequence stratigraphy*

In the Mesozoic evolution of the Lusitanian Basin, the Coimbra Fm is the first unequivocal evidence of marine flooding at a basinal scale, related to the beginning of a carbonate ramp that will be maintained and developed until the end of the Middle Jurassic [see Azerêdo et al., 2014, Soares et al., 1993]. This unit is known for the dolomitic and calcareous-dolomitic facies that dominate a large part of the Sinemurian record in the eastern and proximal areas of the basin. These facies are associated with very restricted marine conditions [see Azerêdo et al., 2010, Dimuccio et al., 2016, Duarte et al., 2010]. On the other hand, in the more distal areas, as is the case of the study area, these facies are limited to the basal portion of the Coimbra Fm (UA and UB), evidenced by the occurrence of dolomitic and microbial (including stromatolites) facies with thin limestone levels displaying low-diversity assemblages of bivalves and gastropods, and typically brackish and restricted marine ostracods [see Azerêdo et al., 2010, Cabral et al., 2013, 2015]. The upwards disappearance of these facies is concomitant with an increase in marine macroinvertebrate fauna (essentially bivalves) in the overlying UC and UD, which also show dominance of marine ostracods, though still bearing restricted marine and even an interval with brackish ostracods. Overall, these features suggest common alternation between more restricted-marine and slightly more open-marine influence, the latter becoming increasingly stronger and indicating a gradual rise in relative sea level [Azerêdo et al., 2010, Cabral et al., 2013, 2015]. Sustained conditions of fully saline (euhaline) conditions and clear marine influence are observed in the uppermost part of the Coimbra Fm (UH), inferred from a marked increase in brachiopods diversity and the sporadic occurrence of ahermatypic corals [see also Paredes et al., 2013, 2016]. Frequent minor movements (induced by differential regional subsidence?), may have promoted the opening and closing pulses of the marine influence in the shallow environment, leading to the common changes from more restricted- into more open marine conditions [Azerêdo et al., 2010]. On the other hand, the disappearance of the endemic ammonite faunas [Dommergues et al., 2010] and the occurrence of *Aegasteroceras* sp., *Gagaticeras gagateum*, *Oxynoticeras simpsoni*, and *Oxynoticeras oxynotum*, recognised in other northwestern European basins, testifies a strong connexion/opening of the Lusitanian Basin to the neighbouring basins during the Oxynotum Chronozone.

At a broad scale within the basin, the sedimentological variation of the different subunits for the Coimbra Fm shows a sequential arrangement, highlighted by recognizing various sedimentary discontinuities and biofacies and the occurrence of the organic-rich intervals. Following the sequential interpretation of Duarte et al. [2010] for the overlying Sinemurian and Pliensbachian units [Água

de Madeiros, Vale das Fontes and Lemede formations; see also Silva et al., 2015], the succession of the Coimbra Fm is part of the transgressive system tracts of a 2nd-order transgressive–regressive facies cycle with its maximum flooding interval around the Sinemurian–Pliensbachian transition [top of Polvoeira Member; see Duarte et al., 2010, 2014a]. This long-lasting transgressive phase involved three 3rd-order subordinate maximum flooding episodes, corresponding to the more argillaceous and organic-rich intervals of the succession, in the middle-upper part of UD (**Fl1**), UF (**Fl2**), and in the lower-middle part of UH (**Fl3**) (Figures 3D, 4B–D and 5). Despite their endemic character, the first two phases of flooding are associated with abundant ammonites (Figure 4B,C). According to the available ammonite data [also based on Dommergues et al., 2010], the sedimentary record of these flooding events (**Fl1**, **Fl2** and **Fl3**) are tentatively dated from the Obtusum Chronozone, with the latter close to the Obtusum–Oxynotum chronozones boundary.

5.4. *Stable carbon isotope chemostratigraphy and organic matter preservation events (OMPIs)*

The stable carbon isotopic data from bulk carbonate presented here for the lower?–upper Sinemurian exposed at S. Pedro de Moel mostly fall within the normal range for carbonate deposits of marine origin, between 0 to 2.5‰ [e.g. Marshall, 1992]. Vertically, the $\delta^{13}C_{carb}$ curve shows several negative excursions (Figure 5). The largest of these (with an amplitude of about 8‰) is observed between UE–UG (~25 m), another relatively large amplitude excursion was previously observed around the Sinemurian–Pliensbachian boundary [see Duarte et al., 2014a].

These two negative $\delta^{13}C_{carb}$ negative excursions are coincident with organic-rich facies. The same is true for the slight shift (IP2) recorded in the most organic-rich part of UH (Figure 5). Considering the relationship between negative $\delta^{13}C_{carb}$ and organic matter deposition, and as previously discussed in Duarte et al. [2014a] for the younger negative excursion contemporaneous with the Sinemurian–Pliensbachian boundary event [S-PBE cf. Korte and Hesselbo, 2011], it is here interpreted that the marked increase bulk carbonate ^{12}C in these intervals (when comparing with the rest of the succession) is likely due to oxidation of organic matter (via anaerobic bacteria for example) and incorporation of organic-related ^{12}C enriched carbon into diagenetic carbonates [e.g. Marshall, 1992]. Although in the case of the Sinemurian–Pliensbachian negative excursion this effect is most evident in a very small number of carbonate beds of clear early diagenetic origin, (likely influenced by anaerobic oxidation products of organic matter), it seems much more pervasive in UF of the Coimbra Fm. In addition, and despite the absence of significant correlation between $\delta^{18}O_{carb}$ and $\delta^{13}C_{carb}$ (see above) suggesting that late burial diagenetic may have had little influence in the generality of stable carbon isotopic data, diagenetic influence in the isotopic signal of UF is particularly evident, highlighted in the better correlation between $\delta^{18}O_{carb}$ and $\delta^{13}C_{carb}$, with a Pearson $R^2 = 0.7$ (Figure 1 in Supplementary data). Therefore, the negative excursions in $\delta^{13}C_{carb}$ from the Coimbra Fm are likely of diagenetic origin and of local/basinal significance; the influence of products derived from the biological oxidation of organic matter in diagenetic carbonates makes it difficult to extract regional/global palaeoenvironmental information from these data, although this information might be imprinted in the observed trends. It is increasingly evident that $\delta^{13}C_{carb}$ curves are very sensitive to diagenetic alteration, and this must be taken into consideration when interpreting these data. Even if the observed excursions of the Coimbra Fm are contemporaneous of regional/global events, their amplitude, stratigraphic location, and absolute values are likely to be biased [e.g. Bougeault et al., 2017, Duarte et al., 2014a, Munier et al., 2021, Silva et al., 2011, 2021, Ullmann et al., 2022].

The organic-rich sediments of UD–UG were suggested to be contemporaneous with the regional late Sinemurian (Obtusum, Obtusum–Stellare) Organic Matter Preservation Interval [OMPI S5; Silva et al., 2021]. By extension, the younger negative carbon isotopic excursion and organic-rich sediments associated with the regional (superregional?) Sinemurian–Pliensbachian OMPI [see Silva et al., 2021] are well dated, both by ammonites and calcareous nannofossils [e.g. Boussaha et al., 2014, Duarte et al., 2014a, Ferreira et al., 2019] and are now also recognized in several European basins [e.g. Franceschi et al., 2019, Korte and Hesselbo, 2011, Masetti et al., 2017, Mercuzot et al., 2020, Munier et al., 2021, Peti et al., 2017, Price et al., 2016, Schöllhorn et al., 2020, Silva et al., 2021, Ullmann et al., 2022]. For a review of

the processes linking dissolved inorganic and organic carbon in seawater, the following sources may be referred to Silva et al. [2017, 2020, 2021].

A negative carbon isotope excursion (CIE) that has recently gained international relevance is the so-called Sinemurian *Liasidium* Event, dated from the Obtusum Chronozone (Denotatus Subchronozone)–Oxynotum Chronozone (Oxynotum Subchronozone) [Hesselbo et al., 2020, Riding et al., 2013] and characterized by the acme of the *Liasidium variabile* dinoflagellate and high abundances of *Classopollis classoides*, suggesting an association of high land and sea temperatures [Hesselbo et al., 2020, Munier et al., 2021, Riding et al., 2013, Schöllhorn et al., 2020, Storm et al., 2020]. Given the nature of the $\delta^{13}C_{carb}$ curve of the Coimbra Fm and its biostratigraphic uncertainty, a correlation with data from neighbouring basins is, at this stage, ill-advised. Isotopic studies in different carbon-bearing substrates are ongoing; it was previously suggested that the organic-rich interval of UH (or even part of UF–UG) could correspond to the Early Jurassic Sinemurian *Liasidium* Event [Silva et al., 2021].

6. Conclusions

From an integrated stratigraphic analysis of the Lower Jurassic carbonate succession (Coimbra Fm) of the Lusitanian Basin cropping out at S. Pedro de Moel, the following conclusions are drawn:

(i) The Coimbra Fm shows a large diversity of calcareous facies and, less abundant, dolostones and shales, and is subdivided into eight informal units (UA to UF), rich in benthic macrofauna and deposited in a shallow-water carbonate ramp.

(ii) The rare occurrence of ammonites, the majority endemic (genus *Ptycharietites*), allows assigning the Coimbra Fm to the lower?–upper Sinemurian (Simpsoni Subchronozone, Oxynotum Chronozone).

(iii) Like the overlying Água de Madeiros Fm, the Coimbra Fm is locally rich in organic matter, especially UF (assigned to the Stellare–Denotatus Subchronozne transition), with total organic carbon reaching values around 10 wt%.

(iv) The studied succession is transgressive and belongs to a long-lasting 2nd-order transgressive phase that shows its maximum flooding around the Sinemurian–Pliensbachian transition. Three 3rd-order maximum flooding intervals are identified across the Coimbra Fm, materialized by an increase in the number of organic-rich levels and ammonite fossils.

(v) The vertical variation in $\delta^{13}C_{carb}$ is characterized by relatively normal marine values (~2‰); however, several negative excursions are associated with the organic-rich sediments, with a maximum amplitude reaching 8‰ in the Obtusum Chronozone. These shifts in bulk carbonate $\delta^{13}C_{carb}$ are interpreted to be of diagenetic origin and, therefore, of local/basinal significance. However, it cannot be discarded that a regional/global signal is imprinted in the observed trends.

Conflicts of interest

Authors have no conflict of interest to declare.

Acknowledgements

This study was supported by Fundação para a Ciência e Tecnologia (FCT), through the strategic project UID/MAR/04292/2019 granted to the Marine and Environmental Sciences Centre (MARE) and to Research Group UCM 910431: Mesozoic Biotic Processes. ACA acknowledges support by FCT, I.P./MCTES, National Funds (PIDDAC) - UIDB/50019/2020, Authors thank the LAFO-UFRJ for the total organic carbon analysis. The authors thank the editor C. Lezin and P. Pellenard and an anonymous reviewer for their helpful comments that much improved the original version of this manuscript.

Supplementary data

Supporting information for this article is available on the journal's website under https://doi.org/10.5802/crgeos.144 or from the author.

References

Azerêdo, A. C., Duarte, L. V., and Silva, R. L. (2014). Configuração sequencial em ciclos (2ª ordem) de

fácies transgressivas-regressivas do Jurássico Inferior e Médio da Bacia Lusitânica (Portugal). *Comun. Geol.*, 101(Especial I), 383–386.

Azerêdo, A. C., Silva, R. L., Duarte, L. V., and Cabral, M. C. (2010). Subtidal stromatolites from the Sinemurian of the Lusitanian Basin (Portugal). *Facies*, 56, 211–230.

Bougeault, C., Pellenard, P., Deconinck, J. F., Hesselbo, S. P., Dommergues, J. L., Bruneau, L., Cocquerez, T., Laffont, R., Huret, E., and Thibault, N. (2017). Climatic and palaeoceanographic changes during the Pliensbachian (Early Jurassic) inferred from clay mineralogy and stable isotope (CO) geochemistry (NW Europe). *Global Planet. Change*, 149, 139–152.

Boussaha, M., Pittet, B., Mattioli, E., and Duarte, L. V. (2014). Spatial characterization of the late Sinemurian (Early Jurassic) palaeoenvironments in the Lusitanian Basin. *Palaeogeogr. Palaeoclimatol. Palaeoecol.*, 409, 320–339.

Brito, M., Rodrigues, R., Baptista, R., Duarte, L. V., Azerêdo, A. C., and Jones, C. M. (2017). Geochemical characterization of oils and their correlation with Jurassic source rocks from the Lusitanian Basin (Portugal). *Mar. Pet. Geol.*, 85, 151–176.

Cabral, M. C., Colin, J.-P., Azerêdo, A. C., Silva., R. L., and Duarte, L. V. (2013). Associações de ostracodos da Formação de Coimbra (Sinemuriano) de S. Pedro de Moel (Bacia Lusitânica): valor paleoecológico e paleobiogeográfico. *Comun. Geol.*, 100(Especial I), 43–47.

Cabral, M. C., Colin, J.-P., Azerêdo, A. C., Silva, R. L., and Duarte, L. V. (2015). Brackish and marine ostracode assemblages from the Sinemurian of western Portugal, with description of new species. *Micropaleontology*, 61(1–2), 3–24.

Choffat, P. L. (1880). *Étude stratigraphique et paléontologique des terrains jurassiques du Portugal. Première livraison - Le Lias et le Dogger au Nord du Tage*. Memórias Secções Trabalhos Geológicos de Portugal. l'Academie royale des sciences, Lisbonne.

Comas-Rengifo, M. J., Duarte, L. V., Goy, A., Paredes, R., and Silva, R. L. (2013). El Sinemuriense Superior (cronozonas Oxynotum y Raricostatum) en la región de S. Pedro de Moel (Cuenca Lusitánica, Portugal). *Comun. Geol.*, 100(Especial I), 15–19.

Comas-Rengifo, M. J., Goy, A., Piñuela, L., García-Ramos, J. C., Suárez Vega, L. C., and Paredes, R. (2021). El Sinemuriense superior: cronozonas Obtusum y Oxynotum en Asturias, España. Ammonoideos y correlación con otras cuencas del oeste de Europa. [Upper Sinemurian: Obtusum and Oxynotum chronozones in Asturias, Spain. Ammonoids and correlation with other western European basins]. *Spanish J. Palaeontol.*, 36(1), 19–50.

Corna, M., Dommergues, J.-L., Meister, C., and Mouterde, R. (1997). Sinémurien. In Cariou, E. and Hantzpergue, P., editors, *Biostratigraphie du Jurassique Ouest-Européen et Méditerranéen: Zonations Parallèles et Distribution des Invertébrés et Microfossiles*, volume 17 of *Bulletin des Centres de Recherche Exploration-Production Elf-Aquitaine, Mémoire*, pages 9–14. Elf Aquitaine, Pau.

Correia, V. F., Riding, J. B., Duarte, L. V., Fernandes, P., and Pereira, Z. (2018). The Early Jurassic palynostratigraphy of the Lusitanian Basin, western Portugal. *Geobios*, (6), 537–557.

Dimuccio, L. A., Duarte, L. V., and Cunha, L. (2016). Definição litostratigráfica da sucessão calco-dolomítica do Jurássico Inferior da região de Coimbra-Penela (Bacia Lusitânica, Portugal). *Comun. Geol.*, 103, 77–96.

Dommergues, J.-L. (1987). L'évolution chez les Ammonitina du Lias Moyen (Carixien, Domerien basal) en Europe occidentale. *Doc. Lab. Géol. Lyon*, 98, 1–297.

Dommergues, J.-L., Meister, C., Neige, P., and Rocha, R. B. (2004). Endemic Sinemurian (Early Jurassic) ammonites from the Lusitanian Basin (Portugal). *Rev. Paléobiol.*, 23(2), 529–549.

Dommergues, J.-L., Meister, C., and Rocha, R. B. (2010). The Sinemurian ammonites of the Lusitanian Basin (Portugal): an example of complex endemic evolution. *Palaeodiversity*, 3, 139–167.

Duarte, L. V. (2004). The geological heritage of the Lower Jurassic of Central Portugal: selected sites, inventory and main scientific arguments. *Riv. Ital. Paleontol. Stratigr.*, 110, 381–388.

Duarte, L. V., Comas-Rengifo, M. J., Silva, R. L., Paredes, R., and Goy, A. (2014a). Carbon isotope stratigraphy and ammonite biochronostratigraphy across the Sinemurian-Pliensbachian boundary in the western Iberian margin. *Bull. Geosci.*, 89, 719–738.

Duarte, L. V., Silva, R. L., Azerêdo, A. C., Paredes, R., and Rita, P. (2014b). A Formação de Coimbra na região de S. Pedro de Moel (Oeste de Portugal).

Caracterização litológica, definição litostratigráfica e interpretação sequencial. IX CNG/2° CoGePLiP, Porto 2014. *Comun. Geol.*, 101(Especial I), 421–425.

Duarte, L. V., Silva, R. L., Félix, F. F., Comas-Rengifo, M. J., Rocha, R. B., Mattioli, E., Paredes, R., Mendonça Filho, J. G., and Cabral, M. C. (2017). The Jurassic of the Peniche Peninsula (Portugal): scientific, educational and science popularization relevance. *Rev. Soc. Geol. España*, 30(1), 55–70.

Duarte, L. V., Silva, R. L., and Mendonca Filho, J. G. (2013). Variação do COT e pirólise Rock-Eval do Jurássico Inferior da região de S. Pedro de Moel. Potencial de geração de hidrocarbonetos. *Comun. Geol.*, 100(Especial I), 107–111.

Duarte, L. V., Silva, R. L., Mendonça Filho, J. G., Poças Ribeiro, N., and Chagas, R. B. A. (2012). High resolution stratigraphy, palynofacies and source rock potential of the Água de Madeiros Formation (Lower Jurassic), Lusitanian Basin, Portugal. *J. Pet. Geol.*, 35(2), 105–126.

Duarte, L. V., Silva, R. L., Oliveira, L. C. V., Comas-Rengifo, M. J., and Silva, F. (2010). Organic-rich facies in the Sinemurian and Pliensbachian of the Lusitanian Basin, Portugal: total organic carbon distribution and relation to transgressive–regressive facies cycles. *Geol. Acta*, 8, 325–340.

Duarte, L. V. and Soares, A. F. (2002). Litostratigrafia das séries margo-calcárias do Jurássico inferior da Bacia Lusitânica (Portugal). *Comun. Inst. Geol. Mineiro*, 89, 135–154.

Ferreira, J., Mattioli, E., Sucherás-Marx, B., Giraud, F., Duarte, L. V., Pittet, B., Suan, G., Hassler, A., and Spangenberg, J. E. (2019). Western Tethys Early and Middle Jurassic calcareous nannofossil biostratigraphy. *Earth-Sci. Rev.*, 197, article no. 102908.

Franceschi, M., Corso, J. D., Cobianchi, M., Roghi, G., Penasa, L., Picotti, V., and Preto, N. (2019). Tethyan carbonate platform transformations during the Early Jurassic (Sinemurian–Pliensbachian, Southern Alps): Comparison with the Late Triassic Carnian Pluvial Episode. *Geol. Soc. Am. Bull.*, 131, 1255–1275.

Hesselbo, S. P., Hudson, A. J. L., Huggett, J. M., Leng, M. J., Riding, J. B., and Ullmann, C. V. (2020). Palynological, geochemical, and mineralogical characteristics of the Early Jurassic Liasidium Event in the Cleveland Basin, Yorkshire, UK. *Newsl. Stratigr.*, 53(2), 191–211.

Hesselbo, S. P., Jenkyns, H. C., Duarte, L. V., and Oliveira, L. C. V. (2007). Carbon-isotope record of the Early Jurassic (Toarcian) Oceanic Anoxic Event from fossil wood and marine carbonate (Lusitanian Basin, Portugal). *Earth Planet. Sci. Lett.*, 253, 455–470.

Hiscott, R. N., Wilson, R. C., Gradstein, F. M., Pujalte, V., Garcia-Mondéjar, J., Boudreau, R. R., and Wishart, H. A. (1990). Comparative stratigraphy and subsidence history of Mesozoic rift basins of North Atlantic. *Am. Assoc. Pet. Geol. Bull.*, 74(1), 60–76.

Howarth, M. K. (2002). The Lower Lias of Robin Hood's Bay, Yorkshire, and the work of Leslie Bairstow. *Bull. Nat. Hist. Mus.*, 58, 81–152.

Knaust, D. (2013). The ichnogenus Rhizocorallium: Classification, trace makers, palaeoenvironments and evolution. *Earth-Sci. Rev.*, 126, 1–47.

Korte, C. and Hesselbo, S. P. (2011). Shallow marine carbon and oxygen isotope and elemental records indicate icehouse-greenhouse cycles during the Early Jurassic. *Paleoceanography*, 26, article no. PA4219.

Kullberg, J. C., Rocha, R. B., Soares, A. F., Rey, J., Terrinha, P., Azerêdo, A. C., Callapez, P., Duarte, L. V., Kullberg, M. C., Martins, L., Miranda, R., Alves, C., Mata, J., Madeira, J., Mateus, O., Moreira, M., and Nogueira, C. R. (2013). A Bacia Lusitaniana: estratigrafia paleogeografia e tectónica. In Dias, R., Araújo, A., Terrinha, P., and Kullberg, J. C., editors, *Geologia de Portugal*, volume II, pages 195–347. Livraria Escolar Editora, Lisboa.

Marshall, J. D. (1992). Climatic and oceanographic isotopic signals from carbonate rock record and their preservation. *Geol. Mag.*, 192, 143–160.

Masetti, D., Figus, B., Jenkyns, H., Barattolo, F., Mattioli, E., and Posenato, R. (2017). Carbon-isotope anomalies and demise of carbonate platforms in the Sinemurian (Early Jurassic) of the Tethyan region: evidence from the Southern Alps (Northern Italy). *Geol. Mag.*, 154, 625–650.

Mendonça Filho, J. G., Menezes, T. R., Mendonça, J. O., Oliveira, A. D., Silva, T. F., Rondon, N. F., and Silva, F. S. (2012). Organic facies: Palynofacies and organic geochemistry approaches. In Panagiotaras, D., editor, *Geochemistry—Earth's System Processes*, pages 211–248. In Tech, Rijeka.

Mercuzot, M., Pellenard, P., Durlet, C., Bougeault, C., Meister, C., Dommergues, J. L., Thibault, N., Baudin, F., Mathieu, O., Bruneau, L., and Huret, E.

(2020). Carbon-isotope events during the Pliensbachian (Lower Jurassic) on the African and European margins of the NW Tethyan Realm. *Newsl. Stratigr.*, 53(1), 41–69.

Mouterde, R. and Ruget-Perrot, Ch. (1975). Esquisse de la paléogéographie du Jurassique inférieur et moyen au Portugal. *Bull. Soc. Géol. Fr.*, XVII(5), 779–786.

Munier, T., Deconinck, J.-F., Pellenard, P., Hesselbo, S. P., Riding, J. B., Ullmann, C. V., Bougeault, C., Mercuzot, M., Santoni, A.-L., Huret, É., and Landrein, P. (2021). Million-year-scale alternation of warm-humid and semi-arid periods as a mid-latitude climate mode in the Early Jurassic (Late Sinemurian, Laurasian Seaway). *Clim. Past Discuss.*, 17, 1547–1566.

Oliveira, L. C. V., Rodrigues, R., Duarte, L. V., and Lemos, V. (2006). Avaliação do potencial gerador de petróleo e interpretação paleoambiental com base em biomarcadores e isótopos estáveis do carbono da seção Pliensbaquiano-Toarciano inferior (Jurássico inferior) da região de Peniche (Bacia Lusitânica, Portugal). *Bol. Geociênc. Petrobras*, 14, 207–234.

Page, K. N. (2003). The Lower Jurassic of Europe: its subdivision and correlation. *Geol. Surv. Denmark Greenland Bull.*, 1, 23–59.

Paredes, R., Comas-Rengifo, M. J., and Duarte, L. V. (2013). Moluscos bivalves da Formação de Água de Madeiros (Sinemuriano superior) da Bacia Lusitânica (Portugal). *Comun. Geol.*, 100(Especial I), 21–27.

Paredes, R., Comas-Rengifo, M. J., Duarte, L. V., García Joral, F., and Goy, A. (2016). The earliest Jurassic brachiopod record in the Lusitanian Basin: palaeoecology insights. Actas de la XXXII Jornadas de la Sociedad Española de Paleontología. *Cuad. Mus. Geominero*, 20, 465–470.

Peti, L., Thibault, N., Clémence, M.-E., Korte, C., Dommergues, J.-L., Bougeault, C., Pellenard, P., Jelby, M. E., and Ullmann, C. V. (2017). Sinemurian-Pliensbachian calcareous nannofossil biostratigraphy and organic carbon isotope stratigraphy in the Paris Basin: Calibration to the ammonite biozonation of NW Europe. *Palaeogeogr. Palaeoclimatol. Palaeoecol.*, 468, 142–161.

Poças Ribeiro, N., Mendonça Filho, J. G., Duarte, L. V., Silva, R. L., Mendonça, J. O., and Silva, T. F. (2013). Palynofacies and organic geochemistry of the Sinemurian carbonate deposits in the western Lusitanian Basin (Portugal): Coimbra and Água de Madeiros formations. *Int. J. Coal Geol.*, 111, 37–52.

Price, G. D., Baker, S. J., VanDeVelde, J., and Clémence, M.-E. (2016). High-resolution carbon cycle and seawater temperature evolution during the Early Jurassic (Sinemurian-Early Pliensbachian). *Geochem. Geophys. Geosys.*, 17(10), 3917–3928.

Riding, J. B., Leng, M. J., Kender, S., Hesselbo, S. P., and Feist-Burkhardt, S. (2013). Isotopic and palynological evidence for a new Early Jurassic environmental perturbation. *Palaeogeogr. Palaeoclimatol. Palaeoecol.*, 374, 16–27.

Rocha, R. B., Matiolli, E., Duarte, L. V., Pittet, B., Elmi, S., Mouterde, R., Cabral, M. C., Comas-Rengifo, M. J., Gómez, J. J., Goy, A., Hesselbo, S. P., Jenkyns, H. C., Littler, K., Mailliot, S., Oliveira, L. C. V., Osete, M. L., Perilli, N., Pinto, S., Ruget, C. H., and Suan, G. (2016). Toarcian stage of lower Jurassic defined by the Global Boundary Stratotype Section and Point (GSSP) at the Peniche section (Portugal). *Episodes*, 39(3), 460–481.

Schöllhorn, I., Adatte, T., van de Schootbrugge, B., Houben, A., Charbonnier, G., Janssen, N., and Föllmi, K. B. (2020). Climate and environmental response to the break-up of Pangea during the Early Jurassic (Hettangian-Pliensbachian); the Dorset coast (UK) revisited. *Glob. Planet. Change*, 185, article no. 103096.

Sêco, S. L. R., Duarte, L. V., Pereira, A. J. S. C., and Silva, R. L. (2018). Field gamma-ray patterns and stratigraphic reinterpretation of offshore well-log data from Lower Jurassic organic-rich units of the Lusitanian Basin (Portugal). *Mar. Pet. Geol.*, 98, 860–872.

Silva, R. L., Carlisle, C., and Wach, G. (2017). The carbon isotopic record of the Lower Jurassic in the Slyne Basin (Ireland). *Mar. Pet. Geol.*, 86, 499–511.

Silva, R. L. and Duarte, L. V. (2015). Organic matter production and preservation in the Lusitanian Basin (Portugal) and Pliensbachian climatic hot snaps. *Glob. Planet. Change*, 131, 24–34.

Silva, R. L., Duarte, L. V., and Comas-Rengifo, M. J. (2015). Carbon isotope chemostratigraphy of Lower Jurassic carbonate deposits, Lusitanian Basin (Portugal): Implications and limitations to the application in sequence stratigraphic studies. In Ramkumar, M., editor, *Chemostratigraphy: Concepts, Techniques, and Applications*, pages 341–371.

Elsevier, Amsterdam.

Silva, R. L., Duarte, L. V., Comas-Rengifo, M. J., Mendonça Filho, J. J., and Azerêdo, A. C. (2011). Update of the carbon and oxygen isotopic records of the Early–Late Pliensbachian: insights from the organic-rich hemipelagic series of the Lusitanian Basin (Portugal). *Chem. Geol.*, 283, 177–184.

Silva, R. L., Duarte, L. V., Wach, G., Morrison, N., and Campbell, T. (2020). Oceanic organic carbon as a possible first-order control on the carbon cycle during the Bathonian–Callovian. *Glob. Planet. Change*, 184, article no. 103058.

Silva, R. L., Duarte, L. V., Wach, G. D., Ruhl, M., Sadki, D., Gómez, J. J., Hesselbo, S. P., Xu, W., O'Connor, D., Rodrigues, B., and Mendonça Filho, J. G. (2021). An Early Jurassic (Sinemurian–Toarcian) stratigraphic framework for the occurrence of Organic Matter Preservation Intervals (OMPIs). *Earth-Sci. Rev.*, 221, article no. 103780.

Soares, A. F., Rocha, R. B., Elmi, S., Henriques, M. H., Mouterde, R., Almeras, Y., Ruget, C., Marques, J., Duarte, L. V., Carapito, M. C., and Kullberg, J. (1993). Le sous-bassin nord lusitanien (Portugal) du Trias au Jurassique moyen: histoire d'un « rift avorté ». *C. R. Acad. Sci., Paris, II*, 317, 1659–1666.

Storm, M. S., Hesselbo, S. P., Jenkyns, H. C., Ruhl, M., Ullmann, C. V., Xu, W., Leng, M. J., Riding, J. B., and Gorbanenko, O. (2020). Orbital pacing and secular evolution of the Early Jurassic carbon cycle. *Proc. Natl. Acad. Sci. USA*, 117(8), 3974–3982.

Suan, G., Mattioli, E., Pittet, B., Lécuyer, C., Suchéras-Marx, B., Duarte, L. V., Philippe, M., Reggiani, M. L., and Martineau, F. (2010). Secular environmental precursors of Early Toarcian (Jurassic) extreme climate changes. *Earth Planet. Sci. Lett.*, 290, 448–458.

Thierry, J. and Barrier, E. (2000). Middle Toarcian. In Dercourt, J., Gaetani, M., Vrielynck, B., Barrier, E. B., Biju-Duval, B., Brunet, M. F., Cadet, J. P., Crasquin, S., and Sandulescu, M., editors, *Atlas Peri-Tethys, Paleogeographic Maps*. CCGM/CGMW, Paris. Map 8.

Ullmann, C. V., Szücs, D., Jiang, M., Hudson, A. J. L., and Hesselbo, S. P. (2022). Geochemistry of macrofossil, bulk rock and secondary calcite in the Early Jurassic strata of the Llanbedr (Mochras Farm) drill core, Cardigan Bay Basin, Wales, UK. *J. Geol. Soc.*, 179(1), article no. jgs2021-018.

Vitón, I., Comas-Rengifo, M. J., and Paredes, R. (2020). Early Jurassic (Sinemurian) gastropods from the Lusitanian Basin (west of Portugal). *Span. J. Palaeontol.*, 35(2), 147–166.

Comptes Rendus
Géoscience — Sciences de la Planète
2022, Vol. 354, Special Issue S3, p. 107-124
https://doi.org/10.5802/crgeos.173

Integrated stratigraphy of the Jurassic and the Cretaceous: a tribute to Jacques Rey /
Stratigraphie intégrée du Jurassique et du Crétacé : un hommage à Jacques Rey

The Oxfordian–Kimmeridgian transition in the Boulonnais (France) and the onset of organic-rich marine deposits in NW Europe: a climatic control?

Johann Schnyder *, [a], **François Baudin** [a] and **Roger Jan Du Chêne** [b]

[a] Sorbonne Université, CNRS-INSU, Institut des Sciences de la Terre de Paris, iSTeP, 4 place Jussieu, 75005 Paris, France

[b] 81 rue Soubiras, 33200 Bordeaux, France

E-mails: Johann.schnyder@sorbonne-universite.fr (J. Schnyder), francois.baudin@sorbonne-universite.fr (F. Baudin), rjdc@hotmail.com (R. Jan Du Chêne)

Abstract. We characterised the organic matter content of marine deposits at the Oxfordian–Kimmeridgian transition in the Boulonnais (France). Organic rich deposits in platform environments are evidenced in the uppermost *Cymodoce* and lowermost *Mutabilis* Zone (early late Kimmeridgian), associated with enhanced planktonic palaeoproductivity and/or developing dysoxia/anoxia. Similar organic rich intervals in early late Kimmeridgian are also evidenced in platform deposits in Normandy and Charentes in France, and in basinal deposits from Yorkshire and Dorset in UK. This refined onset of the organic rich bands (ORB), as described in NW Europe during the late Jurassic, is coeval with seawater warming. We propose that this seawater warming was an important trigger of the onset of the late Jurassic ORB deposition system in NW Europe, which began at the *Cymodoce–Mutabili*s boundary during the early late Kimmeridgian and lasted until the middle part of the Tithonian, over a time span of 6.8 Myr.

Keywords. Jurassic, Organic geochemistry, Palynofacies, Palaeogeography, Palaeoclimate, Palaeoproductivity, Organic rich band.

Published online: 13 January 2023, Issue date: 13 January 2023

1. Introduction

Organic matter enrichments in marine deposits may be driven by a number of factors, such as tectonics, palaeogeography, climate and sea-level changes [Demaison et al., 1983, Tissot, 1979, Tyson, 1995]. Those factors can favour palaeoproductivity changes and/or induce anoxia/dysoxia in sea water masses, therefore leading to enhanced organic matter influx to the seafloor [Tyson, 1995]. During the late Jurassic, the upper Kimmeridgian–Tithonian deposits of several NW European basins do show such remarkable organic matter-rich intervals. Because of their significant contribution to the genesis of the North Sea hydrocarbons, those deposits were intensely stud-

* Corresponding author.

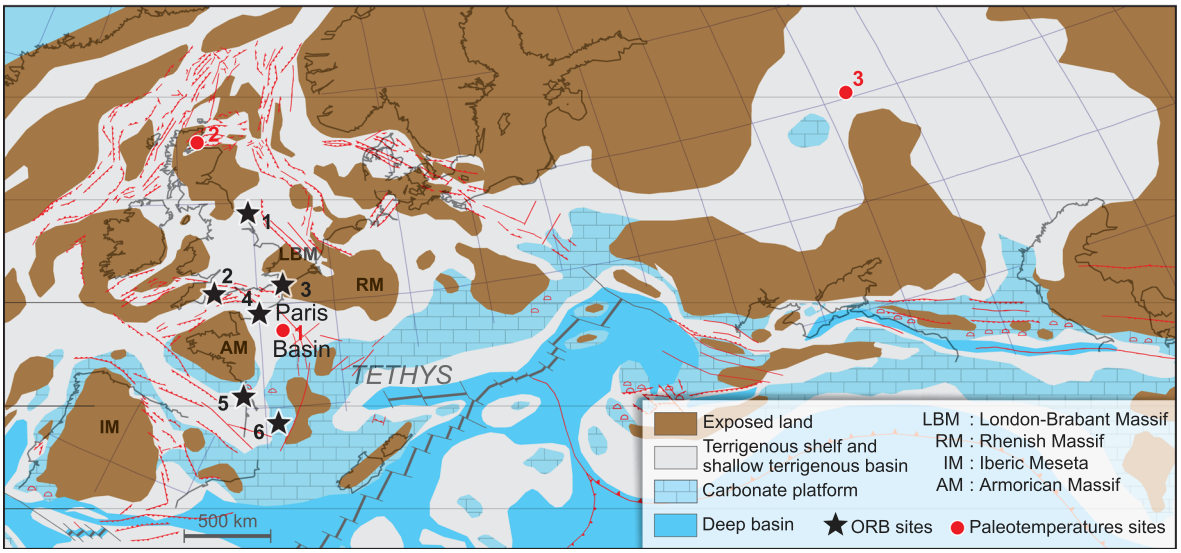

Figure 1. NW Europe paleogeographic map for the Early Kimmeridgian [Cecca et al., 1993]. Black stars: Organic-rich bands (ORB) sites cited in this work, 1: Yorkshire; 2: Dorset, 3: Boulonnais (this work), 4: Normandy, 5: Charentes, 6: Quercy. Red dots: selected sites with published sea-water paleotemperatures, 1: Paris Basin [Brigaud et al., 2008, Dera et al., 2011, Lathuilière et al., 2015]; 2: Scotland [Nunn and Price, 2010]; 3: Russian platform [Price and Rogov, 2009].

ied during the last decades, both in England [e.g. Cox and Gallois, 1981, Herbin et al., 1991, 1993, Huc et al., 1992, Morgans-Bell et al., 2001, Oschmann, 1988, 1990, Tyson, 1996, Tyson et al., 1979, Wignall, 1991] and northern France [e.g. Bialkowski et al., 2000, El Albani et al., 1993, Geyssant et al., 1993, Herbin and Geyssant, 1993, Herbin et al., 1995, Proust et al., 1995, Ramdani, 1996, Tribovillard et al., 2001, Waterhouse, 1999]. Well studied in the basinal facies of the so-called Kimmeridge Clay Formation in Yorshire and Dorset in UK, five ORB, for organic rich bands [Cox and Gallois, 1981] or organic rich belts [Herbin and Geyssant, 1993], have been described and correlated within these basins from the *Eudoxus* ammonite zone (late Kimmeridgian) until the *Hudlestoni–Pectinatus* zones (early Tithonian) [Cox and Gallois, 1981, Herbin and Geyssant, 1993, Herbin et al., 1993, 1995]. In the Boulonnais area in NW France, where more proximal, shoreface to outer platform facies were deposited during the upper Jurassic (Figure 1), the first two ORB as recorded in UK are not observed, and the three following ORB are only partly recorded [Herbin et al., 1995]. Both in UK and France, the largest organic matter enrichments correspond to the highest sea-levels recorded in this time period, in the latest Kimmeridgian to earliest Tithonian [Herbin et al., 1995, Wignall and Ruffell, 1990]. By contrast, the lower Kimmeridgian deposits received little attention because of the lack of oil-generating levels and the relative condensation of the sedimentary sequence and, as a consequence, the onset of this ORB deposition system is not well known.

In this paper, we aim to study the organic matter distribution at the Oxfordian–Kimmeridgian transition in the Boulonnais area in France, in order to detail the initiation of ORB deposition. We then compare the Boulonnais record with that of neighbouring regions in France (Normandy, Charentes, Quercy) and in the UK (Yorkshire and Dorset) and use known relative sea-level changes and a set of palaeoclimate data (namely seawater temperature reconstructions using stable isotopes) during the late Jurassic to discuss the possible triggers controlling ORB initiation and deposition at NW European scale.

2. Material and methods

In the Boulonnais area, late Jurassic deposits crop out on coastal cliffs north of the town of Boulogne-sur-

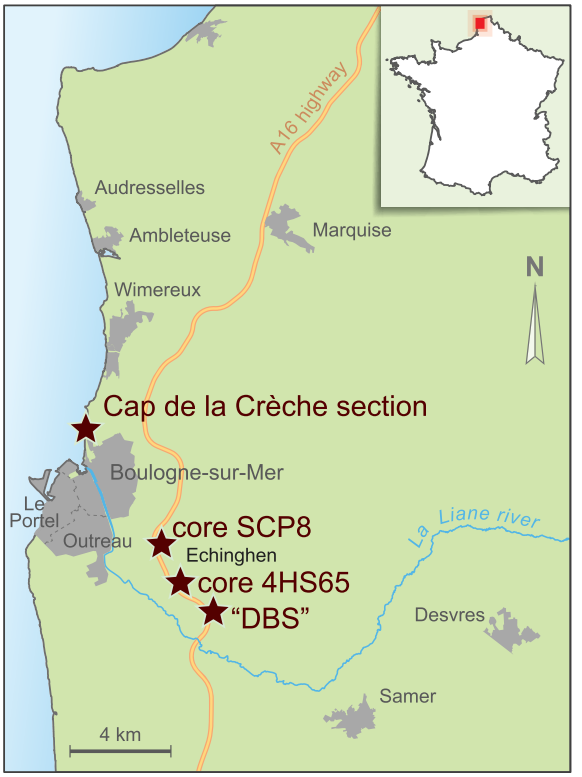

Figure 2. Studied sites for organic matter content in the Boulonnais, France, near the coastal town of Boulogne-sur-Mer. "DBS" is for Diffuseur de Boulogne Sud.

Mer (Cap de la Crèche outcrop, Figure 2), showing deposits from the upper part of the *Mutablis* zone in the late Kimmeridgian (only one metre within this later zone cropping out) onto the *Kerberus* zone in the late Tithonian [Proust et al., 1995]. Mostly shallow, inner platform facies of late Oxfordian and early Kimmeridgian ages are not cropping out nowadays. During the winter 1996, the A16 motorway works allowed observation of the lowermost formations of the Kimmeridgian in the vicinity of Boulogne-sur-Mer. The so-called Oolithe d'Hesdin-l'Abbé, Caillasses d'Hesdigneul and Calcaires de Brecquerecque, as well as the base of the Argiles du Moulin Wibert formations (Figures 3 and 4) were visible for several months before the trench was paved (Diffuseur de Boulogne Sud (DBS) outcrops, Figure 2). Moreover, several cores were drilled for geotechnical purpose. One of them, the SCP8 core (Figure 2), covering the upper Oxfordian–lowermost Kimmeridgian interval, from the Argiles du Mont des Boucards to the Caillasses d'Hesdigneul formation was intensely studied [Schnyder et al., 2000]. The 4HS65 core completes this local stratigraphy, showing the upper part of the Calcaires de Brecquerecque and the base of the Argiles du Moulin Wibert formations (Figures 2 and 3).

The DBS is located just after the place where the A16 motorway crosses the Liane River and 2 km before the toll (Figure 2). The outcrops were studied during the road works along a 500 m-long trench. The two studied cores, SCP8 and 4HS65, are located near the village of Echinghen (Figure 2). Both penetrated the sedimentary deposits over 50 m and 38 m, respectively. The uppermost part of the Argiles du Moulin Wibert was sampled using the Cap de La Crèche outcrop (Figure 2). The stratigraphic extent of each outcrop and core that helped construct the composite log are indicated in Figures 3 and 4.

After detailed sedimentological field observations, the 4HS65 core and the outcrops were sampled at high resolution with a sampling step ranging from 5 to 20 cm. Note that there are some out-

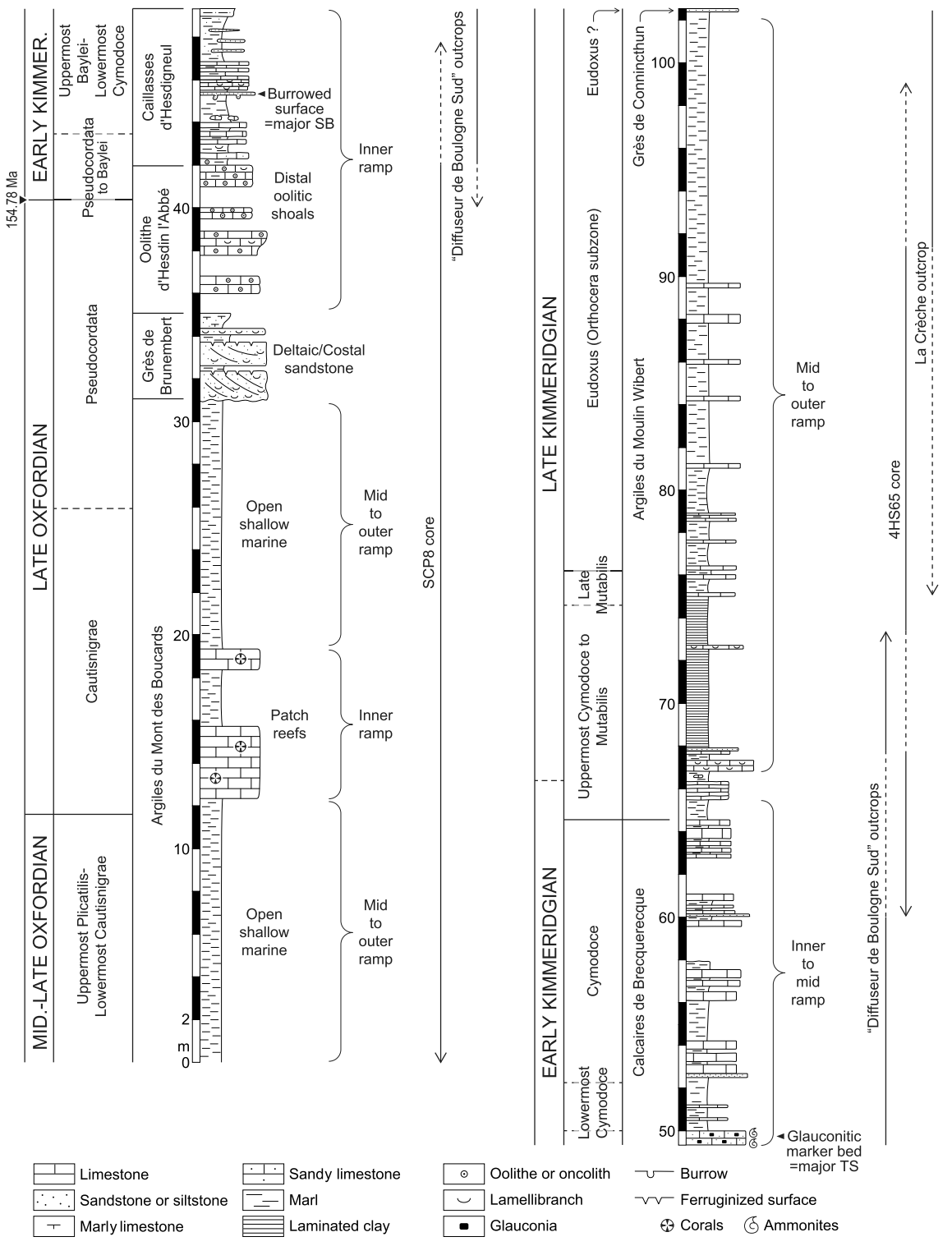

Figure 3. Composite log at the Oxfordian–Kimmeridgian transition in the Boulonnais, France.

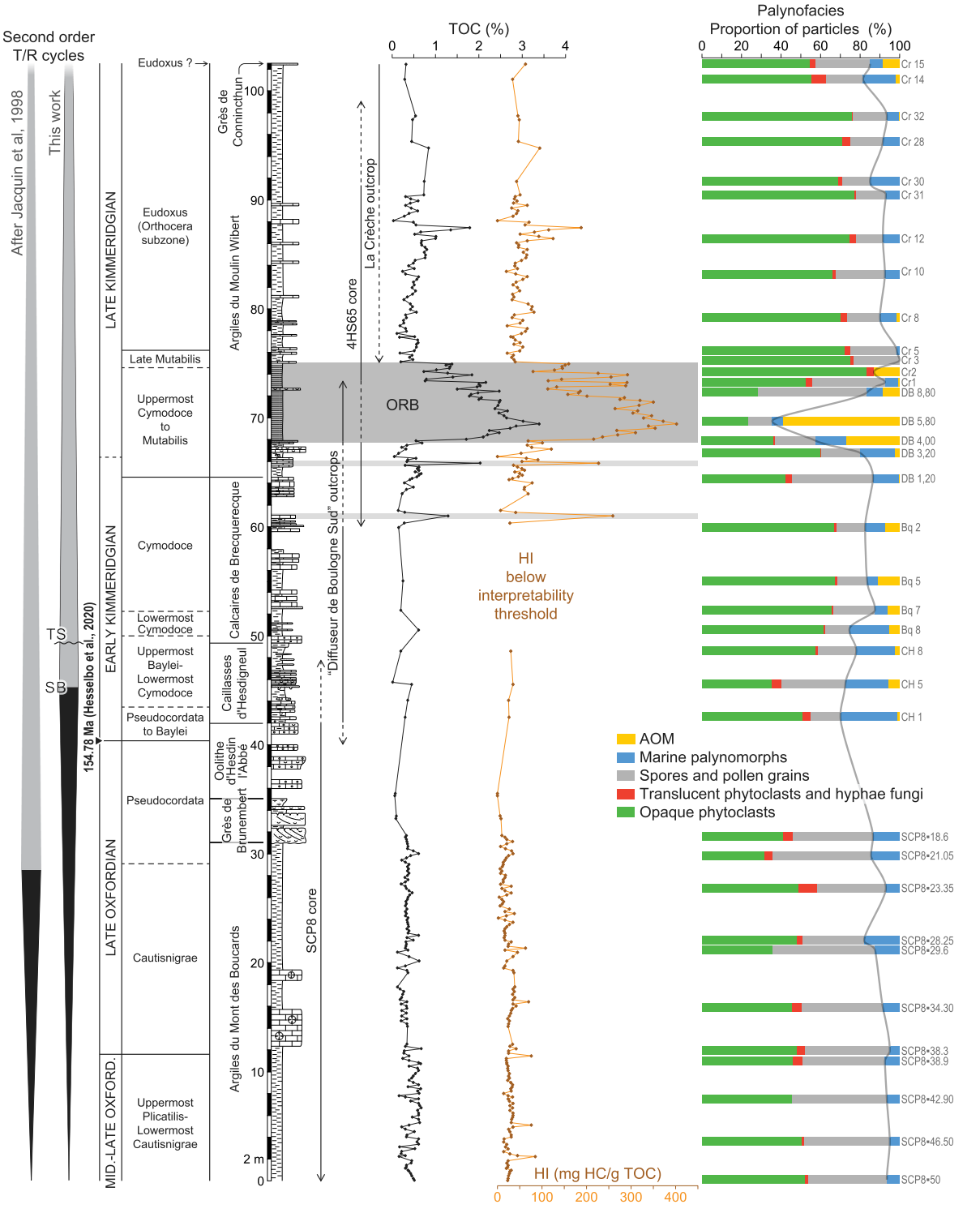

Figure 4. Rock-Eval pyrolysis and palynofacies data against the composite log at the Oxfordian–Kimmeridgian transition in the Boulonnais, France. Note the major organic-rich interval evidenced during the Late *Cymodoce* to late *Mutabilis* zones interval (Early Late Kmmeridgian).

crop gaps (a few decimetres in thickness) on the DBS outcrops. The sedimentary organic matter was characterised using Rock-Eval pyrolysis and palynofacies observations. Facies description, biostratigraphy, Rock-Eval pyrolysis (142 samples) and palynofacies (11 slides) data from SCP8 core have been published in Schnyder et al. [2000] (Figure 4). Additional, newly presented data correspond to 152 samples for Rock Eval pyrolysis and 25 samples for palynofacies slide preparation collected in the DBS outcrops, 4HS65 core and the Cap de la Crèche outcrop (Figure 4). A total of 10 slides were selected among these 25 slides for palynology to help dating the Caillasses d'Hesdigneul, Calcaires de Brecquerecque, and base of Argiles du Moulin Wibert formations. All the above mentioned results, are shown in Figures 3 and 4, in order to present an integrated organic matter dataset at the Oxfordian–Kimmeridgian transition, based on a total of 294 Rock-Eval pyrolysis analyses and 36 palynofacies slides.

Calcium carbonate content was determined using the 152 new samples with a carbonate bomb, and the total carbon content was determined using a LECO WR-12 analyser. Total organic carbon (TOC) content was calculated by determining the difference between total carbon and carbonate carbon, assuming that all carbonate is pure calcite. The source and thermal maturation of the organic matter were estimated using a Rock-Eval instrument using an Oil Show Analyser device [Espitalié et al., 1986]. Standard notations are used: Tmax is expressed in °C; TOC content in weight % and hydrogen index (HI = S2/TOC × 100) in mg HC per g of TOC.

Organic residues were obtained using a standard palynological treatment with HCl-HF maceration to remove the mineral fraction [Steffen and Gorin, 1993]; no oxidation by nitric acid was used. The residues were sieved (10 μm) and directly mounted for palynofacies observations. The classification used is a simplified version of that detailed in McArthur et al. [2016] and Schnyder et al. [2017]. Five constituents categories are retained (Figure 4), which will be used in the diagram illustrating the results. These categories are the amorphous organic matter (AOM), which is generally considered in marine settings as derived from algal–bacterial marine production, the marine palynomorphs (including here dinoflagellate cysts, foraminera linings, and scolecodont remains), the spores and pollen grains, the translucent phytoclasts and the opaque phytoclasts (the latter two derived from terrestrial plants tissues) (see McArthur et al. [2016] and Schnyder et al. [2017] for more details). Palynostratigraphic slides for dinoflagellate identifications were prepared from the organic residues, after a slight oxidation by nitric acid and heavy mineral separation. Ten samples were studied for dinoflagellate identifications, 3 from the Caillasses d'Hesdigneul, 2 from the Calcaires de Brecquerecque, and 5 from the Argiles du Moulin Wibert.

3. The upper Oxfordian and lower Kimmeridgian succession of the Boulonnais

3.1. *Facies and long-term sea-level sequences*

From the mid-Oxfordian up to the early late Kimmeridgian, the sedimentary record from the Boulonnais corresponds to marine deposits with mixed carbonate/siliclastic lithologies and interpreted to be inner to outer ramp (platform) deposits. In ascending order, six successive formations have been described: the Argiles du Mont des Boucards, the Grès de Brunembert, the Oolithe d'Hesdin-l'Abbé, the Caillasses d'Hesdigneul, the Calcaires de Brecquerecque and finally the Argiles du Moulin Wibert formations (Figures 3 and 4). The Argiles du Mont des Boucards Formation is 15–30 m thick and corresponds to homogeneous claystone to marlstones with some mollusc shell layers (*Ostrea*) interpreted to be mid-to-outer ramp deposits. It locally contains patch-reef facies in its middle part (Calcaire de Brucquedal Member) corresponding to inner ramp deposits. The following Grès de Brunembert Formation is 1–10 m thick and consists of bivalves and locally gastropod-rich sandstone beds alternating with silty to sandy marls. These deposits are interpreted to be deltaic/coastal sandstones. The Oolithe d'Hesdin-l'Abbé Formation consists of 6–10 m thick whitish bioturbated poorly-sorted oolitic and oncolitic limestones passing to marls with oolites and is interpreted to be inner ramp, distal oolitic shoals. The Caillasses d'Hesdigneul Formation is 5 m thick and starts with black marls containing oolites and some oysters, passing upward to oolitic sandy limestones with gastropods (*Harpagodes*) and sea-urchins and then to micritic limestones, mostly devoid of fauna. The topmost beds are usually covered

by hard-grounds, with eroded surfaces and small oyster encrustations. The depositional environment is interpreted to be an inner ramp, lagoonal facies. Compared with the underlying Argiles du Mont des Boucards Formation, the Grès de Brunembert, Oolithe d'Hesdin l'Abbé and Caillasses d'Hesdigneul formations evidence a shallowing-up trend at the Oxfordian/Kimmeridgian boundary (Figures 3 and 4). The following Calcaires de Brecquerecque Formation shows a 15 m thick alternation of marls and limestones, containing thin sand to sandstone layers. The faunal content is dominated by bivalves, sea-urchins, and brachiopods, but devoid of ammonites. A peculiar (0.5 m thick) sandy and glauconitic limestone, rich in ammonites, is visible at the base of the formation (Figure 3). This observation suggests an important transgressive event with erosional surfaces, glauconite accumulation, and ammonite condensation or reworkings at the base of the Calcaires de Brecquerecque (Figure 3). The depositional environments in the Calcaires de Brecquerecque are interpreted to be inner to mid-ramp deposits, and a deepening-up trend is obvious with respect to the underlying Caillasses d'Hesdigneul Formation (Figures 3 and 4). The following Argiles du Moulin Wibert Formation directly overlies the Calcaires de Brecquerecque. The formation as seen in the Cap de la Crèche section is around 20 m thick [Mansy et al., 2000], however, the base of the formation is lacking in Cap de la Crèche and the whole thickness reach up to 38 m adding the DBS outcrop sedimentary sequences (Figure 3). The Argiles du Moulin Wibert Formation shows an alternation of gray to black marl and limestone beds, often rich in bivalves [*Nanogyra virgula*, *Trigonia* and *Gervillia*, Mansy et al., 2000]. The dark clays are remarkably laminated between 68 and 75 m (composite section, Figure 3). The Argiles du Moulin Wibert correspond to mid to outer ramp deposits that again mark a deepening-up trend with respect to the underlying Calcaires de Brecquerecque Formation, from the early Kimmeridgian to the base of the late Kimmeridgian (Figures 3 and 4). The Argiles du Moulin Wibert is finally overlain by the Grès de Conincthun Formation (Figure 3).

To summarise, the sedimentary succession of the Boulonnais, from the mid-Oxfordian up to the early late Kimmeridgian, corresponds to two open marine, deeper marl-dominated intervals (i.e. Argiles du Mont des Boucards and Argiles du Moulin Wibert) separated by a shallower marine, sandstone to carbonate platform-dominated interval (comprising the Grès de Brunembert, the Oolithe d'Hesdin l'Abbé, the Caillasses d'Hesdigneul and the Calcaires de Brecquerecque), the latter interval being deposited at around the Oxfordian/Kimmeridgian boundary (Figures 3 and 4). A long-term, second-order relative sea-level regressional and then transgressional trend (T/R cycle) can thus be evidenced in the Boulonnais, with a second order sequence boundary that can be placed at the major hardground in the Caillasses d'Hesdigneul at 45.5 m (uppermost *Baylei*–lowermost *Cymodoce*) and a major transgressive surface corresponding to the glauconitic ammonite-rich marker-bed at 49.5 m (lowermost *Cymodoce*) (Figures 3 and 4). These relative sea-level trends are equivalent to the regressive part of the second-order cycle 8 and the transgressive part of second-order cycle 9, as referred to by Jacquin et al. [1998] at the scale of Western Europe, with a slight difference in the position of the major sequence boundary (Figure 4).

3.2. *Biostratigraphy*

Age determination of the Argiles du Mont des Boucards in the Middle-late Oxfordian until the Argiles du Moulin Wibert in the late Kimmeridgian is based on ammonite and dinocyst distributions [Dutertre, 1925, Debrand-Passard et al., 1980, Mansy et al., 2000, Schnyder et al., 2000, see Figures 3 and 4]. A summary of biostratigraphic information for each formation, based on published data, is provided in the Supplementary Data File. To complete the published data set in some poorly-dated intervals, we performed new dinocyst identification using 10 samples collected in the Caillasses d'Hesdigneul, Calcaires de Brecquerecque and Argiles du Moulin Wibert formations. These new dinocyst identifications are presented in the Supplementary Data File, and the corresponding results are integrated into the biostratigraphic framework as shown on Figures 3 and 4.

4. Organic geochemistry and palynofacies results

The average Tmax value from the Rock-Eval in the entire set of data is 424 °C. This indicates an immature

organic matter, which was not affected by significant burial diagenesis and is therefore suitable for palaeoenvironmental studies [Espitalié et al., 1986].

The Rock-Eval and palynofacies results allow distinction between three parts in the composite log with respect to the organic matter content.

The first interval extends from 0 to 68 m, including the middle-late Oxfordian to early Kimmeridgian deposits, from the Argiles du Mont des Boucards to the Calcaires de Brecquerecque formations (Figure 4). TOC values are mainly below 1 wt% (TOC = 0.38 wt% on average) and HI values mainly below 100 mgHC/gTOC (HI = 30 mgHC/gTOC on average). These results are represented as grey dots on Figure 5, and correspond to a Type III organic matter, probably deriving from terrestrial debris and/or from a relatively degraded marine organic matter and even Type IV organic matter (highly degraded organic matter whose origin cannot be assessed). The palynofacies from this interval show a dominant terrestrial component of 84% of the total assemblage (defined here as opaque+translucent debris+spores and pollen grains+hyphae from fungi) over a marine component of 16% (defined as AOM+ dinoflagellate cysts+foraminifera linings) (Figure 4). These results are in line with those from the Rock-Eval pyrolysis and suggest a mixture of a relatively degraded marine organic matter and strong terrestrial organic influx from the neighbouring emerged lands (Figure 1). Low TOC and IH values and the dominant terrestrial component in palynofacies suggest a moderate or low palaeoproductivity and that the water masses were most probably well oxygenated. An interesting secondary feature is the significant increase in marine palynomorph (dinoflagellate cysts and foraminifera linings) proportions from sample CH1 (42.6 m) to sample Bq8 (50.6 m) within the Caillasses d'Hesdigneul and the base of the Calcaires de Brecquerecque (Figure 4). Marine palynomorph proportions in the total assemblage are comprised between 20 and 28.5% within this stratigraphic interval, whereas marine palynomorph proportions are always below 20% and often below 10% in the other palynofacies samples from our data set. This suggests that periodic planktonic blooms occurred during the deposition of the shallow marine to lagoonal Caillasses d'Hesdigneul and base of Calcaires de Brecquerecque formations.

The second interval extends from 68 to 75 m. It includes a time interval spanning the uppermost *Cymodoce* onto the late *Mutabilis* zones in early late Kimmeridgian, and correspond to the darker, laminated marls well observed at the base of the Argiles du Moulin Wibert Formation deposits (Figure 4). TOC values are largely higher when compared to the first interval, being mainly above 1.5 wt% (TOC = 2 wt% on average) and reaching up to 3.4 wt%. HI values are higher as well, being often above 200 mgHC/gTOC (HI = 244 mgHC/gTOC on average), and reaching up to 402 mgHC/gTOC. These results suggest a Type III to Type II organic matter deposition, the latter most probably deriving from marine organic matter sources, such as planktonic/bacterial materials [Tyson, 1995]. These analyses correspond to the black dots on Figure 5 and the organic-rich interval II will be referred to as "Organic Rich Bands, ORB" in the following. Interestingly, the TOC and HI curves are asymmetric in shape (Figure 4), meaning that there is a sudden increase in TOC and HI values up to a maximum from 68 to 69.75 m, and then a progressive decline in TOC and HI values from 69.75 m to 75 m. The palynofacies from this second interval show a terrestrial component of 71% on average, and a correlative marine component of 29% on average, e.g., an elevated average value compared to our first interval between 0 m and 68 m. The two samples located between 68 and 69.75 m and associated with the sharp TOC increase discussed above, show an even lower terrestrial component and an higher marine component in the palynofacies (64% and 36% respectively on average, Figure 4). This indicates that the peak in TOC and HI values corresponds to a peak of marine components in palynofacies. Both palynofacies and Rock-Eval results thus attest to a mixture of Type III (derived from terrestrial plant debris) and Type II (derived from marine planktonic and/or bacterial production) organic sources during deposition of the second interval, with a large increase in production from marine sources and better preserved organic matter. This indicates enhanced primary productivity in surface waters and/or occurrence of dysoxia to anoxia in water masses during the uppermost *Cymodoce* and part of the *Mutabilis* zones in the Boulonnais area corresponding to the organic-rich interval labelled "C" in Figure 6. In more detail, it seems that this organic-rich interval C is

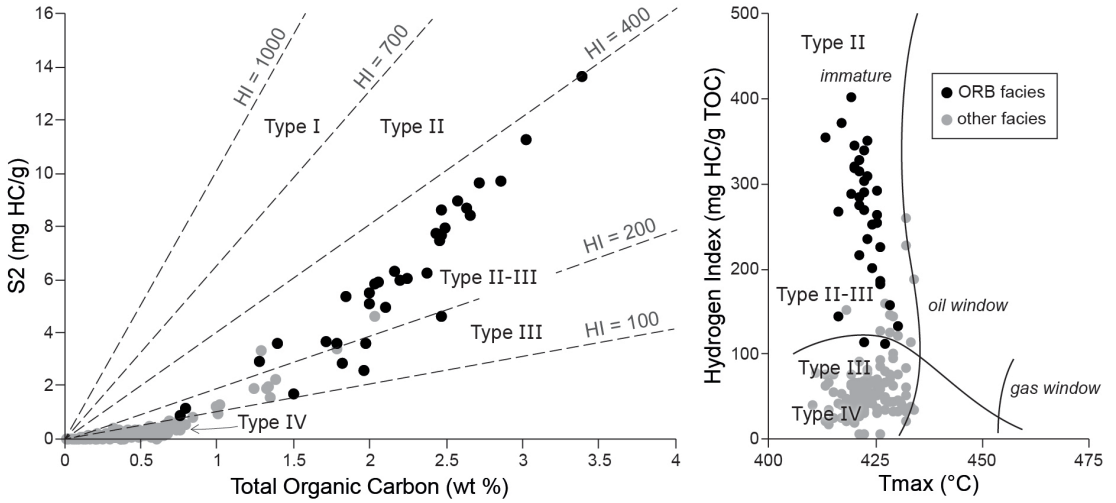

Figure 5. S2/TOC and HI/Tmax from the Oxfordian–Kimmeridgian boundary samples in the Boulonnais. Note the sharp contrast between ORB samples (black dots) and non-ORB samples (grey dots).

announced by two peaks in TOC and HI values centered around 61 m and 65.90 m, TOC reaching up to 1.29 wt% and 2.03 wt% and HI values reaching up to 259 mgHC/gTOC and 227 mgHC/gTOC, respectively, and labelled "A" and "B" in Figure 6. We interpret these peaks as indicating first, short-term phases of increasing marine productivity and/or better preservation of organic matter linked to periodic dysoxia/anoxia development in water masses during the uppermost *Cymodoce* to lowermost *Mutabilis* zone (Figure 6 and Supplementary Data), preceding the deposition of the main organic-rich interval. Furthermore, palynofacies data also evidence a slight increase in marine palynomorph proportions from sample DB1.20 (64.5 m) to sample DB4 (68 m) (Figure 4). Marine palynomorph proportions are comprised between 13 and 17.5% within these samples. This slight increase again predates the major organic-rich interval beginning at 68 m and corresponds to the interval of TOC and HI peaks located in the uppermost *Cymodoce* to the lowermost *Mutabilis* zones. These data most probably evidence planktonic blooms linked to increasing periodic marine influences.

The third interval extends from 75 to 102.50 m, and includes the uppermost *Mutabilis* to *Eudoxus* (*Orthocera* subzone) zones in the late Kimmeridgian, in the upper part of the Argiles du Moulin Wibert and the base of the Grès de Conningthun formations (Figure 4). TOC values are again mainly below 1 wt% (TOC = 0.5 wt% on average) and HI mainly below 100 mgHC/gTOC (HI = 53 mgHC/gTOC on average), similar to what was observed in the first interval between 0 m and 68 m. These results point to a Type III organic matter, and again correspond to the grey dots on Figure 5. The palynofacies indicate a dominant terrestrial component (91% of the total assemblage) over the marine component (9%), a feature again quite similar to the first interval. The organic matter is thus a mixture of strong terrestrial organic sources and oxidized marine sources. The primary productivity levels in surface waters were certainly low or moderate and the water masses rather well oxygenated. Of special interest is a clear increasing trend in TOC and HI values from 78 to 87.50 m in the Argiles du Moulin Wibert in the *Eudoxus* zone, TOC values reaching up to 1.79 wt% and HI reaching up to 188 mgHC/gTOC (Figure 4). This probably correspond to a moderate increase of marine organic matter production and/or preservation. However, this minor trend is not reflected in the palynofacies data by an increase of the marine organic particles (Figure 4). It may be possible that this trend toward higher TOC values should be followed higher up by a symmetric decreasing trend in TOC, from 87.5 m onto the base of the Grès de Conningthun deposition, evidencing a flat-shaped organic cycle (Figure 4). However, the low resolution of our data set above 90 m does not allow us to ascertain this possibility.

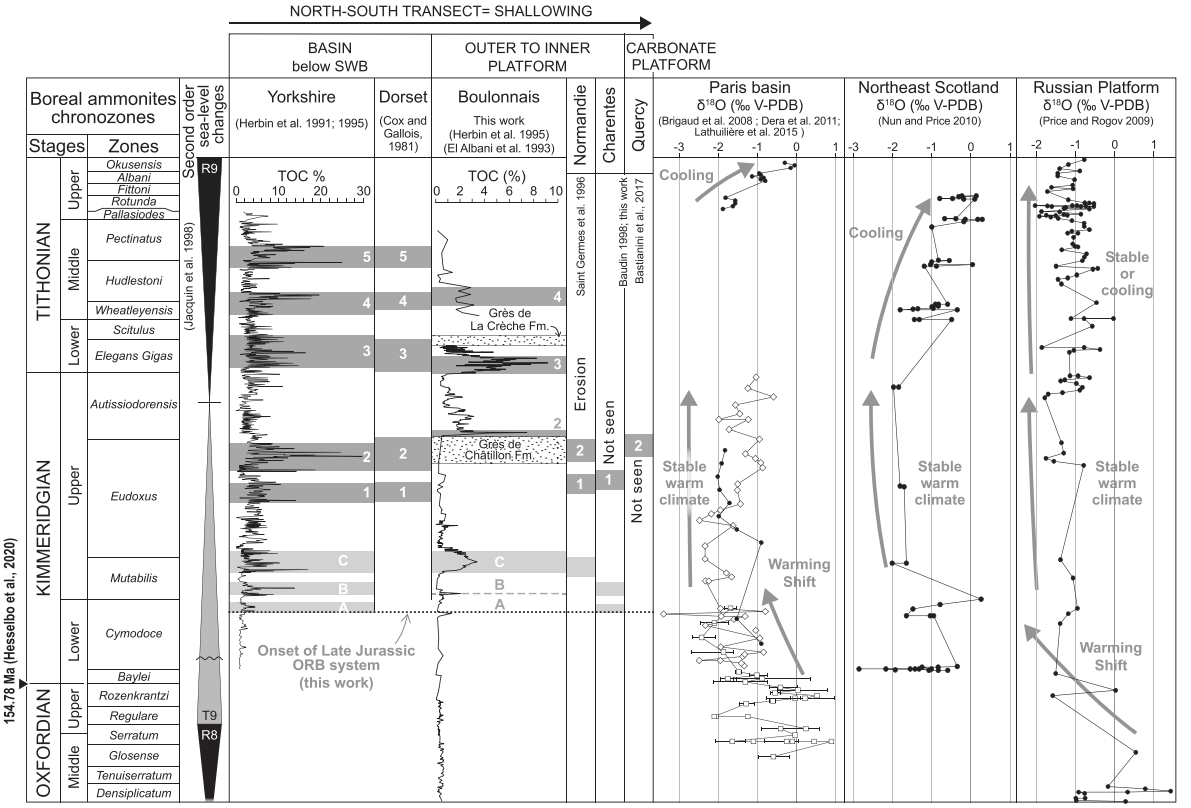

Figure 6. Late Jurassic organic matter enrichments in Yorkshire and Dorset in the UK (basinal facies), and Boulonnais, Normandy, Charentes and Quercy in France (platform facies), showing the simultaneity of ORB system onset (Uppermost *Cymodoce* to late *Mutabilis* zones interval), and the relatively good correlations of the various ORB at large scale. Note (1) the corresponding shift toward warmer climates at the onset of ORB deposition, (2) the association of the ORB system with stable, warm climates and (3), the termination of the ORB system in NW European basins as a large-scale cooling trend is obvious during the middle part/upper part of the Tithonian. Isotopic data from the Paris Basin: white squares after Brigaud et al. [2008] and Lathuilière et al. [2015]; black dots after Dera et al. [2011].

5. Discussion

Significant organic matter enrichments, respectively labelled "A", "B" and "C" (see Figure 6) occur at the topmost part of the Calcaires de Brecquerecque and the base of the Argiles du Moulin Wibert Formation in the Boulonnais, in the uppermost *Cymodoce* and *Mutabilis* zones, at the early/late Kimmeridgian boundary, with TOC reaching up to 3.4 wt% and HI values up to 400 mgHC/gTOC. Marine organic matter planktonic algal/bacterial production was enhanced and/or dysoxia/anoxia did occurred in water masses. This organic matter accumulation strongly contrasts with the underlying middle-late Oxfordian to early Kimmeridgian time interval in the same region, were TOC values are always low to very low and below 1 wt% (Figure 4).

5.1. *Comparison with Normandy, Charentes and Quercy (France)*

In the neighbouring Normandy area (4, Figure 1), the organic matter analyses [Baudin, 1992, Saint-Germès et al., 1996] reveal a low content of organic carbon (<0.5%) in lower Kimmeridgian deposits (*Baylei* and *Cymodoce* zones), whereas the total organic carbon content varies between 1 and 7% in upper Kimmeridgian sediments (*Mutabili*s and *Eudoxus* zones).

The HI-values indicate a recycled and oxidized terrigenous material in lower Kimmeridgian marls and limestones, whereas more or less oxidized marine organic matter dominantly occurs in upper Kimmeridgian black shales. Three organic-rich bands are recognised within the Argiles d'Octeville Formation. The oldest is located in the Argiles du Croquet Member (*Mutabilis* subzone), whereas the others two are from the *Eudoxus* zone. The first one lies in the middle part of the Argiles d'Ecqueville Member (*Orthocera* subzone) and the latest in the upper part of the Argiles d'Ecqueville Member (*Contejeani* subzone). Although the biostratigraphic resolution of the Kimmeridgian is poor in the Boulonnais area, the major organic-rich band from the base of the Argiles du Moulin Wibert (labelled C) seems coeval with the organic-rich band from the Argiles du Croquet Member (Figure 6). The similar evolution of palynological and organic geochemical features observed between Normandy and Boulonnais suggest a common event. This implies a late *Mutabilis* subzone dating for this organic-rich band observed in the two regions (Figure 6), although we have seen that in the Boulonnais, first, older short-lived organic enrichments ("A" and "B", Figure 6) are obvious in the uppermost *Cymodoce*/lowermost *Mutabilis* zones. The Argiles du Moulin Wibert coincide with a major change in lithology (e.g. from dominantly carbonates to dominantly claystones), similar to that occurring at the base of Argiles d'Octeville, both indicating a deepening-up, long-term transgressive trend at the boundary between the early and late Kimmeridgian, beginning in the earliest Kimmeridgian, as revealed by the facies succession described in the Boulonnais (Figure 4).

In the Charentes area (5, Figure 1), organic enrichment intervals are obvious in the upper part of the *Cymodoce* zone, TOC values being above 2 wt% and HI above 400 mgHC/gTOC [Figure 6, Baudin, 1998, this work]. Two other organic-rich intervals are recorded in the *Mutabilis* zone and in the *Eudoxus* zone (*Orthocera* subzone) zone (Figure 6).

In Quercy (6, Figure 1) organic rich intervals are recognized only in the upper part of the *Eudoxus* zone and the basal part of the *Autissiodorensis* zone, TOC values reaching up to 15 wt% and IH values up to 700 mgHC/gTOC, and palynofacies are dominated by AOM within these levels, indicating a dominant marine organic source with enhanced palaeoproductivity and/or dysoxia/anoxia [Figure 6, Baudin, 1998, Bastianini et al., 2017; this work].

5.2. *Onset of late Jurassic organic rich bands (ORB) in NW European margin*

The study of the Kimmeridge Clay Formation in the Cleveland Basin in Yorkshire (UK) has evidenced the cyclic nature of marine organic matter distribution, from primary organic fluctuations less than 1 m in thickness to decametre-thick organic-rich intervals [Herbin et al., 1991, 1995, Herbin and Geyssant, 1993]. Five main concentrations of oil shales with TOC higher than 10 wt%, which can be correlated throughout several cores in Yorkshire in late Kimmeridgian and early Tithonian beds, have been defined as "organic belts" by Herbin et al. [1991, 1993]. They correspond to periods highly favourable for marine organic matter production and preservation, and alternate with unfavourable periods [e.g., most of the *Autissiodorensis* zone, the *Scitulus* zone, middle part of the *Hudlestoni* zone and the top of the *Pectinatus* zone, Herbin et al., 1991, 1993]. Similar organic-rich intervals found in subsurface data in Dorset in the UK were previously described as "organic rich bands" (ORB) [Cox and Gallois, 1981] and have been recognized in outcrops in Dorset as well [Huc et al., 1992]. The five ORB can indeed be correlated from Yorkshire to Dorset and are recognised: in the middle part of the *Eudoxus* zone (ORB1), in the upper part of the *Eudoxus* zone and the lower part of the Autissiodorensis zone (ORB2), in the *Elegans* zone (ORB3), in the upper part of the *Wheatleyensis* zone and the basal part of the *Hudlestoni* zone (ORB4) and finally in the upper part of the *Hudlestoni* zone and the lower part of the *Pectinatus* zone (ORB5), spanning the late Kimmeridgian to part of the late Tithonian time-interval (Figure 6). In Yorkshire, TOC from the ORB are commonly above 5–10 wt% and can reach up 30 wt%, whereas HI values are often above 400–500 mgHC/gTOC and can reach maxima of 800 mgHC/gTOC [Herbin et al., 1991, 1995], pointing mostly to a well-preserved Type II marine organic matter deposition associated with probable dysoxia/anoxia during ORB deposition. No significant organic matter enrichments are observed in beds younger than the *Pectinatus* zone (early Tithonian). The above described ORB

can be correlated throughout the Boulonnais area in France [Herbin and Geyssant, 1993], but only the upper part of ORB2 in the Autissiodorensis zone, the lower part of ORB3 in the *Elegans* zone, and the ORB4 in *Wheatleyensis* and *Hudlestoni* zones are recorded (Figure 6). Furthermore, TOC and HI values are often lower in the Boulonnais when compared to the similar Yorkshire and Dorset intervals, reaching up to 9 wt% and 560 mgHC/gTOC respectively in the Argiles de Châtillon Formation (*Elegans* zone) [El Albani et al., 1993, Herbin et al., 1995]. This has been related to the shallower environments of the Boulonnais, corresponding to outer to inner ramp-type platforms neighbouring emerged lands [Proust et al., 1995, Figure 1], when compared to the deeper, more basinal and often below storm wave base environments of the Kimmeridge Clay Formation in UK [Herbin et al., 1995]. Shallower and nearshore environments in the Boulonnais may have been associated with better oxygenated waters, whereas dysoxia/anoxia could have persisted in deeper environments [Creaney and Passey, 1993, Herbin et al., 1995]. Although, regressive trends may have led in nearshore environments to the deposition of thick sandstone packages not prone to organic matter deposition and even eroding older deposits, such as the Grès de Châtillon and Grès de la Crèche in the Boulonnais [Herbin et al., 1995, see Figure 6]. Furthermore, ORB1 and ORB2 can be partly recognised in Normandy, Charentes and Quercy (Figure 6).

As stated above, our data at the Oxfordian/Kimmeridgian transition in the Boulonnais, compared with that of Normandy, Charentes and Quercy [Baudin, 1992, Saint-Germès et al., 1996, Baudin, 1998, this work] show that a major organic-rich matter interval can already be identified in the (probably late) *Mutabilis* zone (C, Figure 6). Re-interpreting the Rock-Eval data from Herbin et al. [1991, 1995] in Yorkshire, it is remarkable that two significant organic-rich accumulations can be identified in the *Mutabilis* zone, at the base and at the top of the *Mutabilis* zone, respectively (Figure 6), although Herbin and Geyssant [1993] did not define "organic belts" within the *Mutabilis* zone. Those two stratigraphic intervals yield TOC comprised between 2–5 and more than 10 wt%, and HI values comprised between 400 and 600 mgHC/gTOC [Herbin et al., 1995, Figure 6]. Furthermore, a first TOC peak occurs in the late *Cymodoce* zone (Figure 6). We thus propose that these first organic matter enrichments in the late *Cymodoce* and *Mutabilis* stratigraphic intervals are lateral equivalents to those seen in the Boulonnais and labelled "A", "B" and "C" respectively, and also partly recognised in Normandy and Charentes (Figure 6). Therefore, the onset of the Late Jurassic ORB system of the Kimmeridgian Clay Formation and lateral equivalents in France may have been located in the late *Cymodoce–Mutabilis* stratigraphic intervals, at around the early/late Kimmeridgian boundary, and not higher up in the *Eudoxus* zone, as previously stated (Figure 6). This hypothesis is in accordance with faintly bituminous mudstones with *Aulacostephanus eulepidus* in the Black Head section of Dorset [Cox and Gallois, 1981]. As is widely observed in younger strata, maxima of TOC and HI values in the *Mutabilis* zone in the Boulonnais (3.4 wt% and 400 mgHC/gTOC, respectively) are lower that the ones in Yorkshire (above 10 wt% and 600 mgHC/gTOC, respectively) and only the upper *Mutabilis* zone organic-rich interval is well recorded in the Boulonnais and Normandy. This was again probably related to the nearshore environments deposited in Normandy and the Boulonnais, less prone to organic matter preservation when compared to deeper, basinal environments. Therefore, the late Jurassic ORB system in NW Europe would have had a duration of around 6.8 Myr (GTS 2021), starting at the topmost part of *Cymodoce* zone and ending around the top of *Pectinatus* zone (Figure 6).

5.3. *Palaeoenvironmental and palaeoclimatic controls on ORB onset and deposition*

Herbin et al. [1991, 1993, 1995] suggested that transgressions were one of the main driving factors for marine organic matter accumulation in the Kimmeridge Clay Formation, as the five ORB correlate well with deepening trends. They however also remarked that all transgressive trends during the late Jurassic did not led to organic-rich beds, indicating that sea-level variations were not the only controls on organic matter enrichments. Our data from the Boulonnais at the Oxfordian–Kimmeridgian transition support this hypothesis, as the first significant organic enrichment found in the Argiles du Moulin Wibert Formation occur at the onset of a long-term "second-order"

transgressive trend [Jacquin et al., 1998] that led in the Boulonnais to the flooding of the late Oxfordian carbonate platforms (Figures 5 and 6). The end of the ORB system after the *Pectinatus* zone also corresponds to a long-term shallowing-up trend in NW European basins [Jacquin et al., 1998, see Figure 6], accelerating during the late Tithonian, that will lead locally to widespread emersion and/or widespread shallow marine or non-marine deposits (e.g. the so-called Purbecks beds).

Tyson et al. [1979] additionally proposed that the peculiar physiography of the late Jurassic NW European shelf also played a role in the widespread organic-rich matter enrichments as seen in the Kimmeridge Clay Formation. The rapid drowning of the large shallow and flat, carbonate-dominated NW European shelf that existed during the late Oxfordian–early Kimmeridgian would have separated the mixed, well oxygenated surface waters from the sea bottom, initiating water stratification and creating stagnant, anaerobic layer(s), favourable for organic matter preservation [Tyson et al., 1979]. These stagnant water bodies were probably relatively isolated from the oceanic tethyan waters to the south, inhibiting large-scale water mixing [Tyson et al., 1979]. Our work in the Boulonnais shows that the ORB deposition, initiated at the early/late Kimmeridgian boundary, occurred at the very early phases of the long-term transgression and the related late Jurassic platform drowning (Figure 6), as the area was probably only covered by a relatively shallow water. This shows that an efficient system for production and/or preservation of organic matter did exist and formed quickly in relatively shallow water, proximal areas. However, the better preservation of organic-rich intervals and the higher content in organic matter in lateral, deeper facies of Yorkshire (Figure 6) also point out that the production and preservation mechanism(s) of organic matter were more efficient in basinal settings at the onset of the ORB system, as shown previously for the five ORB previously described [Herbin et al., 1991, 1993].

Following Dunn [1974] and House [1985], who had previously investigated the orbital forcing of climate as a control on sedimentary deposits in the Kimmeridge Clay Formation, Herbin et al. [1991, 1995] recognized the cyclic nature of the organic matter accumulation in the Kimmeridge Clay Formation, this being observed from millimetre-scale cycles up to decametre-thick cycles and suggesting a climatic control on organic matter cycles. Studying palynofacies data in the Kimmeridge Clay Formation in Dorset, Waterhouse [1995] evidenced the occurrence of obliquity and precession orbital forcing on palaeoenvironmental variations within cycles. Using trace element data, Tribovillard et al. [1994] evidenced the local development of reducing conditions enhancing organic matter accumulation in the Kimmeridge Clay Formation in Yorkshire, but also stressed that phytoplanktonic production was an important factor—if not the main factor—in organic matter accumulation, a conclusion backed by Bertrand et al. [1994]. Indeed, phytoplanktonic production may be driven, directly or indirectly by climatic fluctuations [Tyson, 1995].

Interestingly, the onset of the late Jurassic ORB at the early/late Kimmeridgian boundary as shown in this work is contemporaneous to a large-scale (global?) climate warming that can be evidenced in the Paris Basin [Brigaud et al., 2008, Dera et al., 2011, Lathuilière et al., 2015], in Scotland, UK [Nunn and Price, 2010] and in the Russian Platform [Price and Rogov, 2009] using oxygen isotopes measured on mollusc or belemnite fossils (Figure 6). All these records show an isotopic shift of around 2‰ toward more negative values, beginning in the middle-late Oxfordian (*Regulare* zone in the Paris Basin) and ending with the more negative values at around the early/late Kimmeridgian boundary (in the top *Cymodoce* or the *Mutablis* zone in the Paris Basin, see Figure 6). Interpreted in term of palaeotemperature changes, this would correspond to a sea-water warming as high as 6 °C during this stratigraphic interval [Brigaud et al., 2008]. Zuo et al. [2019] similarly evidenced a warming trend during the Kimmeridgian in the Lower Saxony Basin (Germany). Using clumped isotope analyses, Wierzbowski et al. [2018] showed that at least a part of the recorded isotopic shift in the early late Kimmeridgian in the Russian Platform may have been due to a salinity decrease, rather than to a temperature change. According to Wierzbowski et al. [2018], enhanced freshwater flows were associated with low sea level and a relative isolation of the Russian Platform, leading to water mass stratifications, ultimately promoting black shales deposition. Indeed, salinity fluctuations in water masses, due to climate changes and/or sea-level fluctuations

are known to locally enhance water stratification and organic matter accumulation, as was evidenced in the Late Tithonian/Berriasian lagoonal facies from the so-called Purbeck Beds of Dorset, UK [Schnyder et al., 2006, 2009] for example. As stressed above, we do think that such stratification processes in shallow, restricted water mass may have favoured, locally, the early record of ORB deposits in NW Europe. It is quite clear that salinity fluctuations through time in marine basins are currently under-estimated, and further studies are urgently required on this topic. However, the late Jurassic warming parallels the long-term late Oxfordian–early Kimmeridgian sea-level rise in the French and British Basins (Figure 6). Such a long-term sea-level rise would certainly not have been associated with a widespread and long-term increase in freshwater inputs. We therefore suggest that climate was an additional major, long-term control on the ORB onset, the general (global) warming at the early/late Kimmeridgian boundary possibly leading to an abrupt increase in phytoplanktonic productivity levels in the epeiric seas that were initiated by the sea-level rise. Oxygen isotope curves appear then to be mostly stable until the top of the *Autissiodorensis* zone, suggesting continuing warm conditions, favourable for primary production in surface waters, during most of the late Kimmeridgian (Figure 6). From the *Elegans* zone to *Wheatleyensis* and up to the Fittoni zone, oxygen isotope curves point to progressive slighly more positive values in all basins, suggesting a climatic deterioration with colder sea water temperatures (Figure 6). Together with the long-term late Jurassic sea-level fall, colder sea water temperatures would have been progressively less favourable for marine organic matter phytoplanktonic production and preservation, finally leading to the termination of the ORB system and to the widespread late Jurassic enrichments in organic matter at the sea bottom in the NW European Basins. In addition, Zuo et al. [2019] evidenced "short term" fluctuations in humid/arid conditions during the Kimmeridgian using clay mineral associations, as shown in the North Aquitaine Platform in France [Colombié et al., 2018]. Such shorter-term climate fluctuations during the Kimmeridgian and the Tithonian, possibly associated with sea-level changes, may have modulated the NW European ORB record, as shown by the succession of several ORB through time and the cyclic pattern of the organic record.

6. Conclusions

Using newly described cores and outcrops, we characterised, thanks to Rock-Eval Pyrolysis and palynofacies observations, the organic matter content of marine platform deposits at the Oxfordian–Kimmeridgian transition in the Boulonnais area (NW France). Organic rich deposits in outer to inner platform environments occur in the uppermost *Cymodoce* to the late *Mutabilis* zone interval (early late Kimmeridgian), with TOC reaching up to 3.4 wt% and HI up to 402 mgHC/gTOC. Organic sources correspond to a mixture of a Type III (continental) and Type II (marine) organic matter, as shown by palynofacies. The organic-rich deposits were associated with enhanced planktonic palaeoproductivity and/or dysoxia/anoxia in water masses. In platform deposits of Normandy and Charentes in France, equivalent organic rich intervals can be evidenced at the Oxfordian–Kimmeridgian transition. Re-interpreting previously published data from Yorkshire and Dorset in the UK, again, similar organic-rich deposits also exist in the late *Cymodoce* and in *Mutabilis* zones in the UK, and can be considered as Organic Rich Bands (ORB), as described in NW Europe during the Late Jurassic. We thus propose that the ORB deposition system at the NW European scale, which lasted until the middle part of the Tithonian over a time span of 6.8 Myr, began earlier than previously thought, at the *Cymodoce–Mutabilis* boundary during the early late Kimmeridgian. This time-interval was also marked by a pronounced sea water warming as high as 6 °C, recorded in NW Europe by most authors. Sea water temperature remained rather stable but elevated during most of the Kimmeridgian and Early Tithonian, an interval corresponding to multiple well-known ORB deposits in NW European basins, followed by a cooling trend during the middle and upper part of the Tithonian, the latter corresponding to the end of the ORB deposition. We thus proposed that early late Kimmeridgian warmer climatic conditions played a role in enhancing palaeoproductivity and/or favouring organic matter preservation on the sea floor as a major trigger for Late Jurassic ORB deposits, together with the long-term sea level rise, the peculiar physiographic conditions in NW European basins, and probably modulated by shorter-term climatic changes.

Conflicts of interest

Authors have no conflict of interest to declare.

Acknowledgments

We thank Diane Vidier and Jean-François Deconinck for fieldworks, and Pierre Hantzpergue and Jean-François Deconinck for discussions. Alexandre Lethiers (Sorbonne Université) took care of the illustrations. We warmly thank M. Pickford for correcting the English. Finally, we acknowledge to the two reviewers, Nicolas Tribovillard and Jacek Graboswki, for their fruitful comments on a previous version of this paper.

Supplementary data

Supporting information for this article is available on the journal's website under https://doi.org/10.5802/crgeos.173 or from the author.

References

Bastianini, L., Caline, B., Hoareau, G., Bonnel, C., Martinez, M., Lézin, C., Baudin, F., Brasier, A., and Guy, L. (2017). Sedimentary characterization of the carbonate source rock of Upper Kimmeridgian Parnac Formation of the Aquitaine Basin (Quercy area). *Bull. Soc. Géol. France*, 188(5), article no. 32.

Baudin, F. (1992). Etude préliminaire du contenu en matière organique du Kimméridgien normand. *Géol. France*, 2, 31–38.

Baudin, F. (1998). *Paléogéographie et sédimentologie de couches mésozoïques riches en matière organique*. PhD thesis, université Pierre-et-Marie-Curie, 98-6.

Bertrand, P., Lallier-Vergès, E., and Boussafir, M. (1994). Enhancement of accumulation and anoxic degradation of organic matter controlled by cyclic productivity: a model. *Org. Geochem.*, 22(3–5), 511–520.

Bialkowski, A., Tribovillard, N., Vergès, E., and Deconinck, J.-F. (2000). Etude haute résolution de la distribution et de granulométrie des constituants organiques sédimentaires dans le Kimméridgien/Tithonien du Boulonnais (Nord de la France). Application à l'analyse séquentielle. *C. R. Acad. Sci. Paris*, 331, 1–18.

Brigaud, B., Pucéat, E., Pellenard, P., Vincent, B., and Joachimski, M. M. (2008). Climatic fluctuations and seasonality during the Late Jurassic (Oxfordian-Early Kimmeridgian) inferred from δ^{18}O of Paris Basin oyster shells. *Earth Planet. Sci. Lett.*, 273, 58–67.

Cecca, F., Azema, J., Fourcade, E., Baudin, F., Guiraud, R., and De Wever, P. (1993). Early Kimmeridgian Palaeoenvironements (146 to 144 M.a). In Dercourt, J., Ricou, L. E., and Vrielynck, B., editors, *Atlas Tethys Palaeonvironnemental Maps*. Beicip-Franlab, Rueil-Malmaison.

Colombié, C., Carcel, D., Lécuyer, C., Ruffel, A., and Schnyder, J. (2018). Temperature and cyclone frequency in Kimmeridgian Greenhouse period (late Jurassic). *Glob. Planet. Change*, 170, 126–145.

Cox, B. M. and Gallois, R. W. (1981). The stratigraphy of the Kimmeridge Clay of the Dorset type area and its correlation with some other Kimmeridgian sequences. *Rep. Inst. Geol. Sci.*, 80(4), 1–44.

Creaney, S. and Passey, Q. R. (1993). Recurring pattern of total organic carbon and source rock quality within a sequence stratigraphic framework. *AAPG Bull.*, 64, 1179–1209.

Debrand-Passard, S., Enay, R., Rioult, M., Cariou, E., Marchand, D., and Menot, J.-C. (1980). Jurassique supérieur. In *Synthèse Géologique du Bassin de Paris, Stratigraphie et Paléogéographie*, volume I of *Mémoire du BRGM 101*, pages 195–253. BRGM, Orléans.

Demaison, G., Holck, A. J. J., Jones, R. W., and Moore, G. T. (1983). Predictive source bed stratigraphy; a guide to regional petroleum occurrences. In *North Sea Basin and Eastern American Eleventh World Petroleum Congress, Vol. 2, Geology Exploration Reserves*, pages 17–29. Wiley, Chichester.

Dera, G., Brigaud, B., Monna, F., Lafont, R., Pucéat, E., Deconinck, J.-F., Pellenard, P., Joachimsky, M. M., and Durlet, C. (2011). Climatic ups and downs in a disturbed Jurassic world. *Geology*, 39, 215–218.

Dunn, C. E. (1974). Identification of sedimentary cycles through Fourier analysis of geochemcial data. *Chem. Geol.*, 13, 217–232.

Dutertre, A.-P. (1925). Observations sur les terrains jurassiques supérieurs dans la vallée de la Liane (Bas-Boulonnais). *Ann. Soc. Géol. Nord.*, 49, 216–236.

El Albani, A., Deconinck, J.-F., Herbin, J.-P., and Proust, J.-N. (1993). Caractérisation géochimique

de la matière organique et minéralogie des argiles du Kimméridgien du Boulonnais. *Ann. Soc. Géol. Nord.*, 2(2), 113–120.

Espitalié, J., Deroo, G., and Marquis, F. (1985–1986). La pyrolyse Rock-Eval et ses applications. *Rev. Inst. Fr. Pétrole*, 40(5), 563–579. 40(6), 755–784; 41(1), 73–89.

Geyssant, J.-R., Vidier, J.-P., Herbin, J.-P., Proust, J.-N., and Deconinck, J.-F. (1993). Biostratigraphie et paléoenvironnement des couches du passage Kimméridgien/Tithonien du Boulonnais (Pas-de-Calais): nouvelles données paléontologiques (ammonites), organisation séquentielle et contenu en matière organique. *Géol. France*, 4, 11–24.

Herbin, J.-P. and Geyssant, J. R. (1993). "Ceintures organiques" au Kimméridgien/Tithonien en Angleterre (Yorkshire, Dorset) et en France (Boulonnais). *C. R. Acad. Sci. Paris*, 317(II), 1309–1316.

Herbin, J.-P., Geyssant, J. R., El Albani, A., Deconinck, J.-F., Proust, J.-N., Colbeaux, J.-P., and Vidier, J.-P. (1995). Sequence stratigraphy of source rocks applied to the study of the Kimmeridgian/Tithonian in the North-West European shelf (Dorset/UK, Yorkshire/UK, et Boulonnais/France). *Mar. Petrol. Geol.*, 12, 177–194.

Herbin, J. P., Geyssant, J. R., Mélières, F., Penn, J. E., and the Yorkim Group (1993). Variation of the distribution of organic matter within a transgressive system tract: Kimmeridge Clay (Jurassic), England. In Katz, B. and Pratt, L., editors, *Source Rocks in a Sequence Stratigraphic Framework*, volume 37, pages 67–100. Am. Assoc. Petrol. Geol. Stud. Geol., Tulsa, OK.

Herbin, J.-P., Muller, C., Geyssant, J. R., Mélières, F., Penn, J. E., and the YORKIM Group (1991). Hétérogénéïté quantitative et qualitative de la matière organique dans les argiles du Kimméridgien du Val de Pickering (Yorkshire, UK). *Rev. Inst. Fr. Pétrole*, 46(6), 675–712.

Hesselbo, S., Ogg, J. G., and Ruhl, M. (2020). The Jurassic period. In *Geologic Time Scale 2020*, pages 955–1021. Elsevier, Amsterdam.

House, M. R. (1985). A new approach to an absolute timesclae from measurments of orbital cycles and sedimentary microrhythms. *Nature*, 316, 721–725.

Huc, A. Y., Lallier-Vergès, E., Bertrand, P., Carpentier, B., and Hollander, D. J. (1992). Organic matter response to change of depositional environment in Kimmeridgian Shales, Dorset, UK. In Whelan, J. K. and Farrington, J. W., editors, *Organic Matter Productivity, Accumulation and Preservation in Recent and Ancient Sediments*, pages 469–486. Columbia University Press, New York.

Jacquin, T., Dardeau, G., Durlet, C., de Graciansky, P.-C., and Hantzpergue, P. (1998). The North-Sea cycle: an overview of 2nd-order transgressive/regressive facies cycles in western Europe. In *Mesozoic and Cenozoic Sequence Stratigraphy of European Basins*, SEPM Special Publication 60, pages 445–466. SEPM Society for Sedimentary Geology, Tulsa, OK.

Lathuilière, B., Bartier, B., Bonnemaison, M., Boullier, A., Carpentier, C., Elie, M., Gaillard, C., Gauthier-Lafaye, F., Grosheny, D., Hantzpergue, P., Hautevelle, Y., Huault, V., Lefort, A., Malartre, F., Mosser-Ruck, R., Nori, L., Trouiller, A., and Werner, W. (2015). Deciphering the history of climate and sea level in the Kimmeridgian deposits of Bure (eastern Paris Basin). *Palaeogeogr. Palaeoclimatol. Palaeoecol.*, 433, 20–48.

Mansy, J.-L., Amédro, F., Auffret, J.-P., Guennoc, P., Lamarche, J., Lefevre, D., Robaszynski, F., Sommé, J., and Vidier, J.-P. (2000). *Carte géologique de Marquise (1/50 000 ème)*. BRGM, Orléans, 2ème edition.

McArthur, A. D., Kneller, B. C., Souza, P. A., and Kuchle, J. (2016). Characterization of deep marine channel-levee complex architecture with palynofacies: an outcrop example from the Rosario Formation, Baja California, Mexico. *Mar. Pet. Geol.*, 73, 157–173.

Morgans-Bell, H. S., Coe, A. L., Hesselbo, S. P., Jenkyns, H. C., Weedon, G. P., Marshall, J. E. A., Tyson, R. V., and Williams, C. J. (2001). Integrated stratigraphy of the Kimmeridge Clay Formation (Upper Jurassic) based on exposures and boreholes in south Dorset, UK. *Geol. Mag.*, 138, 511–539.

Nunn, E. V. and Price, G. D. (2010). Late Jurassic (Kimmeridgian–Tithonian) stable isotopes (δ^{18}O, δ^{13}C) and Mg/Ca ratios: new palaeoclimate data from Helmsdale, northeast Scotland. *Palaeogeogr. Palaeoclimatol. Palaeoecol.*, 292, 325–335.

Oschmann, W. (1988). Kimmeridge Clay sedimentation-a new cyclic model. *Palaeogeogr. Palaeoecol. Palaeoclimatol.*, 65, 217–251.

Oschmann, W. (1990). Environmental cycles in the late Jurassic northwest European epeiric basin: interaction with atmospheric and hydrospheric circulations. *Sedim. Geol.*, 69(3–4),

313–332.

Pellat, E. (1867). Observations sur quelques assises du terrain jurassique supérieur du Bas-Boulonnais. Coup d'oeil sur le terrain jurassique supérieur de cette contrée. *Bull. Soc. Géol. France*, 25(2), 196–215.

Pellat, E. (1878). Terrain Jurassique supérieur du Bas-Boulonnais (étages Oxfordien, Corallien, Kimméridgien, Portlandien). *Ann. Soc. Géol. Nord.*, 5, 173–195.

Price, G. D. and Rogov, M. A. (2009). An isotopic appraisal of the Late Jurassic greenhouse phase in the Russian platform. *Palaeogeogr. Palaeoclimatol. Palaeoecol.*, 273, 41–49.

Proust, J.-N., Deconinck, J.-F., Geyssant, J.-R., Herbin, J.-P., and Vidier, J.-P. (1995). Sequence analytical approach to the Upper Kimmeridgian–Lower Tithonian storm-dominated ramp deposits of the Boulonnais (Northern France). A landward time-equivalent to offshore marine source rocks. *Geol. Rundsch.*, 84, 255–271.

Ramdani, A. (1996). Les paramètres qui contrôlent la sédimentation cyclique de la "Kimmeridge Clay Formation" dans le basin de Cleveland (Yorkshire, GB). Comparaison avec le Boulonnais (France). PhD thesis, University Paris XI Orsay. 259 p.

Saint-Germès, M., Baudin, F., Deconinck, J.-F., Hantzpergue, P., and Samson, Y. (1996). Sédimentologie de la matière organique et des argiles du Kimméridgien de Normandie (region du Havre). *Géol. France*, 3, 21–33.

Schnyder, J., Baudin, F., and Deconinck, J.-F. (2009). Occurrence of organic-matter-rich beds in early Cretaceous coastal evaporitic setting (Dorset, UK): a link to long-term palaeoclimate changes? *Cretaceous Res.*, 30, 356–366.

Schnyder, J., Baudin, F., Deconinck, J.-F., Durlet, C., Jan du Chêne, R., and Lathuilière, B. (2000). Stratigraphie et analyse sédimentologique du passage Oxfordien/Kimméridgien dans le Boulonnais. *Géol. France*, 4, 21–37.

Schnyder, J., Ruffell, A., Deconinck, J.-F., and Baudin, F. (2006). Conjunctive use of spectral gamma-ray logs and clay mineralogy in defining late Jurassic-early Cretaceous palaeoclimate change (Dorset, U.K.). *Palaeogeogr. Palaeoclimatol. Palaeoecol.*, 229, 303–320.

Schnyder, J., Stetten, E., Baudin, F., Pruski, A.-M., and Martinez, P. (2017). Palynofacies reveal fresh terrestrial organic matter inputs in the terminal lobes of the Congo Deep-Sea fan. *Deep-Sea Res. II*, 142, 91–108.

Steffen, D. and Gorin, G. (1993). Palynofacies of the upper Tithonian deep-sea carbonates in the Vocontian trough (SE France). *Bull. Centres Rech. Explor.-Prod. Elf Aquitaine*, 17(1), 235–247.

Tissot, B. (1979). Effects on prolific petroleum source rock and major coal deposits caused by sea-level changes. *Nature*, 277, 463–465.

Tribovillard, N., Bialkowski, A., Tyson, R. V., Lallier-Vergès, H., and Deconinck, J.-F. (2001). Organic facies variation in the Late Kimmeridgian of the Boulonnais area (northernmost France). *Mar. Pet. Geol.*, 18, 371–389.

Tribovillard, N., Desprairies, A., Lallier-Vergès, E., Bertrand, P., Moureau, N., Ramdani, A., and Ramanampisoa, L. (1994). Geochemical study of organic-matter rich cycles from the Kimmeridge Clay Formation of Yorkshire (UK): productivity versus anoxia. *Palaeogeogr. Paleoclimatol. Palaeoecol.*, 108, 165–181.

Tyson, R. V. (1995). *Sedimentary Organic Matter. Organic Facies and Palynofacies*. Chapman and Hall, London.

Tyson, R. V. (1996). Sequence stratigraphical interpretation of organic facies variations in marine siliclastic systems: general principles and application to the onshore Kimmeridge Clay Formation, UK. In Hesselbo, S. P. and Parkinson, D. N., editors, *Sequence Stratigraphy in British Geology*, volume 103, pages 75–96. Geological Society Special Publication, London.

Tyson, R. V., Wilson, R. C. L., and Downie, C. (1979). A stratified water column environment model for the Kimmeridge Clay. *Nature*, 277, 377–380.

Waterhouse, H. K. (1995). High-resolution palynofacies investigation of Kimmeridgian sedimentary cycles. In House, M. R. and Gale, A. S., editors, *Orbital Forcing Timescales and Cyclostratigraphy*, volume 85, pages 75–114. Geological Society Special Publication, London.

Waterhouse, H. K. (1999). Orbital forcing of palynofacies in the Jurassic of France and the United Kingdom. *Geology*, 27, 511–514.

Wierzbowski, H., Bajnai, D., Wacker, U., Rogov, M. A., Fiebig, J., and Tesakova, E. M. (2018). Clumped isotope record of salinity variations in the Subboreal Province at the Middle–Late Jurassic transi-

tion. *Glob. Planet. Change*, 167, 172–189.

Wignall, P. B. (1991). Test of the concepts of sequence stratigraphy in the Kimmeridgian (Late Jurassic) of England and northern France. *Mar. Pet. Geol.*, 8, 430–441.

Wignall, P. B. and Ruffell, A. H. (1990). The influence of a sudden climatic change on marine deposition in the Kimmeridgian of northwest Europe. *J. Geol. Soc. Lond.*, 147, 365–371.

Zuo, F., Heimhofer, U., Huck, S., Adatte, T., Erbacher, J., and Bodin, S. (2019). Climatic fluctuations and seasonality during the Kimmeridgian (Late Jurassic): stable isotope and clay mineralogical data from the Lower Saxony Basin, Northern Germany. *Palaeogeogr. Palaeoclimatol. Palaeoecol.*, 517, 1–15.

Comptes Rendus

Géoscience

Objet de la revue

Les *Comptes Rendus Géoscience* sont une revue électronique évaluée par les pairs de niveau international, qui couvre l'ensemble des domaines des sciences de la Terre et du développement durable. Ils publient des articles originaux de recherche, des articles de revue, des mises en perspective historiques, des textes à visée pédagogique ou encore des actes de colloque, sans limite de longueur, en anglais ou en français. Les *Comptes Rendus Géoscience* sont diffusés selon une politique vertueuse de libre accès diamant, gratuit pour les auteurs (pas de frais de publication) comme pour les lecteurs (libre accès immédiat et pérenne).

À propos de la revue

Toutes les informations concernant la revue, y compris le texte des articles publiés qui est en accès libre intégral, figurent sur le site https://comptes-rendus.academie-sciences.fr/geoscience/.

Informations à l'attention des auteurs

Pour toute question relative à la soumission des articles, les auteurs peuvent consulter le site https://comptes-rendus.academie-sciences.fr/geoscience/.

Contact

Académie des sciences
23, quai de Conti, 75006 Paris, France
Tél. : (+33) (0)1 44 41 43 72
CR-Geoscience@academie-sciences.fr

Comptes Rendus
de l'Académie des sciences

Géoscience
Sciences de la Planète

Volume 354, nº S3, 2022

Special issue / *Numéro thématique*

Integrated stratigraphy of the Jurassic and the Cretaceous: a tribute to Jacques Rey / *Stratigraphie intégrée du Jurassique et du Crétacé : un hommage à Jacques Rey*

Guest editors / *Rédacteurs en chef invités*

Carine Lézin (Laboratoire Géosciences Environnement, Université Paul Sabatier, 31000 Toulouse, France)
Thomas Saucède (Biogéosciences, UMR 6282 CNRS, Université Bourgogne Franche-Comté, 21000 Dijon, France)

Cover illustration / *Illustration de couverture*

1778-7025 (electronic)

Académie des sciences — Paris

COMPTES RENDUS
DE L'ACADÉMIE DES SCIENCES
Géoscience
Volume 354, nº S3, 2022